Department für Angewandte Genetik und Zellbiologie

Vorstand: Ao.Univ.Prof. Dr. Lukas Mach

BetreuerInnen: Ao.Univ.Prof. Dr. Marie-Theres Hauser

Univ.Prof. Dr. Christian Schlötterer (VUW Wien)

GENETIC AND MOLECULAR ANALYSIS OF TRICHOME PATTERNING IN NATURAL ACCESSIONS OF *ARABIDOPSIS THALIANA*

Dissertation zur Erlangung des akademischen Grades
Doctor rerum naturalium technicarum
an der Universität für Bodenkultur Wien

Eingereicht von

Mag. Julia Hilscher

Wien, Februar 2011

»Woran arbeiten Sie?« wurde Herr K. gefragt.

Herr K. antwortete: »Ich habe viel Mühe, ich bereite meinen nächsten Irrtum vor.«

Bertold Brecht

Danksagung

Zusammenfassung

An pflanzlichen Epidermen entwickeln sich Zellen häufig zu Trichomen (Blatthaare) mit hoher Vielgestalt, ihnen werden unterschiedliche Schutzfunktionen vor biotischen und abiotischen Einflüssen zugeschrieben. Natürliche Populationen der Modellpflanze *Arabidopsis thaliana* weisen große Unterschiede in ihrer Trichomdichte auf Rosetteblättern auf und so wird angenommen, dass die jeweilige Dichte einen selektiven Vorteil bieten kann. In *A. thaliana* sind Trichome ein intensiv beforschtes Modellsystem der Zellspezifikation und der Musterbildung. Aktuelle Studien basierend auf klassischen genetischen Experimenten postulieren einen Aktivatorkomplex, dessen Anwesenheit in epidermalen Zellen notwendig ist, um die Entwicklung zu einer Trichomzelle einzuleiten. Dieser besteht aus MYB und bHLH Transkriptionsfaktoren sowie einem WD40-repeat Protein. Gleichzeitig beeinflusst dieser Komplex die Genexpression von Inhibitoren (sogenannte single-repeat R3 MYB Proteine) positiv, die wiederum hindern durch nicht-zellautonome Wirkungsweise die umgebenden Zellen an der Entwicklung zu Trichomen.

Die hier vorliegende Arbeit nutzte nun die vorhandene natürliche Variation der Trichomdichte in *A. thaliana* Populationen, um weitere Informationen zum molekularen Mechanismus der Trichomentwicklung zu bekommen. Eine F2 Kartierungs-Population, basierend auf zwei *A. thaliana* Ökotypen mit extrem unterschiedlicher Trichomdichte, wurde einer „quantitative trait locus" (QTL) Analyse unterzogen. Unter den vier detektierten QTL Regionen befindet sich eine, die die Trichomdichte sehr stark beeinflusst und die im weiteren auf einen 8.4 cM Bereich eingeengt werden konnte. Anschließende funktionelle und populationsgenetische Experimente mit mehreren Kandidatengenen wiesen nach, dass sich das kausale „quantitative trait" Nukleotid (QTN) in der kodierenden Region des single-repeat R3 MYB Gens *ENHANCER OF TRIPTYCHON AND CAPRICE2* (*ETC2*) befindet. Dieses QTN führt zu einem Aminosäureaustausch eines konservierten Lysins zu Glutamat und stellt damit den ersten Hinweis auf eine mögliche Rolle des Prozesses der Ubiquitinierung in der Trichommusterbildung dar. Um ein tieferes Verständnis für den Mechanismus der differentiellen Trichominitiation zu erhalten, wurden Analysen auf zellulärer Ebene durchgeführt, die zeigten, dass die Modulation mit der Anzahl dazwischen liegender Mesophyllzellen gekoppelt ist. Dies ist ein Phänotyp, der eine Mutation in *caprice* (*cpc*), einem single-repeat R3 MYB Gen, widerspiegelt.

Weiters beschreibt diese Arbeit ein neues Pilotprojekt, das einen Zusammenhang zwischen Trichomdichte, Anthocyangehalt und UV-B Toleranz in natürlichen *A. thaliana* Populationen untersucht, da ein WD40/bHLH/R2R3MYB Transkriptionskomplex auch Enzyme der Anthocyanbiosynthese reguliert.

Abstract

Trichomes (leaf hairs) are epidermal cells protruding from aerial surfaces of plants. Morphological and mechanical features of trichomes are thought to influence many aspects of plant physiology and ecology and thus may be of selective importance. In accordance, rosette leaves of *Arabidopsis thaliana* exhibit extensive variation in trichome density among natural accessions. *A. thaliana* trichomes also serve as an intensely studied model system for cell specification. Classical genetic studies identified a set of genes including MYB related and bHLH-like transcription factors and a WD40 repeat gene as trichome activators and a family of single-repeat R3 MYB genes as trichome inhibitors. Molecular characterisation of these and consideration of theoretical models led to the current mechanistic concept of *de novo* trichome patterning: a specific WD40/bHLH/R2R3MYB trichome activator complex acting local is counteracted by single-repeat R3 MYB proteins which act non-cell autonomous to repress trichome initiation of cells neighbouring trichomes.

Existing natural variation for trichome density in *A. thaliana* provides the opportunity to complement well-established information about the genetic pathway of trichome initiation with knowledge about the modulation of trichome density in natural accessions. In this spirit, a quantitative trait locus (QTL) analysis of an F2 mapping population derived from a low and a high trichome density accession was carried out and detected four and seven QTL affecting aspects of trichome patterning and leaf morphology, respectively. Among the former a major QTL for trichome density was fine mapped to an 8.4 cM interval on chromosome two. Further population genetic and functional tests lead to the isolation of a quantitative trait nucleotide (QTN) located in *ENHANCER OF TRIPTYCHON AND CAPRICE2* (*ETC2*), a member of the single-repeat R3 MYB gene family of trichome repressors. The QTN causes an exchange of a conserved lysine to glutamate in low trichome density accessions and therefore presents the first indication that ubiquitination may play a role in modulating trichome density. Furthermore, to better understand the mechanism of differential initiation of leaf trichomes on a mechanistic level, cellular analysis of fully grown leaves showed that a main difference between the low and the high trichome density accession is expressed by the number of cells formed between trichomes and that this phenocopies mutants in *caprice* (*cpc*), a single-repeat R3 MYB gene.

Given that a WD40/bHLH/R2R3MYB transcription activator complex is also being involved in transcriptional regulation of the anthocyanin biosynthesis pathway, the second part of this work describes a pilot study investigating possible relationships between trichome density, anthocyanin content and UV-B tolerance in *A. thaliana* accessions.

TABLE OF CONTENT

1 INTRODUCTION

By definition, in plants the term trichome refers to all outgrowths originating solely from the epidermis. It is more commonly used though for structures present on aerial surfaces, like stems, leaves, petioles, pedicels, sepals, etc. There is an extraordinary diversity of trichomes regarding their morphology, anatomy and physiology, illustrated by the major classification criteria of single celled versus multicellular and secreting versus non-secreting trichomes (Werker, 2000). Familiar examples include the stinging trichomes of the stinging nettle (*Urtica dioica*), trichomes covering leaves of Edelweiss (*Leontopodium alpinum*) resulting in their woolly appearance, trichomes serving as hooks on cleaver (*Galium aparine*), cotton fibers which are trichomes formed on the ovule epidermis of certain *Gossypium* species, menthol producing glandular trichomes of peppermint (*Mentha x piperita*), but also root hairs that are important for water and nutrient uptake. The properties of trichomes in general point to functions in mediating diverse ecological interactions (see chapter 1.4). *Arabidopsis thaliana* trichomes are single, non-secreting cells and can be found on all of the above mentioned aerial surfaces. On *A. thaliana* rosette leaves trichomes are large, distinctive cells and typically have three spikes situated on a stalk, but also two-spiked trichomes are occasionally formed, whereas for example on stems or on sepals they possess usually only one or two branches (Gan et al, 2006; Hülskamp et al, 1994).

Trichomes are idioblasts, i.e. they are specialised cells that differ from an otherwise rather homogenous surrounding tissue. Since *A. thaliana* trichomes formed on the adaxial epidermis of rosette leaves are easily accessible and relatively simple structures, they became a model to study cell fate specification and morphogenesis. Studies characterising genes isolated by classical forward genetic screens for mutants affecting trichome initiation, patterning and morphogenesis have been starting to characterise regulatory mechanisms governing decisions of how cells are chosen to be reprogrammed to undergo a specified cell fate out of a field of initially equivalent cells. The use of *A. thaliana* leaf trichomes as a model for cell specification provides yet another informative source: they show variation in density across natural *A. thaliana* populations (see chapter 1.2.1.5). Therefore, natural variation can be used as a complementary source to investigate the regulation of trichome cell specification and may inherently provide information about ecologically

important trait variation genotypic level. Finally, trichomes are of medical and commercial value since they constitute or are engineered to become the site of production of secondary compounds of interest (f.e. pharmaceuticals, fragrances, food additives, pesticides; (Duke et al, 2000)), further, recent transcriptome (Arpat et al, 2004; Jakoby et al, 2008a) and functional experiments (Guan et al, 2008; Humphries et al, 2005) suggest that initiation of cotton fibers is closely related to that of *A. thaliana* leaf trichomes. Taken together, trichomes combine properties which turn them into an excellent and valuable model for study under diverse aspects.

1.1 Natural variation and the model plant *Arabidopsis thaliana*

Intraspecific natural genetic variation is a complementary source to artificially induced genetic variation for dissecting gene function. Its use in functional biology expands the number of genes and traits to be analyzed, further, the mutations analyzed have the potential to contain information beyond gene function since they harbour information about evolutionary processes acting on them and thus may provide a link to ecologically important trait variation (Alonso-Blanco & Koornneef, 2000).

In *A. thaliana*, classical forward and reverse genetic screens have been carried out in few genetic backgrounds (accessions) and largely focused on strong (qualitative) phenotypic effects. Further, one of the primary sources of analyzed mutants are large collections of T-DNA insertion lines (for example SALK lines (Alonso et al, 2003), GABI-Kat lines (Rosso et al, 2003), etc.) which primarily harbour knock-out alleles. These general characteristics lead to constraints, for example, genes that are functionally weak or null alleles in a genetic background might not be detected by T-DNA mutagenesis since it causes mainly loss-of-function (lof) alleles. Also, mutant genes engaged in epistatic interactions will show phenotypes only in certain genetic backgrounds. Alternatively, working with naturally occurring variation involves screening of many accessions and often description of quantitative traits with more elaborate phenotypic effects. The underlying mutations are not as strongly biased in respect of their type and effect as in using T-DNA insertion mutagenesis, for example large and small indels, as well as single nucleotide polymorphisms (SNPs) of major effect (altering for example gene structure) might be expected. This offers the advantage of analyzing an increasing number of mutations that modulate gene function, i.e. of functional alleles as opposed to lof alleles, which

therefore might inherently provide insights into structure-function relationship of genes and the molecular mechanisms they are involved in (Alonso-Blanco & Koornneef, 2000).

1.1.1 Analysis of natural variation

Natural phenotypic variation is often based on complex traits. Complex traits are typically affected by multiple genes and are often additionally modulated by environmental factors, so that they show quantitative (continuous) variation. The quantitative nature and the vast amount of genetic differences between natural populations makes it more complex to identify underlying causative quantitative trait loci (QTL) and quantitative trait nuclei (QTN) compared to mapping of classical qualitative phenotypes. As a single QTL explains only a fraction of the observed phenotypic variation, and environmental variability often increases the trait variation of individuals with the same genotype, this increases the sample size required for QTL detection in QTL mapping experiments which are based on experimental crosses. An alternative way to map traits of interest in natural populations is association mapping (linkage disequilibrium mapping) which uses segregating variation in natural populations to detect association of phenotypic and genotypic variation (Hill & Mackay, 2004; Lynch & Walsh, 1998). In comparison to experimental crosses association mapping relies on many more informative meioses that occurred during the history of the sample and therefore is also used for fine mapping subsequently to QTL mapping in organisms where linkage disequilibrium decays rapidly with distance (Gaut & Long, 2003). Challenges in association mapping pose spurious associations due to population structure, for example by disproportional sampling of phenotypically different individuals from subpopulations with different allele frequencies at random loci, therefore tests to correct for population structure in association studies are needed (Balding, 2006). Based on the above described benefits and drawbacks of both mapping methods, they are proposed as complementing strategies for identification of candidate intervals/genes. Candidate intervals/genes detected by QTL or association mapping then often contain many polymorphisms which are equally likely to cause phenotypic variation. In general, methods for identification of the molecular cause of natural phenotypic variation are not different to classical genetic studies, however, above described challenges impede unambiguous detection. Therefore, criteria for establishment of gene and/or QTN discovery after QTL and/or association mapping

have been proposed as guidelines (Abiola et al, 2003; Glazier et al, 2002; Weigel & Nordborg, 2005), ranging from circumstantial evidence (gene expression pattern, gene function of candidate genes) to functional tests (f.e. transgenic complementation tests, quantitative complementation tests).

1.1.2 Adaptive natural variation

Natural genetic variation is partly the result of ecologically important trait variation. Adaptive traits that enhance the ability to survive and reproduce by mediating interactions with the biotic and abiotic environment have been suggested to be especially important for sessile terrestrial plants and have been observed on a temporally and geographically small scale (Linhart & Grant, 1996). Comparison of standing patterns of polymorphism to patterns according to neutral evolution is used to identify candidate genes under selection (Storz, 2005; Wright & Gaut, 2005). However, in *A. thaliana* assumptions underlying these tests are violated (Nordborg et al, 2005; Platt et al, 2010; Schmid et al, 2005), i.e. these patterns are confounded by demographic processes. Therefore, population genomics efforts are increasing to describe genome-wide genetic variation (Luikart et al, 2003), since it can be used to more efficiently define outlier genes in neutrality tests, further, it might give insight into the demographic history of *A. thaliana* which can be used to formulate modified neutrality tests. An ultimate goal in this context is to link naturally occurring polymorphism at particular loci with an adaptive advantage by functional tests, i.e. fitness tests of reciprocal transplantation in a common garden (Shimizu & Purugganan, 2005).

There is a current debate whether genetic changes causing adaptive phenotypic changes follow certain patterns (Stern & Orgogozo, 2008). Evolutionary developmental (evo-devo) biologists claim that adaptive morphological variation at species divergence level is predominantly caused by *cis*-regulatory (f. e. promoter elements) changes of transcriptional regulators. They highlight experimental findings that many major morphological changes studied between species are correlated with or caused by changes in expression of regulatory genes, and emphasize that transcriptional regulators themselves are functionally equivalent over large evolutionary distances. One of the central theoretical arguments for their "genetic theory of morphological evolution" is the pleiotropic nature of many transcriptional regulators, in which coding sequence changes might affect several genetic

pathways and might therefore easily be detrimental, whereas *cis*-regulatory regions are modular structures and mutations are likely to affect gene function only in the specific organ or tissue in which the affected module of the *cis*-regulatory element is important in (Carroll, 2008). This is opposed by the view that the theory is premature and it is claimed that (i) there are no compelling theoretical or empirical reasons to formulate a hypothesis specifically for adaptive morphological traits (omitting for example physiological traits), (ii) there are also experimental data linking adaptive variation with changes in coding sequence, and (iii) lines of arguments for the *cis*-regulatory hypothesis can be criticized, for example in the case of pleiotropy by forms of protein evolution circumventing its negative effect (gene duplication, etc.) or by strong selection in small populations, etc. Instead, it is argued for a broader analysis of adaptive variation for all "classes" of traits (morphological, physiological), gene categories (transcriptional regulators, structural genes) and inter- and intraspecific variation to test if and how mutations affecting different gene functions (*cis*-regulatory regions vs. coding sequence) are distributed within these categories. Detected patterns might be used to draw general conclusions on, for example, whether population genetic parameters affect the distribution of *cis*-regulatory and coding sequence variation within these categories, or, whether there is evidence that particular gene categories and/or mutations are favoured to modulate phenotypic change (Hoekstra & Coyne, 2007).

1.1.3 *Arabidopsis thaliana* as a model organism for analysis of natural variation

Currently, advances in marker technologies facilitating genotyping (Appleby et al, 2009), the application of next generation sequencing (Mardis, 2008) and the development of refined methodology in statistical analyses in QTL and association mapping (reviewed in (Balding, 2006; Zou, 2009)) are rapidly promoting analyses of natural variation.

Besides properties that established *A. thaliana* as a genetic model plant (small genome size (~120 Mb), short generation time, inbreeding, large number of offspring, etc.) and lead to a wealth of molecular tools (efficient transformation protocols, public platforms of the sequenced genome of the reference accession Col-0 (AGI, 2000), collections of annotated mutant lines, databases with gene expression data, etc.), *A. thaliana* is now increasingly used to study natural

variation. *A. thaliana* has a widespread distribution and there is a large and expanding collection of *Arabidopsis* accessions available, i.e. of natural populations sampled at different, annotated natural sites. *A. thaliana* is native to Europe and central Asia and it has been naturalized widely in the world (including northern and southern America, Africa, and eastern Asia) and it grows in diverse habitats of naturally open and disturbed sites, over a broad range of altitudes and climatic conditions. Consequently, phenotypic variation for most traits analyzed has been found (life history traits, tolerance to biotic and abiotic factors, organ morphology) (reviewed in (Koornneef et al, 2004; Shindo et al, 2007)). Initially studies using dideoxy resequencing of short fragments dispersed throughout the genome using 12 accessions described genetic variation to vary across the genome, with an average pairwise nucleotide diversity (π) estimate of 0.007 for total sites (Schmid et al, 2005), i.e. an average pair of 1 kb sequence differs at 7 nucleotides, which is consistent to other studies (Borevitz et al, 2007; Nordborg et al, 2005), and therefore nucleotide diversity is similar to *Drosophila melanogaster*, around ten times higher than estimates in humans and lower than in the outcrossing plant *Arabidopsis lyrata*, (Mitchell-Olds & Schmitt, 2006). Recent genome wide array re-sequencing (using 20 accessions; (Clark et al, 2007)) found more than 100,000 amino acid changes, 2,500 polymorphisms altering transcript or protein structure and, in agreement with single feature polymorphism (SFP) detection by hybridizing to the Affymetrix ATH1 gene expression array (using 54 accessions; (Borevitz et al, 2007)), regions that are highly dissimilar in comparison to the Col-0 reference sequence. The former study reports in their dataset ~4% of the genome being highly polymorphic or deleted, the latter found on average 135 deletions per accession with an average length of ~970 b and 34 duplicated regions per accession with an average length of 1.1 kb. These studies indicate that accessions also differ considerably on the genetic level. The above mentioned data on natural genetic polymorphisms in *A. thaliana* accessions and polymorphism data of further studies are available in public databases for the scientific community. An ongoing project called "1001 Genomes" (http://www.1001genomes.org/) has the goal to completely sequence many *A. thaliana* accessions. Further, whole genome sequences of the two closely related species *Arabidopsis lyrata* and *Capsella rubella* are currently being generated (DOE Joint Genome Institute) and will be integrated together with *A. thaliana* sequences in a publicly available platform (ARelatives project by D. Weigel and NSF 2010 project by M. Nordborg). This will allow comparative analyses of natural variation and

6

adaptation across these species.

A. thaliana is a highly inbreeding plant, reported selfing rates are greater than 95 % (reviewed in (Shindo et al, 2007)) and thus accessions are highly homozygous (Platt et al, 2010) facilitating sequencing and haplophase determination, further any accession needs to be genotyped only once and genotypic data can be used in multiple studies. The amount of outcrossing, however, is sufficient for gene flow to happen, which leads to genetic variation also within local populations (Platt et al, 2010; Shindo et al, 2007). Further, although local populations show extensive linkage disequilibrium (LD), on a global scale it decays on average within 10 kb which is faster than expected and attributed partly to a large effective population size (Kim et al, 2007). This suggests that association mapping at high resolution is possible when using diverse accessions, however, studies detected population structure on a global scale ((Atwell et al, 2010; Borevitz et al, 2007; Platt et al, 2010; Schmid et al, 2006) and references therein) which might lead to spurious associations and have to be accounted for; to account for population structure several statistical methods for plant genomes have been developed and are being tested (Atwell et al, 2010; Kang et al, 2008; Yu et al, 2006; Zhao et al, 2007b). A recent genome-wide association study (Atwell et al, 2010) of 107 phenotypes in a core set of 95 accessions using 250,000 tag SNPs (250k SNP-chip; (Kim et al, 2007)) is spearheading identification of natural genetic variation for a multitude of traits, these data are publicly available. Further, an online platform is in the works where researchers can statistically analyze *A. thaliana* GWAS of phenotypes of interest and where data after publication are collected in a common format (http://walnut.usc.edu/2010/GWA). GWAS will be further assisted by an effort to genotype a panel of 1300 *A. thaliana* accessions with the 250k tag SNPs (http://walnut.usc.edu/2010/2010-project).

For QTL mapping, there is an increasing number of established mapping populations, for example recombinant inbred lines (RILs) derived of various parental accessions (the very first one being derived from the accessions Ws and W100 (Reiter et al, 1992)), a collection of multiparent advanced generation inter-cross (MAGIC) lines (Kover et al, 2009), chromosome substitution strains (CSS) and derived stepped aligned inbred recombinant strains (STAIRS) for the accessions Ler-0 and Col-0 as well as Nd and Col-0 (Koumproglou et al, 2002). QTL mapping in an F2 mapping population is facilitated by general attributes of *A. thaliana* as a model plant, and marker establishment and use has been supported by collection of

different types of markers in public databases (for example at TAIR).

Taken together, *A. thaliana* thaliana is increasingly used in and tools are being established to support in analysis of the study of natural variation. Moreover, it has already been shown that it is feasible in *A. thaliana* to map and functionally verify the effect of natural variation on phenotypic expression (examples listed in (Shindo et al, 2007)).

1.2 Epidermal patterning in *Arabidopsis thaliana*

1.2.1 Trichome patterning

Trichome cell specification starts early in leaf development. Visual inspection of the first true leaves, which are smaller in size than successive leaves, of the accessions Col and L*er* showed that trichomes become visible as soon as the primordium reaches a size of ~100 µm in length and most of the trichomes are initiated upon reaching a primordium size of ~600 µm, after which epidermal cell proliferation is still ongoing (Larkin et al, 1996). Observations on young leaves of the accession Col showed an average distance of four epidermal cells between incipient trichomes, and the distance is enlarged by a factor of ten by further cell divisions through leaf development (Hülskamp et al, 1994). Trichome initiation is regulated in a basipetal manner, it starts at the tip of the leaf and proceeds towards the base (Hülskamp et al, 1994) This may be interpreted as a basipetal movement of a temporal zone of competence, visualized also on leaves covered with trichomes only at the tip or the base in an experiment complementing a glabrous mutant (*transparenta testa glabra1* (*ttg1*)) with a dexamethasone (DEX) inducible maize RED (R) gene fused to the glucocorticoid receptor (Lloyd et al, 1994). However, the basipetal development is not exclusive, since young trichome primordia can be formed between older ones (Hülskamp et al, 1994). Epidermal cells that have entered the trichome pathway increase in cell and nuclear volume. The nuclear enlargement in developing trichomes is correlated with the start of endoreduplication, since nuclei of mature trichomes reach an average DNA level of 20-32C (Hülskamp et al, 1994; Melaragno et al, 1993). The trichome then begins to expand out of the epidermis and branching follows, succeeded by elaboration of a thickened secondary cell wall. Trichomes are surrounded by 10-12 accessory cells that appear morphologically specialized (Hülskamp et al, 1994). Trichome mutants for trichome initiation, morphogenesis and patterning were originally detected in genetic screens (Hülskamp et al, 1994;

Koornneef, 1981; Koornneef et al, 1982).

The spatial distribution of leaf trichomes is non-random, since they develop next to each other less frequently than would be expected by chance, suggesting that an active mechanism exists to govern trichome spacing (Hülskamp et al, 1994; Larkin et al, 1994). Clonal sector analyses of trichomes and their accessory cells showed that the spacing pattern is not governed by a cell lineage derived process (Larkin et al, 1996; Schellmann et al, 2002). Instead, trichome initiation and patterning is thought to be regulated by communication of neighbouring cells, identification of a transcription factor complex promoting trichome initiation and members of a small gene family of negative trichome regulators lead to a general model of trichome initiation and patterning based on a regulatory process called local self-activation – lateral inhibition and is categorized as a *de novo* patterning mechanism, that is, a patterning mechanism in the absence of any pre-existing spatial information (LALI; reviewed in (Ishida et al, 2008; Pesch & Hülskamp, 2009)). It was originally formulated by Meinhardt and Gierer in 1974 to explain biological pattern formation who were inspired by a concept of Alan Turing that described pattern formation by substances with different diffusion rates (reviewed in (Meinhardt & Gierer, 2000)).

1.2.1.1 Key regulators form an activator complex that is counteracted by members of the family of single-repeat R3 MYB proteins

Originally, forward genetic screens led to the identification of several key regulators affecting trichome number and patterning at the adaxial surface of *A. thaliana* rosette leaves. Based on their phenotypes detected genes have been classified as positive and negative regulators of trichome initiation (reviewed in (Ishida et al, 2008)).

Positive regulators detected by genetic screens (Hülskamp et al, 1994; Koornneef, 1981; Koornneef et al, 1982; Zhang et al, 2003) include the genes *GLABRA1* (*GL1*), *GLABRA3* (*GL3*) and its paralog *ENHANCER OF GLABRA3* (*EGL3*), *TRANSPARENTA TESTA GLABRA1* (*TTG1*) and *GLABRA2* (*GL2*). Strong mutant alleles of *GL1* and *TTG1* abolish trichome initiation on rosette leaves (Hülskamp et al, 1994; Koornneef, 1981; Koornneef et al, 1982). *GL1* encodes an R2R3 MYB transcription factor (Oppenheimer et al, 1991) and *TTG1* a protein with a WD40 domain, a domain which in general is thought to be involved in protein-protein interactions (Walker et al, 1999). *gl3-1* causes a reduced trichome number and
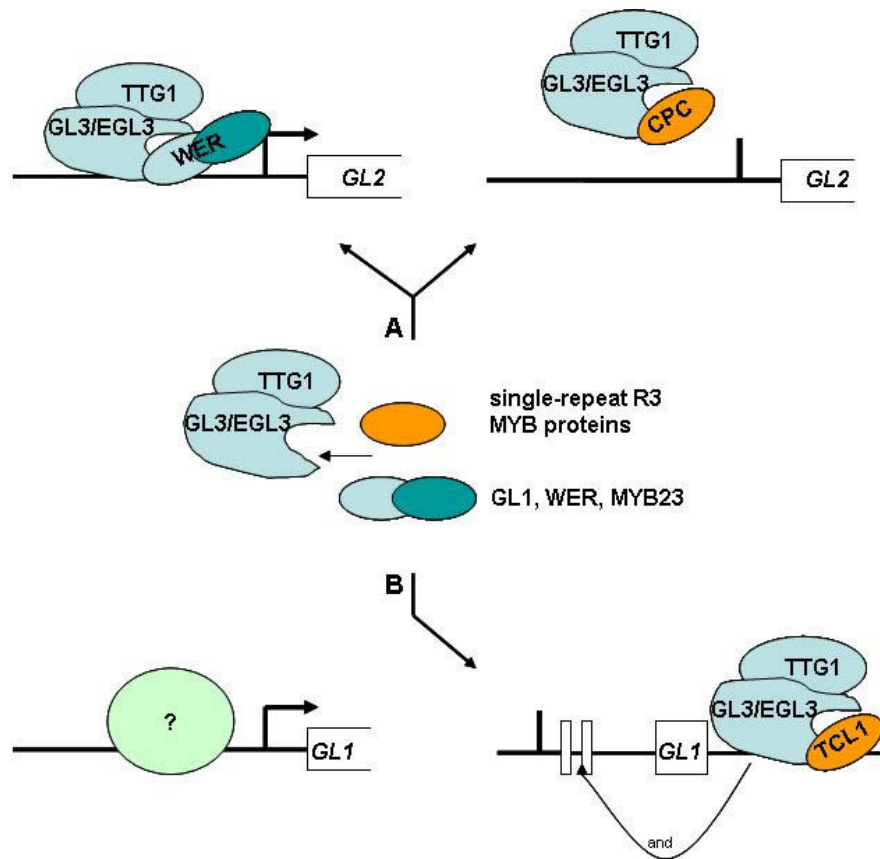
Figure 1.1. Formation of the WD40/bHLH/R2R3MYB activator complex enhancing gene expression in trichome and root hair patterning and its repression by single-repeat R3 MYB proteins. (A) Repression of GL2 expression by CPC in the root does not involve binding of CPC to GL2 regulatory sequences (Tominaga et al, 2007). (B) Repression of *GL1* expression by TCL1 in leaves showed proximity of TCL1 to *GL1* regulatory regions (introns 1 and 3´UTR) in a ChIP assay (Wang et al, 2007). The question mark indicates unknown transcription factors enhancing GL1 expression.

reduced trichome branching (Hülskamp et al, 1994; Payne et al, 2000). An enhancer screen in the *gl3-1* mutant background that produced glabrous lines identified *EGL3* (Zhang et al, 2003), *GL3* and *EGL3* are paralogs and encode basic helix-loop-helix (bHLH)-type transcription factors (Payne et al, 2000; Zhang et al, 2003). *gl2-1* mutants form a reduced trichome number (Hülskamp et al, 1994), however, closer inspection showed that they also form small aborted trichomes aberrantly expanding in the epidermal plane (Rerie et al, 1994). *GL2* encodes a homeodomain-leucine zipper (HD-Zip) transcription factor (Rerie et al, 1994)

The phenotypes of mutants in *TRIPTYCHON* (*TRY*) and *CAPRICE* (*CPC*) suggested that they are negative regulators of trichome initiation; *try* alleles lead to

trichomes forming directly next to each other (termed trichome nests) whereas *cpc-1* increases trichome density but otherwise does not affect leaf trichome distribution (Hülskamp et al, 1994; Wada et al, 1997). Subsequent studies identified a family of six single-repeat R3 MYB genes (comprising *TRY*, *CPC, ENHANCER OF TRIPTYCHON AND CAPRICE1* (*ETC1*), *ENHANCER OF TRIPTYCHON AND CAPRICE2* (*ETC2*), *ENHANCER OF TRIPTYCHON AND CAPRICE3/CAPRICE-LIKE3* (*ETC3*/(*CPL3*) and *TRICHOMELESS1* (*TCL1*)), all of which have been shown to act as negative trichome regulators (described in more detail in 1.3.3.1); (Esch et al, 2004; Kirik et al, 2004a; Kirik et al, 2004b; Schellmann et al, 2002; Tominaga et al, 2008; Wada et al, 1997; Wang et al, 2007).

The proteins TTG1, GL3, EGL3 and GL1 have been shown to interact in a number of protein-protein interaction studies *in vitro* and *in vivo* to form a WD40/bHLH/R2R3 MYB activator complex (Figure 1.1) (reviewed in (Ishida et al, 2008; Pesch & Hülskamp, 2009)). Specifically, yeast two-hybrid interaction assays showed that GL3 and EGL3 homo- and heterodimerise and that GL1 and TTG1 interact with both, GL3 and EGL3 (reviewed in (Pesch & Hülskamp, 2009)). GL1 and TTG1 themselves do not interact directly, but were found to be in a complex containing GL3 in an *in vivo* pull down experiment (Zhao et al, 2008). Therefore the activator complex is generally drafted as containing a homo- or heterodimer of GL3/EGL3 bound to TTG1 and GL1, although the exact stochiometry especially of GL3 and EGL3 has not been determined. A complex consisting of the above proteins is also termed WD40/bHLH/R2R3MYB complex and is a general module which in various compositions of members of the indicated protein families is involved in regulation of different developmental pathways in plants (see chapter 1.2.4; Figure 1.4). In turn, members of the single-repeat R3 MYB family have also been shown to bind to GL3 and EGL3 using various protein-protein interaction assays (reviewed in (Pesch & Hülskamp, 2009)) and to compete with *GL1* for *GL3*/*EGL3* binding in yeast three-hybrid assays (Esch et al, 2003; Esch et al, 2004; Tominaga et al, 2007; Wester et al, 2009), and accordingly, a complex exchanging GL1 with a member of the single-repeat R3 MYB family is termed repressor complex (Figure 1.1). The formation of alternate complexes and consequently, activation or repression of target genes is thought to determine epidermal cell fate (Ishida et al, 2008; Schellmann et al, 2007). One of the key downstream targets of the activator complex is *GL2*, whose expression in trichomes is thought to be one of the first detected stable outcomes and which has been shown to regulate cell morphogenesis in epidermal patterning

in the root (reviewed in (Schellmann et al, 2007)).

The molecular cause of the ability of the single-repeat R3 MYB family members to act as repressors might generally be accounted for by their lack of an acidic transactivation domain which is present in the GL1/WER/MYB23 R2R3 MYB subfamily (Kranz et al, 1998; Lee & Schiefelbein, 2001), and, additionally, single-repeat R3 MYB family members might be unable to bind to promoter sequences of target genes (Figure 1.1A). The inability of CPC to bind putative MYB-binding-sites in its own promoter which are recognized by WEREWOLF (WER; a functional paralog of GL1 involved in root hair patterning, see chapter 1.2.2) has been shown by gel mobility shift assays and yeast one-hybrid assays (Koshino-Kimura et al, 2005). Furthermore, swapping of only two conserved amino acid residues in the WER R3 MYB domain to the corresponding residues of CPC abolished binding of the chimeric WER protein to *GL2* promoter sequences. *In planta*, the same chimeric WER construct failed to complement the *wer* phenotype by its inability to ensure wild type gene expression of *GL2*, visualized by a GL2::GUS reporter construct (Figure 1.5B) (Tominaga et al, 2007). The swapped residues are conserved in WER and GL1, but are distinct to all of the single-repeat R3 MYB family members. However, to date no general conclusions can be made about DNA binding abilities of single-repeat R3 MYB proteins. Also, selective recruitment of single-repeat R3MYB repressors to different promoters - directly by DNA binding or indirectly by interaction with GL3/EGL3 or other proteins - might be a determinant of functional differences within the single-repeat R3 MYB family members. In line with this, *TCL1* has been shown to negatively affect *GL1* expression and ChIP experiments visualized recruitment of TCL1 to *GL1* regulatory sequences in intron 1 and in the 3´UTR (Figure 1.2B) (Wang et al, 2007).

1.2.1.2 Current models of trichome initiation involve the central concept of non-cell autonomy

Excluding the involvement of cell-lineage based regulation of trichome initiation and the finding that single-repeat R3 MYB proteins act non cell-autonomous have been important steps towards current models of trichome initiation and patterning. To date, trichome patterning is thought to be a *de novo* patterning mechanism, that is, it is carried out without pre-existing spatial information (Ishida et al, 2008; Schellmann et al, 2007).Characterisation of the gene expression pattern of the trichome

activators and repressors provided the first indication to adopt a general model as guidance for the understanding of trichome initiation and patterning. Expression of the trichome activators *GL1*, *GL3*, *EGL3* and *TTG1* using promoter-GUS reporter constructs showed that all are initially expressed ubiquitously in the area of the developing leaf competent for trichome initiation and that later expression becomes more prominent in incipient trichomes; apart from that they differ in other dynamics of gene expression, for example *GL1* expression ceases in mature trichomes, whereas *GL3* expression is maintained (Bouyer et al, 2008; Kirik et al, 2005; Larkin et al, 1993; Zhao et al, 2008). Surprisingly, the same general expression pattern was detected for the trichome repressors *TRY*, *CPC* and *ETC2* (Kirik et al, 2004b; Schellmann et al, 2002), furthermore, *GUS* expression driven by the *ETC1* and *TCL1* promoters was also detected in trichomes (Esch et al, 2004; Kirik et al, 2004a; Wang et al, 2007).

The finding that the repressors of trichome initiation are themselves expressed in trichomes was explained by a mechanism based on lateral inhibition that together with local self-activation has been shown in simulations to lead to pattern formation ((Gierer & Meinhardt, 1972), reviewed in (Pesch & Hülskamp, 2004)). The LALI mechanism is based on the actions of an activator and an inhibitor (Figure 1.2A). The activator possesses the ability to activate itself in a fashion containing non-linear elements, to activate the inhibitor and its action is local. The inhibitor in turn inhibits the activator and is able to diffuse. A homogenous distribution of the activator and inhibitor is unstable, since small stochastic fluctuations lead to local amplification of the activator and inhibitor. High concentration of the activator stays local, while, since the inhibitor is diffusible, high concentration of the inhibitor is further distributed and downregulates the activator in the surrounding field. In case the activator can diffuse, the diffusion rate of the inhibitor must be larger.
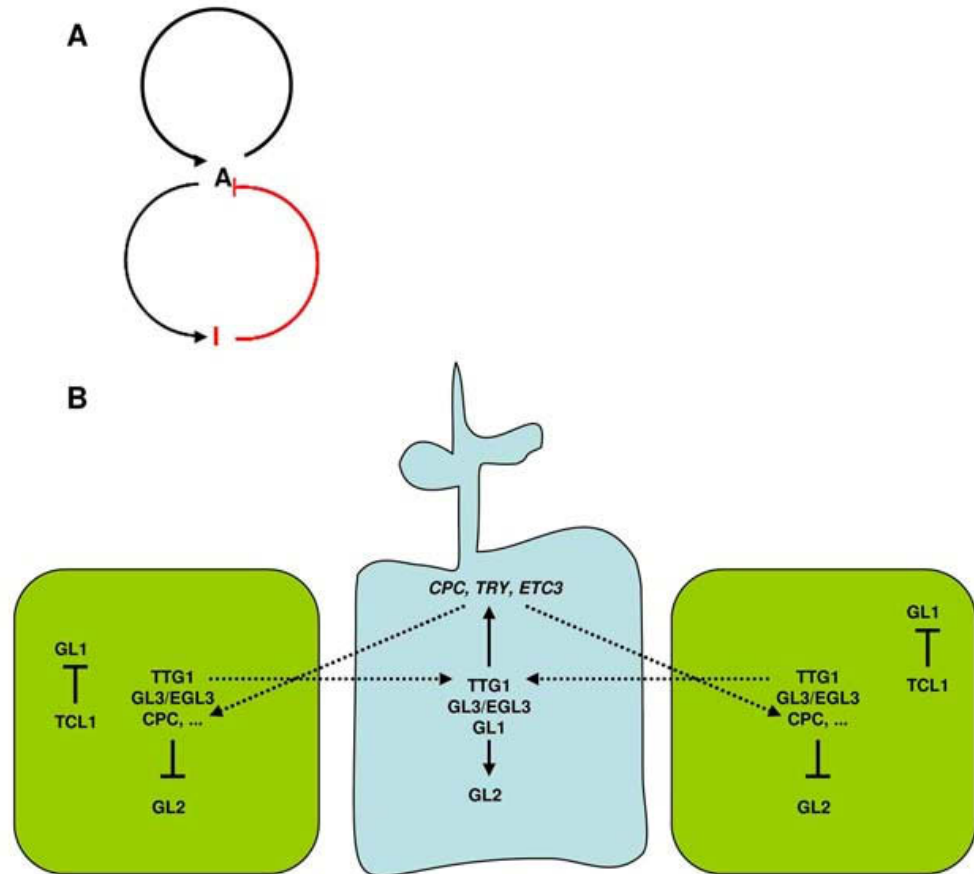
Figure 1.2. Model of trichome patterning. (A) Model of local self-activation - lateral inhibition (LALI), taken from (Pesch & Hülskamp, 2004). A: activator, I: inhibitor. (B) Schematic representation of transcriptional regulation events and cell-cell movement of proteins during leaf trichome initiation discussed in the text. Modified from (Ishida et al, 2008). Arrows and stunted lines indicate positive and negative regulatory interactions, respectively, broken arrows indicate intercellular movement of proteins. Green cell: basal epidermal cell, blue cell: trichome.

Derived from the predictions of the local self-activation and lateral inhibition model, it was postulated that the activator is given by the TTG1-GL3/EGL3-GL1, complex, which must act cell autonomous. Random fluctuations in concentration of member(s) of the activation complex lead to local self-enhancement of trichome initiation activity. At the same time, expression of the single-repeat R3 MYB genes is promoted which repress trichome cell fate in neighbouring cells by competing for GL3/EGL3 binding and thereby render the complex inactive. Further, a first stable outcome of trichome patterning is thought to be the establishment of the *GL2* expression in cells destined to become trichomes (Figure 1.2B) (reviewed in (Pesch

14

& Hülskamp, 2004)).

On the theoretical basis of the described mechanism, predictions were made regarding the expression regulation of genes and the action of proteins involved in trichome initiation (Pesch & Hülskamp, 2004). First, as trichome patterning takes place in a field of cells, the inhibitors are predicted to act non cell-autonomous. Initially, cell to cell movement has been shown for CPC in the root (for a description of root-hair patterning see chapter 1.2.2); plants transformed with a CPC::2xrsGFP construct showed GFP fluorescence only in root cell files where the endogenous *CPC* promoter is active, that is atrichoblast cell files, whereas GFP fluorescence was also found in trichoblast cell files upon transformation of plants with CPC::CPC-2xrsGFP constructs (Kurata et al, 2005). It was proposed (Kurata et al, 2005) that CPC movement takes place via plasmodesmata since CPC-tandemGFP fusions were only able to move until they reached a size of ~119 kDa, indicative of a size exclusion limit (SEL). Micro-projectile bombardment of *A. thaliana* cotyledons or rosette leaves with fluorescently labeled fusion proteins expressed under the 35S promoter found that CPC, TRY and ETC3 can, in contrast to the trichome activator proteins GL1, GL2 and GL3, move to neighbouring cells in leaves (Digiuni et al, 2008; Wester et al, 2009; Zhao et al, 2008).

Second, the model predicts several cross-regulatory interactions between the activators and the inhibitors. A summary of to date known regulatory interactions on the transcriptional level can be found in (Pesch & Hülskamp, 2009). To date the strongest established cross regulatory interaction is the activation of transcription of members of the single-repeat R3 MYB trichome repressors and of *GL2* by the trichome activator complex (Figure 1.2B). It has been shown in *A. thaliana* mesophyll protoplasts, which *per se* possess undetectable levels of *GL1*, *WER*, *GL3*, *EGL3* and *TTG1*, as well as of *ETC1* and *ETC3*, that transient expression of combinations of *GL1* or *WER* together with *GL3* or *EGL3* are sufficient to induce expression of *ETC1* and *ETC3* and increase expression of *TRY* and *CPC*, whereas expression levels of *TCL1* and *ETC2* remained unchanged and seemed to decrease, respectively (Wang et al, 2008). Similarly, it was demonstrated *in planta* that TTG1 and GL3 are able to directly induce expression of *CPC* and *ETC1* as well as *GL2,* using *ttg1* and *gl3/egl3* mutant plants transformed with 35S::TTG1-GR and 35S::GL3-GR, respectively, treated with dexamethasone (DEX) and cycloheximide (CHX) (Morohashi et al, 2007; Zhao et al, 2008). A direct role of TTG1, GL3 and GL1 proteins in activation of *CPC*, *ETC1* and *GL2* is further substantiated by

chromatin immunoprecipitation (ChIP) experiments which demonstrated that all three proteins are recruited to the respective promoters (Morohashi & Grotewold, 2009; Morohashi et al, 2007; Zhao et al, 2008). Further, it was shown that *GL1* and *GL3* are necessary to activate *TRY* expression visualized by the absence of TRY::GUS reporter activation in a *gl1* and *gl3* mutant background at the leaf zone where TRY is expressed ubiquitously before its expression is confined to trichomes (Digiuni et al, 2008).

Inhibition of transcription of the activator by the inhibitor – another cross-regulatory interaction predicted by the model – was shown for *GL1* transcription which is negatively regulated by TCL1 (Figure 1.2B) (Wang et al, 2007). Seedlings overexpressing HA-TCL1 which showed a glabrous phenotype, possessed, besides reduced *GL2* transcript levels, reduced *GL1* transcript levels in RT-PCR analyses, whereas *GL3* and *TTG1* transcript levels remained unaffected (Wang et al, 2007). Several lines of evidence suggest this being a direct effect on *GL1* transcription by TCL1, for example, TCL1 was recruited specifically to regulatory regions of *GL1* in ChIP experiments, and specifically upregulated *GL1* while not affecting *GL2*, *GL3* and *TTG1* transcript levels when overexpressed as a TCL1-VP16 fusion protein *in planta* (Wang et al, 2007). A second example is provided in the context of root hair patterning, in a *cpc* mutant background *WER* transcription was upregulated and WER::GFP reporter lines showed GFP fluorescence in all cell files, indicating that *CPC* is necessary to confine *WER* expression to non-hair cell files (Figure 1.3) (Lee & Schiefelbein, 2002).

Evidence for the third regulatory interaction necessary to yield pattern formation, a positive autoregulatory loop of the activator, is missing. More specifically, *GL2* and *TRANSPARENTA TESTA GLABRA2* (*TTG2*) are the only known targets of activator proteins that also have an established activator function in trichome initiation (Ishida et al, 2007; Morohashi & Grotewold, 2009; Morohashi et al, 2007; Wang & Chen, 2008; Zhao et al, 2008), and in the root *WER* positively regulates *MYB23* which in turn shows positive autoregulation (Figure 1.3) (Kang et al, 2009), however, based on their mutant phenotypes and expression patterns *GL2*, *TTG2* and *MYB23* are thought to play roles at later steps in trichome initiation and root hair formation as opposed to being involved in early decisions (in the context of trichome patterning – *de novo* decisions) (for example (Hülskamp et al, 1994; Johnson et al, 2002; Kang et al, 2009)).

The lack of experimental evidence for a positive autoregulatory feedback loop

necessary for explanation of patterning in the context of the LALI model has stimulated further research to explain trichome initiation dynamics. A mathematical modelling study showed that in the absence of a positive feedback loop bistability of trichome forming versus non-trichome forming cells can be achieved (Siegal-Gaskins et al, 2009). The model incorporated (i) CPC production and degradation, (ii) GL3-GL1 and GL3-CPC complex formation and (iii) GL3-GL1 complex binding to the *CPC* promoter resulting in CPC production. In this framework bistability was a possible outcome when either the GL3-GL1 complex binds as a tetramer (two interacting GL3-GL1 complexes) to the *CPC* promoter or as a GL3-GL1 monomer to distinct binding sites in a sequential cooperative manner. Though not investigated under that aspect, in general both modelled requirements for bistability may comply with experimental evidence. For example, GL3 has been shown to interact with itself and its paralog EGL3 (Payne et al, 2000; Zhang et al, 2003), and thus an active trichome initiation complex has been proposed to contain a dimer of these bHLH transcription factors, however, the stochiometry of the activation complex has not yet been analyzed in detail. Alternatively, the *CPC* promoter has been shown to harbour two MYB-binding-sites in a region required for epidermal cell-specific expression and this region has been shown to be targeted by WER using gel mobility shift assays and yeast one-hybrid assays (Koshino-Kimura et al, 2005).

Recently, a second distinct mechanism termed activator-depletion model has been proposed based on novel experimental evidence and mathematical modelling (Bouyer et al, 2008). Central to that were two experimental findings, the ability of TTG1 to move between leaf epidermal cells and GL3-dependent depletion of TTG1 protein from trichome neighbouring cells (Figure 1.2B). Depletion of TTG1 protein was shown by quantitative fluorescence measurement of TTG1–YFP expressed under its endogenous promoter in a *ttg1-13* mutant background. Relative YFP fluorescence was lowest in cells next to trichomes and increased again with distance, which is in contrast to the *TTG1* transcriptional expression pattern visualized by TTG1::GUS constructs where GUS expression peaks in incipient trichomes but is distributed evenly at a lower level in other cells, as well as in contrast to GFP abundance of TTG1::GFP-NLS transgenic plants, which recapitulate the GUS expression pattern and therefore also show no depletion in cells surrounding trichomes. Further, depletion was shown to be independent of protein degradation, since the fluorescent pattern remained unaltered in *TTG1::TTG1–YFP* transformed plants upon treatment with the proteasomal inhibitor

17

epoximicin. However, in a *gl3* mutant background depletion of fluorescence in trichome neighbouring cells was abolished and the fluorescence pattern visualizing TTG1 protein abundance resembled the transcriptional pattern. Mathematical modelling indicated that a patterning resembling wildtype trichome distribution can be achieved based on the described activator-depletion mechanism (Bouyer et al, 2008).

1.2.1.3 Developmental and hormonal regulation of trichome initiation

The density and distribution of *A. thaliana* trichomes gradually changes on vegetative and reproductive organs formed as plants pass through different phases during their life cycle (Chien & Sussex, 1996; Gan et al, 2006; Martinez-Zapater et al, 1995; Telfer et al, 1997). Post-embryonic developmental phases have been divided into early and late vegetative phase and reproductive phase, where early and late reproductive phase might be distinguished by their different ability to respond to signals for reproductive development (Poethig, 1990). Visible phenotypic markers for early and late reproductive phase are heteroblastic traits, a term referring to age dependant changes in foliage leaf morphology (Tsukaya et al, 2000); in *A. thaliana* examples are changes in leaf form or the onset of abaxial trichome formation (Willmann & Poethig, 2005). Heteroblastic behaviour of trichome density and patterning on *A. thaliana* rosette leaves involves an increase in adaxial and abaxial trichome density on subsequently formed leaves, further rosette leaves formed during early vegetative phase are characterized by the absence of abaxial trichomes (Chien & Sussex, 1996; Martinez-Zapater et al, 1995; Telfer et al, 1997). On cauline leaves adaxial and abaxial trichome number decreases and increases, respectively with increased leaf position in a unique spatially distributed manner (Chien & Sussex, 1996; Telfer et al, 1997). Further, trichome number decreases on subsequent internodes of the main inflorescence stem and of paraclades (Gan et al, 2006).

There is little information about the regulation of gradual changes during the life cycle of the plant in general and of heteroblastic behaviour of trichomes during vegetative and reproductive phase in particular. It should be noted though that several of vegetative phase change mutants were mapped to genes involving sRNA biogenesis (Willmann & Poethig, 2005). Light and temperature are important environmental signals in timing of reproductive phase change and the

phytohormone gibberellin (GA) plays an important role in flowering time control by upregulation of specific floral integrator genes (reviewed in (Davis, 2009)) and has been shown to regulate vegetative phase change in several species (Telfer et al, 1997). Therefore most of what is known about heteroblastic behaviour of trichome patterning has been studied in the context of mutants in flowering time and GA biosynthesis and signalling.

The onset of abaxial trichome formation is delayed in late-flowering mutants and, accordingly, of plants grown under short day (SD) conditions in comparison to continuous light (CL) conditions. However, the fact that the late flowering mutant *terminal flower1* (*tfl1*) does not show a delay in the onset of abaxial trichome production together with the lack of a quantitative correlation between the delay in abaxial trichome onset and the delay in flowering time, points to further independent regulatory factors timing the onset of abaxial trichome production (Chien & Sussex, 1996; Telfer et al, 1997). Exogenous application of GA leads to earlier onset of abaxial trichome production, accordingly, mutants in GA biosynthesis and signalling are delayed and mutant alleles of *GIBBERELLIC ACID1* (*GA1*), a mutant in GA biosynthesis, abolishes trichome formation on adaxial leaf surfaces (Chien & Sussex, 1996; Telfer et al, 1997). In the context of the inducing effect of GA on trichome formation several regulatory steps have been elucidated. GA is perceived by the nuclear receptor GA-INSENSITIVE DWARF1 (GID1) and together they bind to DELLA proteins which induces DELLA protein degradation mediated by the F-Box protein SLEEPY (SLY1) via the 26S proteasome (Hirsch & Oldroyd, 2009). DELLA plant growth repressors, a subfamily of the GRAS family of putative transcription factors, repress rapidly but indirectly, i.e. requiring *de novo* protein synthesis, the action of *GLABROUS INFLORESCENCE STEM* (*GIS*), *GIS2* and *ZINC FINGER PROTEIN8* (*ZFP8*), putative C2H2 transcription factors (Gan et al, 2007b). In turn, these C2H2 transcription factors are positive regulators of trichome initiation acting upstream of the trichome TTG1/GL3-EGL3/GL1 activator complex and directly or indirectly affect the expression of *GL1* and possibly *GL3*, but not *TTG1* (Gan et al, 2006; Gan et al, 2007a). DELLA proteins might also provide a link to light signalling, upon GA presence they are also prevented from binding to PHYTOCHROME INTERACTING FACTORs (PIFs) that promote growth (Hirsch & Oldroyd, 2009). Recently, an independent pathway to the above regulating trichome distribution on the inflorescence stem has been discovered (Yu et al, 2010). It affects trichome distribution via direct regulation of *TRY* and *TCL1* by SQUAMOSA PROMOTER

19

BINDING PROTEIN LIKE9 (SPL9) which in turn is negatively regulated by miRNA156 (Yu et al, 2010).

Further phytohormones that have been shown to have an effect on trichome production are cytokinin, jasmonate (JA) and salicylic acid (SA). Cytokinin positively influences trichome initiation in the inflorescence meristem and has been shown to act via *GIS2* (Gan et al, 2007a). The – opposing - effects of JA and SA on trichome initiation are described in chapter 1.4 in the context of trichome function.

1.2.1.4 Trichome morphogenesis

Analogous to trichome patterning, mutants for trichome morphogenesis have been isolated. Molecular mapping and characterisation of mutants include genes involved in regulation of endoreduplication and mitosis, and genes coding for cytoskeletal proteins and regulators of their polymerization and structure. Several of these genes are involved in morphogenesis of several cell types and are thus not specific to trichome morphogenesis (reviewed in (Guimil & Dunand, 2007; Ishida et al, 2007)).

The observation that trichome branching is accompanied by cycles of endoreduplication has been corroborated by mutants affecting both, the number of endoreduplication cycles and/or mitosis and trichome branching, as in, for example, *try*, *gl3* and *kaktus* (*kak*) mutants (reviewed in (Guimil & Dunand, 2007)). How these genes influence endoreduplication remains unknown. Contrary, the molecular function of *SIAMESE* (*SIM*), mutants of which possess multicellular trichomes with an increased branch number and a decreased nuclear DNA content, has been shown to suppress mitosis by binding to cyclinD/cyclin dependant kinase A1 (CYCD/CDKA1) complexes, together with transcriptional repression of a *bona fide* gap2 (G2)/mitosis (M) phase specific cyclin, CYCB (Churchman et al, 2006; Walker et al, 2000).

The cytoskeleton affects two processes, trichome branching and expansion (reviewed in (Guimil & Dunand, 2007; Ishida et al, 2008)). Trichome branching is affected by mutants in α-tubulin genes (*TUA4*, *TUA6*) and a correlation between the stability of microtubules and trichome branching could be detected. This is corroborated by drug treatments, application of taxol, which stabilizes microtubules, lead to branch formation in a *zwichel* (*zwi*) mutant background, which untreated shows trichomes with only two branches and a shortened stalk. *ZWI* codes for kinesin-like calmodulin-binding protein. Further, mutants in tubulin-folding cofactors

20

A and C, (*KIESEL* (*KIS*) and *PORCINO* (*POR*), respectively) possess trichomes with less branches. The integrity and regulation of actin filaments on the other hand is thought to be important for the expansion of trichomes (reviewed in (Guimil & Dunand, 2007; Ishida et al, 2008)). Mutants of a group of genes named *DISTORTED* (*DIS*), due to their distorted or stunted trichome growth, were mapped to genes coding for subunits of actin-related protein (ARP) 2/3 complex and the WAVE complex which regulates the former in its function in nucleating actin filaments.

Finally, in the root *GL2* has been shown to directly regulate the expression of the cell wall biosynthesis genes cellulose synthase 5 (*CESA5*) and of xyloglucan endotransglucosylase (*XTH1-33*) (Figure 1.3) (Tominaga-Wada et al, 2009)). It is thought that changing tensile forces due to altering cell wall components might be a mechanism to drive morphogenesis (Boudaoud, 2010).

1.2.1.5   Natural variation of trichome density

A. thaliana accessions show quantitative variation in trichome density (Hauser et al, 2001; Larkin et al, 1996; Symonds et al, 2005). Natural genetic variation for trichome density in *A. thaliana* has been analyzed by QTL mapping (Larkin et al, 1996; Mauricio, 2005; Pfalz et al, 2007; Symonds et al, 2005), association analysis of the candidate gene *GL1* (Hauser et al, 2001) and recently by genome wide association mapping (Atwell et al, 2010).

QTL mapping analyses of trichome density on *A. thaliana* rosette leaves have detected at least ten different QTLs using five recombinant inbred line (RIL) populations with partly overlapping parental accessions (Larkin et al, 1996; Mauricio, 2005; Pfalz et al, 2007; Symonds et al, 2005). Accurate comparison of QTL positions across studies is difficult due to different genetic maps, however, a study analysing four RIL populations in parallel aligned the linkage maps to the physical map for better comparisons (Symonds et al, 2005). There are two regions in the genome where a QTL was mapped to the same location in multiple RIL populations and in different studies, a QTL on the lower arm of chromosome 2, which was mapped in all but one QTL analysis as major QTL (however, in the latter a QTL for trichome number at leaf edges was mapped to the same location), and a QTL on the upper arm of chromosome 4. Epistasis was reported in two studies and in both may include the same QTL on the lower arm of chromosome 4, however, it interacts with

different QTLs in the two studies (Pfalz et al, 2007; Symonds et al, 2005). With the exception of the QTL on the lower arm of chromosome 2, estimates of the explained variation of mapped QTLs in the same RIL population differs across studies, most likely due to differences in growth conditions and methods of phenotyping.

In an alternative approach to detect functional genetic variation, polymorphisms at *GL1* were tested for an association with phenotypic variation for trichome density using 28 *A. thaliana* accessions (Hauser et al, 2001). The polymorphisms detected at *GL1* grouped the accessions with high statistical support into two main clades, however, neither these two clades nor other cladistic levels were correlated with trichome density. While *GL1* is an important gene for trichome initiation, it might not be the cause for modulating natural variation for trichome density, alternatively, low statistical power due to large within-accession variance or masking by large effects at other loci might have hampered the detection of an association (Hauser et al, 2001). QTL analyses showed that the genomic location of *GL1* coincides with a QTL location (Symonds et al, 2005). Further, naturally occurring glabrous *A. thaliana* accessions and *Arabidopsis* lyrata populations have been shown to be harbour GL1 alleles with larger deletions or with mutations leading to premature stop codons (Hauser et al, 2001; Kivimaki et al, 2007). Finally, genome wide association mapping using 95 accessions detected several known trichome initiation genes associated with trichome density, for example the locus on chromosome 2 harbouring single-repeat R3 MYB proteins, as well as *CPC*, *TTG1*, *GL1* and *ETC3* (Atwell et al, 2010).

1.2.2   Root hair patterning in *Arabidopsis thaliana*

Important to the mechanism of *A. thaliana* root-hair patterning is the anatomy of the outer cell layers of the primary root. Epidermal root cells are arranged in approximately 15-25 cell files produced by transverse anticlinal cell divisions and overlie – nearly invariantly - eight cortical cells (Dolan et al, 1993; Galway et al, 1994). Newly formed epidermal cells mature by passing through the meristematic, elongation and specialization zone where cell division, expansion and final
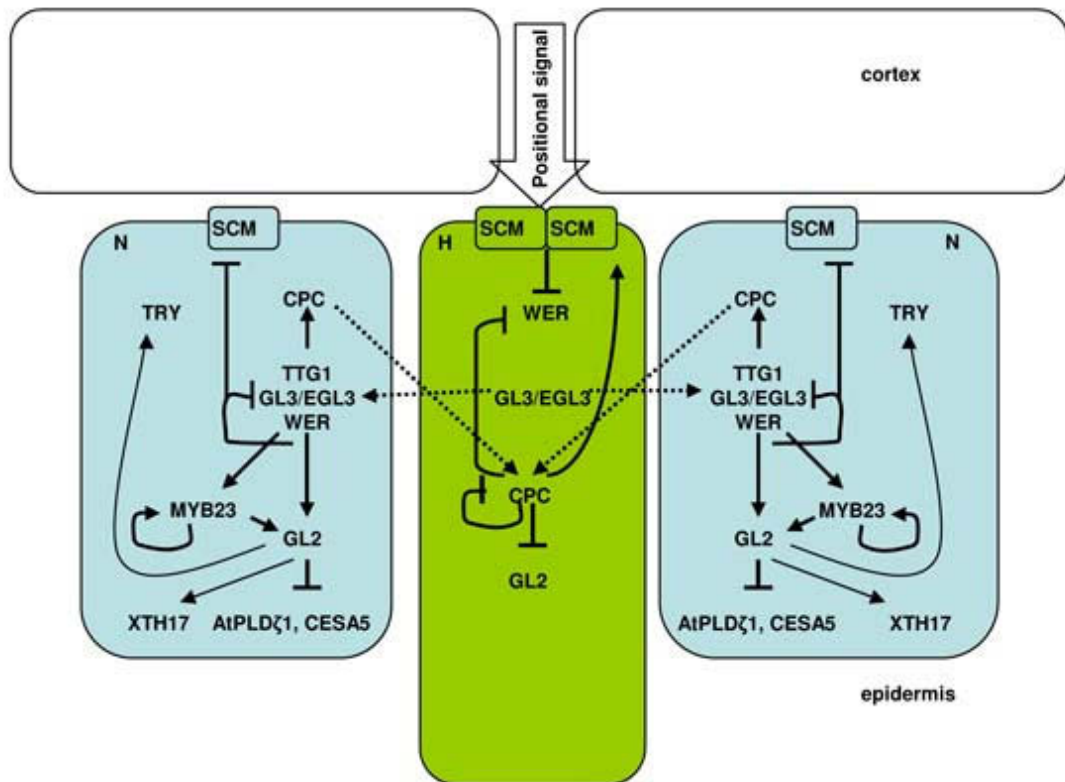
Figure 1.3. Schematic representation of transcriptional regulation events and cell-cell movement of proteins during root-hair patterning. Modified from (Schiefelbein et al, 2009). Arrows and stunted lines indicate positive and negative regulatory interactions, respectively, broken arrows indicate intercellular movement of proteins. Blue cells: non root-hairs, green cell: root-hair, white cells: cortex cells.

morphological differentiation take place, respectively (Schiefelbein & Benfey, 1991). Root epidermal cells are differentiated into only two distinct cell types, root-hair cells (trichoblasts) and hairless cells (atrichoblasts). Most epidermal cells contacting the radial cell wall of cortical cells (hair (H) position) form into root-hair cells while intervening cell files contacting only tangential cortical cell walls (N (non-hair) position) mostly form into hairless cells (Figure 1.3) (Dolan et al, 1993; Galway et al, 1994). The arrangement in cell files which are positioned differently regarding underlying cortex cells and which possess different cell fates points to the existence of a positional signal influencing root-hair patterning. In accordance, rare longitudinal anticlinal divisions of trichoblasts (giving rise to T clones) cause daughter cells to adopt atrichoblast cell fate in response to changed position in respect to underlying cortex cells (Berger et al, 1998).

Current evidence suggests that in the root a WD/bHLH/R2R3MYB activator complex consisting of TTG1, GL3/EGL3 and WEREWOLF (WER, a R2R3MYB transcription

factor; (Lee & Schiefelbein, 1999)) specifies non-hair cell fate by positively regulating *GL2* expression in N cell files, whereas lateral inhibition mediated by single-repeat R3 MYB family members in H cell files leads to competition with WER for binding to GL3/EGL3 and thus repression of *GL2* transcription (Figure 1.3). Further, WER is expressed preferentially in N position cells due to repression in H position cells by an unknown signal which is mediated by SCRAMBLED (SCM; (Kwak et al, 2005)), a leucine-rich repeat receptor-like kinase (LRR-RLK) (reviewed in (Schiefelbein et al, 2009)).

Figure 1.3 summarizes currently deduced regulatory events in root hair specification leading to and maintaining the above described differential expression pattern of *GL2* in the alternative cellular fates (reviewed in (Schiefelbein et al, 2009)). Positional signalling is thought to be mediated by a yet unknown non-uniformly distributed apoplastic signal stemming from tissue underlying the epidermal cell layer. The signal might preferentially activate SCM in H position cells, which is located in the plasma membrane of all root epidermal cells, leading to repression of *WER* expression in H position cells. Therefore *WER* is expressed preferentially in N position cells where, potentially in a complex with TTG1 and GL3/EGL3, it positively regulates expression of *GL2* and of *CPC.* The latter acts in lateral inhibition by movement of CPC protein to H position cells. *WER* also positively regulates the expression of its closely related paralog *MYB23*, which in turn engages in a positive autoregulatory feedback loop in N position cells. Furthermore, in N position cells *WER* negatively regulates *SCM, GL3* and *EGL3* expression – all potentially in a complex with GL3/EGL3 and TTG1. Negative regulation of *SCM* by *WER* in N position cells re-enforces positionally regulated expression of *WER.* In turn H position cells accumulate CPC protein, which is expressed in N position cells, moves to H position cells, and there represses *GL2* expression. Furthermore, CPC negatively regulates itself and *WER,* and positively regulates *SCM* expression in the H cell position, thereby re-enforcing differential *WER* expression in the alternative root cell fates. GL3 and EGL3 expression in H position cells is positively regulated by *CPC* and *TRY*, however, GL3 and likely EGL3 protein accumulate preferentially in N position cells by cell-cell movement, where they again engage in non hair cell fate determination for example by positively regulating *GL2* expression. Finally, *GL2* has been shown to promote *TRY* expression which re-enforces lateral inhibition. GL2 has also been shown to (i) directly repress phospholipase Dζ1 expression, indicating a possible downstream effect of *GL2* might be to influence phospholipid

signalling, and to directly promote and repress cellulose synthase 5 (*CESA5) and* xyloglucan endotransglucosylase 17 (*XTH17*) expression, respectively (reviewed in (Schiefelbein et al, 2009)).

1.2.2.1 Selected experiments highlighting root hair patterning

Phenotypes of the above mentioned root hair patterning regulators are the following: roots of *wer-1* and *gl3-1 egl3-1* mutants form almost only root hair cells, roots of *ttg1* and *gl2-1* mutants form an excessive number of hair cells at non-hair cell positions, and *myb23-1* roots show a slight but statistically significant increase in hair cells at N positions, while *cpc-1* roots form fewer hair cells and the *cpc-1* phenotype is enhanced in the *cpc-1 try-82* and *cpc-1 etc1-1* double mutants, where roots form no and very few hair cells, respectively (Bernhardt et al, 2003; Galway et al, 1994; Kang et al, 2009; Kirik et al, 2004a; Lee & Schiefelbein, 2002; Masucci et al, 1996). *scm* was isolated in a forward genetic screen for mutants misexpressing *GL2::GUS* reporter constructs where *GL2* expression lacked a position dependent pattern, further, *scm* mutant plants form a root hair density similar to the wild-type, however, the positioning of hair and non-hair cells confined to specific cell files is less tightly regulated (Kwak et al, 2005). SCM protein is located at the plasma membrane in every root epidermal cell file in the early meristematic zone, later SCM accumulates preferentially in H position cells (Kwak & Schiefelbein, 2008) by the above described regulatory events. SCM is allelic to *STRUBBELIG* (*SUB*; (Chevalier et al, 2005)), which has been characterized in the floral meristem to regulate cell shape and correct cell division planes.

WER has been designated a master regulator of root hair patterning (Ryu et al, 2005) since it seems to be the target of positional signalling via SCM and determines both, non-hair and hair cell fate, by positively regulating *GL2* and *CPC* expression, respectively. This view is based on the observations that (i) WER expression is increased in *scm-2 cpc-1* compared to *cpc-1* plants (Kwak & Schiefelbein, 2007), (ii) residual *GL2* expression in *wer-1* plants lacks position dependent patterning and (iii) undirected overexpression of *WER* in the *wer-1* background leads to randomized formation of both cell types rather than formation of only non-hair cells (Lee & Schiefelbein, 1999). Evidence for direct transcriptional regulation of *GL2* and *CPC* by *WER* was further supported by expressing WER by the glucocorticoid receptor (GR) inducible system (Ryu et al, 2005), furthermore,

WER bound to promoter sequences of *GL2* and *CPC* in gel mobility shift assays (Koshino-Kimura et al, 2005).

In contrast to trichome patterning, *GL3* and likely *EGL3* act non cell-autonomous in root hair specification (Bernhardt et al, 2005). Movement from H position cells to N position cells has been documented by comparing transcriptional expression pattern to protein localisation. *GL3* and *EGL3* are expressed in H position cells, as visualized for example by GUS reporter constructs, however, GL3 protein accumulates predominantly in N position cells visualized by *GL3::GL3-YFP* reporter constructs in the *gl3-1* background (Bernhardt et al, 2005).

MYB23 is to date the only gene involved in root hair patterning for which positive autoregulation has been shown (Kang et al, 2009). It is functionally equivalent with *WER* as shown by promoter-swap experiments, i.e. it also positively regulates *GL2* transcription. However, MYB23 is unlikely to be the factor that constitutes the local activation mechanism necessary for the LALI model, since *MYB23* mutant alleles show only a subtle phenotype and its expression in the root initiates later than *WER* expression. Instead, *MYB23* is thought to reinforce the differential *GL2* expression pattern of N position cells, as under destabilized patterning conditions lack of MYB23 activity becomes more evident. For example N position cells derived from epidermal T clones in the *myb23-1* background more often misspecify their cell fate due to lack of *GL2* expression than wildtype plants, further *myb23-1* attenuates the *cpc-1* phenotype and this is correlated with a decrease in *GL2* expression in comparison to the *cpc-1* single mutant (Kang et al, 2009).

The finding that there is mutual interaction between the two cell fates in the root, i.e. CPC and GL3 movement in opposing direction from N to H and H to N cell position, respectively, (Bernhardt et al, 2005; Kurata et al, 2005) and the lack of experimental evidence for local self-activation of WER lead to modelling of the gene regulatory network in the root according to an alternative mechanism called lateral inhibition with feedback (LIF, also termed mutual support mechanism; (Savage et al, 2008)). In LIF mutual signals of neighbouring cells with different fates account for cell patterning which is in contrast to a unilateral signal together with local self-activation in the LALI mechanism. Mathematical modelling of LIF for root hair patterning incorporating (i) active CPC and GL3 protein movement, (ii) initial ubiquitous expression of WER in all root epidermal cells, (iii) repression of WER expression by CPC and (iv) bias of *WER* transcription by a cortical signal showed that local self-activation of WER is dispensable for obtaining root hair patterning and that only LIF

26

modelling recapitulated the ectopic expression of WER in H cell positions seen experimentally in *cpc* mutants (Savage et al, 2008).

1.2.3 Epigenetic regulation epidermal patterning

Recently, epigenetic regulation has been shown to be part of the regulatory epidermal patterning mechanisms of root-hairs and trichomes. 3D fluorescence *in situ* hybridisation (3D FISH) visualized that chromatin at the *GL2* locus is more accessible for probes in atrichoblast than in trichoblast cell files, termed "open" versus "closed" chromatin conformation, respectively, which positively correlates with *GL2* expression state (Costa & Shaw, 2006). *CPC* supposedly is involved in regulating the closed chromatin state at *GL2*. Atrichoblast cell files ectopically express *GL2* in *cpc-1* mutants and possess an "open" *GL2* chromatin conformation, however, *wer-1* mutants which lack *GL2* but also *CPC* expression possess still an "open" *GL2* chromatin conformation. Inspection of epidermal T clones showed that remodelling of the *GL2* locus from "closed" to "open" conformation is established already after the first longitudinal anticlinal division, more precisely, a clear *GL2* probe signal was visible in mitotic in contrast to G1 phase trichoblasts suggesting that the chromatin state at *GL2* is reset after each cell cycle possibly to be able to respond to present positional signals (Costa & Shaw, 2006). Further evidence for involvement of chromatin state in root hair patterning was provided by the *FASCIATA2* (*FAS2*) mutant which exhibits very few cells with "closed" chromatin state at *GL2* and these lack position dependent localization; the molecular phenotype correlates with a severe reduction in root hairs (Costa & Shaw, 2006). *FAS2* is a subunit of the chromatin assembly factor 1 (CAF-1) which is thought to be for correct assembly of histones H3 and H4 into chromatin during replication and in maintenance of epigenetic states in higher eukaryotes (van Nocker, 2003). Analyses on the nature of specific epigenetic marks underlying different chromatin states in epidermal patterning have focused on histone acetylation and methylation. It was shown that treatment of roots with trichostatin A (TSA), an inhibitor of histone deacetylases (HDACs), leads to an increase of root hairs and a decrease of trichomes (Xu et al, 2005). It affects the level and patterning of *CPC*, *GL2* and *WER* expression which is accompanied by changes of H3 and H4 acetylation in their promoter (*CPC*, *GL2*, *WER*) and transcribed regions (*CPC*). In a reverse genetic screen of 18 known TSA sensitive HDACs, five showed an increase in root hair number (Xu et al, 2005). A further epigenetic regulator involved in epidermal

patterning is *GL2 EXPRESSION MODIFIER* (*GEM*), encoding a protein lacking significant homology to other known proteins, and it is involved in sustaining of a repressive epigenetic status at the *GL2* and *CPC* locus (Caro et al, 2007). ChIP assays showed that GEM is recruited to the promoters of *GL2* and *CPC*, at both loci, *gem-1* plants gained and lost epigenetic marks indicative of active (histone H3 acetylation [H3K9acK14ac] and methylation (H3K9me3)) and of silent chromatin (histone H3 methylation [H3K9me2]), respectively. Concomitantly, *gem-1* mutants had elevated *GL2* and *CPC* expression levels and exhibited decreased and increased root hair and trichome density, respectively. *GEM* also provides a link between epidermal patterning and cell division, since *gem-1* mutants showed increased cell number in root epidermal and cortex cells and GEM interacted with the *A. thaliana* homolog of CDT1, in animals a subunit of the pre-replication complex involved in DNA replication licensing (DePamphilis et al, 2006), and with TTG1 in yeast two-hybrid assays (Caro et al, 2007). Taken together, epigenetic mechanisms are involved in regulation of root hair and trichome cell patterning and to date, *GL2* and *CPC* expression have been shown to be epigenetically regulated. *GEM* has been identified as a link between cell fate specification and cell division processes and is suggested to be recruited to the *GL2* and *CPC* promoters possibly via interaction with TTG to mediate repressive epigenetic status and thus repression of *GL2* and *CPC* expression (Caro et al, 2007).

1.2.4 The WD40/bHLH/R2R3MYB module

The WD40/bHLH/R2R3MYB protein complex constitutes a general module which in *A. thaliana* is involved in expression regulation of several developmental and biosynthetic pathways, including epidermal patterning and flavonoid biosynthesis (Figure 1.4). Any active module is thought to be composed of a WD40 protein which interacts with a homo- or heterodimer of bHLH proteins that in turn interact with an R2R3 MYB protein (reviewed in (Broun, 2005)). In *A. thaliana* the WD40 component of the WD40/bHLH/R2R3MYB module is specified solely by *TTG1*, which may act – by deduction from common roles of WD40 proteins (Stirnimann et al, 2010) - as a scaffold facilitating protein-protein interaction. Accordingly, it is *per se* not a transcriptional activator and in *A. thaliana* its function in respect to trichome patterning and anthocyanin accumulation can be complemented by overexpression of bHLH activity (Lloyd et al, 1994). GL3, EGL3 and TT8 participate as bHLH proteins in the WD40/bHLH/R2R3MYB module. They, together with MYC1,

constitute subfamily IIIf of the large bHLH transcription factor family in *A. thaliana*, also designated R/B like subfamily due to homology to maize R/B bHLH genes which in maize are involved in anthocyanin pigment production and also function together with MYB proteins (Damiani & Wessler, 1993). It has been shown for GL3 in the context of transient expression studies in protoplasts that the N-terminal domain preceding the bHLH domain, which is conserved in the bHLH subfamily IIIf, functions as transcriptional activation domain (Wang & Chen, 2008). R2R3 MYB genes are described in more detail in chapter 1.3.2. The ability of the complex to be involved in diverse pathways on the one hand and the functional specificity on the
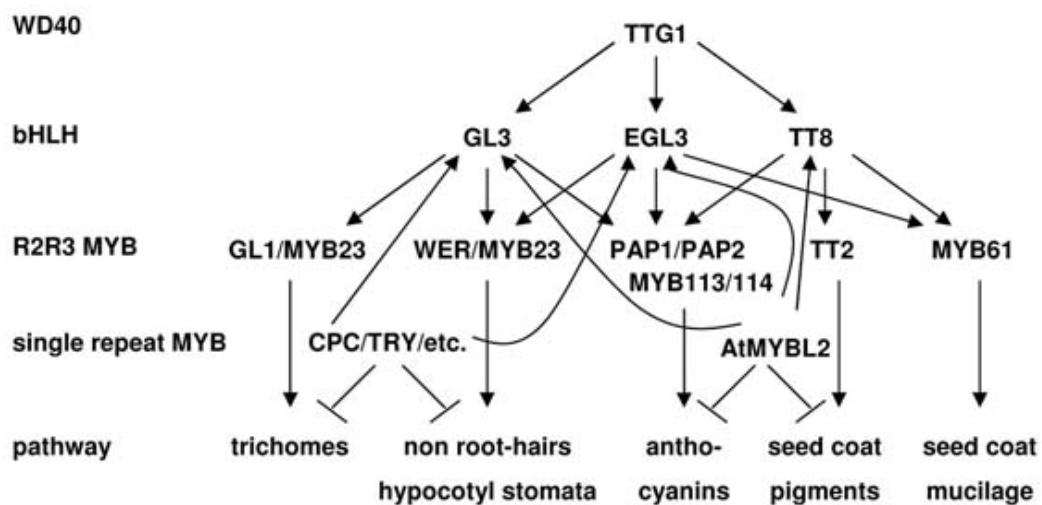
Figure 1.4. Composition of the WD40/bHLH/R2R3 MYB complex and its involvement in cell specification and biosynthesis pathways. Modified from (Zhang et al, 2003). Affiliation to protein families is shown to the left. Arrows indicate documented protein interactions. Arrows and stunted lines pointing towards pathways indicate positive and negative regulation. Not all members of the single-repeat R3 MYB protein family are functioning in all shown cell fate specification processes, see chapter 1.3.3 for details. TT2,8: TRANSPARENTA TESTA2,8; PAP1,2:PRODUCTION OF ANTHOCYANIN PIGMENT1,2; all other gene name abbreviations are documented in the text.

other hand is given by certain combinations of members of the bHLH and R2R3 MYB transcription factor family in each sub-complex. The modular hierarchy of the complex is also reflected by the pleiotropic behaviour of genetic mutants, like high pleiotropy of *ttg1* mutants with phenotypes in all depicted pathways and specific phenotypes of for example *gl1* mutants restricted to trichome patterning (reviewed in (Broun, 2005)).

The protein families involved in the regulatory complex are not plant specific, WD40, bHLH and MYB gene families are found in all eukaryotes and there are prokaryotic

transcription factors with HLH domains. However, there are indications that the functioning in a WD40/bHLH/R2R3MYB complex has evolved in land plants and is mostly involved in specification of certain developmental aspects of epidermal cells across plant species (reviewed in (Ramsay & Glover, 2005)). Interestingly, it has been speculated that although single celled trichomes of *A. thaliana* and cotton (both belonging to the rosid division) are specified by a WD40/bHLH/R2R3MYB complex, this may be not the case of multicellular trichomes in the asterid division and thus their formation might be governed by convergent mechanisms (discussed in (Serna & Martin, 2006)). Although in asterids R2R3MYB proteins are also involved in multicellular trichome initiation (for example AmMIXTA in *Anthirrinium majus*, PhMYB1 in *Petunia hybrida*) they lack the conserved bHLH interaction motif, and it has been shown that *MIXTA* is unable to complement *A. thaliana gl1* mutants. Further, there was no phenotypic effect on trichome production of (i) overexpression of bHLH activity in asterids in contrast to overexpression in *A. thaliana* and (ii) petunia mutants and overexpressors of *ANTHOCYANIN11* (*AN11*), the single WD40 protein in petunia. Finally, phylogenetic analysis grouped AmMIXTA and PhMYB1 in a clade together with *A. thaliana* MIXTA-like proteins, separated from GL1, MYB23 and GaMYB2 (discussed in (Serna & Martin, 2006)).

1.3 Arabidopsis thaliana MYB genes

1.3.1 The MYB domain

The MYB DNA binding domain is conserved in animals, plants and yeast and was first described for the vertebrate genes c-Myb, A-Myb and B-Myb, which are functioning in cell proliferation and differentiation, and of the derived and truncated R3 MYB domain of the v-Myb oncogene of avian myeloblastosis virus (Weston, 1998). The MYB DNA binding domain consists of up to three imperfect MYB repeats (R1, R2 and R3) each of around 50 amino acids in length. Based on structural studies of vertebrate MYB proteins, each MYB repeat is suggested to adopt a helix followed by a helix-turn-helix conformation, within which three regularly spaced tryptophan residues contribute to maintain a hydrophobic core (in the context of the R3 MYB domain see Figure 1.5B) ((Frampton et al, 1991; Ogata et al, 1992); in most plant R2R3 MYB proteins the first tryptophan residue of R3 is exchanged for a phenylalanine or isoleucine residue (Stracke et al, 2001)). Helices 3 of the R2 and R3 MYB repeat are thought to function as recognition helices for DNA binding, and

both, the R2 and R3 MYB repeat, are thought to be necessary for sequence-specific DNA binding, with the R3 MYB repeat contacting the core of the MYB consensus binding sites (Frampton et al, 1991).

1.3.2 Arabidopsis thaliana MYB gene families

In plants, MYB proteins are categorized depending on the number and similarity of their MYB repeats to MYB R1-3 into the three subfamilies of R1R2R3 MYB proteins, R2R3 MYB proteins and MYB-related proteins (Jin & Martin, 1999; Rosinski & Atchley, 1998; Stracke et al, 2001; Yanhui et al, 2006). In *A. thaliana*, the R1R2R3 MYB family has five members of which some have been shown to be involved also in cell cycle control like vertebrate MYB proteins (Stracke et al, 2001; Yanhui et al, 2006). R2R3 MYB proteins constitute the largest transcription factor family with at least 125 members (Stracke et al, 2001). Characterized members of these are involved in diverse processes, including regulation of cell fate, of organ morphogenesis and of secondary metabolism, many are responsive to environmental factors or hormones and/or are expressed in an organ specific manner (Stracke et al, 2001; Yanhui et al, 2006). R2R3 MYB proteins are divided into several subgroups based on sequence motifs located C-terminal to the MYB domain (Kranz et al, 1998; Stracke et al, 2001; Yanhui et al, 2006). The proteins GL1, WER and MYB23 constitute an R2R3 MYB subgroup sharing the conserved amino acid signature [DE]Lx2[RK]x3Lx6Lx3R necessary for interaction with R/B-like bHLH proteins located on helices 1 and 2 in the R3 MYB repeat (Figure 1.5B) (Zimmermann et al, 2004) and a 19 aa long conserved motif embedded in the acidic C-terminus (Kranz et al, 1998), which for WER has been shown to act as a transcriptional activator (Lee & Schiefelbein, 2001). The third subfamily, MYB-related proteins, is a heterogeneous group and contains 64 members with one or two MYB repeats. It has further divided into five subgroups, these include the single-repeat R3 MYB gene family (Yanhui et al, 2006).

Although sharing the conserved MYB DNA binding domain DNA binding specificity varies between plant MYB proteins, possibly due to the global context of the MYB domain and due to specific changes within the MYB domain. Using gel mobility shift assays, for WER a DNA consensus binding site has been deduced (5´-C(C/T)AACNG-3´; (Koshino-Kimura et al, 2005) and two of these consensus binding sites were detected in both the *GL2* and *CPC* promoter, where for *GL2* it has been

shown that the promoter region containing the consensus binding sites has is necessary for proper *GL2* expression in the root and in leaves (Hung et al, 1998; Szymanski et al, 1998). Since WER, GL1 and MYB23 are functionally redundant proteins regarding cell fate determination (Kirik et al, 2005; Lee & Schiefelbein, 2001), it is likely that GL1 and MYB23 are also able to bind to this consensus sequence. Contrary, it has been shown that binding ability is lost upon swapping two particular amino acid residues in helix 2 of the WER R3 MYB domain to that of the corresponding residues of CPC (Tominaga et al, 2007)). To date it is not clear whether members of the single-repeat R3 MYB family are able to directly bind to DNA, however, ChIP analyses indicate presence of TCL2 at *GL1* regulatory sequences (Wang et al, 2007). Further, it has been shown for other plant MYB proteins encoding only one MYB repeat that they are capable of specific DNA binding (Baranowskij et al, 1994; Wang et al, 1997).

1.3.3 The single-repeat R3 MYB gene family

To date, the single-repeat R3 MYB gene family consists of six members, *TRY*, *CPC*, *ETC1*, *ETC2*, *ETC3* and *TCL1* (Esch et al, 2004; Kirik et al, 2004a; Kirik et al, 2004b; Schellmann et al, 2002; Tominaga et al, 2008; Wada et al, 1997; Wang et al, 2007) localized on chromosomes 1, 2, 4 and 5 (Figure 1.5A) (Wang et al, 2008). They encode proteins between 77 and 112 amino acids in length and their common feature is a single R3 MYB domain which is homologous to the R3 repeat of the classical MYB DNA binding domain (Figure 1.5B). One hallmark residue of the R3 MYB domain, the first tryptophan or phenylalanine residue in vertebrate and plant R3 MYB repeats, respectively, is changed to methionine in the single-repeat R3 MYB family proteins. All of the single-repeat R3 MYB proteins lack the two aa necessary for binding of WER to *GL2* regulatory sequences (Figure 1.5B) (Tominaga et al, 2007). TRY and ETC2 are the only two members with short carboxy-terminal tails, but within these tails they do not share any similarity. Within their R3 MYB domain the bHLH interaction motif $[DE]LX_2[RK]X_3LX_6LX_3R$ is conserved (Figure 1.5B) and interaction with the bHLH proteins GL3 and EGL3 has been functionally verified for most of the single-repeat R3 MYB family members (Pesch & Hülskamp, 2009).

Figure 1.5. The single-repeat R3 MYB gene family. (A) Genome localisation of the single-repeat R3 MYB genes (Wang et al, 2008). (B) Alignment of the single-repeat R3 MYB family proteins and the R3 MYB repeat of GL1 and WER. Similarity shading was done according to the PAM120 matrix. H1, 2, 3 correspond to the aa forming α-helices 1, 2, 3 of the R3 MYB domain and filled circles indicate the regularly spaced tryptophan (phenylalanine/methionine) residues contributing to a hydrophobic core (Frampton et al, 1991; Ogata et al, 1992; Stracke et al, 2001). Asterisks indicate the bHLH interaction motif [DE]Lx2[RK]x3Lx6Lx3R (Zimmermann et al, 2004). Triangles indicate aa residues necessary for binding of WER to the GL2 promoter (Tominaga et al, 2007). Orange bars mark aa residues required for CPC cell-cell movement (Kurata Dev 05). Numbers to the right are equivalent to the number of aa residues of respective proteins.

1.3.3.1 Single-repeat R3 MYB gene functions

The founding members of the single-repeat R3 MYB family, *TRY* and *CPC,* were detected by forward genetic screens for mutants in trichome and root hair

patterning, respectively (Schellmann et al, 2002; Wada et al, 1997). Later it was shown that they are pleiotropic and act in both, trichome and root hair patterning, and that they show genetic interaction in both processes (Schellmann et al, 2002). Regarding trichome patterning, *TRY* and *CPC* mutants form trichome nests (trichomes formed without intervening epidermal cells) and an increased trichome density, respectively, and thus they were categorized as trichome repressors (Hülskamp et al, 1994; Schellmann et al, 2002). In the framework of the LALI model of pattern formation and based on further experimental evidence they were proposed to counteract the WD40/bHLH/R2R3MYB activator complex by competitive binding with GL1 and WER to GL3/EGL3 in trichome and root hair patterning, respectively, thereby forming an inactive repressor complex and suppressing expression of the downstream target gene *GL2* (Figure 1.1 A). Further, since they are expressed in trichomes and non-root hair cells in leaves and roots, respectively, and repress cells to acquire the same cell fates, that is trichomes and non-root hair cells, single-repeat R3 MYB members were modelled to act by lateral inhibition (Figure 1.2 B, Figure 1.3) (reviewed in (Ishida et al, 2008)).

Experimental evidence regarding single-repeat R3 MYB proteins to support the LALI model will be briefly described below. Protein interaction with GL3 and EGL3 has been shown for all of the single-repeat R3 MYB proteins, but for TCL1-EGL3 interaction, which has not been analyzed yet (reviewed in (Pesch & Hülskamp, 2009)). It has also been demonstrated that all tested single-repeat R3 MYB proteins can compete with GL1 for GL3 binding in yeast three-hybrid experiments, as well as CPC with WER for GL3 and EGL3 binding (Esch et al, 2003; Esch et al, 2004; Tominaga et al, 2007; Wester et al, 2009). Negative regulation of *GL2* expression by members of the single-repeat R3 MYB family has been visualized in roots by ectopic expression of *GL2::GUS* reporter constructs in H cell files in the *cpc-1*, *try* and *etc1* background (Lee & Schiefelbein, 2002; Simon et al, 2007; Wada et al, 2002). Gene expression patterns in accordance with the LALI model have been visualized by *promoter::GUS* constructs in leaves. The expression pattern of *TRY, CPC, ETC1, ETC2, ETC3* and *TCL1* is generally characterized by a diffuse staining in young leaves with stronger staining in incipient trichomes, later, diffuse staining is restricted to the leaf base in the trichome initiation zone, again, strongest staining is visible in incipient and developing trichomes; further, expression of *TRY, CPC* and *ETC1* is maintained in trichomes of developed leaves, whereas *ETC2* and *ETC3* expression ceases (Esch et al, 2004; Kirik et al, 2004a; Kirik et al, 2004b; Koshino-Kimura et al,

2005; Schellmann et al, 2002; Tominaga et al, 2008; Wang et al, 2007). In roots, the spatial resolution of gene expression and protein localisation has been shown in detail for *CPC* (Kurata et al, 2005; Wada et al, 2002). Visualized by *promoter::GUS* and *promoter::2rsGFP* constructs, *CPC* is expressed in N cell files, however, in *CPC::HA-CPC cpc-1* lines, which are fully complemented, HA-CPC was only detected in H cell files (Kurata et al, 2005). Truncation and amino acid substitution experiments mapped two signals in CPC necessary for intercellular movement: an N-terminal region not conserved between the single-repeat R3 MYB proteins and two conserved residues (W76 and M78) in H3 of the R3 MYB domain, further, W76 was shown to be necessary for nuclear localisation (Figure 1.5 B) (Kurata et al, 2005). Spatially restricted expression in N cell files has also been shown for *TRY* and *ETC1* (Simon et al, 2007). Intercellular movement ability in leaves has been documented for TRY, CPC and ETC3 (Digiuni et al, 2008; Wester et al, 2009; Zhao et al, 2008). Recently, it has been shown that intercellular movement ability might correlate with the strength of GL3/EGL3 binding (Wester et al, 2009).

The regular pattern of trichomes on leaf blades is disturbed by mutants of single repeat R3 MYB family members in two different ways, an increase of regularly spaced trichomes and/or formation of trichomes next to each other (nests). *try* alleles display trichome nests, i.e. depending on the allele approximately 4-12% of trichome initiation sites (TIS) display (up to four) trichomes formed next to each other, surrounded by a common ring of accessory cells (Hülskamp et al, 1994; Schellmann et al, 2002; Wang et al, 2008). At the same time, *try* single mutants have a decreased number of TIS (Schellmann et al, 2002). None of the other single-repeat R3 MYB family show significant increased nest formation as single-mutants, but certain combinations of double mutants (e.g. *cpc-1 etc3-1*, *cpc-1 tcl1-1*) or triple mutants do; most severe nest formation is seen in combination with *try* alleles, *try cpc-1* double mutants have an increased trichome number and also larger nests (~ 80% of TIS are nests with up to 30 trichomes) and *try cpc-1 etc1-1* triple mutant leaves are nearly covered with trichomes forming next to each other, except near the midvein region (Kirik et al, 2004a; Schellmann et al, 2002; Wang et al, 2008; Wester et al, 2009). Clonal analysis showed that trichome nests are more likely formed due to destabilisation of processes acting in intercellular communication than in mitosis (Schnittger et al, 1999). *cpc-1*, *etc2-1* and *etc3-1* single mutants or higher order mutants increase trichome density without disturbing regular patterning (Wang et al, 2008; Wester et al, 2009).

Based on phenotypic data of mutants, single-repeat R3 MYB genes function in several developmental processes, most conclusive in trichome initiation and patterning on different organs, trichome morphogenesis, root hair patterning and, recently, evidence suggests a role in stomata patterning in the hypocotyl (Figure 1.4) (Esch et al, 2004; Kirik et al, 2004a; Kirik et al, 2004b; Schellmann et al, 2002; Serna, 2008; Simon et al, 2007; Tominaga et al, 2008; Wada et al, 2002; Wang et al, 2008; Wang et al, 2007; Wester et al, 2009). For these processes, some members are pleiotropic and *ETC2* is the only member which acts exclusively in trichome patterning, while for example lof mutants of all other family members have been shown to affect also root hair patterning, although the effect of some members is masked by redundancy. For example, the phenotype of *tcl1* mutants is visible in both leaf trichome and root hair patterning only in the triple mutant background of *cpc1-1 etc1 etc3*; or, while *try* single mutants show wild-type roots and *cpc-1* mutants show a decreased root hair number, *cpc-1 try* double mutants are devoid of root hairs. In accordance to that, all members but *ETC2* have been shown to be expressed in leaves and roots (Kirik et al, 2004a; Simon et al, 2007; Tominaga et al, 2008; Wada et al, 2002).

Single-repeat R3 MYB family members repress trichome initiation also on other organs than the leaf blade. *ETC2* together with *TRY* and *CPC* redundantly suppress trichome formation on petioles (Kirik et al, 2004b). *tcl1-1* shows ectopic trichome formation on pedicels and on certain internodes of the inflorescence stem, and the phenotype is enhanced in *tcl1-1 cpc-1* double mutants (Wang et al, 2007). Further, ectopic trichomes were formed on hypocotyls, siliques and cotyledons in *try-82 cpc-1 etc1-1*, *try-29760 cpc-1 etc1-1 tcl1-1* and *try-29760 cpc-1 etc1-1 etc3-1 tcl1-1* mutants, respectively (Kirik et al, 2004a; Wang et al, 2008). *TRY* also affects trichome morphogenesis. *try* alleles possess trichomes with supernumerary branches and this is correlated with increased endoreduplication (Hülskamp et al, 1994; Szymanski & Marks, 1998). Further, *try* mutants possess an increased epidermal cell number (Szymanski & Marks, 1998), thus *TRY* plays a role in constricting endoreduplication and mitotic cycles depending on the cell type. *ETC3* has also been implicated in regulation of endoreduplication, contrary to *try-EM1*, *etc3-1* mutants increase endoreduplication in epidermal cells and concomitantly possess trichomes with a reduced branch number (Tominaga et al, 2008). However, the phenotypes could not be recapitulated in an independent study (Wester et al, 2009).

There is evidence that single-repeat R3 MYB proteins are involved in stomata patterning in the hypocotyl. Recently it was shown that *cpc-1* and *try* mutants decrease stomata formation in the hypocotyl, and accordingly, *CPC* but also *ETC1* are preferentially expressed in the non-stomata cell files in the hypocotyl as visualized by promoter::GUS constructs (Kirik et al, 2004a; Serna, 2008). There seems to be a difference in the regulation of stomata patterning in the hypocotyl and in cotyledons/leaves: *cpc-1 try* double mutants abolish stomata formation in the hypocotyl, but stomata density on cotyledons stays unaffected (Kirik et al, 2004b; Serna, 2008). However, *ETC2* and *ETC3* expression was also detected in stomata of leaves and/or cotyledons (Kirik et al, 2004b; Tominaga et al, 2008). Additional evidence for a role of *ETC3* in stomata patterning in the hypocotyl provide *35S::ETC3* expressing lines that show a randomized stomata distribution in hypocotyl cell files (Tominaga et al, 2008).

The single-repeat R3 MYB gene family members have been shown to have redundant and distinct roles in the above described developmental processes. The precise roles and comparison of function of members in parallel regarding the two main patterning processes, i.e. trichome and root hair patterning, have been started to be investigated but gave rise to slightly differing results as to, for example, the extent of which each member is involved in each patterning process and genetic interactions between the family members, hence hampering precise conclusions about which genes are essential for the patterning processes or the extent of redundancy between the members. These discrepancies arise due to analysis of different alleles in different studies, in some cases analysis in different genetic backgrounds. A specific problem in testing the interaction between *ETC2* and *TCL1* poses their tight linkage (encoded *in tandem* on chromosome 2; Figure 1.5A). However, some general conclusions can be drawn from parallel analyses of phenotypes of family members in respect to trichome and root hair patterning so far. As mentioned, *ETC2* is the only family member which seems to function exclusively in trichome patterning (Kirik et al, 2004b; Simon et al, 2007; Wang et al, 2008). *TRY*, *CPC*, *ETC2* and *ETC3* show significant phenotypes in leaf trichome patterning as single mutants, whereas the tested loss of function alleles of *ETC1* and *TCL1* show phenotypes only in higher order mutants (Hülskamp et al, 1994; Kirik et al, 2004a; Kirik et al, 2004b; Tominaga et al, 2008; Wada et al, 2002; Wang et al, 2008; Wang et al, 2007; Wester et al, 2009). Contrary, to date only single mutants of *CPC* and *ETC3* show significant phenotypes in root hair patterning (a decrease in root hairs),

however, in combination with *cpc-1*, mutants in *TRY* and *ETC1* form no and drastically decreased root hairs, respectively (Kirik et al, 2004a; Schellmann et al, 2002; Tominaga et al, 2008; Wada et al, 2002). The impact of *TCL1* on root hair patterning could only be uncovered in a quadruple mutant (Wang et al, 2008). Further, functional redundancy between family members was tested using complementation tests in two studies. First, complementation of a *try* mutant by *ETC1* was tested. As described, *try* plants show trichome clusters and trichomes with supernumerary branches. Interestingly, *ETC1* expressed under the regulatory regions of *TRY* was able to complement the trichome branching phenotype but failed to complement trichome clustering. Therefore, regarding regulation of trichome branching *TRY* and *ETC1* are functionally equivalent proteins and changes in *cis*-regulatory regions of *TRY* lead to its functional diversification, contrary to regulation of trichome spacing where changes in protein coding sequence have contributed to functional diversification of *TRY* (Esch et al, 2004). *TCL1* failed to complement the trichome clusters and the increased root hair density of *try* mutants when expressed under *TRY* regulatory sequences and completely abolished trichome formation and partially restored root hair patterning when expressed under the *CPC* promoter in *cpc-1* mutant (Wang et al, 2007). Finally, the ability of *TRY*, *ETC1*, *ETC2* and *ETC3* expressed under *CPC* regulatory sequences to complement *cpc-1* mutant phenotypes was tested (Simon et al, 2007). While all tested genes were able to complement the increased trichome density of *cpc-1* mutants, *TRY* and *ETC2* were outperformed by *ETC1* and *ETC3* in complementing root patterning defects. The latter experiment is in line with the observation of *ETC2*´s exclusive functioning in trichome patterning. Direct evidence of differences in transcriptional regulation of single-repeat R3 MYB genes were provided by expression analyses. *A. thaliana* protoplasts *per se* do not express *GL1*, *WER*, *GL3*, *EGL3* and *TTG1* and were therefore used as a system to test their affect on single-repeat R3 MYB gene expression (Wang et al, 2008). *TRY*, *TCL1*, *ETC2* and *CPC* expression was detected in the absence of above mentioned regulators in *A. thaliana* protoplasts. Further, expression of *TRY*, *CPC*, *ETC1* and *ETC3*, but not *ETC2* and *TCL1*, was enhanced by the combined action of *GL1* or *WER* together with *GL3* or *EGL3*. Further, expression analysis of *gl3 egl3* mutant seedlings showed that *GL3* and *EGL3* are essential only for *ETC1* but not for *ETC3* gene expression (Wang et al, 2008) and expression analysis in a *gl2* mutant background showed that *GL2* is essential for *TRY* but not *CPC* or *ETC1* expression in the root (Simon et al, 2007).

Taken together, both, changes in *cis*-regulatory regions and in protein function, contribute to functional diversification of single-repeat R3 MYB proteins.

1.4 Biological functions of *Arabidopsis thaliana* trichomes

Plant trichomes are very diverse in morphology, anatomy and physiology and are formed on various plant organs. Therefore, they may serve very different functions, however, many of them are unknown and of the hypothesized functions few have been experimentally tested. In general many functions suggested for trichomes located on plant leaves can be summarized as protective functions against biotic and abiotic stressors. This is particularly evident for glandular trichomes that secrete an array of compounds (polysaccharides, sugars, salts, lipids, essential oils, etc.) that serve for example from immobilization of insects to acting as feeding deterrent of herbivores. In regard to mediating protection against abiotic stressors, the factors light, UV-B radiation, extreme temperatures and water stress are suggested, and trichomes were found to be sites of heavy metal accumulation (reviewed in (Wagner et al, 2004; Werker, 2000)). As described, *A. thaliana* possesses non-glandular trichomes, i.e. they are non-secreting cells and may exert their functions by physiological pathways present in trichomes and/or simply by their morphological features.

An emerging function of *A. thaliana* trichomes is their protective role against herbivores. Initially, field experiments comparing plants sprayed with pesticides (thus grown under less exposition to herbivores) to untreated plants showed that trichome density is positively correlated to a reduction of damage by natural enemies (Mauricio, 1998) and that natural enemies impose selection favouring increased trichome density (Mauricio & Rausher, 1997). Recently, experiments carried out with the specialist herbivore *Plutella xylostella* (diamondback moth) demonstrated a negative correlation between trichome density and the number of eggs positioned on the leaf, on the other hand, trichome density did not affect resistance to larval feeding (Handley et al, 2005). Similar lines of evidence linking trichomes to protection against biotic stressors were found in the close relative *Arabidopsis lyrata* (Clauss et al, 2006; Kivimaki et al, 2007; Loe et al, 2007).

Other putative functions of *A. thaliana* trichomes are primarily suggested by a diverse set of gene expression and protein profiling studies that detected genes to be differentially expressed in trichomes in comparison to for example leaf epidermal

cells. The high resolution to the cell level is made feasible on the one hand by the properties of trichomes which can be sampled manually and on the other hand by microcapillary sampling in which the cell sap of single cells can be collected (Kryvych et al, 2008; Lieckfeldt et al, 2008; Wienkoop et al, 2004). In an *in situ* hybridization study the enzymes γ-glutamyl-cysteine synthetase (*GSH1*) and glutathione synthetase (*GSH2*) were found to be present at a high level in leaf trichomes, possibly leading to the 300-fold higher amount of glutathione (GSH) in trichomes compared to other epidermal cells (Gutierrez-Alcala et al, 2000). Among other functions, GSH acts as an anti-oxidant and plays a role in detoxification processes by sequestering toxic compounds to the vacuole (Rea et al, 1998). In accordance, protein profiling of *A. thaliana* trichomes in comparison to leaf epidermal cells identified differential expression of a glutaredoxin-like protein (At5g40370) and a glutathione S-conjugate ABC transporter (At*MRP1*; (Wienkoop et al, 2004)) and gene expression profiling reported a high expression of glutathione S-transferases (*GST9*, *GST12*, *GST16*; (Lieckfeldt et al, 2008)). Notably, these genes are picked from a large list of differentially or highly expressed genes in *A. thaliana* trichomes. By validation of the transcriptional profile on a larger scale it was found that, according to the Gene Ontology (GO) annotation, genes categorized as "response to biotic or abiotic stimulus" and as "response to stress" are overrepresented among genes expressed in trichomes in comparison to other functional categories, (Jakoby et al, 2008c; Kryvych et al, 2008) and (Kryvych et al, 2008), respectively. In a further study comparing the transcriptional profile of trichomes to leaves abrased of trichomes, high expression of glucosinolate and flavonoid pathway genes were found (Jakoby et al, 2008c). Upon inspection, for example chalcone synthase (*CHS*) and flavonol synthase (*FLS*) of the flavonoid pathway are listed as being overexpressed in trichomes in the above studies (Kryvych et al, 2008; Lieckfeldt et al, 2008). Both pathways produce secondary metabolites; glucosinolates are a common feature of the Brassicales and mediate defense against herbivores, flavonoids perform a wide range of functions, from plant-animal interaction to protection against UV-B irradiation (Kliebenstein, 2004).

Further approaches to deduce *A. thaliana* trichome function assessed stimulation of trichome formation upon exposition to factors of interest. These experiments also led to the identification of genetic pathways involved in stimulated trichome formation. Initially, central to that was the weak *gl1-2* allele (Esch et al, 1994) that lacks the 29 C-terminal AA comprising the acidic transactivation domain and shows

a glabrous phenotype. It was shown that exposition to γ-irradiation (Nagata et al, 1999b) and wounding of leaves (Yoshida et al, 2009) restores trichome formation in the *gl1-2* background, further both factors enhance trichome formation in a wild-type background but fail to restore trichome formation in plants harbouring the strong *gl1-1* allele (Nagata et al, 1999a; Traw & Bergelson, 2003; Yoshida et al, 2009) indicating that a functional WD40/bHLH/R2R3MYB trichome initiation complex is necessary for induced trichome formation. It was speculated that the common feature in restoring trichome formation in the *gl1-2* background by γ-radiation and wounding may be the formation of reactive oxygen species, since prior treatment with antioxidants abolished induction of trichomes by γ-irradiation (Nagata et al, 1999a; Yoshida et al, 2009). It could be shown that wounding induced formation of trichomes depends on jasmonate (JA) signalling because plants mutant for *ALLENE OXIDASE SYNTHASE* (*AOS*), a central enzyme in JA biosynthesis, cannot increase trichome formation upon wounding, and, further, exogenous application of JA also induces trichome formation (Traw & Bergelson, 2003; Yoshida et al, 2009). Besides functioning in developmental processes, JA mediates systemic defenses especially against herbivores and necrotrophic pathogens (Browse & Howe, 2008). A genetic screen detected *UNARMED9* (*URM9*) as a suppressor of the JA induced formation of trichomes in the *gl1-2* mutant background (Yoshida et al, 2009). *URM9* is identical to *SUPER SENSITIVE TO ABA AND DROUGHT2* (*SAD2*; (Verslues et al, 2006)) and codes for an importin β-like protein. Although *sad2/urm9* did not affect nuclear targeting of *GL1*, *TTG1* and *GL3* (Gao et al, 2008; Yoshida et al, 2009), the subnuclear distribution of a*:GL3-2xGFP* fusion protein was altered in jasmonate treated *gl1-2 urm9* mutant plants (Yoshida et al, 2009). *GL3* regulates trichome initiation in a dosage dependent manner (Payne et al, 2000) and, in turn, jasmonate has been shown to increase *GL3* expression (Maes et al, 2008; Yoshida et al, 2009). These and further findings led to the hypothesis that a key event in wound induced trichome formation is the upregulation of *GL3* via jasmonate signalling and *URM9* – by a yet unknown mechanism – plays a pivotal role in regulating GL3 function (Yoshida et al, 2009). Contrary to JA, salicylic acid (SA), a phytohormone known to mediate plant resistance for example by induction of the hypersensitive response (HR) especially effective against biotrophic pathogens (Smith et al, 2009), downregulates trichome initiation (Traw & Bergelson, 2003).

1.5 Leaf development

In order to understand the patterning and density of trichomes on *A. thaliana* rosette leaves which starts during early leaf development, processes regulating final leaf size and shape have to be taken into account. *A. thaliana* leaves are determinate organs, they are heteroblastic, i.e. they show differences in leaf size and morphology depending on the time they are formed during the plant´s life cycle, and, they show phenotypic plasticity, i.e. final leaf size also depends on environmental factors like light, temperature, water abundance, etc. (Tsukaya, 2005; Tsukaya et al, 2000).

A. thaliana rosette leaves are initiated at the shoot apical meristem (SAM) during the vegetative phase. The ordered formation of leaf primordia (phyllotaxis) is thought to be coordinated by the phytohormone auxin, since high concentrations of auxin correlate with incipient leaf primordia. The actual cause triggering outgrowth of primordia is not known, however, it is thought that altering tensile forces via rearranging of cell wall structure might lead to local outgrowth, and a class of proteins called expansins might be implicated in that process. Primordia then grow lateral, to become flat structures, and along the proximo-distal axis, to become longer (reviewed in (Fleming, 2005)). For the former to occur, it is necessary to generate a dorso-ventral polarity giving rise to different leaf tissues, i.e. the adaxial epidermis, the palisade mesophyll and spongy mesophyll cell layer, and the abaxial epidermis. The spongy mesophyll cell layer embeds the vasculature. Early events in causing the gradient involve an unknown signal from the meristem, a complex regulatory network of transcription factors and regulation by small RNAs (Szakonyi et al, 2010).

Growth along the proximo-distal leaf axis has been analyzed by a stably transformed GUS-reporter construct driven by the regulatory region of a B-type cyclin (Donnelly et al, 1999) to monitor cell cycling, and by measurement of mesophyll cell size (Pyke et al, 1991) to monitor cell elongation, in dependence to the position along the proximo-distal axis and over time. By that it has been shown that growth occurs in a basipetal manner, that is in a gradient starting from the tip moving towards the base of the leaf which correlates to the observed gradient in trichome formation (Hülskamp et al, 1994). Leaf development has been divided into three different stages based on kinematic analysis, cell proliferation, cell expansion and maturation phase and these phases correlate with gene expression profiles

(Beemster et al, 2005). In contrast to monocotyledonous plants (reviewed in (Granier & Tardieu, 2009), these phases are not strictly separated in a temporal or spatial manner, but occur in a gradient as described above. Individual tissue layers follow the same proximo-distal development, i.e. a common basic regulatory mechanism might act in all cell layers. However, for example the palisade mesophyll layer possesses a broader gradient of proliferating cells and they are present over a longer period of time in comparison to the epidermal cell layer (Donnelly et al, 1999). Trichomes are formed starting early during leaf development (see chapter 1.2.1), therefore the regulatory events leading to trichome cell specification take place in a field of actively dividing and subsequently elongating cells and final trichome density and number may be influenced by these processes.

Several genes affecting leaf shape and size by modulating cell proliferation or elongation have been detected by mutational analyses, with examples specifically affecting either of these growth mechanisms in the leaf width (for example *ANGUSTIFOLIA* (*AN*)) or leaf length (for example *ROTUNDIFOLIA* (*ROT*)) direction (reviewed in (Tsukaya, 2005)). Cell proliferation and cell expansion in turn are not strictly independent processes, as reduced cell proliferation may result in increased cell elongation, a process termed compensation (reviewed in (Tsukaya, 2005)). Natural variation for leaf shape has initially been analyzed by phenotypic screening of ~190 *A. thaliana* accessions which were then grouped into different phenotypic classes and F2 crosses showed that tested leaf shape phenotypes have multigenic architecture (Perez-Perez et al, 2002). QTL analyses conducted in several RIL populations detected a large number of loci for leaf size and shape traits, as well as for epidermal cell number and size (reviewed in (Perez-Perez et al, 2010)). These growth traits are correlated and dependent not only to each other but also to the total number of leaves formed during the plants life cycle, which has been shown by co-localisation of QTLs and by structural equation modeling (SEM) in a RIL population with L*er* as one of the parental accessions (Tisne et al, 2008). Interestingly, a QTL linked to the *erecta* locus radically changed most of the growth relationships in the same study (Tisne et al, 2008).

1.6 The role of anthocyanins in UV-B protection and their regulation by the WD40/bHLH/R2R3MYB complex

Phenylalanine
↓ PAL
trans-Cinnamate
↓ C4H
4-Coumarate
↓ 4CL
4-Coumaroyl CoA
↓ CHS (*tt4*)
Chalcones
↓ CHI (*tt5*)
Flavanones → Flavones
↘ Isoflavones
↓ F3H
Dihydrokaempferol
↓ F3′H
Dihydroflavonols → Flavonols
FLS
↓ DFR
Leucoanthocyanidins → Proanthocyanidins
LAR
↓ LDOX
Anthocyanidins
↓ UGT
Anthocyanins

(early / late brackets at left of pathway)
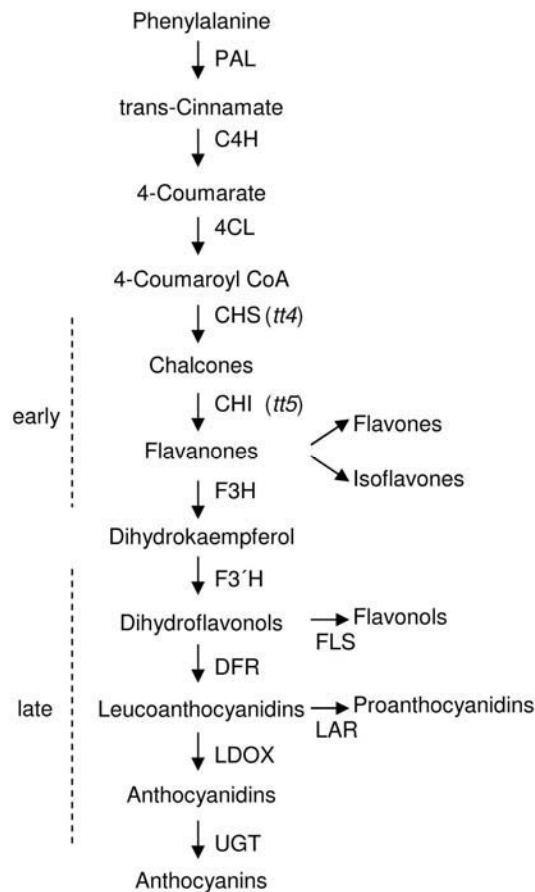
Figure 1.6. Simplified overview of the flavonoid biosynthetic pathway leading to anthocyanins. Arrows to the right depict branch points of the flavonoid pathway leading to flavones, isoflavones and flavonols. The diagramme follows the Arabidopsis flavonoid pathway described in the MetaCyc Database (Caspi et al, 2006). Arabidopsis early and late flavonoid biosynthetic pathway enzymes are categorized based on late genes being regulated by the WD40/bHLH/R2R3MYB complex (Gonzalez et al, 2008). PAL: phenylalanine ammonia lyase; C4H: cinnamate 4-hydroxylase; 4CL: 4-coumarate coenzyme A ligase; CHS: chalcone synthase; CHI: chalcone isomerase; FH3: flavanone 3β-hydroxylase; F3′H: flavonoid 3′- hydroxylase; FLS: flavonol synthase; DFR: dihydroflavonol 4-reductase; LDOX: leucoanthocynidin dioxygenase; tt4, 5: transparenta testa 4, 5; UGT: anthocyanidin 3-O-glucosyltransferase.

Anthocyanins are secondary metabolites generated by the flavonoid biosynthetic

pathway (Figure 1.6). Per definition, secondary metabolites do not play roles in essential, basic processes of growth and development and thus specific secondary metabolites generally show restricted distribution to certain taxonomic groups in the plant kingdom. Flavonoids have a basic structure of C6(A)-C3-C6(B) and are grouped based on the degree of oxidation of the carbon bridge and the position of the B phenol ring, for example, into flavones, isoflavones, flavonols, proanthocyanidines and anthocyanins. Anthocyanins are glycosylated and further modified at the B phenol ring by hydroxyl- and methoxyl-groups as well as at the glycosyl moieties (Tanaka et al, 2008).

Anthocyanins are most prominently known for their function as red, pink, purple and blue plant pigments which may both attract and repel animal species. Among further endogenous roles proposed for anthocyanins are protection of photolabile defence compounds, reduction of photoinhibition by absorbing excess photons, scavenging of free radicals, and enhancing resistance to osmotic stress imposed upon by various abiotic factors, like drought or chilling in (reviewed in (Gould, 2004)). A general role of anthocyanins in UV-B protection is discussed controversial (reviewed in (Close & Beadle, 2003; Harborne & Williams, 2000; Steyn et al, 2002)). While there are anthocyanins that do absorb strongly UV-B wavelengths, anthocyanins often contribute less to total UV-B absorbance. Further, anthocyanins are produced in many species in mesophyll cell layers and are absent from epidermal cell layers, and there are no general correlations between anthocyanin accumulation and UV-B exposure or UV-B resistance. *A. thaliana* mutants in the flavonoid biosynthetic pathway that responded sensitive to UV-B targeted early genes in the pathway (*tt4*, *tt5*; see Figure 1.6), which impair biosynthesis of several different flavonoid compounds (Li et al, 1993). Additionally, more definitive conclusions about the behaviour of anthocyanins in respect to UV-B exposure is hampered by experimental conditions that often poorly reflect biological situations (Kliebenstein, 2004). To date, the more general function ascribed to anthocyanins in UV-B protection is thought to be its protective role in photoinhibition induced upon UV-B exposure (Close & Beadle, 2003; Steyn et al, 2002), however, the difficulty to come to general conclusions about anthocyanin function in UV-B protection might be inherent in it being a secondary metabolite. Generally, a major role in UV-B protection is attributed to flavones and flavonols (for example kaempferol and quercetin) based on the above mentioned criteria (Harborne & Williams, 2000).

The biosynthetic pathway leading to anthocyanins is divided into early and late

biosynthetic steps on the basis of absence and presence, respectively, of transcriptional regulation by a specific WD40/bHLH/R2R3MYB module which has been shown in several species (Figure 1.3,) (Gonzalez et al, 2008). Recently it was shown in *A. thaliana* that GL3 and TTG1 directly regulate the expression of the late biosynthesis genes *F3´H*, *DFR* and *LDOX* (Figure 1.6) by overexpression of DEX-inducible fusion proteins in respective mutant backgrounds concomitant with CHX treatment (Gonzalez et al, 2008). The redundancy of the R2R3 MYB transcription regulators *PAP1*, *PAP2*, *MYB113*, and *MYB114* and their tight linkage precluded the same experiment, however it has been shown that downregulation of *PAP1* and its paralogs by RNAi lead to a reduction in expression of the late biosynthetic genes mentioned above, as well as of *UGT75C1*, one of the necessary glycosyltransferases converting anthocyanidins to anthocyanins (Figure 1.6). As a repressor of the WD40/bHLH/R2R3MYB complex in respect to flavonoid biosynthesis a single-repeat R3MYB like protein has been detected called MYB like 2 (Figure 1.4) (MYBL2; (Dubos et al, 2008; Kirik & Baumlein, 1996; Matsui et al, 2008)). MYBL2 is different to the single-repeat R3MYB family members in that it harbours a ~100 aa long carboxy-terminal domain which is important for its repressor activity, possibly due to the presence of an EAR-like repressor motif. Mutant and overexpression lines of *MYBL2* showed that it strongly represses the expression of the late biosynthetic genes *DFR* and *LDOX*, as well as to a lesser extent of *F3H* and *F3´H* (Figure 1.6). Yeast two-hybrid interaction tests showed that it interacts with GL3, EGL3 and TT8 and that it is able to counteract TT8/TT2 and EGL3/PAP1 mediated upregulation of DFR in transiently co-transformed protoplasts (Dubos et al, 2008; Matsui et al, 2008).

In *A. thaliana*, upon UV-B exposure an increase in transcription has been shown for the early biosynthetic genes coding for *PAL*, *CHS*, *CHI* but also for *DFR* in two studies (Figure 1.6) (Brown & Jenkins, 2008; Kubasek et al, 1992), whereas UV-B mediated upregulation of *DFR* could not be recapitulated in another study (Cominelli et al, 2008). However, Cominelli *et al.*, (2008) showed an induction of *DFR* and *LDOX* upon exposure to UV-A, which is preceded by transcriptional induction of *PAP1* and *PAP2,* as well as induction of the same genes by various other changes in light regimes.

1.7 Aim of the thesis

Trichome density is modulated in natural *A. thaliana* populations (Hauser et al, 2001; Symonds et al, 2005) and studies suggest that this may be of ecological significance (Handley et al, 2005; Mauricio, 1998; Mauricio & Rausher, 1997). To date, molecular regulation of natural variation in trichome density modulation is unknown, despite a wealth of knowledge of regulation of trichome initiation derived from classical genetic analyses (reviewed in (Ishida et al, 2008)). Therefore, this study aimed to characterize natural variation for trichome density in *A. thaliana* populations.

Pivotal for this aims was an F2 mapping population derived of two accessions selected due to their opposing extreme trichome density phenotypes, which was already established in the lab. Here, a QTL analysis describes the genomic architecture for trichome density modulation between these two accessions using the F2 mapping population. A major QTL was subjected to fine mapping and candidate genes annotated within the narrowed QTL candidate interval to further genetic, population genetic and functional analyses in order to isolate the molecular cause for trichome density modulation in natural *A. thaliana* populations. Further, trichome density between the two accessions was analysed in relation to intervening cells between trichomes to collect insight from the cellular level into the mechanism of trichome density modulation. Part of this work was published in (Hilscher et al, 2009).

In a second part, a pilot study was undertaken to search for natural variation in UV-B tolerance and anthocyanin content in *A. thaliana* and to start to investigate a possible role of non-secreting trichomes in UV-B tolerance.

2 MATERIALS AND METHODS

2.1 Chemicals

Chemicals were purchased from the companies Roth, Fluka, Merck and GibcoBRL, enzymes were purchased from MBI-Fermentas, Finnzymes, Invitrogen, New England Biolabs, and Roche, if not indicated otherwise.

2.2 Escherichia coli and Agrobacterium tumefaciens strains

The *E. coli* strains DH5α [*supE*44 Δ*lac*U169 (Φ80*lacZ* ΔM15) *hsdR*17 *recA*1 *endA*1 *gyrA*96 *thi*-1 *relA*1; (Sambrook & Russell, 2001)] and TOP10 [F- *mcr*A Δ(*mrr*-*hsd*RMS-*mcr*BC) Φ80*lacZ*ΔM15 Δ*lac*X74 *rec*A1 *ara*D139 Δ(*araleu*)7697 *gal*U *gal*K *rps*L (StrR) *end*A1 *nup*G; (Invitrogen)] were used for cloning. The *A. tumefaciens* strain GV3101::pMP90 with chromosomal background C58 was used for plant transformation (Koncz & Schell, 1986).

2.3 Plant material

A. thaliana accessions used were obtained from the Nottingham *Arabidopsis* Stock Centre (NASC) or were gifts from Philip Benfey, Gerd Jürgens, Ken Feldman, Karl Schmid, Hans Stenoien and Heike Schmuths. Details of *A. thaliana* accessions used are listed in Table 7.1. Ws *cpc-1* and L*er* t*ry-82* were a gift from Martin Hülskamp (Hülskamp et al, 1994; Wada et al, 1997). The SALK T-DNA insertion line (Alonso et al, 2003) Col *etc2* (NS40390) was obtained from NASC and the homozygous line Col *etc2* D5 was used in described experiments. It corresponds to *etc2-2* (Simon et al, 2007). The Gr-1×Can-0 mapping population is described in chapter 2.10.1.

2.4 General molecular biological methods

2.4.1 Polymerase chain reaction (PCR) with *Taq* polymerase

Reactions were performed in total volumes of 10 µl or 20 µl and were containing 1× PCR buffer (10 mM Tris/HCl pH 8.5, 50 mM KCl, 1.5–3 mM MgCl$_2$, 0.15% Triton X-100), 200 µM dNTPs, 10 pmol forward and reverse primer, 0.5 U of *Taq* polymerase and DNA template. Generally, approximately 10-20 ng gDNA and 50-100 pg plasmid DNA was used as template. Cycling conditions were specified according to

the nature of the PCR, and consisted of an initial denaturation step at 95 ℃ for 3 minutes, followed by 30-35 cycles each consisting of a denaturation step at 95℃ for 30 seconds, an annealing step at 50-60 ℃ for 30 seconds and an extension step at 72 ℃ for 30 seconds to 2 minutes.

2.4.2   DNA precipitation

DNA Precipitation using isopropanol

$1/10^{th}$ volume of 3 M sodium-acetate and 0.6^{th} volume of isopropanol was added to the sample, mixed and then centrifuged at 10,000 g for 20 minutes at 4 ℃. The supernatant was discarded and the pellet washed with 70% ethanol followed by centrifugation at 10,000 g for 15 minutes at 4 ℃. The supernatant was discarded, the pellet dried and finally taken up in dH_2O or TE buffer (10 mM Tris/HCl pH 7.4, 1 mM EDTA).

DNA Precipitation using ethanol

$1/10^{th}$ volume of 3 M sodium-acetate and 2.5× the volume of 96% ethanol was added to the sample, mixed and incubated for 20 minutes on ice. DNA was pelleted by centrifugation at 10,000 g for 20 minutes at 4 ℃. The supernatant was discarded and the pellet washed with 70% ethanol followed by centrifugation at 10,000 *g* for 15 minutes at 4 ℃. The supernatant was discarded, the pellet dried and finally taken up in dH_2O or TE buffer.

DNA Precipitation using polyethylenglycol (PEG)

In order to purify DNA from low molecular weight DNA (primers, etc.) PEG precipitation was carried out by addition of $1/10^{th}$ volume of 3 M sodium-acetate and an equal volume of 30% PEG 6000. After incubation for 15 minutes on ice the sample was centrifuged for 30 minutes, 10,000 *g*, and 4 ℃. The supernatant was discarded and the pellet washed with 70% ethanol. Finally, the pellet was resuspended in dH_2O or TE buffer.

2.4.3   Restriction enzyme digest of DNA

Restriction enzymes were used from Fermentas. Restriction digests were generally performed in 20 µl reactions containing the respective buffer and were incubated for at least 90 minutes at 37 ℃. If necessary, reactions were stopped by heat inactivation according to the manufacturer's instructions. The restriction enzyme

amount for a given digest was calculated from the molar amount of DNA used, the number of cutting sites and the unit definition of the respective restriction enzyme.

2.4.4 Dephosphorylation of DNA sticky-end termini

Shrimp alkaline phosphatase (SAP; Roche) was used for dephosphorylation of vector DNA linearized by a single restriction enzyme in order to prevent vector religation. Dephosphorylation reactions were adjusted with 1/10 volume of 10× dephosphorylation buffer (0.5 M Tris/HCl, 50 mM $MgCl_2$, pH 8.5) and the appropriate SAP unit amount according to the present molar amount of DNA termini. Reactions were incubated at 37 ℃ for 1 hour and stopped at 65 ℃ for 15 minutes.

2.4.5 Phosphorylation of DNA 5´-termini

Rephosphorylation of plasmid DNA 5´-termini

In order to test cut and dephosphorylated target vector for its ability of ligation (i.e. for intact DNA termini) plasmids were rephosphorylated and subsequently ligated. T4 Polynucleotide Kinase (T4 PNK; Fermentas) was used for phosphorylation of DNA 5´-termini. Phosphorylation reactions were done in 20 µl reactions containing 1× Reaction Buffer A (50 mM Tris-HCl pH 7.6, 10 mM $MgCl_2$, 5 mM DTT, 0.1 mM spermidine and 0.1 mM EDTA), 1 mM rATP, 5 U T4 PNK and 50 ng of cut and dephosphorylated plasmid DNA. Reactions were incubated at 37 ℃ for 1 hour and stopped at 65 ℃ for 20 minutes.

Phosphorylation of primer DNA 5´-termini

Reactions were done in 50 µl containing 300 pmol primer, 1 × Reaction Buffer A (50 mM Tris/HCl pH 7.6, 10 mM $MgCl_2$, 5 mM DTT, 0.1 mM spermidine and 0.1 mM EDTA), 1 mM rATP and 10 U T4 PNK. The reaction was incubated at 37 ℃ for 30 minutes and inactivated at 65 ℃ for 20 minutes. Phosphorylated primers were stored at -20 ℃.

2.4.6 DNA ligation

Ligation reactions were done in 20 µl volume containing 1× Reaction Buffer A (50 mM Tris/HCl pH 7.6, 10 mM $MgCl_2$, 5 mM DTT, 0.1 mM spermidine and 0.1 mM EDTA) or 1 × Ligation buffer (40 mM Tris-HCl pH7.8, 10 mM $MgCl_2$, 10 mM DTT, 0.5 mM ATP), both supplemented with 1 mM rATP, 3 Weiss U of T4 DNA Ligase

(Fermentas) and a 3:1 to 10:1 molar ratio of insert:vector. Generally, 50 ng of vector DNA was used for one ligation reaction. Reactions were incubated at 22 °C for at least 1 hour to overnight and subsequently used for transformation or stored at -20 °C. Alternatively, ligation reactions were carried out using the Quick Ligation™ Kit (NEB) according to manufacturere´s instructions.

2.4.7 TOPO® cloning

For fast subcloning without the need of digestion of PCR amplicons TOPO TA Cloning® Kit for Sequencing (Invitrogen) was used. Amplicons were cloned into the vector pCR®4-TOPO® after manufacturer's instructions, with the exception that 5 ng pCR®4-TOPO® vector was used and the TOPO reaction was transformed into smaller aliquots of purchased TOP10 chemically competent cells where applicable. In case PCR amplicons were derived from a polymerase with proofreading activity, 3´A overhangs were added to the either purified or non-purified amplicon by incubation in the presence of 1× PCR buffer supplemented with 1.5 mM MgCl$_2$, 200 µM dATP and 0.5 U *Taq* polymerase at 72 °C for 10 minutes.

2.4.8 Agarose gel electrophoresis of DNA

Samples were mixed with 6× loading solution (Fermentas; 10 mM Tris/HCl pH 7.6, 0.03% (w/v) bromophenol blue, 0.03% (w/v) xylene cyanol, 60% (v/v) glycerol, 10 mM EDTA). Depending on amplicon size, agarose gels in the range of 0.8-2% (w/v) agarose in 1× TAE (40 mM Tris, 5.71% (v/v) acetic acid, 1 mM EDTA) supplemented with 0.5 µg/ml ethidiumbromide were run in 1× TAE at a speed of 5 Vcm^{-1}.

2.4.9 DNA isolation from agarose gels

DNA isolation using the "Freeze-Squeeze" method

The gel slice containing DNA was frozen at -80 °C for 30 minutes, or alternatively, two hours to overnight at -20 °C. The sample was then centrifuged at 10,000 g for 30 minutes at 4 °C. The supernatant was transferred to a new tube, ethanol precipitated and finally resuspended in dH$_2$O.

DNA Isolation using commercial kits

Commercial kits used were QIAEX® II Gel Extraction Kit (QIAGEN) and Silica Bead

DNA Gel Extraction Kit (Fermentas). Extraction was done according to manufacturer's instructions. In general, DNA elution from silica particles was done with two repetitions of 20 µl and 10 µl dH$_2$O.

2.4.10 Sanger sequencing of DNA

DNA was sequenced using using ABI Prism Dye Terminator Cycle Sequencing Kit (Applied Biosystems). For sequencing of DNA templates, 200-500 ng of plasmid DNA or 5-50 ng of PCR amplicons (according to fragment size; see ABI Prism Dye Terminator Cycle Sequencing Kit manual; Applied Biosystems) was used. Template DNA and 6 pmol primer was added to 4 µl DYEnamic ET Dye Terminator sequencing chemistry (GE Healthcare) and the reaction was cycled in a total volume of 20 µl using the following parameters: 24 cycles consisting each of 96 °C for 30 seconds, 50 °C for 15 seconds and 60 °C for 4 minutes. Reactions were ethanol precipitated and dried. Sequencing reactions were sent for analysis on an ABI Prism 3100 Genetic Analyser (Applied Biosystems). Obtained sequence data were assembled and edited using the SeqMan^{TM} II software (DNASTAR, Inc.).

2.4.11 Media and growth conditions of bacterial cells

E. coli was grown in liquid YT medium (1% (w/v) yeast extract, 1% (w/v) peptone, 256 mM NaCl) or LB medium (0.5% (w/v) yeast extract, 1% (w/v) peptone, 512 mM NaCl) with shaking (180 rpm on rotary platform) or on solid YT or LB medium (media containing 1.5% (w/v) agar), both supplemented with appropriate antibiotics (Table 2.1), at 37 °C overnight. *A. tumefaciens* was grown in liquid YT or LB medium with shaking (120 rpm at a rotary platform) or on solid YT medium, both supplemented with appropriate antibiotics (Table 2.1) at 28 °C for 12-60 hours.

Table 2.1 Antibiotics used for selection of bacterial cells

E. coli

Selection for	Antibiotic	Stock solution	Solvent	Working concentration
pCR®4-TOPO® [1]	Ampicillin	100 mg/ml	dH2O	100 mg/l
pCR®4-TOPO® [1]	Kanamycin	100 mg/ml	dH2O	50 mg/l
pPZP211, pPZP221 [2]	Spectinomycin	50 mg/ml	dH2O	100 mg/l
pBIC20 [3]	Tetracyclin	15 mg/ml	50% EtOH	15 mg/l

A. tumefaciens

Selection for	Antibiotic	Stock solution	Solvent	Working concentration
pTiC58ΔT-DNA [4]	Gentamycin	50 mg/ml	dH2O	50 mg/l
A. tumefaciens genomic background C58 [4]	Rifampicin	25 mg/ml	DMSO	100 mg/l
pBIC20 [3]	Kanamycin	100 mg/ml	dH2O	50 mg/l
pPZP211, pPZP221 [2]	Spectinomycin	50 mg/ml	dH2O	100 mg/l

1: Invitrogen; 2: (Hajdukiewicz et al, 1994); 3: (Meyer et al, 1996); 4: (Koncz & Schell, 1986).

2.4.12 Production and transformation of chemical competent *E. coli* cells after Chung and Miller

A single colony of *E. coli* DH5α was inoculated in 5 ml YT medium and was grown at 180 rpm on a rotary platform overnight at 37 °C. The overnight culture was diluted 1:1000 in 50 ml of YT medium and grown to an OD_{600} of 0.3-0.6 at 180 rpm, 37 °C (early log phase). The cell suspension was harvested by centrifugation in 50 ml Falcon tubes at 5600 rpm (Heraeus Christ Minifuge, Rotor 816) for 10 minutes at 4 °C. The cell pellet was carefully resuspended in 2.5 ml of cold TSB medium (YT medium containing 9.5% (w/v) PEG 4000, 5% (v/v) DMSO, 0.1 mM $MgCl_2$ and 0.1 mM $MgSO_4$) and incubated on ice for 10 minutes. Aliquots of 100 µl were snap frozen in liquid N_2 and stored at -80 °C.

100 µl of competent cells were thawed on ice and mixed with 100 µl 1× KCM buffer (0.1 M KCl, 0.03 M $CaCl_2$, 0.03 M $MgCl_2$) containing approximately 10 ng of plasmid DNA or ligation reactions to be transformed and incubated for 30 minutes on ice. Following a heat shock at 42 °C for 90 seconds the transformation reaction was cooled on ice for 1-2 minutes. After addition of 800 µl YT medium it was incubated

at 180 rpm on a rotary platform for 50 minutes at 37℃. Finally, the transformation reaction was plated on YT plates supplemented with the appropriate antibiotic.

2.4.13 Blue-White colour screening of transformed *E. coli* cells

For blue-white colour screening for inserts 20 µl X-Gal (50 mg/ml) and 2.5 µl IPTG (100 mg/ml) were added to 100 µl YT liquid medium and spread on selective YT plates prior to plating of transformed *E. coli* DH5α cells.

2.4.14 Stock cultures of bacterial cells

One ml of overnight culture was mixed with 400 µl 86% glycerol, snap frozen in liquid N_2 and stored at -80 ℃.

2.4.15 Plasmid DNA mini preparation from *E. coli*

Single clones were inoculated in 5 ml YT medium supplemented with the appropriate antibiotic and grown overnight at 37 ℃ at 180 rpm on a rotary platform. 3 ml overnight culture were harvested by centrifugation at 10,000 *g* for three minutes, resuspended in 200 µl GTE solution (50 mM glucose, 10 mM EDTA, 25 mM Tris/HCl pH 8.0) and incubated for five minutes at room temperature. For cell lysis, 400 µl alkaline SDS solution (0.2 N NaOH, 1% SDS) was added, mixed by several inversions of the tube and incubated on ice for 5-10 minutes. The sample was neutralized by addition of 300 µl 3 M sodium-acetate pH 4.8, mixed immediately by several inversions of the tube and incubated on ice for 10 minutes. Afterwards, the sample was centrifuged at 10,000 *g* for 15 minutes at 4 ℃, followed by transfer of the supernatant to a fresh tube. Plasmid DNA was isopropanol precipitated and dissolved in 20 µl dH_2O supplemented with 2 µl RNaseA (10 mg/ml).

2.4.16 Plasmid DNA midi preparation from *E. coli*

For Plasmid DNA midi preparation a single colony was inoculated in 20 to 100 ml (high and low copy plasmids, respectively) YT medium supplemented with the appropriate antibiotic and grown at 180 rpm on a rotary platform overnight at 37 ℃. Plasmid purification was done using NucleoBond® Xtra Midi Kit (Macherey-Nagel) following manufacturer's instructions. Plasmid DNA was resuspended in 100 µl dH_2O. Plasmid yield was quantified using agarose gel electrophoresis.

2.4.17 Preparation and transformation of electrocompetent *A. tumefaciens* cells

6 ml LB medium containing the appropriate antibiotics were inoculated with a single *A. tumefaciens* colony and incubated at 120 rpm on a rotary platform overnight at 28 °C. Next day, 500 ml of LB selection medium was inoculated with five ml of the overnight culture and grown to an OD_{600} of 0.6-0.8. Starting from this stage, every step was done on ice and with cold solutions: cells were transferred into 50 ml Falcon tubes, chilled on ice for 15 minutes and pelleted at 4000 g for 15 minutes at 4 °C. The supernatant was discarded and the cells were resuspended in 250 ml sterile dH_2O. The centrifugation step was repeated three times, and the cells were resuspended subsequently in 25 ml sterile dH_2O, 2 ml sterile dH_2O, and 2 ml sterile 10% glycerol. Finally, aliquots of 100 µl of cells in 10% glycerol were snap frozen in liquid N_2 and stored at -80 °C.

For electroporation, cuvettes were sterilized by treatment with 6000× 100 µJ (254 nm) in a cross linker. After electroporation, they were cleaned by incubation in dH_2O containing 1% TritonX-100 for 30 minutes followed by incubation in 0.25 N HCl for 30 minutes. In between incubation steps cuvettes were rinsed with dH_2O, finally incubated in 96% ethanol for 5 minutes and left to dry.

For electroporation, 100 µl aliquots of competent cells were thawed on ice, mixed with approximately 100 ng plasmid DNA and transferred to cuvettes. Electroporation was carried out with BIO-RAD MicroPulser Electroporation system at 2.45 kV, 25 µF and 200 ohm. Under ideal conditions the time constant is between 4.4–4.8 ms. After electroporation, the cells were transferred back to Eppendorf tubes, mixed with 700 µl YT medium and incubated at 120 rpm on a rotary platform for one hour at 28 °C in darkness. Finally, cells were plated on appropriate selective plates.

2.4.18 Plasmid DNA mini preparation of *A. tumefaciens*

The protocol is adapted after Li, Stahl and Brown (Li et al, 1995). Single *A. tumefaciens* colonies were inoculated in 5 ml YT medium supplemented with appropriate antibiotics and grown overnight at 120 rpm on a rotary platform at 28 °C. 4 ml overnight culture was harvested by centrifugation at 10,000 g for 5 minutes, resuspended in 200 µl GTE solution and incubated for 5 minutes at room temperature. For cell lysis, 400 µl alkaline SDS solution was added, mixed by several inversions of the tube and incubated for 15 minutes on ice. The solution was

neutralized by addition of 300 µl 5 M K/3 M acetate solution pH 4.8, mixed immediately by several inversions of the tube and incubated for 30 minutes on ice. After centrifugation at 10,000 g for 15 min at 4 °C to pellet cell debris and transfer of the supernatant to a fresh tube the plasmid prep was further purified by addition of 500 µl of phenol/chloroform/isoamylalcohol (24/24/1) solution and subsequent mixing for one minute. Centrifugation at 10,000 g for 5 minutes lead to phase separation of organic and aqueous phases and the aqueous supernatant was transferred to a new tube. Plasmid DNA was isopropanol precipitated and the dried pellet was resuspended in 20 µl of TE buffer supplemented with 2 µl RNaseA (10 mg/ml).

2.5 RNA methods

2.5.1 Total RNA isolation

Total RNA isolation was done using TRI Reagent[®] (MRC) after the manufacturer´s instructions. Generally, 50-100 mg plant tissue was sampled, quickly snap frozen in liquid N_2 and stored at -80 °C. After isolation, RNA was taken up in ddH_2O and stored at -80 °C. Quantification and quality check of RNA was done by UV spectrophotometry (Beckmann DU 640 Spectrophotometer) and agarose gel electrophoresis, respectively.

2.5.2 Reverse Transcriptase (RT) PCR

Reverse transcription was carried out with SuperScript[TM] Reverse Transcriptase (Invitrogen) using 2 µg of total RNA. Prior to the reverse transcription reaction, a DNaseI digest was carried out in a 7.25 µl volume containing 2 µg of total RNA, 1 mM $MgCl_2$ and 3 U DNaseI (RNase free, Roche) at 37 °C for 30 minutes. The reaction was stopped at 75 °C for 10 minutes and put on ice. In a final volume of 15 µl containing 1× First-Strand Buffer (Invitrogen), 1mM dNTPs, 10 mM DTT, 2.5 µM $d(T)_{18}$ and 200 U M-MLV Reverse Transcriptase (Invitrogen) the DNaseI digested total RNA was reverse transcribed by incubation at 37 °C for 1 hour and the reaction was stopped by incubation at 95 °C for 5 minutes. The resulting cDNA was diluted 1:10 with ddH_2O and stored aliquoted at -20 °C. Generally, 1 µl of the diluted cDNA was used for PCR or quantitative real-time PCR reactions.

2.5.3 Quantitative real-time PCR

Primers used are listed in Table 7.4. Quantitative real-time PCR was done using SYBR$^{®}$ Green I (Roche) for detection and using the principle of relative quantification, with *UBIQUITIN5* (*UBQ5*) and *TUBULIN9* (*TUB9*) as standard reference genes.

Real-time PCR reactions were done in a total volume of 20 µl containing 1× PCR buffer (10 mM Tris/HCl pH 8.5, 50 mM KCl, 2 mM MgCl$_2$, 0.15 % Triton X-100), 200 µM dNTPs, 5 pmol forward and reverse primer, 1 U of *Taq* polymerase (Fermentas), 1 µl of SYBR$^{®}$ Green I (Roche) and 1 µl cDNA template (1:10 diluted; see chapter 2.5.2). The reactions were cycled in a Rotor-Gene 2000 or 3000A machine (Corbette Research) using the following parameters: an initial step at 94 ℃ for 90 seconds, followed by 30 cycles each consisting of 94 ℃ for 10 seconds, 55 ℃ for 5 seconds and 72 ℃ for 10 seconds. Fluorescence was captured after each extension step for 1 second at 72 ℃, 81 ℃ and 84 ℃. Finally, a melting curve was measured ranging from 65 ℃ to 99 ℃.

2.6 Plant methods

2.6.1 Plant growth conditions

Non-selective growth conditions

All seeds were plated on MS 4.5% sucrose media (1× Murashige and Skoog basal salt mixture (Sigma), 1% agar (Fluka), 4.5% sucrose, pH 6.7) as described in (Hauser et al, 1995). Briefly, seeds were sterilized in 5% sodium-hypochlorite supplemented with 1 drop Tween-20 per 5 ml solution for three minutes. Afterwards, seeds were washed twice with dH$_2$O, taken up in 1% low melting agarose and plated on MS plates. After stratification for one week at 4 ℃ seeds were cultivated under constant light at 22 ℃. Approximately 14 DAG seedlings were transferred to soil (1:1 mixture of soil with perlite) and grown in a chamber under long day conditions (16 hrs light (75 µEinstein m^{-2} s^{-1})/8 hrs dark cycles) at 20 ℃.

Selective growth conditions

T$_0$ and T$_1$ or T$_2$ seeds of transgenic *A. thaliana* plants were plated on MS 1% and MS 4.5% sucrose plates, respectively, supplemented with 100 µg/ml kanamycin and gentamycin for binary vector transformants with pPZP211 and pPZP221

(Hajdukiewicz et al, 1994), respectively, and on MS plates supplemented with 100 µg/ml kanamycin for transformants with pBIC20 (Meyer et al, 1996) transformants.

2.6.2 Quick genomic plant DNA mini preparation

The quick genomic DNA Miniprep protocol used was adapted by Farhah Assaad from Rogers and Bendichs CTAB based protocols. Briefly, plant material the size of a small leaf was harvested and stored at -20 ℃. For isolation, the tissue was ground in liquid nitrogen (N_2). The ground tissue was resuspended in 200 µl 2✕ CTAB buffer (2% (w/v) hexadecylammoniumbromid, 100 mM Tris, 20 mM EDTA, 1.4 M NaCl, 1% (w/v) polyvinylpyrrolidon, pH 8.0) and incubated for a minimum of 5 min at 65 ℃. 1✕ volume of chloroform was added, the sample was mixed and centrifuged for two minutes, 10,000 g to separate organic and aqueous phases. The upper aqueous phase was transferred to a new tube and gDNA was isopropanol precipitated. The dried pellet was resuspended in 50 µl dH_2O supplemented with 2 µl RNaseA (10 mg/ml).

2.6.3 Transformation of *A. thaliana*

Transformation of *A. thaliana* was following the floral dip protocol after Clough and Bent (Clough & Bent, 1998). 2 ml of YT selection medium were inoculated with a single colony of *Agrobacterium tumefaciens* in 50 ml Falcon tubes and grown at 120 rpm overnight at 28 ℃. In the morning the overnight culture was diluted to 10 ml using the same selection medium and was grown at 120 rpm and at 28 ℃ to a dense culture until evening. Prior to dipping, the culture was filled up to 50 ml with dH_2O and supplemented with 8% (w/v) sucrose and 0.03% (v/v) Silwet L-77. Generally, five plants were dipped sequentially into the culture for 10 minutes with occasional stirring, after which they were put into a humid chamber for overnight incubation. The following day plants were transferred to a growth chamber and cultivated under described conditions (chapter 2.6.1).

2.7 Quantitative phenotyping and definition of phenotypic traits

Trichome patterning and leaf size and morphology traits

Phenotypic measurements were carried out on one symmetrical half of leaf blades and where necessary, extrapolated to the whole leaf; analyses involving palisade

mesophyll cell traits corresponding second halves of the leaf blades were used for phenotyping mesophyll cell parameters. Leaves were removed, put on glass slides and photographed with a digital camera mounted on a stereomicroscope (Leica MZ FLIII) to visualize trichomes. Leaves were then fixed with adhesive tape to paper, scanned (300 dpi, grayscale) and saved in tiff format.

Trichome number was counted using the point selection tool in ImageJ. Leaf area was measured of binary pictures converted from grayscale scans using ImageJ´s wand tool with a set measurement scale. Leaf width and length were measured directly from the taped leaves using a ruler, where both parameters represent the largest distance on leaf blades along and perpendicular to the midrib, respectively. Further traits are derived from above measurements: trichome density was derived by division of trichome number by leaf area, trichome number at leaf edges corresponds to trichomes counted directly at leaf edges divided by trichome number, heteroblasty of trichome number corresponds to the increase k of trichome number from leaf to leaf derived by linear regression and leaf index is derived by the division of leaf length by leaf width.

Palisade mesophyll cell traits

Leaves were removed and incubated in 20% methanol, 0.24 N HCl for 15 minutes at 57 ℃, followed by incubation in 7% NaOH, 60% ethanol for 15 minutes at room temperature. Subsequently, leaves were incubated in a rehydration series of 70%, 40%, 20% and 10% ethanol, and finally mounted in 50% glycerol on microscope slides. Pictures were taken with a Nikon D70 digital camera mounted on an inverted Axiovert microscope (Zeiss).

The number of palisade mesophyll cells per 0.135 mm^2 or 0.03375 mm^2 was counted and mesophyll cell density was defined as the number of mesophyll cells per mm^2. Of this parameter mesophyll cell number per leaf, mesophyll cells per trichomes, mesophyll cell area and diameter were derived by calculations.

Flowering time traits

Flowering time was recorded as the rosette leaf number of the primary shoot apical meristem prior to the initiation of a flowering meristem, designated as leaf number at flowering, and as the number of days to initiate a visible flowering meristem, designated as days to flowering.

2.8   Anthocyanin measurement using spectrophotometry

Green tissue was sampled, weighed and immediately frozen in liquid N_2. Samples were stored at -80 °C. For anthocyanin extraction, samples were ground to powder under cooling with liquid N_2, followed by addition of 500 µl extraction solution (1% (v/v) HCl in methanol) per 200 mg sample and samples were incubated at 4 °C overnight with shaking. After diluting the samples with dH_2O to reach a final concentration of 60% methanol, the samples were extracted from cell debris by vortexing with an equal volume of chloroform. After centrifugation at 10,000 g the aqueous supernatant was transferred to a new tube. Samples were measured at 530 nm and 657 nm with a spectrophotometer (BIO-RAD Smart Spec TM 3000) and anthocyanin absorbance units were calculated as $[A_{530} - A_{657}]$ g^{-1} fresh weight; values were multiplied ×1000 for better visualization.

2.9   Marker analysis

Primer sequences for marker analysis can be found in Table 7.2.

2.9.1   Native polyacrylamide (PAA) gel electrophoresis of DNA

Native polyacrylamide gel electrophoresis for marker analysis was done using Protean[TM] Dual Vertical Slab Gel Electrophoresis Cell (BIO-RAD). Gels (1.5×90×130 mm) were cast as either 5% or 8% PAA (19:1 acrylamide:bisacrylamide) gels containing 1× TBE (89 mM Tris/HCl, 89 mM boric acid, 2 mM EDTA, pH 8.0) and 1.075% (v/v) glycerol, polymerization was started with addition of TEMED and APS to a final concentration of 0.04% (v/v) and 0.09% (w/v), respectively. Samples were mixed with 6× loading solution (Fermentas) and gels were run in 1× TBE first at 150 V with cooling, after samples had migrated into the gel at 200 V with cooling for approximately 100 minutes. After the run gels were stained with ethidiumbromide solution (1 µg ethidiumbromide/ml dH_2O) for 10 minutes and documented under a transilluminator.

2.9.2   Heteroduplex analysis

Heteroduplex analysis followed the protocol by Hauser et al., (Hauser et al, 1998). For Heteroduplex analysis the PROTEAN® II xi Cell (BIO-RAD) was used. Gels (0.75×160×200 mm) were based on MDE[TM] gel solution (1× MDE (Cambrex), 0.6×

TBE, 2.5 M urea) and polymerization was started by addition of TEMED and APS to a final concentration of 0.06% (v/v) and 0.09% (w/v), respectively. Samples were prepared as follows: 50-100 ng of PCR amplicons in a 5 µl volume were transferred into Eppendorf tubes, covered with mineral oil and incubated on a heating block at 95 °C for 5 minutes. Afterwards, the metal block was put at room temperature, upon reaching approximately 37 °C the samples were mixed with 1 µl Triple Dye (50% (w/v) sucrose, 0.6 % (w/v) bromophenol blue, 0.6 % (w/v) xylene cyanol, 0.6 % (w/v) Orange G) and loaded. MDE Gels were run with 0.6× TBE for approximately 4,800 Vh at a maximum of 500 V. After the run gels were stained with ethidiumbromide solution (1 µg ethidiumbromide/ml dH$_2$O) for 10 minutes and documented under a transilluminator.

2.9.3 Denaturing polyacrylamide (PAA) gel electrophoresis of radioactively labelled DNA

Denaturing PAA gel electrophoresis of radioactively labelled DNA followed procedures described in (Schlötterer et al, 1999).

Labeling reaction of primers

To ^{32}P-end-label primers using T4 polynucleotide kinase (PNK; Fermentas), 20 pmol of primer were incubated in the presence of 1× PNK buffer (Fermentas) and 5 U T4 PNK with 1 µl γ^{32}-ATP in a total volume of 5 µl at 37 °C for 30 minutes. The reaction was stopped by incubation at 96 °C for 2 minutes.

PCR conditions

Reactions were performed in 10 µl containing 1× BioTherm^{TM} buffer (supplemented with 1.5 mM MgCl$_2$), 0.2 U BioTherm^{TM} *Taq* polymerase, 10 pmol forward and reverse primer, 200 fmol ^{32}P-end-labeled forward primer, 200 pmol dNTPs and approximately 1-20 ng of DNA template. Reactions were overlaid with paraffin oil. Cycling conditions were as follows: an initial step at 94 °C for 3 minutes, 32 cycles consisting each of 94 °C for 50 seconds, 50-60 °C (depending on primer pair) for 50 seconds and 72 °C for 50 seconds, and a final elongation step at 72 °C for 45 minutes.

Preparation of size standard

The following procedure was used to produce a ^{32}P-end-labeled size standard containing bands corresponding to 254 b and 142 b in length. First, the primer M13-40 was ^{32}P-end-labeled in a final volume of 5 µl in the presence of 1× PNK buffer

(Fermentas), 3 U PNK and 1 µl of γ^{32}-ATP at 37 °C for 30 minutes. The reaction was stopped at 95 °C for 2 minutes. The labelling reaction was added to a PCR reaction, further containing 1× PCR buffer (300 mM KCl, 50 mM Tris-HCl pH 9.0, 100 mM MgCl$_2$, 1% (v/v) Triton-X100, 1.5 mM MgCl$_2$), 50 pmol M13-48R primer, 50 pmol M13-243-r primer, 10 pmol dNTPs and 20 ng of M13mp19 DNA template in a total volume of 50 µl. The cycling conditions were as follows: an initial step at 94 °C for 3 minutes, 30 cycles each consisting of 94 °C for 50 seconds, 50 °C for 50 seconds and 72 °C for 50 seconds, and a final elongation step at 72 °C for 5 minutes. The PCR product was diluted 1:20 and 2 µl were used for loading on gels.

Denaturing PAA gel electrophoresis

Denaturing PAA gels were prepared containing 7% PAA (19:1 acrylamide:bisacrylamide), 32% formamide, 5.6 M urea and 1× TBE. Polymerization was started by adding APS and TEMED to a final concentration of 0.1% (w/v) and 0.06% (v/v), respectively. 1× TBE was used as buffer system. Gels were prerun at 95 V for 30 minutes, prior to loading samples were mixed with 5 µl of loading dye (95% formamide, 20 mM EDTA, 0.05% (w/v) bromophenol blue, 0.05% (w/v) xylene cyanol), loaded on the gel and run at 95 V for 2-3 hours. After the run the PAA gel was mounted onto Whatman paper, wrapped in plastic foil and exposed to film at -20°C for 2 days.

2.10 QTL analysis

2.10.1 Mapping population

An F2 mapping population derived by the cross Gr-1×Can-0 and subsequent selfing of the F1 generation was already established in the lab.

2.10.2 Growth conditions of parental accessions and mapping population individuals

Seeds were sterilized and plated on MS 4.5% sucrose media as described in chapter 2.6.1. After stratification for two days and one week at 4 °C, for mapping population individuals and parental accessions, respectively, seedlings were cultivated under constant light at 22 °C for 14 days. Seedlings were transferred to soil (1:1 mixture of soil with perlite) and grown for four weeks under long day conditions (16 hrs light (75 µEinstein m^{-2} s^{-1})/8 hrs dark cycles) at 20 °C.

2.10.3 Estimation of broad-sense heritability H^2

Broad-sense heritability (H^2) was calculated as V_G/V_P and $V_P=(V_G+V_E)$, where V_G, V_P and V_E are genetic, phenotypic and environmental variation, respectively. V_E was estimated by averaging the parental trait variance and V_G was estimated by subtracting the average parental trait variance from the variance of the F2 mapping population (as an estimate of phenotypic variation).

2.10.4 Construction of the genetic map

The genetic map for QTL mapping was obtained with the module Emap implemented in WinQTL Cartographer (Wang et al, 2005). It is based on 266 F2 mapping population individuals genotyped with 24 microsatellite markers (primer sequences can be found in Table 7.2). Kosambi mapping function was used to convert recombination frequencies to centimorgan distances (Kosambi, 1944).

At the population level the segregation ratio of the parental alleles was close to that expected (Can-0/Gr-1 = 48%/52%). There was no segregation distortion detected at any marker ($P>0.05$; chi-square test) after Bonferroni-correction for multiple testing. All markers were assigned to the expected linkage group in the expected order. The five linkage groups represent a total of 263 cM. The average genetic distance between two adjacent markers is 10.97 cM, with a maximum distance of 26 cM and a minimum of 2 cM.

2.10.5 QTL mapping

All traits measured in the F2 mapping population (n=266) were normally distributed ($P>0.05$; One-Sample Kolmogorov-Smirnov test), except trichome density, which was ln-transformed to achieve normality, and edge trichomes. The flowering time traits days to flowering and number of leaves at day of flowering were measured on a subset of 140 F2 mapping population individuals and were also normally distributed ($P>0.05$; One-Sample Kolmogorov-Smirnov test).

The software package WinQTL Cartographer version 1.17e (Wang et al, 2005) was used to identify and locate QTLs on the linkage map using composite interval mapping (CIM; (Zeng, 1993; Zeng, 1994)). CIM performs interval mapping while statistically accounting for QTL located outside the tested interval by fitting background markers in the statistical model which were determined independently

for each trait by forward selection-backward elimination stepwise regression. A 3 cM scan window was used for all analyses and the likelihood ratio (LR0) test statistic, comparing the two hypotheses of there being a QTL present versus there being no QTL present, was calculated every 2 cM. 95% significance thresholds for QTL identification were determined for each trait separately by permutation test (Churchill & Doerge, 1994). For each trait 1000 permutations were performed.

2.10.6 Fine mapping

Primer sequences used for fine mapping are listed in Table 7.2 and the strategy is described in the result section (chapter 3.1.5).

2.11 Genomic *A. thaliana* (L*er*) library screen for contigs of the major QTL candidate interval of chromosome 2

Briefly, midi preparations of subpools of a genomic cosmid library were screened by PCR for pools containing sought after genomic regions. Positive pools were then plated, colonies were transferred to nylon membranes and screened for clones with the desired insert by using the Digoxigenin (DIG) DNA Labeling and Detection Kit (Roche).

2.11.1 L*er* Cosmid library description and PCR screen of the subpools

The *A. thaliana* genomic library used for isolating genomic regions located in the QTL candidate interval was a gift of Erwin Grill (Meyer et al, 1994). It was constructed using the Landsberg *erecta* genome and consists of three genome equivalents inserted as 10-25 kb *Hind*III fragments in the binary vector pBIC20 (Meyer et al, 1996) and is split in 41 subpools.

To search the library pools for clones harbouring genomic regions located in the QTL candidate interval, midi preparations of the library pools were screened with primers designed to probe for locations covering the QTL candidate interval approximately every 15 kb in distance. Primer sequences and the distribution of clones in the 41 pools are listed in Table 7.3 and shown in Fig. Figure 7.1, respectively.

2.11.2 Digoxigenin (DIG) labeling and quantification of probes

DIG DNA Labeling and Detection Kit (Roche) was used to produce probes labelled with DIG-11-dUTP by asymmetric PCR. Defined PCR amplicons were used as templates to generate probes. PCR reactions were carried out in a total volume of 100 µl and were containing 1× PCR buffer supplemented with 1.5 mM MgCl$_2$, 20 µM dATP, dCTP, and dGTP, 13 µM dTTP, 7 µM DIG-11-dUTP, 250 pmol primer and 2 µl of *Taq* polymerase. Standard PCR cycling conditions as described were used with the exception that the cycle number was increased to 40.

Quantification of labelled probes was done by comparison of a dilution series of the probe (1:50 to 1:50,000 in tenfold steps) and a DIG-labelled Control DNA (Roche; 5 ng/µl digoxigenin labelled DNA). 2 µl of each dilution were spotted on a nylon membrane and cross-linked (1200× 100 µJ, 254 nm). The membrane was incubated subsequently in 1× maleic acid buffer (100 mM maleic acid, 150 mM NaCl, pH 7.5) for 5 minutes on a rocker platform and in 1× blocking solution (1× Blocking reagent (Roche) in 1× maleic acid buffer) for 5 minutes. Following incubation with Anti-Digoxigenin-AP Antibody Conjugate (Roche; 1:10,000 in blocking solution) for 10 minutes the membrane was washed twice with maleic acid buffer for 5 minutes and subsequently incubated with detection buffer (100mM NaCl, 100 mM Tris-HCl, pH 9.5) for 5 minutes. The membrane was incubated with CSPD$^{®}$ ready-to-use substrate solution (Roche) for 5 minutes, enclosed in a plastic membrane and exposed to an X-ray film for approximately 30-45 minutes at 37 ℃.

2.11.3 Colony lift

Nylon membranes for Colony and Plaque Hybridization (Ø 132 mm; Roche) were placed on cooled (30 min at 4℃) agar plates (Ø 132 mm diameter; containing approximately 1,400 colonies) for 1 minute and marked by orientation. Then, nylon membranes were incubated subsequently on whatman filter paper soaked with denaturation solution (0.5 N NaOH, 1.5 M NaCl), neutralization solution (1.5 M NaCl, 1 M Tris/HCl, pH 7.4) and 2× SSC (300 mM NaCl, 30 mM Na$_3$Citrate, pH 7.0) for 15, 15 and 10 minutes, respectively. In between, nylon membranes were dried by placing on Whatman filter paper. Membranes were crosslinked twice with 1200 × 100 µJ (254 nm; Hoefer Stratalinker), incubated with Proteinase K solution (2 mg/ml) at 37℃ for one hour and afterwards cell debris was removed by putting moistened Whatman filter paper on the membrane, applying soft pressure and

peeling the filter paper off. Membranes were either used directly for DIG detection procedure or dried and stored enclosed in plastic membranes.

2.11.4 Colony lift membrane hybridization and detection with DIG system

Membranes were prehybridized with 15 ml of DIG Easy Hyb solution (Roche) at 42 ℃ for 30 minutes. Hybridization solution was prepared by diluting quantified probes to 25 ng/ml in DIG Easy Hyb solution. For that, probes were first denatured by boiling at 95 ℃ for 5 minutes, rapidly placed on ice and subsequently mixed with preheated DIG Easy Hyb solution; hybridization solution was reused and stored at -20 ℃. Reused hybridization solution was incubated at 68 ℃ for 10 minutes prior to hybridization. Membranes were incubated with 15 ml of hybridization solution at 42 ℃ overnight on a rocker platform. Membranes were then washed twice in washing solution I (2× SSC, 0.1% SDS) for 5 minutes followed by washing twice in washing solution II (0.1× SSC, 0.1% SDS) at 68 ℃ for 15 minutes. After equilibration in 1× maleic acid buffer (100 mM maleic acid, 150 mM NaCl, pH 7.5) for 5 minutes, membranes were incubated in 1× blocking solution (1× Blocking reagent (Roche) in 1× maleic acid buffer) for 2 hours. Following incubation with Anti-Digoxigenin-AP Antibody Conjugate (1:10,000 in blocking solution) for 30 minutes membranes were washed twice with maleic acid buffer in a fresh dish for 15 minutes and subsequently incubated with detection buffer (100 mM NaCl, 100 mM Tris-HCl, pH 9.5) for 5 minutes. Finally, membranes were covered with CSPD® ready-to-use substrate solution (Roche) for 5 minutes, enclosed in plastic membranes and exposed to X-ray films at 37 ℃ for 15 minutes to overnight exposure.

Isolated cosmids are listed in Table 7.5.

2.12 Determination of the exon-intron structure of *TCL2*

The amplification product generated with the primer combination oRNA264_F2/2goRNA_264_R using Col-0 rosette leaf cDNA was PEG precipitated and sequenced using the primer 2goRNA_264_R. The obtained sequence was aligned to gDNA with the program Spidey (http://www.ncbi.nlm.nih.gov/IEB/Research/Ostell/Spidey/). Sequence information of primers used can be found in Table 7.3.

2.13 Cloning strategies

Primer sequences used for cloning can be found in Table 7.3. *ETC2* corresponds to the AGI referenced gene At2g30420. Primer titled with 30432 and oRNA264 refer to the AGI referenced genes At2g30432 (corresponding to *TCL1* (Wang et al, 2007)) and the recently annotated gene At2g30424 (designated *TCL2*), respectively.

2.13.1 Cloning of Can-0 alleles of *ETC2*, *TCL1* and *TCL2* into binary vector pPZP211

Genomic Can-0 alleles of *ETC2*, *TCL1* and *TCL2* including 2489/358 bp, 2158/351 bp and 1616/1425 bp of flanking upstream/downstream sequences were PCR amplified with High Fidelity PCR Enzyme Mix (Fermentas) according to the manufacturer's instructions using the primers ETC2_F5_EcoRI/ETC2_R4_EcoRI, 30432_F4_XbaI/30432_R4_XbaI and oRNA264_F1_XbaI/oRNA264_R1_XbaI, respectively. The primer names indicate the introduced restriction sites for cloning.

ETC2 was directly cloned into pPZP211 by ligation of the *Eco*RI digested PCR amplicon into pPZP211. *TCL1* and *TCL2* were first cloned into the vector pCR®4-TOPO® (Invitrogen) and then recloned into pPZP211 (Hajdukiewicz et al, 1994). After an analytic plasmid digest positive clones were checked by sequencing for correct sequence of the coding region. *TCL1* and *TCL2* were recloned into the binary vector pPZP211 by a preparative restriction digest of positive pCR®4-TOPO® clones with *Xba*I and ligated into pPZP211. Positive clones were isolated by an analytic restriction digest.

2.13.2 Cloning of Gr-1 alleles of *ETC2*, *TCL1* and *TCL2* into binary vector pPZP211

In general, Gr-1 alleles were amplified and cloned using the same strategies as described above with Can-0 alleles: *ETC2* and *TCL1* were cloned first into pCR®4-TOPO and then recloned into pPZP211, *TCL2* was directly cloned into pPZP211.

2.13.3 Cloning of *ETC2* Gr-1 and Can-0 alleles into binary vector pPZP221

$ETC2^{Can}$ and $ETC2^{Gr}$ were recloned from pPZP211_$ETC2^{Can}$ and pCR®4_$ETC2^{Gr}$ into pPZP221 (Hajdukiewicz et al, 1994) using *Eco*RI sites. Clones were screened for correct insert and in the case of pPZP221_$ETC2^{Can}$ for correct vector by analytic

restriction digests.

2.13.4 Site directed mutagenesis of *ETC2* Can-0 and Gr-1 alleles

Phusion™ Site-Directed Mutagenesis Kit (Finnzymes) was used for site directed mutagenesis of *ETC2* Can-0 and Gr-1 alleles. Primers that incorporate the desired point mutations swapping the -53 and +55 nt between the Gr-1 and Can-0 alleles were designed and bought as HPLC purified primers according to the manufacturer's instructions. Subsequently primers were phosphorylated at their 5´-termini (see chapter 2.4.5). As templates for the mutagenesis reaction pCR®4_*ETC2*^{Can} and pCR®4_*ETC2*^{Gr} were used. For that, the insert of pPZP221_*ETC2*^{Can} was recloned into an empty pCR®4 vector using the *Eco*RI sites, for mutagenesis of *ETC2*^{Gr} allele the already existing pCR®4_*ETC2*^{Gr} clone was used. Primer combinations were as follows: 2g30420_Gr-53F_Phusion/2g30420_Gr-53R_Phusion, 2g30420_Gr+55F_Phusion/2g30420+55R_Phusion, 2g30420_Can-53F_Phusion/2g30420_Can-53R_Phusion, and 2g30420_Can+55F_Phusion/2g30420+55R_Phusion to construct pCR®4_*ETC2*^{Gr}-53Gr>Can (i.e. Gr-1 allele with swapped nt position -53 to Can-0), pCR®4_*ETC2*^{Gr}+55 Gr>Can (i.e. Gr-1 allele with swapped nt position +55 to Can-0), pCR®4_*ETC2*^{Can}-53Can>Gr (i.e. Can-0 allele with swapped nt position -53 to Gr-1) and pCR®4_*ETC2*^{Can}-55Can>Gr (i.e. Can-0 allele with swapped nt position +55 to Gr-1), respectively. PCR amplifications were done in 20 µl volume containing 1× Phusion™ Flash High Fidelity PCR Master Mix (Finnzymes), 10 pmol forward and reverse primer and 500 pg template using the following cycling parameters: an initial step of 98 ℃ for 30 seconds, 35 cycles consisting each of 98 ℃ for 10 seconds, 67 ℃ for 10 seconds and 72 ℃ for 2 minutes, followed by a final single step of 72 ℃ for 5 minutes, except for the amplification of pCR®4_*ETC2*^{Gr}+55, where the annealing temperature used was 69 ℃. 25 ng of respective PCR amplicons were ligated according to the manufacturer's instruction, transformed into *E. coli* and plated onto selective plates. Positive clones confirmed by sequencing were recloned into pPZP221 using *Eco*RI restriction sites.

2.14 Data sets and statistical analyses

Statistical analyses were carried out with Microsoft Office Excel 2003 and SPSS

16.0.

2.14.1 Genetic interaction test of the major QTL for trichome density and number with *CPC* and *TRY*

To test genetic interaction of the major QTL at chromosome 2 with *TRY* and *CPC*, *cpc-1*^{Ws} and t*ry-82*^{Ler} were crossed to Gr-1 and Can-0. The F1 generation was selfed and F2 and F3 offspring were screened for individuals with homozygous allelic combinations QTL^{Gr-1};*CPC*$^{Gr-1}$, QTL^{Gr-1};*cpc-1*^{Ws}, QTL^{Can-0};*CPC*$^{Can-0}$, QTL^{Can-0};*cpc-1*^{Ws} and QTL^{Gr-1};*TRY*$^{Gr-1}$, QTL^{Gr-1};*try-82*^{Ler}, QTL^{Can-0};*TRY*$^{Can-0}$, QTL^{Can-0};*try-82*^{Ler}, for interaction with *CPC* and *TRY*, respectively, using following primer combinations: LB_CPC_I/2g46410R and 2g46410F/2g46410R at *CPC*; nga5g53150F/nga5g53150R at *TRY*; nga3034F/nga3034R at the QTL in combination with *try-82*^{Ler}; nga30420F/nga30420R and nga3098F/nga3098R at QTL^{Gr-1} and QTL^{Can-0}, respectively, in combination with *cpc-1*^{Ws}. Primer sequences are listed in Table 7.3. In order to account for the segregating genomic background two or three independent lines were isolated of each allelic combination.

Of each isolated line ten individuals were phenotyped for leaves at position 8-10. Ln-transformed data satisfied the normal distribution criterion ($P>0.05$, One-Sample Kolmogorov-Smirnov Test), however, the dataset for the interaction of the major QTL with *TRY* deviated marginally from a normal distribution ($P=0.047$). To test for interaction, a full factorial ANOVA was carried out using the accession genotypes at the QTL and *CPC* or *TRY* as fixed effects and leaf position as random effect. For the interaction with *try-82*^{Ler}, which develops trichome clusters, analysis of trichome initiation sites (TIS) is reported, and analysis based on trichome density derived from the total trichome number leads to the same interpretations.

2.14.2 F1 complementation test of *etc2-2*^{Col}

For the F1 complementation test of *etc2-2*^{Col}, *etc2-2*^{Col} was crossed to the accessions Can-0 and 20-13 (both high trichome density accessions) and Gr-1 and Ler (low trichome density accessions). Of each heterozygous F1 genotype, *etc2-2*^{Col}/*ETC2*^{Can}-0, *etc2-2*^{Col}/*ETC2*$^{Gr-1}$, *etc2-2*^{Col}/*ETC2*$^{20-13}$, and *etc2-2*^{Col}/*ETC2*^{Ler}, ten individuals were phenotyped for trichome number at rosette leaf positions 8-10. Ln-transformed traits were normal distributed ($P>0.05$, One-Sample Kolmogorov-Smirnov Test). A factorial ANOVA design incorporating genotype as fixed factor and

leaf position as random factor was carried out. A significant main effect of genotype on trichome number ($P>0.001$) was further analyzed by Tukey HSD Post Hoc test (variances of groups were equal according to Levene´s of Test Equality of Error Variances; $P=0.054$).

2.14.3 Transgenic complementation test of etc2[Col] with chimeric ETC2 alleles

The transgenic complementation dataset consisted of 44, 38, 22 and 23 *etc2*-2[Col] T1 lines transgenic for pPZP221_*ETC2*[Gr]+55Gr>Can (i.e. Gr-1 allele with swapped nt position +55 to Can-0), pPZP221_*ETC2*[Gr]-53Gr>Can (i.e. Gr-1 allele with swapped nt position -53 to Can-0), pPZP221_*ETC2*[Can]+55Can>Gr (i.e. Can-0 allele with swapped nt position +55 to Gr-1) and pPZP221_*ETC2*[Can]-53Can>Gr (i.e. Can-0 allele with swapped nt position -53 to Gr-1), respectively.

Each T1 line was phenotyped at three subsequent rosette leaf positions; the exact rosette position could not be determined in this dataset since T1 lines were brought to the next generation. After ln-transformation the distribution of trait values did not deviate from normality ($P=0.198$, One-Sample Kolmogorov-Smirnov Test). Full factorial ANOVA incorporating the -53 bp/+55 bp status and allele background (*ETC2*[Gr-1] or *ETC2*[Can-0]) as fixed factor and leaf position as random factor was carried out.

2.14.4 Characterisation of trichome patterning at the cellular level: mesophyll cell analysis

Gr-1, Can-0, Ler, Ler *try*, Ws and Ws *cpc* were grown for phenotyping as described in chapter 2.7. Rosette positions 9-12, 9-11 and 8-10 of 5-10 individuals were phenotyped in the datasets comparing Gr-1/Can-0, L*er*/L*er try* and Ws/Ws *cpc*, respectively. All traits were normally distributed ($P<0.05$, One Sample Kolmogorov Smirnov Test) except trichome density in the comparison between Gr-1 and Can-0, which was ln-transformed to achieve normality. For Ler *try*, trichome initiation sites (TIS) were used for analysis, since trichomes in nests are formed directly next to each other, however, here it was of interest to analyze trichome spacing modulation as in Can-0 and Gr-1. In each dataset the effect of leaf position on traits was tested using ANOVA incorporating leaf position as random and the respective genotypes as fixed factor. Since no genotype×leaf position interaction effects were detected and, if present, main effects of leaf position were significant at α-levels close to 0.05,

Student´s t tests incorporating all leaf positions were chosen to test for significant differences of trichome and mesophyll cell parameters in the three datsets.

2.14.5 Functional characterization of *Arabidopsis thaliana* accessions exhibiting extreme trichome numbers: UV-B tolerance and anthocyanin content

Seeds of the *A. thaliana* accessions Gr-1, Ler, Can-0, Tsar/1 and Uk-3 and of Gr-1, Ler, Can-0, Tsar/1, Uk-3 and 20-13, for day 18 (late) and day 3 (early) UV-B response experiment, respectively, were sterilized and plated on MS 4.5% sucrose. After stratification for seven days at 4 ℃, 12 DAG seedlings cultivated under constant light were transferred to soil and were allowed to adapt for three days under long day conditions (16 hrs light/8 hrs dark cycles). Afterwards plants were transferred to a Percival growth chamber and subjected to chronic UV-B stress at two different regimes, hereafter designated as moderate and strong regime corresponding to 4 µmol m^{-2} s^{-1} UV-B for 1 h/day and to 4 µmol m^{-2} s^{-1} UV-B for 1.5 h/day, respectively. The UV-B regimes were carried out for 18 and 3 days, for the late and early UV-B response experiment, respectively. Control plants were grown under the same conditions without UV-B exposure.

Plant rosette diameter was measured at day 10, 14 and 18 of UV-B exposure and plant fresh weight was measured at day 18 of UV-B exposure in the late UV-B response experiment. Anthocyanin content was measured at day 18 and at day 3 of UV-B exposure in the late and the early UV-B response experiment, respectively.

Statistical analyses described below were applied to data obtained at day 18 of UV-B exposure. The data set consisted of 17-20 and 8-10 measured individuals of each accession for the parameters rosette diameter and fresh weight, respectively. Both growth parameters, rosette diameter and fresh weight, were not normally distributed (P=0.013 and P=0.002, One Sample Kolmogorov-Smirnov Test, for rosette diameter and fresh weight, respectively), however, several data transformation strategies failed to lead to a normal distribution, therefore untransformed measurements were used for statistical analysis. To statistically analyze the effect of UV-B exposure on both plant growth parameters, full factorial ANOVAs incorporating accession and treatment as fixed factors were carried out. A significant main effect of treatment (P<0.001) for both growth parameters was analyzed using Games-Howell Post Hoc test. To further analyze the interaction effect of accession×treatment detected for

both growth parameters (P<0.001, ANOVA), the measurements for rosette diameter and fresh weight of the accessions under moderate and strong UV-B exposure were normalized and expressed as percentage to the mean value of the respective accessions under control conditions. ANOVAs carried out separately for the normalized values of moderate and strong UV-B exposure detected a main effect of accession for both, rosette diameter and fresh weight (all P<0.001), confirming the accession×treatment interaction effect on the non-normalized dataset. Games-Howell Post Hoc tests were used to further investigate the significant main effect of accession, which was interpreted as differences in UV-B tolerance of *A. thaliana* accessions.

To analyze the response of trichome number and density to UV-B exposure, trichome number, trichome density and leaf area were measured at day 18 upon moderate UV-B exposure and under control conditions at leaf positions 8-10 of 8-10 individuals per accession. The measurements were restricted to the accessions Gr-1 and Uk-3, a low and a high trichome number accession, respectively, and the moderate UV-B treatment since the remaining accessions possessed damaged leaves poorly amenable for phenotyping of trichome number and density. Trichome number and leaf area were normally distributed and trichome density was ln-transformed to achieve normal distribution (all P>0.05, One Sample Kolmogorov-Smirnov Test). Reported p-values are based on an ANOVA incorporating accession and treatment as fixed factor and leaf position as random factor.

For measurements regarding anthocyanin content, only the datset of the late UV-B response experiment under control conditions was amenable for statistical analyses, since for the UV-B treatment condition and the early UV-B response experiment the sample size was too small. Anthocyanin content measured in six biological replicates of each accession at day 18 under control conditions was normally distributed (P=0.282, One Sample Kolmogorov-Smirnov Test). To test whether there is natural variation in anthocyanin content an ANOVA incorporating accession as fixed effect was performed (P=0.419, ANOVA).

2.14.6 Sequencing of *ETC2*, *TCL1* and *TCL2* in *A. thaliana* accessions

Genomic DNA was isolated and genomic regions of *ETC2*, *TCL1* and *TCL2* were PCR amplified. Amplicons were Sanger sequenced, obtained sequences were assembled and edited using the SeqMan[TM] II software (DNASTAR, Inc.).

Sequences were aligned using Clustal X (2.0) and manually adjusted. Based on genomic regions including 866 bp, 676 bp and 580 bp of 5´uptream sequences for *ETC2*, *TCL1* and *TCL2*, respectively, and 6 bp and 580 bp of 3´downstream sequences for *TCL1* and *TCL2*, respectively, Neighbour joining (NJ) trees were calculated with Clustal X (v2.0; (Larkin et al, 2007)) and visualised with TreeView 1.6.6 (Page, 1996). Primer sequences are listed in Table 7.3. Sequences have been deposited at GenBank (accession numbers FJ972633-FJ972681).

3   RESULTS

3.1   Quantitative trait locus (QTL) analysis of trichome patterning, leaf size and morphology and flowering time traits in *A. thaliana*

In a phenotypic survey of *A. thaliana* accessions (Hauser et al, 2001), the
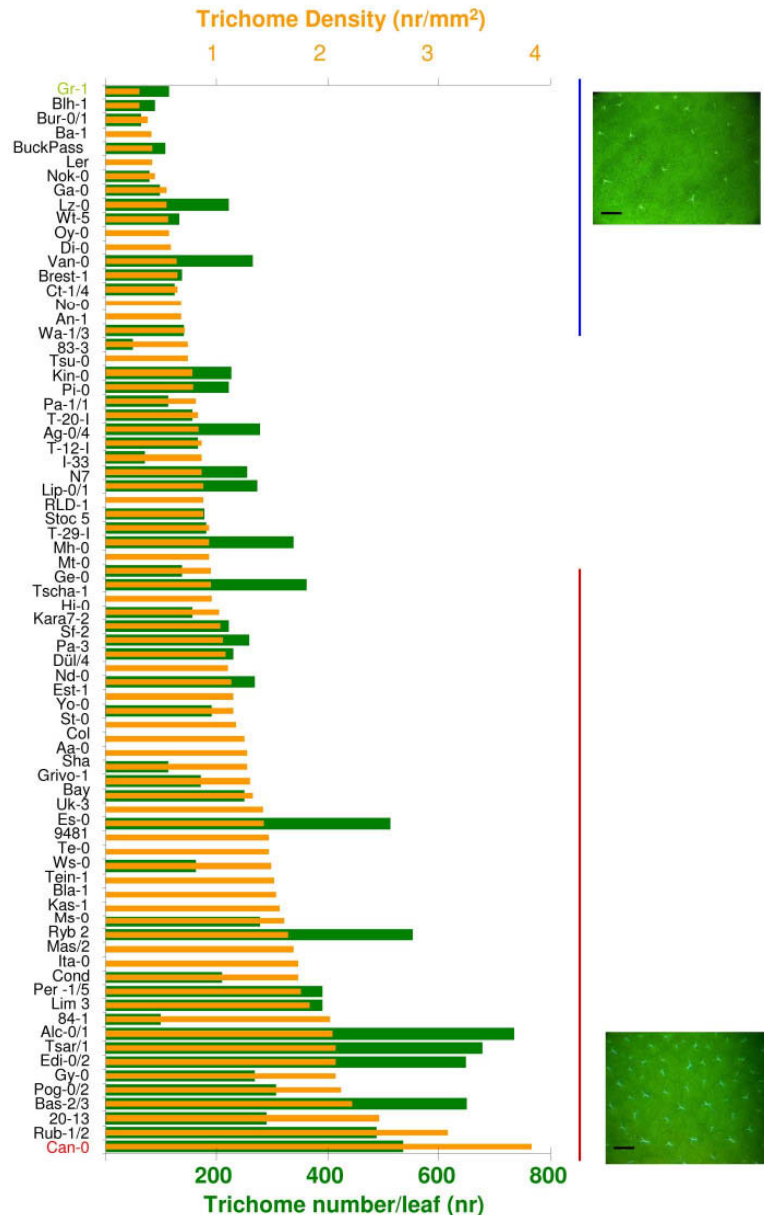
Figure 3.1. Trichome number and density distribution of Arabidopsis accessions. Trichome density (orange) and trichome number (green) were measured on late rosette leaves. Each value represents a mean of n = 1-8 individuals. The blue and the red bar symbolize the range of low and high trichome trichome density accessions used for association mapping (chapter 3.3.2). The insets depict typical trichome distribution on late rosette leaves of Gr-1 and Can-0. Scale bar, 1.5 mm. The figure incorporates data from (Hauser et al, 2001).

accessions Gr-1 and Can-0 have been shown to develop opposite extreme phenotypes for trichome density on rosette leaves (Figure 3.1). Therefore they had been chosen as parental accessions to construct an F2 mapping population. This strategy increases the chance of detecting major quantitative trait loci for a given trait. Here, the already established F2 mapping population was used to carry out a QTL analysis jointly mapping trichome patterning, leaf size and morphology and flowering time traits.

3.1.1 Characterisation of the parental accessions Gr-1 and Can-0 shows differences in phenotypic traits amenable for QTL mapping

To set up phenotyping of the F2 mapping population, the parental accessions Gr-1 and Can-0 were characterised in detail for trichome patterning and leaf size and morphology traits. This was critical since it is known that *A. thaliana* exhibits heteroblasty, i.e. aspects of for example trichome patterning or leaf morphology change on subsequent leaves formed during the ontogeny of the plant (Tsukaya et al, 2000). Therefore each leaf position in the rosette of six week old plants was analysed (Figure 3.2). As expected, trichome patterning and leaf morphology traits on subsequently formed leaves showed heteroblasty and the analysis visualised leaf positions with the most pronounced differences in trichome number and density that were subsequently analyzed in QTL mapping. Leaf positions were categorized into early and late leaf positions solely in regard to growth conditions, the former are primarily initiated and developed while grown on MS medium (indexed as position I-V), the latter while grown on soil (indexed as position 6-14).

Gr-1 has a smaller trichome number and trichome density than Can-0 on all leaf positions examined (Figure 3.2), however, the difference increases on leaf position 7-14 and 10-14 for trichome number and density, respectively. The number of edge trichomes formed is similar in the two accessions. Leaf size traits are similar at leaf positions I and II, at later positions Can-0 forms larger leaves. The size difference diminishes again at leaf positions 12-14. The two accessions possess the same leaf shape index on the first leaf positions, on later positions Can-0 has a larger leaf index, i.e. Can-0 leaves are more elongated than Gr-1 leaves. The plot of trichome patterning and leaf size and morphology against leaf position visualises differences in heteroblastic behaviour; for example, trichome number increases gradually with
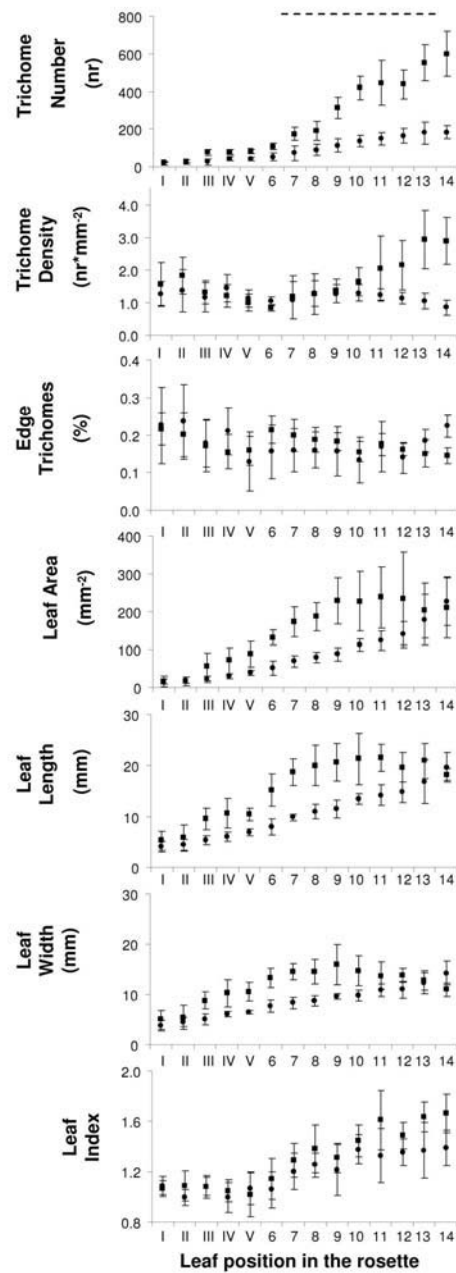
Figure 3.2. Heteroblastic behaviour of trichome patterning and leaf size and morphology traits shown as a function of leaf position in the rosette of A. thaliana accessions Can-0 and Gr-1. Can-0 and Gr-1 graphs are represented by squares and dots, respectively. The latin numeral I indicates the first formed rosette leaf, etc.; latin and arabic numerals correspond to leaves formed while growing on nutrient agar plates and on soil, respectively. The dotted line indicates the range of rosette positions of which three leaves were sampled for further phenotypic analyses. Bars represent mean ± sd of 7 individuals.

76

leaf position, but the increase in Can-0 is larger than in Gr-1 (Figure 3.2) and trichome density increases at later leaf positions in the accession Can-0, whereas it stays nearly constant in Gr-1. Trait differences between the two accessions were statistically tested averaging across leaf positions 7-14, i.e. the positions with the largest differences in trichome number and density, and shown to be significantly different also for heteroblasty in regard to trichome number, leaf area, length and width, as well as for leaf shape index (Table 3.1).

Table 3.1 Characterization of the accessions Gr-1 and Can-0 and quantitative genetic parameters of the F2 mapping population in regard to trichome patterning and leaf size and morphology traits.

Trait	Can-0	Gr-1	Mean of F2	H^2
Trichome Number** [nr]	383 ± 45	137 ± 18	215 ± 89	0.85
Trichome Density** [nr/mm^2]	1.9 ± 0.4	1.2 ± 0.1	1.6 ± 0.9	0.89
Edge Trichomes [nr]	0.17 ± 0.02	0.17 ± 0.03	0.19 ± 0.04	0.56
Heteroblasty**	60.5 ± 17.5	16.8 ± 10.2	22 ±16.4	0.24
Leaf Area* [mm^2]	211 ± 57	127 ± 20	147 ±48	0.21
Leaf Length** [mm]	20.2 ± 2.3	14 ± 1.5	16.6 ± 3	0.59
Leaf Width** [mm]	14 ± 1.8	10.6 ±- 0.7	11.2 ± 2	0.51
Leaf Shape Index**	1.48 ± 0.08	1.31 ±.07	1.5 ± 0.17	0.78

Phenotypic values (mean ± s.d.; n = 7) of the accessions Gr-1 and Can-0 were averaged over rosette positions seven to fourteen. The genetic (V_G) and the environmental variance (V_E) were used to estimate broad sense heritabilities (H^2) as described in chapter 2.10.3.
*, **, *** indicate significant difference at 0.05, 0.01, and 0.001 significance level (Kolmogorov-Smirnov test with two samples (n = 7)) of the accessions Gr-1 and Can-0 in regard to respective traits.

Taken together, all traits measured show heteroblasty with the exception of edge trichomes, and heteroblasty can be differently modulated in *A. thaliana* accessions, as quantified for trichome number. Due to the detailed analysis, leaf positions 7-14 were chosen for phenotyping of F2 mapping population individuals for QTL

mapping.
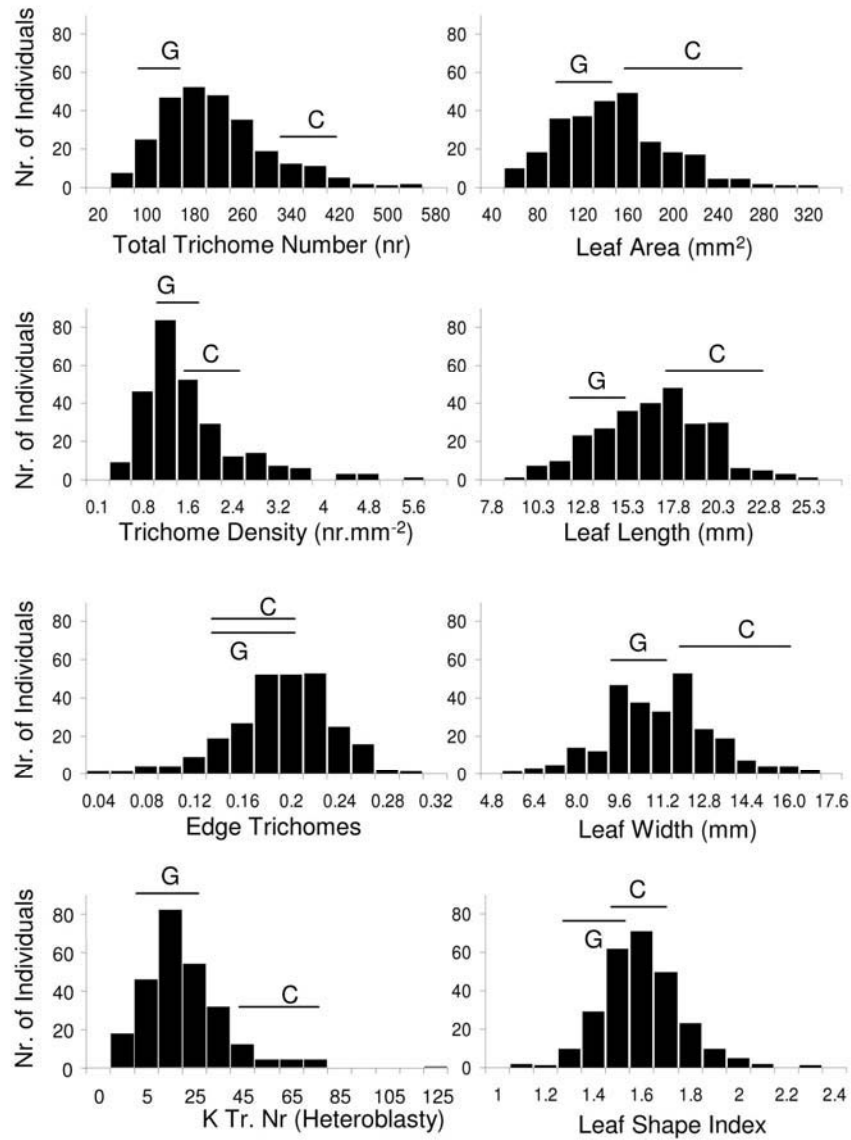
Figure 3.3. Frequency distributions of non-normalized data of trichome patterning and leaf size and morphology traits of F2 mapping population individuals. The mean parental values are indicated above the respective bins with the letters C and G, for Can-0 and Gr-1, respectively; horizontal bars indicate their standard deviation (n = 7).

3.1.2 Characterisation of the F2 mapping population

Analysis of the frequency distribution of the traits in the F2 population showed that they were normally distributed (P>0.05; One-Sample Kolmogorov-Smirnov test) except for trichome density and edge trichomes. All traits showed transgressive segregation, also edge trichomes where parental accessions did not differ. Transgressive segregation is an indicator of parents carrying alleles both increasing and decreasing respective traits, of under- and overdominant gene action and /or of epistasis. Broad-sense heritability H^2 estimates, a measure of the extent to which individuals phenotypes are determined by their genotypes ((Falconer & Mackay, 2005)), are very diverse and range from 0.21 (leaf area) to 0.89 (trichome number) (Table 3.1).

The measured H^2 estimates and the significant differences between parents suggested that QTL mapping was likely to detect QTLs for analysed traits, although detection might be hampered for some traits by heteroblastic behaviour and trait variance influenced by environmental conditions (the latter shown for example by H^2 estimates of 0.24 and 0.21, for heteroblasty in regard to trichome number and for leaf area, respectively (Table 3.1).

3.1.3 Phenotypic correlation of traits among F2 individuals

Phenotypic correlations between traits arise by two general causes, modification by the same environmental factors operating on individuals or genetic correlations. The latter can arise by two mechanisms: linkage of loci or pleiotropy of a locus influencing different traits. Phenotypic correlations are often used as surrogate estimates for genetic correlations, as they normally have the same sign and are also of similar magnitude (Lynch & Walsh, 1998).

Phenotypic correlations of trichome patterning and leaf size and morphology traits were structured by principal component analysis (Table 3.2). The first three principle components explain 41%, 30%, and 14% of the variation in the F2 population, respectively. Principal component 1 has a high positive loading for all leaf size traits. Principal component 2 shows a high positive loading for total trichome number, trichome density and heteroblasty together with a high positive loading for leaf shape and leaf length and principle component 3 reveals a high positive loading for edge trichomes and a positive loading for leaf shape. This indicates that leaf size traits are highly correlated and that trichome density is mostly explained by a strong

negative correlation to leaf size and by a positive correlation to trichome number. Moreover, trichome number is to some extent independent of leaf size traits.

Table 3.1 Principal component analysis of trichome patterning and leaf size and morphology traits in the F2 mapping population

Trait	Component		
	1	2	3
Trichome Number	-0.17	0.91	-0.20
Trichome Density	-0.76	0.54	-0.08
Edge Trichomes	0.22	0.13	0.78
Heteroblasty	-0.37	0.70	-0.24
Leaf Area	0.92	0.35	-0.09
Leaf Length	0.84	0.51	0.07
Leaf Width	0.94	0.16	-0.26
Leaf Shape Index	-0.17	0.59	0.56
% variation explained	41	30	14

Based on n=266 mapping population individuals

3.1.4 QTL mapping

QTL LR0 likelihood graphs for all traits are shown in Figure 3.4 A-C, and summarized in Figure 3.5 and Table 3.3.

3.1.4.1 QTL mapping detects a major QTL for trichome number and density on chromosome 2

Composite interval mapping (CIM) detected three QTL for trichome number, three QTL for trichome density, and two QTL each for edge trichomes and heteroblasty. QTL are located on all chromosomes except chromosome 1. A major QTL explaining 33% of the variation for trichome number (and 9% for trichome density) was mapped to the lower arm of chromosome 2. The remaining QTL detected explain between 4-9% of the variation. Taken together, 44% and 18% of the variance can be accounted for by detected QTL for trichome number and trichome density, respectively. Additive allele effects of detected QTL for trichome number, trichome density and edge trichomes were unidirectional, i.e. Can-0 possessed only alleles increasing trichome number and trichome density and decreasing edge trichomes, only the two QTL for heteroblasty showed opposite additive allele effects.

The prevalent gene action modelled was partial dominance (five out of ten QTL), three loci show overdominance and two complete dominance. The major QTL detected for trichome number is linked to marker nga361 on chromosome 2. It was assigned to an 8.4 cM interval (which in this mapping population equals 2.56 Mb) flanked by the markers ngaT3B23 and nga2g3470. Its gene action is partially dominant towards lower trichome number. The modelled gene action of QTL allows drawing conclusions about the underlying effect of transgressive segregation in the F2 mapping population: genetic evidence for transgressive segregation is provided by overdominant gene action for total trichome number and heteroblasty. Transgressive phenotypes for trichome density and edge trichomes are either due to environmental variance or due to several QTLs with effects beyond the detection limit, because detected QTL show no overdominance, epistasis was not detected, and the parental accessions code for QTL with only unidirectional additive effects.

The major QTL and the QTL on the upper arm of chromosome 4 are potentially identical to QTL which have been detected in multiple RIL mapping populations (Larkin et al, 1996; Mauricio, 2005; Pfalz et al, 2007; Symonds et al, 2005). The major QTL harbours several candidate genes in its interval, among these three members of the single-repeat R3 MYB family, *ETC2* and *TCL1* (Kirik et al, 2004b; Wang et al, 2007) and the novel member *TCL2* (see chapter 3.3.2.1) (Table 3.3).
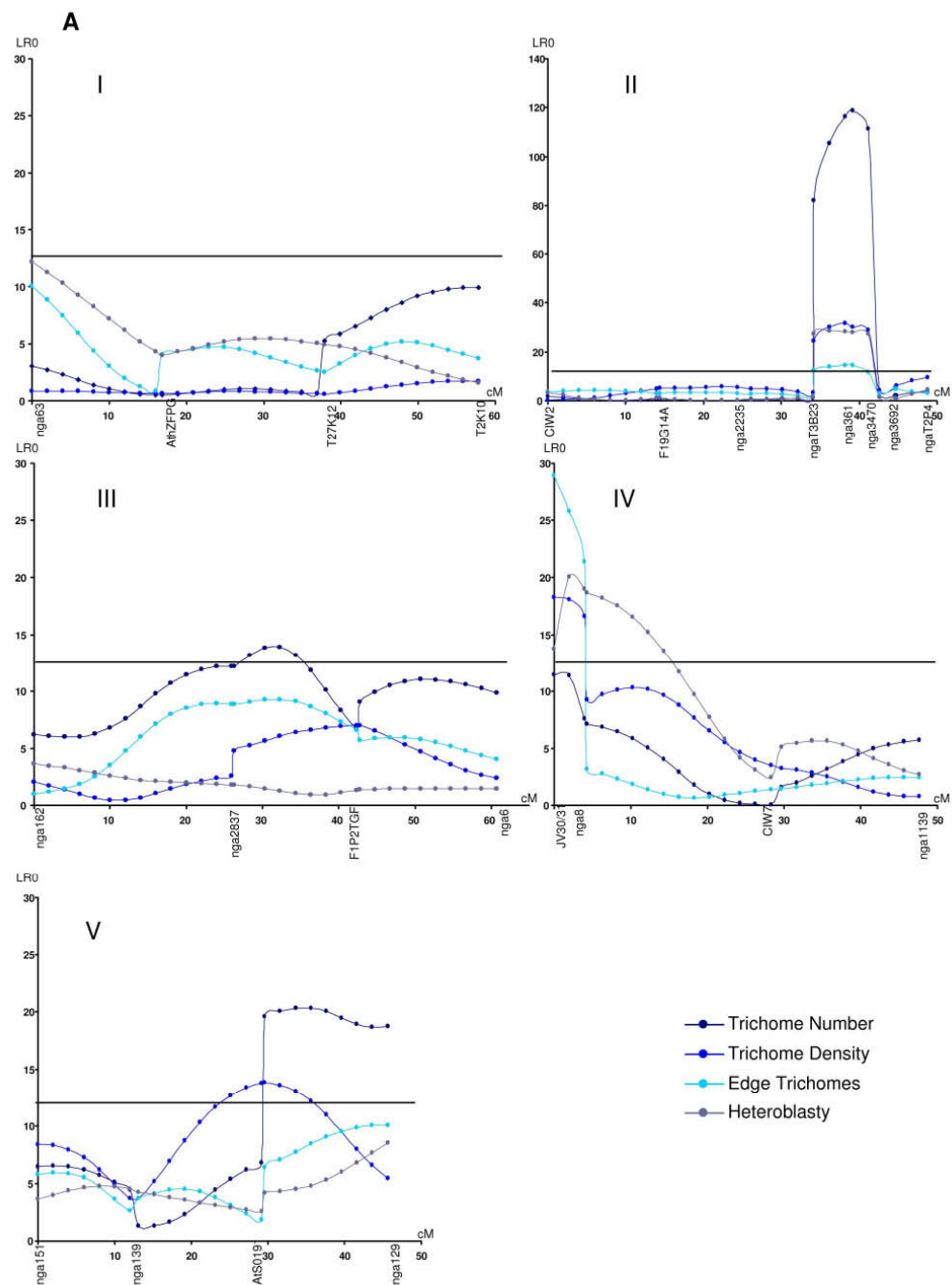
Figure 3.4. LR0 likelihood graphs of QTL mapping. (A) trichome patterning, (B) leaf size and morphology and (C) flowering time traits. Horizontal lines indicate the significance threshold determined by 1000 permutations. Marker positions are indicated below the graphs. cM: centimorgan; LR0: likelihood ratio test statistic, comparing the two hypotheses of there being a QTL present versus there being no QTL present. Chromosomes are marked I-V.

Figure 3.4 (B) legend see page 82.

C
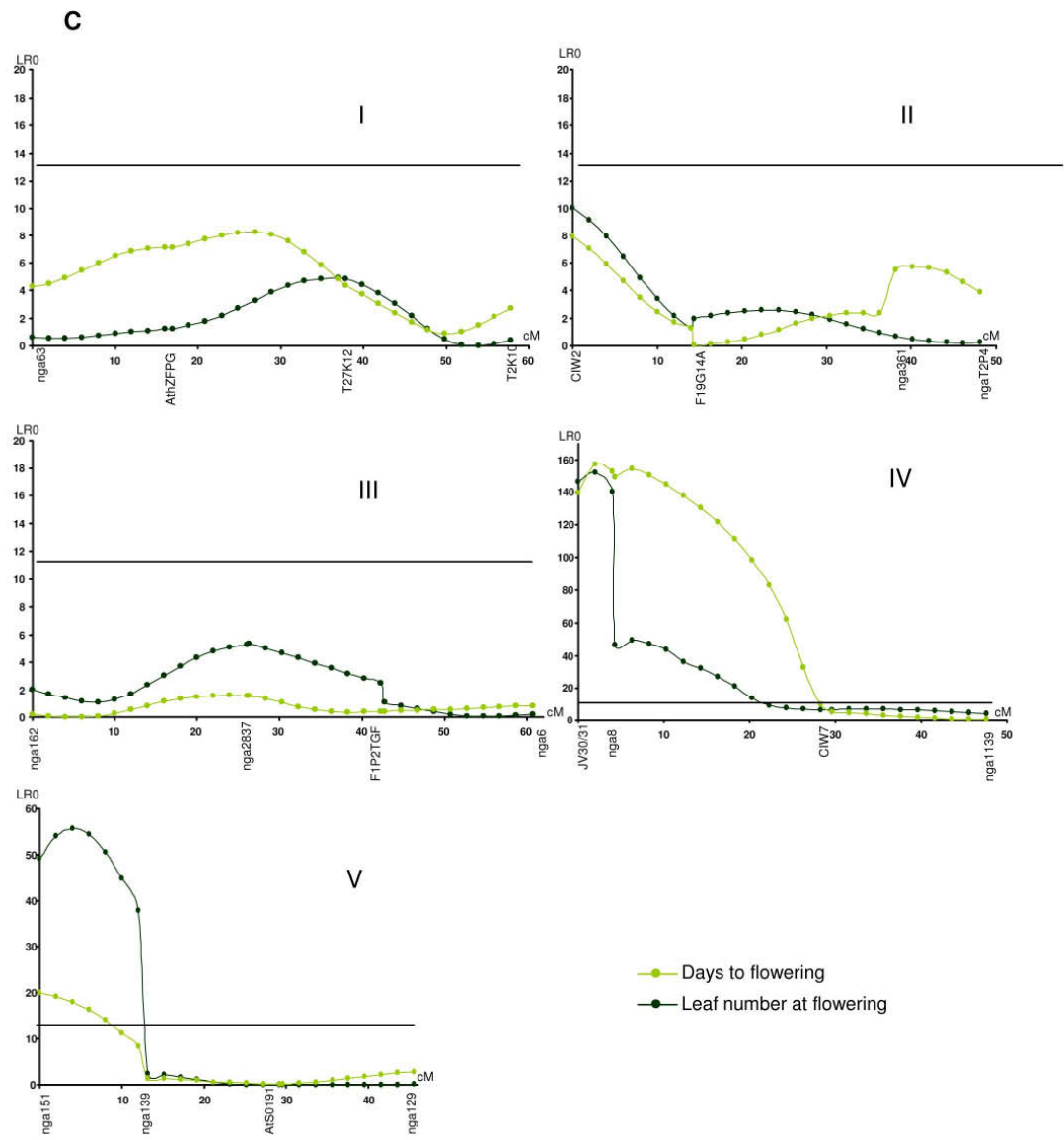
Figure 3.4 (C) legend see page 82.
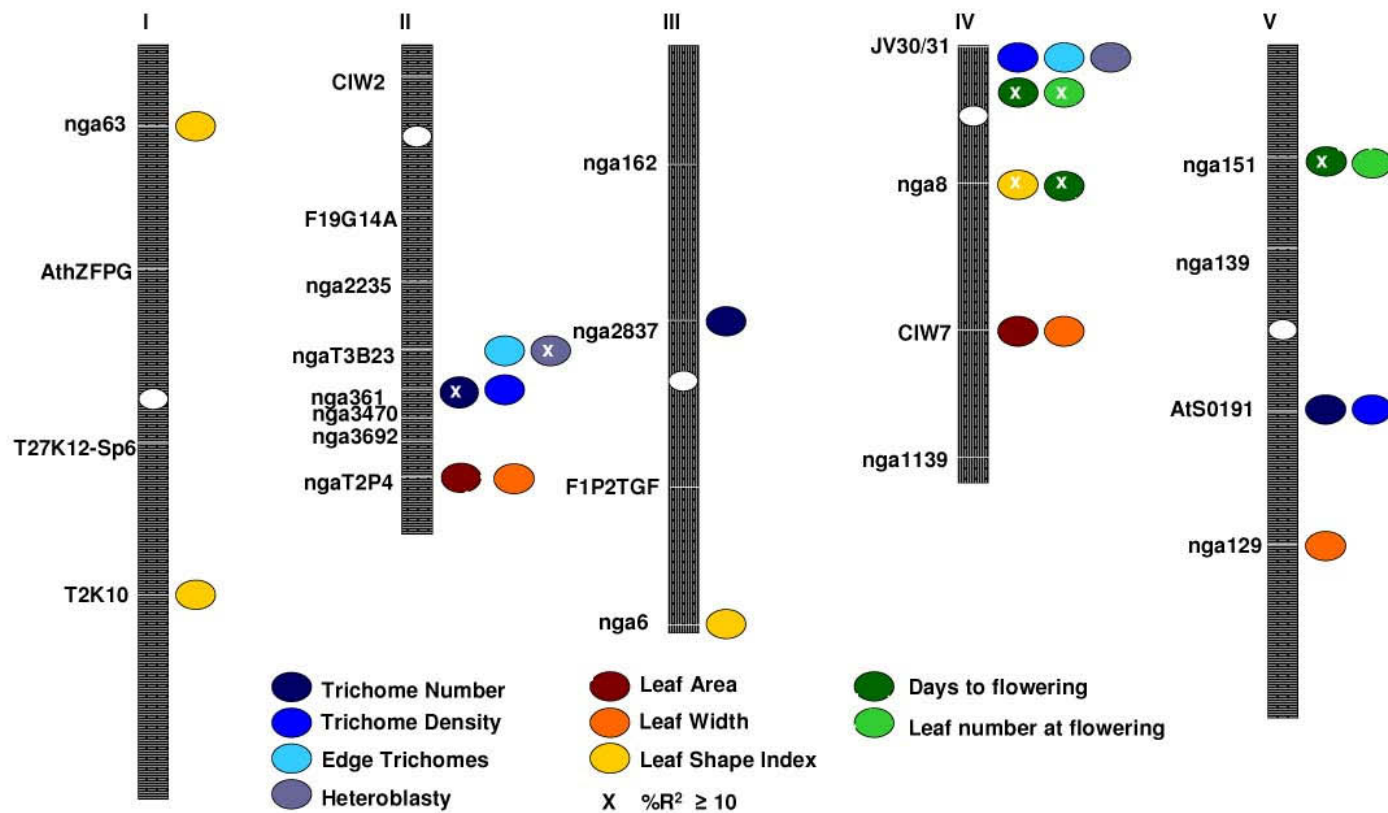
Figure 3.5. Schematic representation of trichome patterning, leaf size and morphology and flowering time QTLs. Markers are indicated to the left of the chromosomes. Centromers are indicated by white ovals. %R^2 is the proportion of the variance explained by the QTL conditioned on the background markers.

Table 3.3 Summary of QTL parameters for trichome number and leaf size and morphology traits in the F2 Can-0×Gr-1 mapping population estimated by WinQTL Cartographer

Trait	Chromosome	Marker[a]	Position (cM)[b]	%R²[c]	Additive Effect a[d]	Dominance Effect d[e]	Dominance Ratio[f]	LR Score	Threshold	Candidate Genes
Tr. Number	II	nga361	39	33	37.99	-10.19	-0.27	119	12.6	ETC2,TCL1, CDT1, URM9/SAD2
	III	nga3g2837	32	5	6.84	17.09	2.50	14		GL1
	V	AtS0191	34	6	14.96	-6.12	-0.41	20		MYB23, GL3, TRY, CPR5
Tr. Density	II	nga361	38	9	0.33	-0.08	-0.25	32	12.7	ETC2,TCL1, CDT1, URM9/SAD2
	IV	JV30/31	0	5	0.12	-0.13	-1.16	18		GeBP, ETC3, GA1
	V	AtS0191	30	4	0.11	-0.12	-1.05	14		MYB23, GL3
Edge Trichomes	II	ngaT3B23	38	5	-0.01	0.01	0.69	15	12.7	ETC2, TCL1, CDT1, URM9/SAD2
	IV	JV30/31	0	9	-0.02	-0.01	-0.76	29		GeBP, ETC3, GA1
Heteroblasty	II	ngaT3B23	38	10	0.34	0.02	0.06	28	12.9	ETC2, TCL1, CDT1, URM9/SAD2
	IV	JV30/31	2	7	-0.07	-0.40	-6.01	21		GeBP, ETC3, GA1
Leaf Area	II	ngaT2P4	49	5	-6.82	9.01	1.32	13	12.5	AtGRF3
	IV	CIW7	30	4	6.65	5.19	0.78	13		
Leaf Width	II	ngaT2P4	49	6	-0.11	0.46	4.00	16	12.4	AtGRF3
	IV	CIW7	16	9	0.13	0.54	4.28	13		
	V	nga129	46	5	0.14	0.38	2.75	14		
Leaf Shape Index	I	nga63	8	5	0.05	0.01	0.27	14	12.4	AN
	I	T2K10	58	8	-0.07	0.00	0.03	24		
	III	F1P2-TGF/nga6	47	9	-0.07	0.04	0.64	24		
	IV	nga8	0	10	-0.03	-0.10	-2.87	34		
Days to flowering	IV	JV30/31	2	55	19.89	15.88	0.80	151	12.8	FRI, LD, GA,
	IV	nga8	6	18	10	16.28	1.63	49		CRY1, PHYD, FCA, VRN2, PHYE
	V	nga151	4	23	14.72	-3.51	-0.24	55		PRR7, TFL1, ELF6, AtMYB33, FLC, FY, CO, FRL1, TFL2
Leaf Number at flowering	IV	JV30/31/nga8	2	71	11.88	13.9	1.17	157	12.9	FRI, LD, GA, CRY1, PHYD, FCA, VRN2, PHYE
	V	nga151	0	8	3.24	5.46	1.69	19		PRR7, TFL1, ELF6, AtMYB33, FLC, FY, CO, FRL1, TFL2

Table legend see next page.

Table 3.3 legend, see Table at previous page.

a markers nearest to the QTL position (inside the 2 LOD drop support interval)

b approximate position of QTL on genetic map estimated from the data set (position of highest LR0 score)

c %R2 is the proportion of the variance explained by the QTL conditioned on the background markers

d Additive Effect a indicates the mean change of the trait of replacement of an Gr-1 allele by an Can-0 allele

e A negative value indicates a dominance deviation towards lower trait values

f Dominance ratio is calculated as d/|a| and indicates the form of gene action. d/|a| < -1, d/|a| > 1: under- and overdominance, respectively; 1 > d/|a| > -1: partial dominance; d/|a| = 0: additivity

g likelihood ratio (LR0) test statistic compares the two hypotheses of there being a QTL present versus there being no QTL present
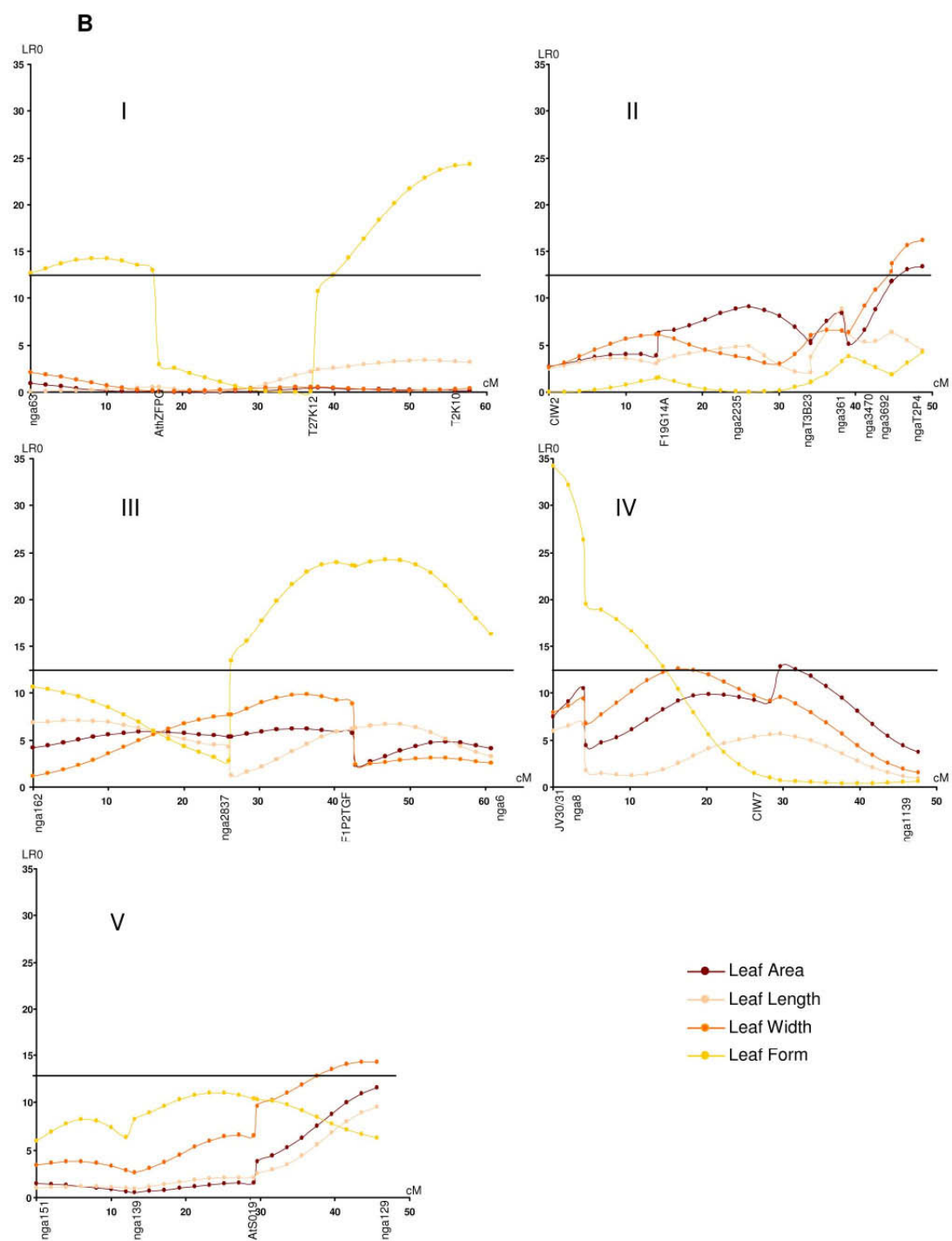
3.1.4.2 Leaf size and morphology QTL

CIM detected nine QTL for leaf size and morphology traits, two for leaf area, and three and four for leaf width and leaf shape, respectively (Figure 3.4 B, Figure 3.5). There was no QTL detected for leaf length. Individual QTL explain between 4-10% of the variation, overall most variation is explained for leaf shape (32%) which might indicate robustness against environmental variation in contrast to for example leaf area (9% of variation explained). Additive allele effects of the QTL detected for each trait were bidirectional, i.e. each parent possesses QTL loci increasing and decreasing respective traits. The predominant gene action is overdominance (five out of nine QTL), three loci show partial dominance and one additive gene action. Genetic impact on transgressive segregation can therefore be explained by two mechanisms: first, both parental accessions possess QTL with increasing and decreasing effects for each trait, and second, each trait is influenced by at least one QTL with overdominant gene action.

Although several QTL were detected for leaf size and morphology traits, only two candidate genes were found to colocalize with QTL candidate intervals (Table 3.3), *GROWTH REGULATING FACTOR3* (GRF3; (Horiguchi et al, 2006)) with a QTL for leaf area and leaf width on chromosome 2, and *ANGUSTIFOLIA* (*AN*; (Tsukaya, 2005)) with a QTL for leaf shape index on top of chromosome 1.

3.1.4.3 Flowering time QTL

Since Can-0 and Gr-1 differ in their flowering time behaviour with Can-0 flowering very late, approximately 9 weeks after germination, and Gr-1 approximately 5 weeks after germination, also flowering time was mapped in a subset of F2 mapping population individuals. Three and two QTL were detected for the traits days to

flowering and leaf number at flowering, colocalizing at the ends of the upper arms of chromosome 4 and 5 (Figure 3.4 C, Figure 3.5). They are major QTL and together explain 96% and 79% of the variation for days to flowering and leaf number at flowering, respectively. Gene action is modeled overdominant and partial dominant.

There are several candidate genes in the QTL intervals (Table 3.3), and some of them have been shown to underlie natural variation in flowering time, for example *CRYPTOCHROME2* (*CRY2*), *FLOWERING LOCUS C* (*FLC*), *FLOWERING LOCUS M* (*FLM*), and *FRIGIDA* (*FRI*) (listed in (Shindo et al, 2007)).

3.1.4.4 Clustering of QTL

Clustering of QTL at genomic positions allows drawing conclusions which factors might correlate to influence a phenotypic trait. Generally, clustering can be explained by pleiotropy of single genes or by linkage of genes affecting different traits.

Co-localisation of loci for total trichome number, trichome density and edge trichomes was found at the major QTL on chromosome 2 (ngaT3B23, nga361). Trichome density, edge trichomes and leaf shape show overlap on top of chromosome 4 (JV30/31), and leaf area and leaf width cluster at the bottom of chromosome 2 (ngaT2P4). There was no extensive overlap detected between QTL important for trichome number and leaf size, except for trichome number and leaf width on the bottom of chromosome 5. Furthermore, there is overlap for trichome patterning QTL with flowering time QTL on top of chromosome 4 (Table 3.3, Figure 3.5).

3.1.5 Fine mapping of the major QTL for trichome number and density on chromosome 2

A major QTL explaining 33% of variation for trichome number and 9% of trichome density was mapped to a QTL candidate interval of 2.56 Mb on the lower arm of chromosome 2 between the markers ngaT3B23 and nga2g3470 (Figure 3.6 A). In order to decrease the QTL candidate interval, fine mapping using the strategy of selective genotyping (Lynch & Walsh, 1998) was carried out. First, an additional number of individuals were scored for the trait of interest and a selected subset of these with an extreme trichome number and density phenotype were chosen for genotyping with further markers in the QTL candidate interval. Extreme individuals

were defined as being among the approximately 12.5% of individuals in the phenotypic distribution with either highest or lowest trichome number and density. In the hypothetical case of a quantitative trait governed by a single gene with purely additive gene action the defined extreme high and low individuals are homozygous for the respective alleles at the quantitative trait nucleotide (QTN). However, due to several QTL governing trichome number and density and the gene action of the major QTL modelled partially dominant, the association of extreme individuals might be weaker than in the hypothetical case.

Phenotyping of additional 459 further F2 mapping individuals lead to a total of 465 individuals exhibiting an extreme (low and high) phenotype. 193 were chosen from the newly phenotyped population of 459 individuals, 133 were of the base population used for QTL mapping and 139 individuals were established earlier in the lab (Im U II and Nicole Schlager). These were chosen and genotyped with the markers flanking the QTL candidate interval, ngaT3B23 and nga2g3341, to detect informative mapping population individuals. Of these, 66 individuals were recombinant between the two markers (34 and 32 of high and low trichome phenotype, respectively) and were genotyped with further nine markers located inside the QTL candidate interval (Figure 3.6 A). For extremely low individuals there were 17/514 and 18/514 recombinant chromosomes at markers ngaT3B23 and nga3341, respectively, detected and the number of recombinant chromosomes dropped to 8/514 and 9/514 at the markers HDUP3038 and nga3098. The physical distance between these markers is ~240 kb. The number of recombinant chromosomes for extremely high individuals was 21/414 and 14/414 at the flanking markers ngaT3B23 and nga3341, respectively, and the number of recombinant chromosomes dropped to 6/416 at the marker HDUP3038 and did not increase until marker nga3168 (5/414), which lies ~530 kb downstream of HDUP3038. The recombinant chromosomes of the extremely low individuals decrease the QTL candidate interval to ~240 kb, the extremely high individuals share this decreased interval, however, the QTL candidate interval is larger and extends at least ~530 kb downstream until marker nga3168.
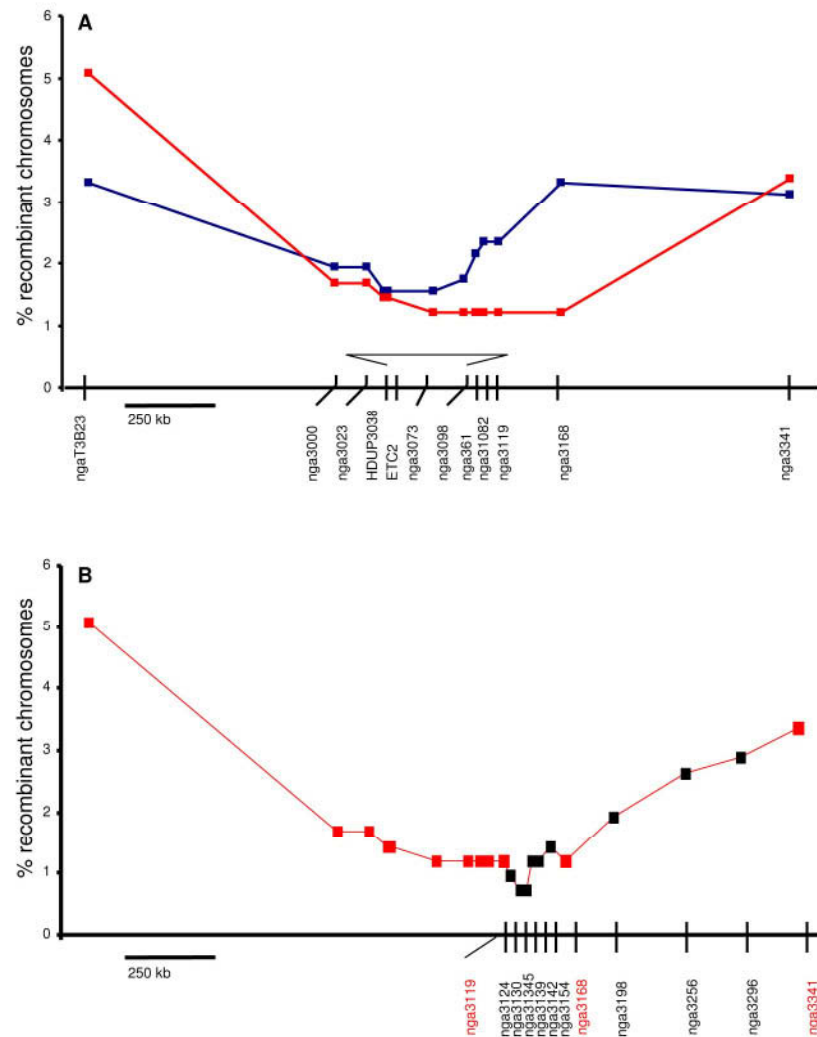
Figure 3.6. Fine mapping of the major QTL for trichome number and density on chromosome 2.(A) Fine mapping of 34 and 32 informative high (red) and low (blue) trichome phenotype F2 mapping population individuals, respectively, using 9 additional markers inside the QTL interval marked by ngaT3B23 and nga3341. The bracket indicates the genomic interval which was functionally tested by complementation analysis (chapter 3.3.1). (B) Fine mapping of a potential second QTL locus visualized by high trichome density individuals using further 9 markers (marked in black). The x–axes provide the marker positions (in bp), the y-axes shows the percentage of recombinant chromosomes (chromosomes with alleles not corresponding to phenotype/per total number of chromosomes) detected for high (red line) and low (blue line) trichome number individuals.

The discrepancy might be explained by two non-exclusive scenarios: first, the QTL was modeled to exhibit partially dominant gene action towards lower trichome density. This gene action could lead to individuals heterozygous at the QTN grouped as extremely low individuals and therefore lead to a distorted QTL candidate interval

for low trichome density indviduals. Secondly, the QTL candidate interval might harbour two QTL and the second QTL situated downstream exhibits epistasis, since it cannot be visualized with low trichome density individuals. In order to get a better resolution of the second QTL visualized by high trichome density individuals, they were genotyped with further 9 markers between markers nga3119 and nga3341 flanking the marker nga3168 (Figure 3.6 B). Fine mapping of the region showed that the lowest percentage of recombinant chromosomes occur between the markers nga3124 (4/416) and nga3168 (5/414), which flank a 184 kb interval.

Taken together, fine mapping reduced the QTL candidate interval from 2.56 Mb to a ~240 kb region on chromosome 2 and it visualized that there is a potential second linked QTL downstream, visualized by high trichome density individuals only. This second potential QTL could be fine mapped to a 184 kb interval. The fine mapped region located upstream harbours three strong candidate genes, members of the single-repeat R3 MYB family, *ETC2*, *TCL1* and *TCL2* (Kirik et al, 2004b; Wang et al, 2007), (see chapter 3.3.2.1) The downstream fine mapped QTL interval based on high trichome density individuals harbours the strong candidate genes *CDT1*, which has been shown to interact with GEM, an epigenetic regulator of trichome initiation (Caro et al, 2007), and *SAD2/URM9*, a suppressor of JA induced formation of trichomes (Yoshida et al, 2009).

3.2   Genetic interaction test of the major QTL for trichome number and density with *CPC* and *TRY*

In order to test genetically if and how the major QTL for trichome number and density functions in the framework of the proposed trichome initiation mechanism (Ishida et al, 2008), genetic interaction tests were carried out. Since it was evident from fine mapping that *ETC2* and *TCL1* were candidate genes, genetic interaction with *CPC* and *TRY*, two other members of the single-repeat R3 MYB family, was to tested.

For that, individuals harbouring the homozygous allelic combinations of either the QTL^{Gr} or QTL^{Can} allele together with the wildtype or mutant alleles of *CPC* and *TRY* were established and phenotyped for trichome density (Figure 3.7). The major QTL and *CPC* show additive gene action (*P*=0.205, ANOVA), whereas a significant interaction term was detected between the major QTL and *TRY* (*P*=0.025, ANOVA). Moreover, *TRY* was shown to be epistatic to the major QTL since individuals harbouring the try-82^{Ws} mutant allele form the same trichome density irrespective of their allele status at the QTL. Based on the present genetic interaction with *TRY*, the major QTL for trichome number is likely functioning in the same genetic pathway that has been intensely analyzed by classical genetic analyses (Ishida et al, 2008). The difference in interaction of the major QTL with *CPC* and *TRY* are further evidence for functional differences of the two repressors in trichome initiation and patterning.
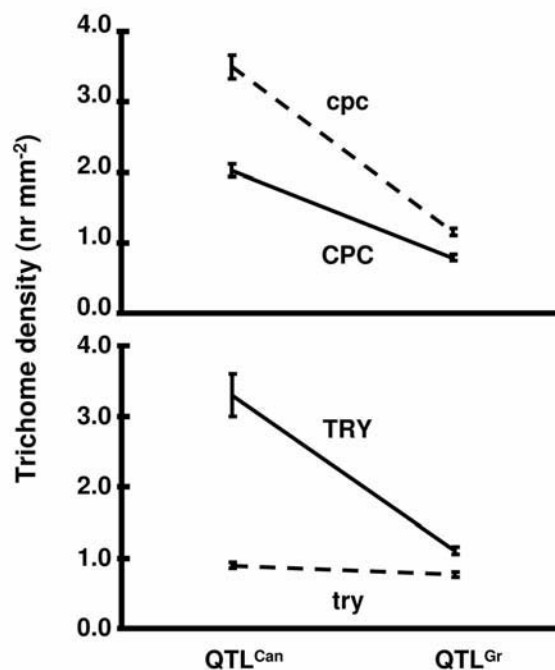
Figure 3.7. Genetic interaction test of the major QTL with *TRY* and *CPC*. For both interactions, trichome density was measured of individuals homozygous for the four allelic combinations. Each data point corresponds to the mean ± s.e.m of ten individuals of at least two independent lines. Shown are non-ln transformed trait values. Additive gene action was detected for the major QTL with *CPC* (*P*=0.205, ANOVA) and a significant interaction term of the major QTL with *TRY* (*P*=0.025, ANOVA) reveals that *TRY* is epistatic to the QTL.

3.3 Identification of the quantitative trait nucleotide (QTN)

To identify the locus harbouring the QTN two strategies were followed in parallel, a systematic transgenic complementation test of the fine mapped QTL candidate region (chapter 3.3.1) and a candidate gene approach (chapter 3.3.2).

3.3.1 Systematic transgenic complementation analysis of the fine mapped QTL candidate region

A systematic screen of the QTL candidate region for chromosomal regions with ability to alter trichome number and density was carried out by complementation analysis. For that, a cosmid library based on the L*er* genome was screened and used to transform Can-0 plants. The L*er* genome has been shown to harbour the low trichome density QTL on chromosome 2 (Larkin et al, 1996; Mauricio, 2005; Symonds et al, 2005), and transformation of the low allele into a high density background is advantageous since the QTL displays partial dominance towards lower trichome density (chapter 3.1.4.1).

For that, an *A. thaliana* L*er* genomic cosmid library was screened systematically for inserts covering the QTL candidate region; details of the 15 isolated cosmids are listed in Table 7.5. It was possible to isolate the region with the cluster of the three single-repeat R3 MYB genes *ETC2*, *TCL1* (see chapter 3.3.2.1) and *TCL2*, strong candidate genes, cosmid_At2g30420 harbours *ETC2* and cosmid_At2g30432 harbours *ETC2* and *TCL2* and a truncated 3´portion of *TCL1*. All isolated cosmids were transformed into Can-0 and phenotyped qualitatively for trichome number and density Phenotyping was started in the T1 generation; although T1 plants are heterozygous in respect to their insertion site, the transformation procedure is expected to lead to some extent to multiple insertions, moreover, individual insertion sites may harbor multiple copies of the insert ((De Neve et al, 1997) and references therein). Also, already a single copy of the alternative allele might be sufficient to visibly change the phenotype in the T1 generation.

There was no difference observed in trichome number and density irrespective of the cosmid transformed in any of the T1 plants, specifically, there was no difference observed in eleven and three independent T1 lines transformed with cosmid_At2g30420 and cosmid_At2g30432, respectively. 8-10 independent T1 lines transformed with c_At2g30420, c_At2g30520 and c_At2g30600 were brought into T2 generation and analyzed for insert number and phenotype. Most of the lines had

a single insertion event (P>0.05, n=20; CHI^2 test), three and one lines transformed with c_At2g30530 and c_At2g30600, respectively, showed indication of more than one insertion (P<0.05, CHI^2 test; n=20). None of the T2 individuals showed a qualitative difference in trichome number and density to Can-0 plants transformed with empty pBIC20, furthermore, there was no phenotypic segregation detected in respect to trichome number and density in T2 families.

3.3.2 Candidate gene approach

The genetic interaction test of the major QTL with *TRY* showed that TRY is epistatic to the major QTL and thus may show that the major QTL is involved in the same genetic pathway of trichome initation as *TRY*. The locus in the QTL candidate interval coding for *ETC2* and *TCL1,* two members of the single-repeat R3 MYB family, therefore, was a strong candidate locus and was further investigated for evidence of harbouring the QTN.

3.3.2.1 Identification of *TRICHOMELESS 2* (*TCL2*), a novel single-repeat R3 MYB family member

Inspection of the genomic locus harbouring *ETC2* and *TCL1* led to the identification of a novel member of the single-repeat R3 MYB family, designated *TRICHOMELESS 2* (*TCL2*). An expressed sequence tag (EST_7611927; (Asamizu et al, 2000)), previously mapped to the genomic location between *ETC2* and *TCL1* (Figure 3.8 A) in a systematic search for transcribed regions of the *A. thaliana* genome not annotated before (Riano-Pachon et al, 2005) and given the identifier *A. thaliana* orphan RNA 264 (At_oRNA_264), showed homology to transcripts of the six members of the single-repeat R3 MYB gene family. The full gene structure of *TCL2* was annotated *in silico* by BLASTX search. Three genomic regions with extensive homology to coding sequences of the single-repeat R3 MYB genes deduced a gene structure for At_oRNA_264 spanning three exons and two introns (Figure 3.8 A,B).

Figure 3.8: See legend next page.

Figure 3.8. Characterisation of *TCL2*. (A) Localisation of TCL2 between ETC2 and TCL1 reveals a locus with three single-repeat R3 MYB genes in tandem on chromosome 2. (B) Gene structure and expression analysis of TCL2. Arrows indicate primer positions used for expression analysis. UBQ: UBIQUITIN. NTC: non template control. (C) Alignment of protein sequence of TCL2 to the other members of the single-repeat R3 MYB family and the R3 MYB repeat of GL1 and WER. Similarity shading was done according to the PAM120 matrix. H1, 2, 3 correspond to the aa forming α-helices 1, 2, 3 of the R3 MYB domain and filled circles indicate the regularly spaced tryptophan /(phenylalanine/methionine) residues contributing to a hydrophobic core (Frampton et al, 1991). Asterisks indicate the bHLH interaction motif [DE]Lx2[RK]x3Lx6Lx3R (Zimmermann et al, 2004). Triangles indicate aa residues necessary for binding of WER to the GL2 promoter (Tominaga et al, 2007). Orange bars mark aa residues required for CPC cell-cell movement (Kurata et al, 2005). Numbers to the right are equivalent to the number of aa residues of respective proteins. (D) NJ tree are based on the protein sequence of the single-repeat R3 MYB proteins and were generated with ClustalX 2.0. Numbers indicate bootstrap values. The R3 MYB repeat of GL1[Col] was used as an outgroup.

In order to analyse whether the putative novel member of the small R3 MYB gene family is expressed in *A. thaliana*, expression analysis was carried out using cDNA from leaf tissue of *A. thaliana* seedlings. PCR targeting *TCL2* amplified a single fragment sized between 100-200 b and expression of *TCL2* was detected in all four analyzed *A. thaliana* accessions (Figure 3.8 B).

To verify the gene structure deduced *in silico*, exon/intron borders were mapped by comparison of sequenced amplicons of *TCL2* cDNA to gDNA. The analysis confirmed a structure of three exons and two introns (Figure 3.8 B). Starting from an ATG codon deduced from previous bioinformatic analysis, *in silico* translation of the CDS predicted a 100-amino-acid protein (Figure 3.8 C). Alignment of the *TCL2* protein sequence to the six members of the single-repeat R3 MYB protein family and the R3 MYB repeat of GL1 and WER showed that TCL2 possesses a R3 MYB repeat resembling the singlre-repeat R3 MYB family with three regularly spaced tryptophane residues where the first residue is substituted by a methionine residue and a conserved bHLH interaction motif. The C-terminal motif found in CPC to be important for intercellular movement and nuclear localisation is partly conserved, and is identical to the residues of TRY, ETC1 and TCL1. Further, TCL2 possesses a short C-terminal tail after the R3 MYB domain as do TRY and ETC2. TCL2 is grouped together in a clade with ETC2 and TCL1 in a NJ tree and shows 80% identity to TCL1 and 67% identity to ETC2 (Figure 3.8 D).

Therefore, *TCL2* is a novel single-repeat R3 MYB gene family member. Together

with *ETC2* and *TCL1*, *TCL2* constitutes an approximately 9.5 kb genomic locus harbouring three single-repeat R3 MYB gene family members *in tandem* located inside the major QTL candidate interval on chromosome 2.

3.3.2.2 Transgenic complementation of the single-repeat R3 MYB genes *ETC2, TCL1* and *TCL2* identifies *TCL1* as a strong suppressor of trichome initiation

A transgenic complementation test was carried out in order to establish if and which of the three single-repeat R3 MYB candidate genes located in the QTL candidate interval act as natural modifier of trichome density in *A. thaliana* accessions. For that, Can-0 and Gr-1 genomic alleles of *ETC2*, *TCL1* and *TCL2* (Figure 3.9 A) were transformed each into the genetic backgrounds of Can-0 and Gr-1. This setup results in four different classes of transformants for each gene in regard to genotypic background and extra copy of allele. Quantitative assessment of the different classes allows analyzing the following questions: (i) is the gene capable of repressing trichome number; (ii) if yes, do alternative alleles of the gene have different strengths of repression; (iii) is there a gene dosage effect; and (iv) is the allele difference caused by differences in expression level or protein function.

The experimental setup allows to test whether there is a gene dosage effect, i.e. if higher protein abundance, for example due to higher gene expression, altered protein stability, etc., has a larger functional effect. Dosage effect can be measured either in segregating T2 families due to an expected 1:2:1 phenotypic segregation of transgenic lines with a single insertion, further by comparison of T3 lines with different insertion number. Further, the experimental setup based on the four classes of transformants makes it possible to distinguish whether the allelic difference is based on altered protein function or on expression level difference, however, this distinction is only possible in case a difference in protein function is not related to increasing or stabilizing the protein amount. An allelic difference based on expression difference is expected to decrease trichome number in all four different classes, but, as discussed above, there should be a clear distinction between the stronger and the weaker allele. Alternatively, if the functional difference is based on other mechanisms than a dosage effect, the largest difference should arise upon transformation of the strong allele into the background coding for the weak allele.
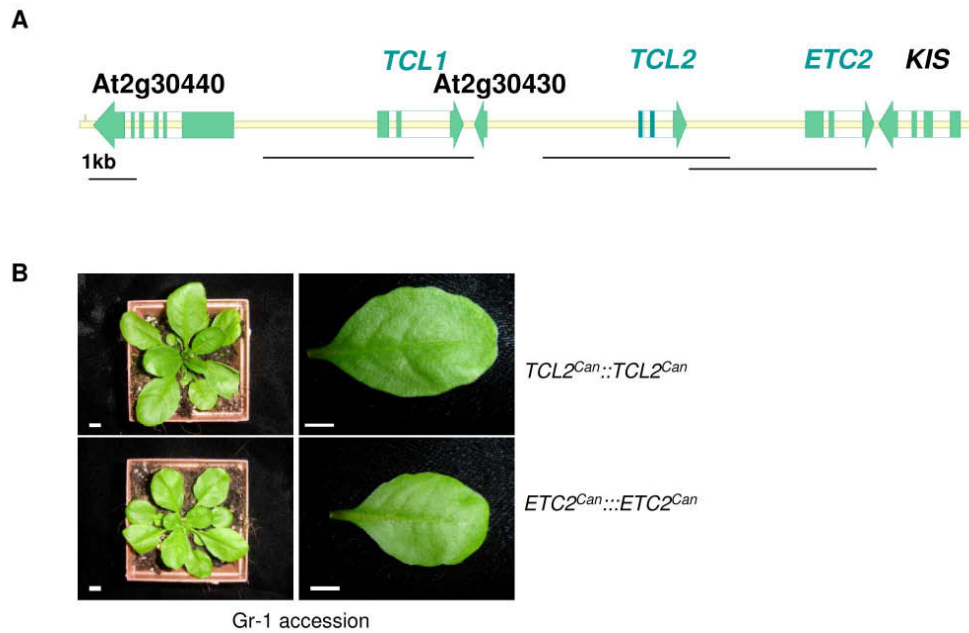
Figure 3.9. Transgenic complementation of Gr-1 and Can-0 using alternative alleles of *ETC2*, *TCL1* and *TCL2*. (A) Schematic representation of genomic alleles of *ETC2*, *TCL1* and *TCL2* used for transformation. Horizontal lines indicate length of respective genomic constructs. Green arrows indicate genes. **(B)** Glabrous T2 lines of Gr-1 transformed with genomic constructs of *TCL2*^{Can} and *ETC2*^{Can}. Shown are the rosette of 6 week old plants to the left and a rosette leaf to the right. Bars represent 0.5 cm.

Qualitative inspection of the transgenic T1 lines (Table 3.4) showed unexpected glabrous phenotypes (for glabrous phenotypes of T2 individuals see Figure 3.9.B) with occasional formation of trichomes on the leaf edge or the midvein. Transformation of *TCL1* resulted in the highest proportion of glabrous plants, 30% upon transformation of *TCL1*$^{Gr-1}$ into the Gr-1 genome, and 45% and 36% upon transformation of the *TCL1*$^{Can-0}$ allele into Gr-1 and Can-0 genome, respectively. Glabrous phenotypes of selected lines could be confirmed in the T2 generation. There were also 12% glabrous individuals detected upon transformation of *ETC2*$^{Can-0}$ into Gr-1 genomic background, however, there were no glabrous individuals detected upon transformation of the same allele into Can-0 genomic background and upon transformation of *ETC2*$^{Gr-1}$ into the Gr-1 genomic background.

The lack of glabrous phenotypes in later cases might be due to low penetrance of glabrous phenotypes in response to *ETC2* in relation to the gene regulatory network, position effects of insertion, lack of multiple insertion lines or a combination of these.

Individuals transformed with *TCL2* alleles lacked glabrous phenotypes in all four different classes. All plants were also inspected under the binocular for quantitative trichome density phenotypes, i.e. a reduction in trichome number. Transgenic plants with disturbed trichome patterning could be observed; these individuals showed a reduced trichome number because of glabrous leaf patches next to wildtype trichome patterning. Individuals with a reduction in trichome number but otherwise wildtype trichome patterning could not be observed by simple visual inspection under the binocular. These possible quantitative effects on trichome number in these transgenic plants remain to be determined in selected T2 or T3 lines phenotyped quantitatively for trichome density and number.

Table 3.2 Qualitative assessement of the effect of ETC2, TCL1 and TCL2 on trichome density on transgenic Gr-1 and Can-0 T1 lines.

		genomic background	
Locus	**Allele**	**Gr-1[a]**	**Can-0[a]**
ETC2 ::ETC2		0% (21)	n.d.
TCL1::TCL1	**Gr-1**	30% (20)	n.d.
TCL2::TCL2		0% (5)	0% (49)
ETC2 ::ETC2		12% (56)	0% (28)
TCL1::TCL1	**Can-0**	45% (57)	36% (19)
TCL2::TCL2		0% (50)	0% (26)

[a]Percentage of glabrous T1 lines (total number of T1 lines analyzed)

Transgenic *ETC2*[Can-0] and *TCL1*[Can-0] Gr-1 plants were also analyzed in the T2 generation to (i) confirm phenotypes observed in the T1 generation, (ii) test whether further lines develop a trichome patterning phenotype upon homozygous insertion state, (iii) test for a dosage effect, i.e. whether in the segregating T2 families (1:2 homozygous:heterozygous transgenic insert state; individuals without transgene are lost due to selective conditions) a phenotypic segregation can be observed and for a correlation of insertion number and glabrousness.

For *ETC2*[Can-0] transgenic plants observed T1 phenotypes could be confirmed in the T2 generation with the exception of one line being categorized glabrous in T1 but forming a wildtype trichome phenotype in T2. None of the lines categorized as wildtype in T1 formed glabrous individuals in T2 families, further, there was neither phenotypic segregation in T2 families detected, nor a correlation of insertion events

and occurrence of glabrousness (the two glabrous lines analyzed possessed one insertion event). Therefore, a gene dosage effect of $ETC2^{Can-0}$ in the Gr-1 background could not be detected. Basically the same findings were made for $TCL1^{Can-0}$ transgenic lines; all glabrous phenotypes of T1 lines could be confirmed in T2 families, with the exception of one line, and there was no gene dosage effect detected in segregating T2 families, nor a correlation of insertion events and occurrence of glabrousness (7 out of 8 analyzed glabrous lines possessed one insertion event and the 8th glabrous line showed a marker gene segregation indicative of gene silencing).

Taken together, since a thorough quantitative phenotyping of all genotypic classes was not carried out and strong (glabrous) phenotypes occurred, an interpretation of the transgenic complementation assay as described in the beginning was not feasible. However, transgenic complementation studies of the three single-repeat R3 MYB genes in tandem confirmed *ETC2* and also implicated *TCL1* as a trichome initiation repressor. Overexpression of *ETC2* under the strong 35S CaMV promoter has been shown to lead to glabrous plants (Kirik et al, 2004b; Wang et al, 2007), while here it was shown that addition of one genomic copy of *ETC2* and *TCL1* suffices to abolish trichome initiation. The high occurrence of glabrous lines upon transformation with *TCL1* in comparison to *ETC2* points to a strong repressor activity of *TCL1*. *TCL2* transgenic lines did not show any glabrous plants, nor could there be detected any strong quantitative effects on trichome number, therefore, here *TCL2* cannot be assigned a functional role as trichome repressor gene. Furthermore, transformation of Can-0 alleles of *ETC2* and *TCL1*, isolated from an accession with high trichome number and therefore expected to harbour weak alleles, lead to the occurrence of glabrous lines indicating that these genes do not code for null alleles. Finally, there was no gene dosage effect detected of *ETC2* and *TCL1* on trichome initiation repression.

3.3.2.3 Association analysis of candidate genes indicates *ETC2* as a possible cause of natural variation in trichome density

Association mapping (linkage disequilibrium (LD) mapping) is an alternative approach to QTL mapping. Association mapping uses segregating variation in natural populations and has the potential to lead to high mapping resolution since it is based on a large number of meioses accumulated during the history of the

sampled accessions. On a global scale *A. thaliana* LD has been shown to decline over 10 kb (Kim et al, 2007). The candidate locus harbours three candidate genes in close proximity (~10 kb), and therefore, association mapping might be powerful in discerning if and which of the candidate genes is causal to trichome density variation. For that, *A. thaliana* accessions exhibiting either extremely high or low trichome number and density phenotypes were sequenced at the three loci and NJ cladograms were constructed for each locus based on respective genomic sequences (Figure 3.10). The cladogram for *ETC2* reveals a strict grouping of accessions according to their phenotypic classification contrary to genetic variation present at *TCL1* and *TCL2*. Furthermore, visual inspection did not detect a single polymorphic site at *TCL1* and *TCL2* grouping high and low trichome number accessions separately.

The phenotypic grouping at *ETC2* is based on a large number of polymorphic sites that differ between low and high trichome number accessions. In order to decrease the number of potential quantitative trait nucleotides (QTN), further extreme accessions were sequenced to reveal recombination breakpoints; taken together, 33 *A. thaliana* accessions were sequenced (Figure 3.11 A). In the putative promoter region only few polymorphic sites were regarded as potential QTN, of these two polymorphic sites at -799 bp and -499 bp could be excluded and one polymorphic site at -53 bp remained strongly associated with the phenotype. On the contrary, the region downstream of the start codon exhibited a large number of polymorphic sites and indels strictly grouping high and low trichome number accessions. Most of the polymorphic sites associated with trichome density were present in introns which mostly harbour extensive indels, and there were one synonymous (+54 bp) and three non-synonymous substitutions (L15F, K19E and Y25H) present in exons. However, the allele of the high trichome density accession Uk-3 excluded all of the polymorphic sites downstream of the start codon except the non-synonymous substitution resulting in K19E. Uk-3 harbours an interesting and informative *ETC2* allele. Uk-3 codes for a high trichome density allele up to the -53 bp polymorphism after which a recombination breakpoint renders it to a low trichome density allele with the exception of the non-synonymous substitution (K19E) at +55 bp. Since there are further highly associated polymorphisms at +54 bp and +73 bp in close proximity, the +55 bp polymorphism might be a reversion event (Figure 3.11 B).
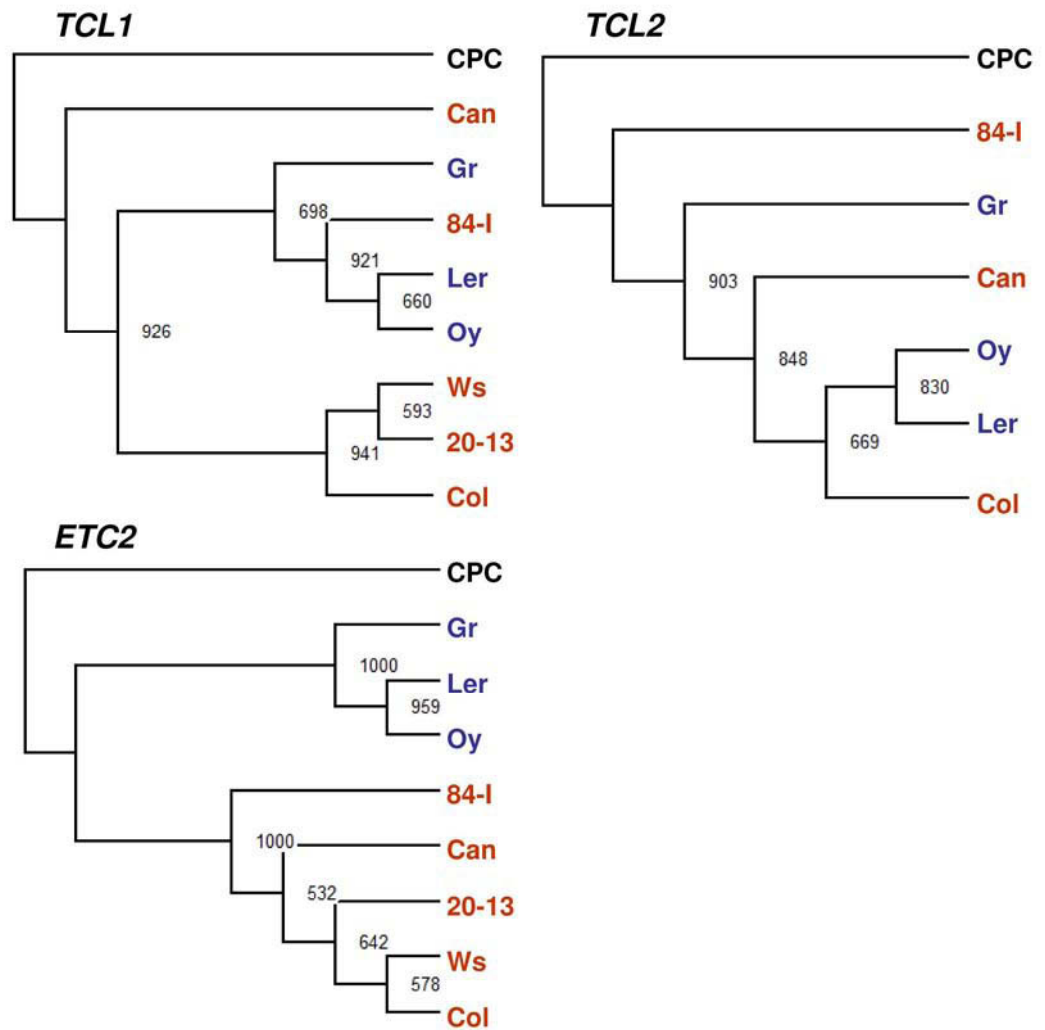
Figure 3.10. Association mapping at the candidate genes *ETC2*, *TCL1* and *TCL2*.

NJ trees are based on genomic sequence of *ETC2*, *TCL1* and *TCL2* (see chapter 2.14.6 for details). Numbers indicate bootstrap values (1000 repetitions). The genomic sequence of *CPC^Col* was used as an outgroup. *A. thaliana* accessions are colour coded in red and blue for high and low trichome density accessions, respectively.
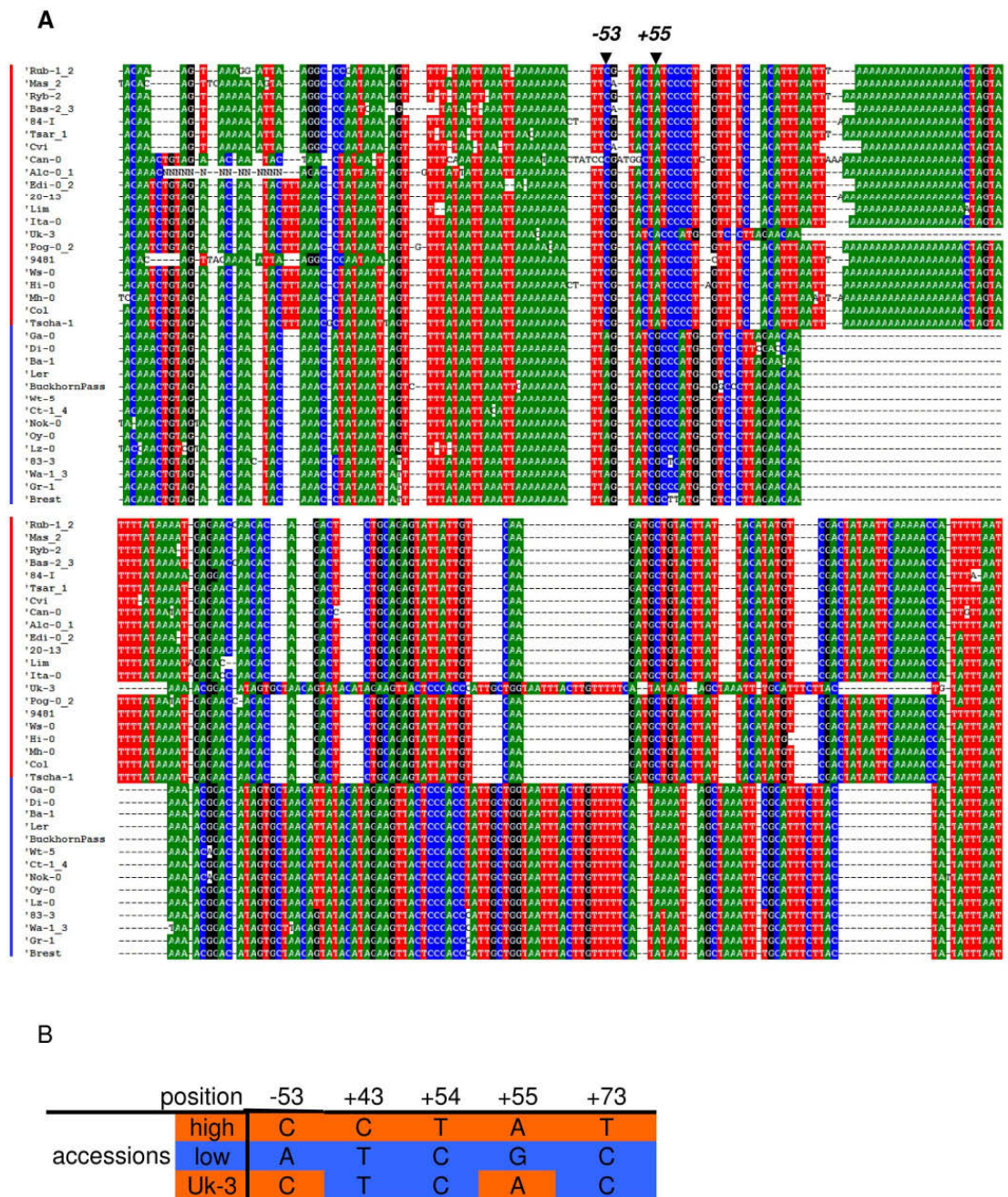
Figure 3.11. Association mapping at *ETC2*. A) Alignment of polymorphic sites and indels at ETC2 locus of 33 Arabidopsis accessions with high (red bar) and low (blue bar) trichome density phenotype. -53 and +55 corresponds to nucleotide positions in respect to the adenosine of the ETC2 start codon which are the only two positions strictly associated with trichome density in this dataset. **(B)** Critical nucleotide positions at the *ETC2* allele of the high trichome density accession Uk-3. Nucleotide positions are given in respect to to the adenosine of the *ETC2* start codon.

Therefore, analysis of natural variation present at the candidate loci *ETC2*, *TCL1* and *TCL2* in *A. thaliana* accessions with extreme trichome density phenotypes allowed to discriminate closely linked loci in regard to being the cause for natural variation in trichome density. Lack of association of polymorphic sites at *TCL1* and *TCL2* and association of two polymorphic sites with trichome number at positions -53 bp and +55 bp within the *ETC2* locus renders these as the primary candidate QTN.

3.3.2.4 F1 complementation test of *etc2-2*^{Col} is in accordance with *ETC2* being allelic to the QTL

To gain further evidence of *ETC2* being the cause of the major QTL on chromosome 2, a modified version of an F1 quantitative complementation test was carried out. In its classical form, wildtype and mutant lines for the gene of interest are crossed to lines carrying alternative QTL alleles, resulting in four different classes of F1
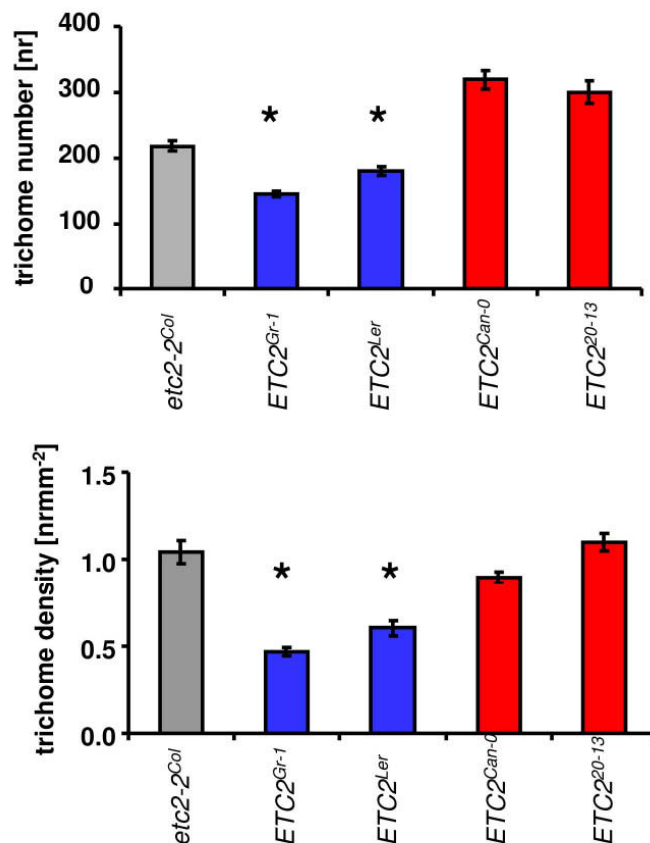
Figure 3.12. F1 complementation test of *etc2-2*^{Col}. Trichome number and trichome density were quantified from F1 individuals heterozygous for etc2-2Col and the low or high trichome density ETC2Gr-1, ETC2Ler, ETC2Can-0, and ETC220-13. Bars represent mean ± s.e.m. of ten individuals. Asterisks indicate significant differences of etc2-2Col/ETC2Can-0 and etc2-2Col/ETC220-13 to etc2-2Col/ETC2Ler and etc2-2Col/ETC2Gr-1 (Tukey´s and Games-Howell HSD Post Hoc test, for trichome number and density, respectively, all *P*<0.001).

individuals with genotypes m(mutant)/QTL^a, wt(wild type)/QTL^a, m/QTL^b and wt/QTL^b. In case the mean difference of phenotype between the m/QTL^a, wt/QTL^a and m/QTL^b, wt/QTL^b genotypes is different, detected by an interaction effect in a two-way ANOVA, it is interpreted as a quantitative failure of the QTL alleles of complementation of the gene of interest and, therefore, as indication of the QTL alleles corresponding to the gene of interest (Long et al, 1996). The design of the modified F1 complementation test used in this study is based on the assumptions that etc2-2^{Col} is a null allele and that the extreme QTL alleles are recessive in combination with a putative distinct functional QTL^{Col}. In case the tested extreme QTL alleles are allelic to *ETC2*, a phenotypic difference is expected in a hemizygous and, therefore, destabilized background. Alternatively, if they were not allelic to *ETC2* and paired with a distinct QTL^{Col}, their effect should be masked by the presence of this locus harbouring a functional allele.

For that, *A. thaliana* accessions carrying extreme QTL alleles for trichome number were crossed to the destabilized etc2-2^{Col} background and the resulting F1 phenotypes were compared to etc2-2^{Col}. F1 individuals derived from low trichome density accessions (etc2-2 ^{Col}/ETC2^{Gr-1} and etc2-2^{Col}/ETC2^{Ler}) exhibited a lower trichome number and density than F1 individuals derived from high trichome density accessions (etc2-2^{Col}/ETC2^{Can-0} and etc2-2^{Col}/ETC2$^{20-13}$)(P<0.05, Tukey HSD and Games-Howell Post Hoc Test, for trichome number and density, respectively) (Figure 3.12). Furthermore, F1 individuals derived from low trichome accessions also formed a lower trichome number and density than the etc2-2^{Col} line (P<0.05, Tukey HSD and Games-Howell Post Hoc Test, for trichome number and density, respectively). These results are in accordance with the extreme QTL alleles being allelic to *ETC2*.

3.3.2.5 Transgenic complementation of *etc2-2*^{Col} suggests a nonsynonymous polymorphism within *ETC2* to be the cause of natural variation for trichome density

Association analysis of natural genetic variation with variation in trichome density narrowed down potential QTNs at *ETC2* to two polymorphic sites, that is position -53 bp and +55 bp in respect to the *ETC2* start codon. In order to test which of the two polymorphic sites is the causal QTN of natural variation for trichome density in *A. thaliana* accessions, transgenic complementation tests of *etc2-2*^{Col} using genomic

$ETC2^{Gr\text{-}1}$ and $ETC2^{Can\text{-}0}$ alleles with exchanged candidate QTN positions were carried out. To this end, the potential QTN positions -53 bp and +55 bp of the $ETC2^{Can}\text{-}_0$ and $ETC2^{Gr\text{-}1}$ alleles were swapped to the alternative nucleotide (Figure 3.13) and transformed into $etc2\text{-}2^{Col}$ plants.

The resulting trichome number phenotypes of T1 lines were analyzed quantitatively together with $etc2\text{-}2^{Col}$ plants transformed with an empty vector (Figure 3.13). Two main findings strongly indicate the +55 bp position at $ETC2$ being causal for the observed quantitative variation for trichome density in *A. thaliana* accessions. First, $etc2\text{-}2^{Col}$ transgenic for $ETC2$ constructs harbouring the Gr-1 nucleotide at the +55 bp position formed a lower trichome number than lines transgenic for $ETC2$ constructs harbouring the Can-0 nucleotide, independent of the allele background ($P<0.05$, ANOVA). Second, the allele background did not have a significant effect on trichome number ($P=0.35$; ANOVA). Finally, independent of the $ETC2$ construct, all transgenic lines had a tendency towards a lower trichome number than $etc2\text{-}2^{Col}$ control lines, although the effect was only significant for lines transformed with $ETC2$ alleles with the +55 position from Gr-1 ($P<0.05$, ANOVA). Together, these findings indicate that all alleles code for a functional trichome repressor gene, that the +55 bp position affects the strength of repressor activity and thus, a nonsynonymous SNP changing lysine to glutamate (K19E) in high trichome density accessions constitutes a QTN for trichome density.

Among the transgenic complementation lines there were several lines with abolished trichome initiation or patterning, i.e. glabrous lines or lines with trichomes formed only at leaf edges or at the midrib. These phenotypes, however, were only found upon transformation of $ETC2$ alleles derived from the Gr-1 genomic background; 18% and 9% of lines transgenic for Gr-1 alleles with swapped residues at -53 bp and +55 bp position, respectively. This strong repressor effect might be either due to methodical procedure, i.e. position effects or multiple insertion events of transgenes or due to an existing biological effect of the allele background. Whatever the underlying mechanism, however, the above findings and their statistical significance showing the modification of trichome number initiation mediated by the +55 bp polymorphism at $ETC2$ remain significant, whether these strong phenotypes are included or omitted in the described analysis.
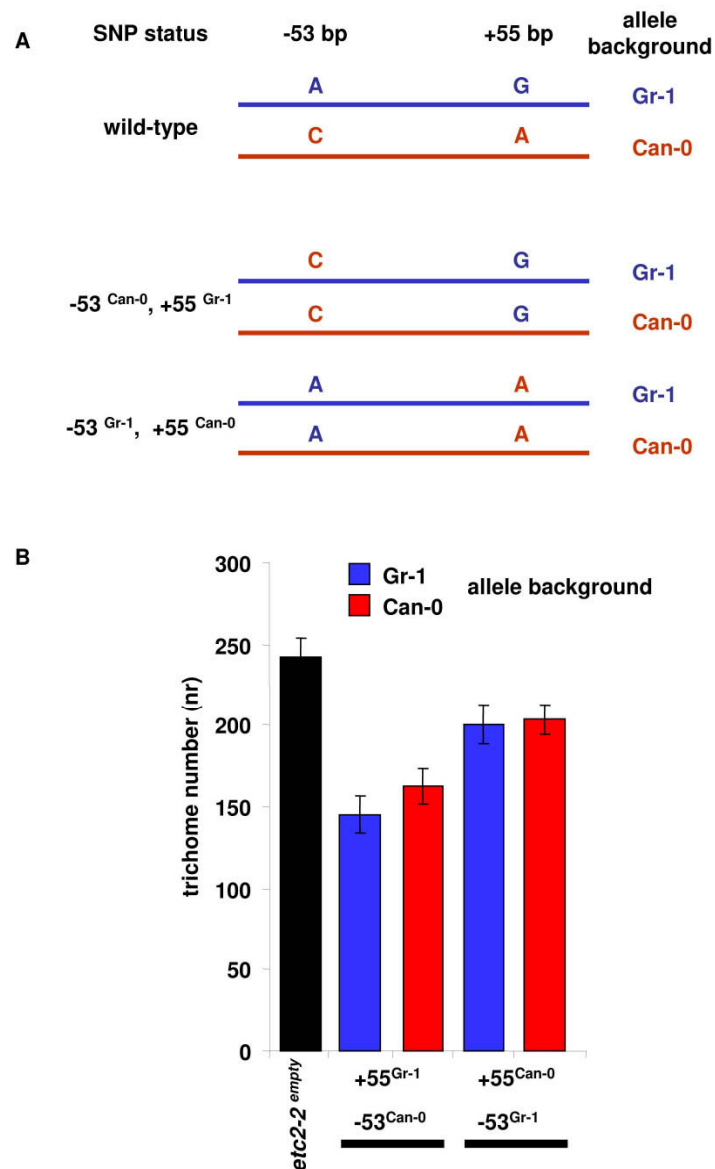
Figure 3.13. Transgenic complementation test of *etc2-2^Col*. (A) Schematic representation of chimeric ETC2 constructs with swapped candidate QTNs used for transgenic complementation testing. (B) Chimeric ETC2 constructs were transformed into etc2-2Col. Data points represent mean ± s.e.m. The main effect of the SNP state is significant (P=0.001, ANOVA); the main effect of the background allele is not significant (P=0.35, ANOVA).

3.4 Characterisation of trichome patterning at the cellular level

Trichome cell specification is a highly regulated process acting early during the dynamics of leaf development and defines which epidermal cells undergo trichome cell fate. Here it was shown that a QTN in the trichome repressor gene *ETC2*, located in the major QTL candidate interval on chromosome 2, contributes to natural variation in trichome number and density, however, fine mapping of the QTL candidate region points to a possible further locus(i). In the light of these findings and to understand which processes are affected by the major QTL on chromosome 2 between Can-0 and Gr-1, a detailed analysis at the cellular level was carried out to find evidence excluding or corroborating the following models explaining trichome number and density modulation: (i) trichome number is a function of leaf cell number; (ii) specified trichomes are spaced by subsequent cell division and/or expansion of intervening epidermal cells; (iii) trichome number and density is modulated by a window of competence for trichome initiation (Larkin et al, 1996); (iv) the rate of trichome initiation is altered, i.e. the activity of trichome cell fate regulators, trichome activators and repressors, is modulated. To test these models, Can-0 and Gr-1 leaves were phenotyped for trichome number and density as well as leaf cell number to estimate the average number of cells formed between trichomes, and leaf cell size. As a surrogate for epidermal leaf cell number and size, palisade mesophyll cells were analyzed.

The results of the leaf cell measurements are summarized in Table 3.5 and visualized schematically in Figure 3.14 A. The data obtained by cellular analysis cannot explain the first two models, stating trichome number and density are determined either by total leaf cell number or by the number and/or size of cells formed in between trichomes after trichome cell specification. Contrary to what would be expected for the first model, Gr-1 has a similar total mesophyll cell number as Can-0 ($P>0.05$, Student's t-test). For the second model Gr-1 is predicted to form a similar number of trichomes spaced over a larger area due to a higher cell number or larger cell size, however, Gr-1 forms significantly less trichomes ($P<0.05$, Student's t-test) and the same number of leaf cells which are smaller in size ($P>0.05$ and $P<0.05$, Student's t-test, respectively). Interestingly, Gr-1 and Can-0 differ significantly in the number of cells present between trichomes ($P<0.05$, Student's t-test), on average Gr-1 forms ~4.2× the number of cells between trichomes of Can-0, which reflects the inverse quantitative effect size difference of trichome number and

Table 3.3 Characterisation of the accessions Can-0 and Gr-1, and mutants for *CPC* and *TRY* in regard to leaf mesophyll cell and trichome traits

Trait	Accession	Mean	SEM[a]	*P* (Student´s t-test)
Mesophyll Cells per Trichomes	Gr-1 Can-0	1778.6 421.8	76.6 15.9	0.000
Mesophyll Diameter [µm^2]	Gr-1 Can-0	34.4 38.9	1.0 1.1	0.005
Total Mesophyll Cell Number [nr]	Gr-1 Can-0	169745 192481	7723 10773	0.092
Trichome Number [nr]	Gr-1 Can-0	96.5 456.1	3.3 20.3	0.000
Trichome Density [nr mm^{-2}]	Gr-1 Can-0	0.66 2.19	0.03 0.13	0.000
Leaf Area [mm^2]	Gr-1 Can-0	150.1 218.2	5.5 8.5	0.000

Trait	Genotype	Mean	SEM[a]	*P* (Student´s t-test)
Mesophyll Cells per Trichomes	CPC^{Ws} cpc^{Ws}	382.6 285.8	28.6 13.9	0.002
Mesophyll Diameter [µm^2]	CPC^{Ws} cpc^{Ws}	32.8 33.4	1.0 0.8	0.628
Total Mesophyll Cell Number [nr]	CPC^{Ws} cpc^{Ws}	120783 129282	11335 10383	0.582
Trichome Number [nr]	CPC^{Ws} cpc^{Ws}	301.2 459.8	23.4 25.1	0.000
Trichome Density [nr mm^{-2}]	CPC^{Ws} cpc^{Ws}	3.40 4.48	0.23 0.25	0.003
Leaf Area [mm^2]	CPC^{Ws} cpc^{Ws}	92.1 108.1	4.5 7.8	0.089

Trait	Genotype	Mean	SEM[a]	*P* (Student´s t-test)
Mesophyll Cells per Trichomes	TRY^{Ler} try^{Ler}	1176.2 922.0	94.0 78.2	0.041
Mesophyll Diameter [µm^2]	TRY^{Ler} try^{Ler}	49.5 66.0	1.7 2.2	0.000
Total Mesophyll Cell Number [nr]	TRY^{Ler} try^{Ler}	131377 68459	10434 6372	0.000
Trichome Number [nr]	TRY^{Ler} try^{Ler}	117.7 72.7	7.4 3.2	0.000
Trichome Density [nr mm^{-2}]	TRY^{Ler} try^{Ler}	0.53 0.38	0.04 0.03	0.003
Leaf Area [mm^2]	TRY^{Ler} try^{Ler}	232.9 209.9	11.2 13.6	0.205

SEM: Standard error of the mean

density between Gr-1 and Can-0 (~0.21× and ~0.3×, respectively). The detected modulation of the number of cells formed in between trichomes can be explained either by a different window of competence for trichome initiation, i.e. the duration/time during leaf development where the genetic regulatory process of trichome initiation is switched on, or by differences of the activity of factors acting to regulate trichome cell fate, as for example the described *ETC2* alleles.

Since the QTL candidate interval harbours three members of the single-repeat R3 MYB gene family of trichome repressors (*ETC2*, *TCL1* and *TCL2*), the nature of the modulation of leaf cell parameters between Gr-1 and Can-0 was investigated further by analyzing mutants in *CPC* and *TRY* in respect to wild type lines (Table 3.5, Figure 3.14 B). In contrast to *ETC2*, mutant lines of *CPC* and *TRY* show stronger trichome number and density phenotypes facilitating analysis. In accordance to (Schellmann et al, 2002)*, cpc*^{Ws} leads to a higher trichome number and density (1.5× and 1.3×, respectively; both *P*<0.05 Student's t-test), although the effect is smaller than that between Gr-1 and Can-0. Interestingly, modulation of leaf cell parameters followed a pattern similar to that between Gr-1 and Can-0. The increase of trichome number and density in *cpc*^{Ws} was accompanied by a decrease (0.75×) of the number of cells formed between trichomes (*P*<0.05 Student's t-test), and again as for Gr-1 and Can-0 these parameters are inversely related in their effect size. Cell size between mutant and wild type lines was unaltered (*P*>0.05, Student's t-test) and therefore does not seem to play a role in modulation of trichome density. The same conclusion is true for Gr-1 and Can-0 where there is a significant, however, small difference in cell size which cannot explain the large modulation in trichome density.

Mutants in *TRY* are characteristic by forming trichomes next to each other and at the same time less trichome initiation sites (TIS). Further, *try* leads to increased trichome branching accompanied by a higher endoreduplication level (Hülskamp et al, 1994; Schellmann et al, 2002) indicative of *TRY* interacting with cell cycle processes. The number of TIS was used for further analysis since the spacing of trichomes over a field of cells was of interest and trichome nests were not observed in Gr-1 and Can-0. In contrast to *cpc*^{Ws}, changes in leaf cell parameters due to *try*^{Ler} were distinct to those observed between Gr-1 and Can-0. First, decreased TIS in *try*^{Ler} were intervened by a lower number of cells, i.e. an inverse relation of trichome number and density with cells formed in between trichomes was not detected, contrary to *cpc*^{Ws} and to Gr-1 versus Can-0. Secondly, *try*^{Ler} lead to dramatic changes in cell diameter and number (both *P*<0.05, Student's t-test) while

maintaining approximately the same leaf area; cell diameter of try^{Ler} increased by ~33% and cell number decreased by ~52%. While no significant changes in cell size and number were observed due to cpc^{Ws}, cell size was modulated between Gr-1 and Can-0 albeit to a smaller extent (~13% difference in cell diameter).
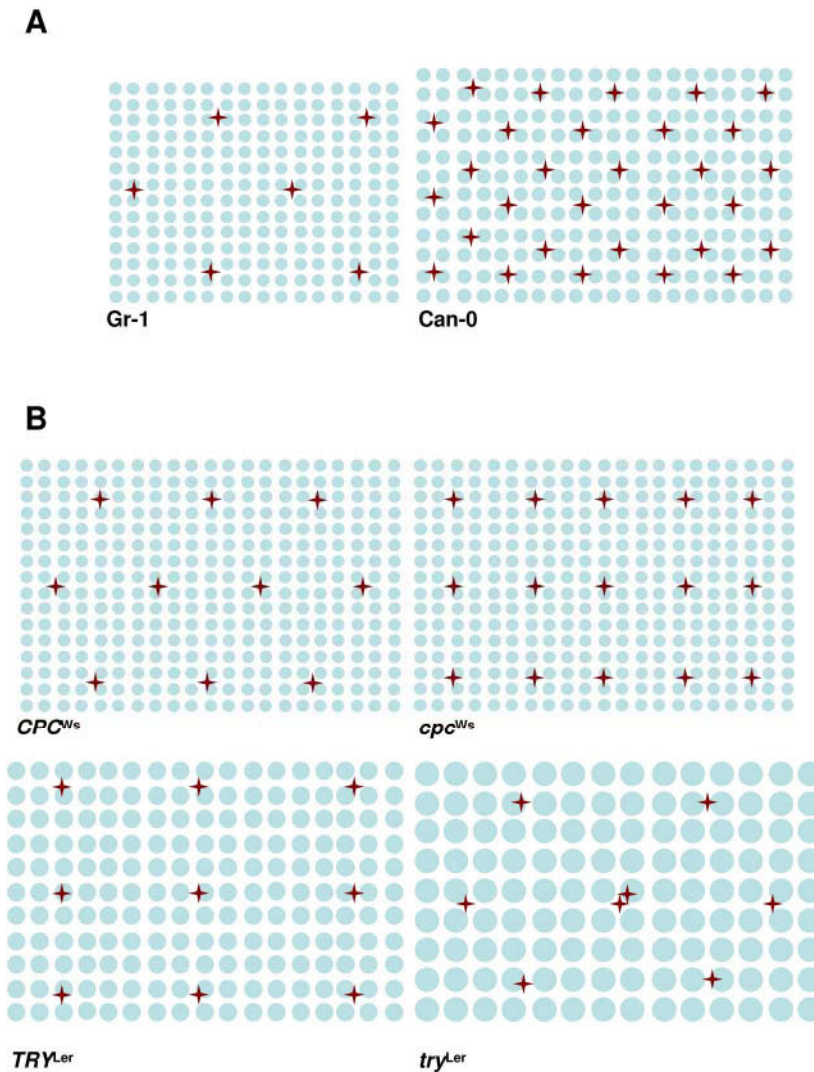
Figure 3.14. Schematic representation of trichome patterning at the cellular level. (A) Gr-1 versus Can-0. (B) CPC^{Ws} versus cpc^{Ws} and TRY^{Ler} versus try^{Ler}. Blue circles represent mesophyll cells, brown crosses represent trichomes. Size of mesophyll cells, number of trichomes and leaf area are drawn in proportion to one another separately for each of the three genotypic comparisons.

Taken together, the modulation of the number of cells formed between trichomes between Gr-1 and Can-0 phenocopies a mutant in *CPC,* indicating that the

111

difference of trichome spacing between Gr-1 and Can-0 at the cellular level can potentially be explained by loss of trichome repressor activity. It is crucial, however, to pinpoint the timing of the modulation of the number of cells between trichomes and the dynamics of trichome initiation in Gr-1 and Can-0 with further experiments. These allow to draw conclusions whether the variation in the number of cells between trichomes arise mainly as a consequence of differences in the activity of factors acting to define trichome cell fate, with a major effector being *ETC2*, or if genes functioning in other pathways contribute to trichome spacing, for example, by modulation of cell cycling or by modulation of a window of opportunity of trichome formation.

3.5 Functional characterization of *Arabidopsis thaliana* accessions exhibiting extreme trichome density: Ultraviolet-B (UV-B) tolerance and anthocyanin content

In *A. thaliana*, a WD/bHLH/MYB transcription initiation complex is central to several developmental processes and biosynthetic pathways, among these trichome initiation and anthocyanin/flavonoid biosynthesis. Although a matter of debate, trichomes and/or anthocyanin content have been implicated in UV-B protection in several plant species (Cominelli et al, 2008; Karabourniotis et al, 1992; Skaltsa et al, 1994; Steyn et al, 2002). The collection of *A. thaliana* accessions phenotyped for trichome density established in this lab prompted to investigate a co-regulation of these traits with and/or without UV-B exposure using natural variation. Specifically, *A. thaliana* accessions with extreme low and high trichome density were exposed to UV-B to address the following questions, (i) is there natural variation in UV-B tolerance and/or anthocyanin content, (ii) is there a correlation of trichome density and anthocyanin content and (iii) is there a correlation of trichome density and/or anthocyanin content in regard to UV-B tolerance.

A. thaliana accessions show natural variation in UV-B tolerance

The *A. thaliana* accessions Gr-1and L*er* (low trichome density accessions) and Can-0, Uk-3, Tsar/1 and 20-13 (high trichome density accessions) were chosen for analysis of UV-B tolerance based on their phenotypic categorization as possessing extreme and opposing trichome density phenotypes. UV-B tolerance of these *A. thaliana* accessions was monitored at two different exposures of chronic UV-B stress, 4 µmol m^{-2} s^{-1} UV-B for 1 h day^{-1} (further designated moderate UV-B
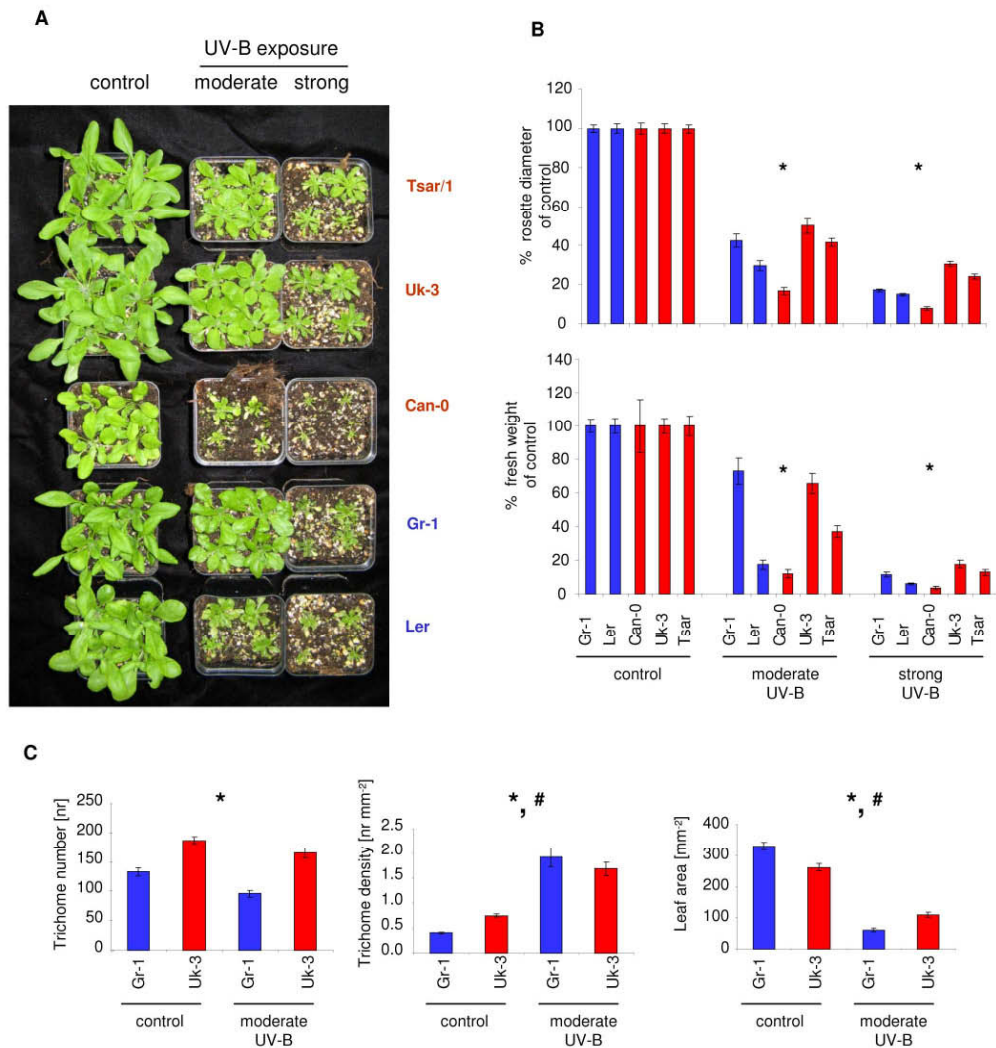
Figure 3.15. UV-B exposure of A. thaliana accessions. (A, B) Natural variation in UV-B tolerance. (A) Representative rosettes of Arabidopsis accessions Tsar/1, Uk-3, Can-0, Gr-1 and Ler at day 14 of moderate (4 µmol m-2 s-1 UV-B for 1 h/day) and strong (4 µmol m-2 s-1 UV-B for 1.5 h/day) UV-B exposure and under control (no UV-B) conditions. (B) Measurements of rosette diameter and fresh weight of Arabidopsis accessions at day 18 of moderate and strong UV-B exposure and of control conditions. Measurements of accessions are normalized to the mean value under control conditions and shown as mean ± sem of n=17-20 and n=8-10 for rosette diameter and fresh weight, respectively. * indicates a significant main effect of accession (P<0.001, ANOVA). (C) Trichome number and density upon UV-B exposure. Measurement of trichome number, trichome density and leaf area of the accessions Gr-1 and Uk-3 at day 18 under moderate UV-B exposure and control conditions. Shown are mean values ± sem of n=8-10 individuals measured in triplicate on leaf positions 8-10. * indicates significant main effect of UV-B exposure on respective traits (P<0.001, ANOVA). # indicates a significant accession×treatment interaction affect (P<0.01, ANOVA). Blue and red correspond to low and high trichome number accessions, respectively, as categorized under control conditions.

113

treatment) and for 1.5 h day^{-1} (further designated strong UV-B treatment) for 18 days in comparison to control conditions. The plant growth parameters of rosette diameter and fresh weight were used as indicator for UV-B tolerance.

Upon UV-B exposure *A. thaliana* accessions were heavily impaired in vegetative growth (Figure 3.15 A). For example, at day 18 of moderate and strong UV-B exposure there was on average a 50% and 75% decrease of rosette diameter, respectively, in comparison to control conditions ($P<0.05$, Games Howell Post Hoc Test). Furthermore, the accessions exhibited differences in UV-B tolerance detected by an accession×treatment interaction effect present for both growth parameters ($P<0.05$, ANOVA). Under the moderate UV-B treatment the accessions L*er* and Can-0 exhibited a significantly stronger reduction in rosette diameter and fresh weight relative to control conditions than the accessions Tsar/1, Uk-3 and Gr-1 ($P<0.05$, Games Howell Post Hoc Test) and the same trend of relative growth reduction was observed under the strong UV-B treatment. The negative impact of UV-B exposure on rosette diameter in general and a stronger reduction of rosette diameter of L*er* and Can-0 in comparison to the other accessions were already manifested at day 10 and 14 of UV-B treatment albeit with varying degrees of significance (data not shown).

A low and a high trichome density accession, L*er* and Can-0, respectively, exhibited less UV-B tolerance in contrast to other low and high trichome density accessions, therefore, under these experimental conditions no correlation between high trichome number - exhibited under control conditions - and UV-B tolerance could be detected. *A. thaliana* trichomes have been shown to be inducible by stress, upon artificial damage newly formed leaves formed an increased number of trichomes mediated by the hormone jasmonate (Traw & Bergelson, 2003; Yoshida et al, 2009). Similarly, if trichomes play a role in UV-B tolerance, they might be upregulated upon UV-B exposure. At day 18 of moderate UV-B exposure, the accessions Gr-1 and Uk-3, possessing low and high trichome number under control conditions, respectively, form significantly less trichomes under UV-B conditions compared to control conditions ($P<0.001$, ANOVA), however, both possess a significantly higher trichome density under UV-B conditions ($P<0.001$, ANOVA) (Figure 3.15 B). Since upon UV-B exposure there is also a significant decrease in leaf area ($P<0.001$, ANOVA), it remains to be determined by cellular analysis if the increase of trichome density under UV-B is a controlled response of trichome initiation or a consequence of decreased leaf area. Interestingly, for trichome density and leaf area there is also

a significant accession×treatment interaction effect present (both P<0.01, ANOVA), indicating that Gr-responds stronger than Uk-3 to moderate UV-B treatment in respect to these traits.

Natural variation of anthocyanin content in A. thaliana populations
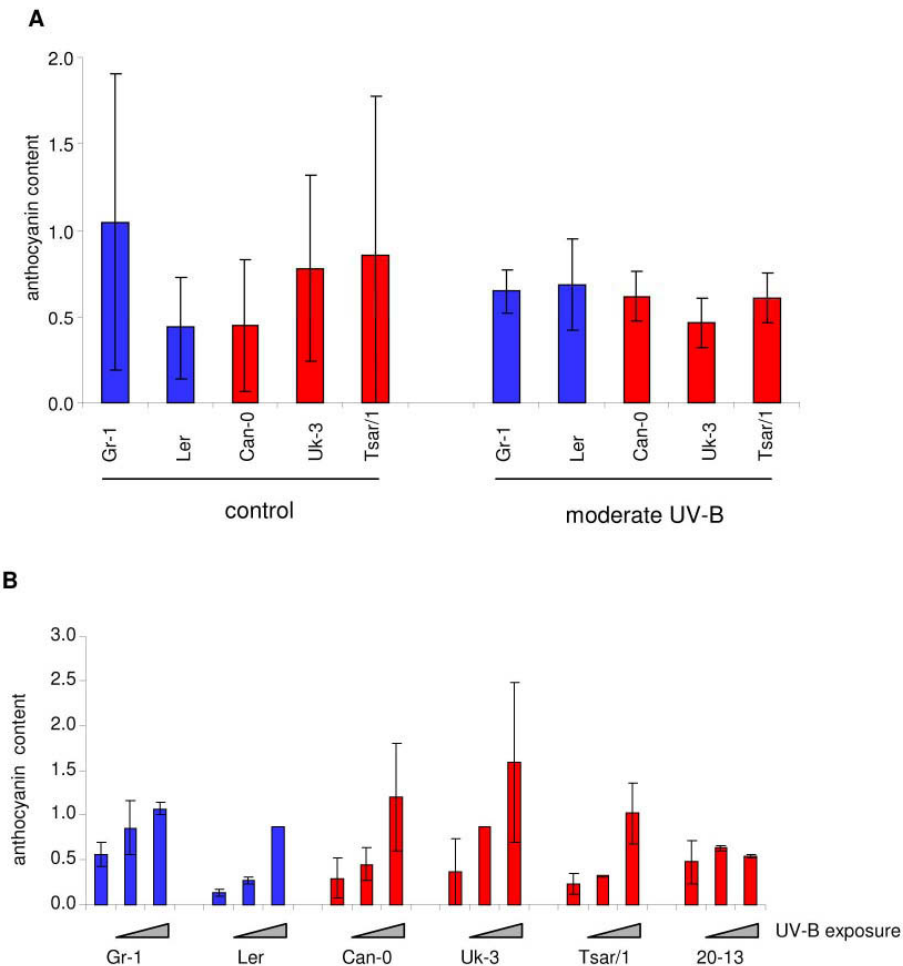
Figure 3.16. Anthocyanin content of *A. thaliana* accessions. Late (A) and early (B) response to UV-B exposure. (A) Anthocyanin content measured at day 18 of moderate UV-B exposure and under control conditions. (B) Anthocyanin content measured at day 3 of moderate and strong UV-B exposure and under control conditions. The y-axes represent anthocyanin content expressed as OD$_{530}$ - OD$_{657}$ mg fresh weight^{-1} 1000. Shown are mean ± stdev of n=6 measurements for control conditions, n=2-6 measurements for moderate UV-B conditions (A) and n=1-2 measurements in (B). Blue and red bars correspond to low and high trichome density accessions, respectively, as categorized under control conditions.

To start analysing whether *A. thaliana* accessions show natural variation in anthocyanin content and/or in regulation of anthocyanin content upon UV-B exposure, anthocyanin content of the above individuals exposed to moderate UV-B and control conditions for 18 days was analyzed (Figure 3.16 A). Due to severe growth reduction and tissue damage individuals grown under strong UV-B conditions (Fig) were excluded from this analysis. For anthocyanin measurement, acidic methanol extracts from leaves were analyzed photometrically at OD_{530}. This method, however, has a low resolution since the extraction procedure does not distinguish between anthocyanin and other flavonoids which also absorb at an OD_{530}, albeit to a low extent (Franz Hadacek, personal communication).

Under control conditions without UV-B exposure there was no significant difference in anthocyanin content detected between the accessions (P=0.419, ANOVA; Figure 3.16 A). Further, moderate UV-B exposure generally did not seem to increase anthocyanin content in comparison to control conditions nor lead to differences in anthocyanin content between the accessions, however, significance testing was not possible for UV-B treated samples due to too few data points. Measurement at day 18 of UV-B exposure monitors late response to UV-B exposure and, therefore, to detect possible early, transient changes six *A. thaliana* accessions were analyzed for anthocyanin content after three days of UV-B exposure (Figure 3.16 B). At three days of UV-B exposure, the strong UV-B treatment already resulted in a clear decrease of fresh weight in comparison to control and moderate UV-B conditions (P<0.001, Games Howell Post Hoc Test). At day three, anthocyanin content seemed to increase with UV-B exposure in each accession but 20-13. A possible increase of anthocyanin content in response to UV-B was therefore detected in low as well as in high trichome density accessions. Since there were at most two datapoints measuring anthocyanin content per accession and condition, the experiment could not be subjected to significance testing.

Taken together, natural variation for UV-B tolerance is present among *A. thaliana* accessions, and UV-B exposure of *A. thaliana* accessions lead to formation of a higher trichome density in comparison to control conditions, however, a detailed anatomical analysis is needed to distinguish whether this is due to regulation of trichome initiation or of cell size and/or number. In this pilot analysis *A. thaliana* accessions grown for 33 days under control conditions showed no significant differences in anthocyanin content and they lacked a clear response upon moderate UV-B exposure after prolonged treatment, however, there seemed to be an early

response to UV-B exposure in regard to anthocyanin accumulation, measured on accessions treated with UV-B for three days. The possible increase in anthocyanin content, however, was seen low and high trichome density accessions.

4   DISCUSSION

4.1   Genetic architecture of trichome patterning and leaf size and morphology traits in *Arabidopsis thaliana*

As discussed by Symonds et al. (2005), in order to draw firm conclusions about natural genetic variation for a given trait, results from several mapping populations derived from different accessions need to be gathered, since a single mapping population will only reveal a conservative estimate of QTL that are polymorphic between the used parental accessions. Therefore, to understand the underlying genetics of the extensive phenotypic variation for trichome density in surveys across *A. thaliana* accessions (Hauser et al, 2001; Symonds et al, 2005), it will be of interest to compare results across several mapping populations in independent experiments, as well as with a recent genome wide association study (Atwell et al, 2010), to more thoroughly estimate for example how many loci contribute quantitatively to natural variation in trichome density, how many alleles are segregating at these loci, estimate their effect size, epistatic interactions, etc. However, accurate comparison of studies is hampered by differences in phenotyping of trichome density and by large confidence intervals especially in the case of minor QTLs (Mauricio 2005) and similar difficulties arise when comparing QTL results across different mapping populations, where different sets of markers for construction of genetic maps were used.

To date, five sets of recombinant inbred (RI) derived from a total of eight different accessions (Bay, Col-4, Cvi, Da-12, Ei-2, L*er*-0, L*er*-2, No-0, and Sha) have been used to map QTLs for trichome number or trichome density with different emphases: (i) to gain knowledge about the large difference of trichome density between Col-4 and L*er*-0 (Larkin et al, 1996), (ii) to describe trichome density modulation across mapping populations (Symonds et al, 2005), (iii) to compare QTL architecture between juvenile and adult leaves (Mauricio, 2005) and (iv) to find trichome density QTL colocalising for herbivore resistance (Pfalz et al, 2007). At least ten QTL regions affecting trichome number or density have been detected in these studies scattered across all chromosomes. Here, in an effort to jointly map QTLs for trichome patterning and leaf size and morphology traits in a Gr-1×Can-0 F2 mapping population four different QTL regions for the traits trichome number,

trichome density, edge trichomes and heteroblasty were detected. These probably colocalise with previously mapped QTL (Figure 3.4 A) (Table 3.3). The lack of novel candidate regions could point to near saturation of identifiable QTL in mapping studies of currently used sample size and marker density. Interestingly, two QTL candidate regions implicated in trichome patterning previously named *REDUCED TRICHOME NUMBER* (*RTN*; (Larkin *et al.* 1996) or *TRICHOME DENSITY LOCUS2* (*TDL2*, (Symonds *et al.* 2005)) and *TRICHOME DENSITY LOCUS5* (*TDL5* (Symonds *et al.* 2005)), have been detected in all studies, and they are located on the middle of chromosome 2 and on top of chromosome 4, respectively. A GWA also detected an association at the genomic regions of *TDL2* and *TDL5*, and lists the strongest candidate genes as *TCL2*, *TCL1* and *ETC2* and *ETC3*, respectively (Atwell et al, 2010). In this study, the QTL colocalising with *TDL2/RTN* has been modelled as a major QTL, explaining 33% and 9% of the variation for trichome number and density, respectively. In other studies there have been diverse estimates of its effect size depending on the mapping population and on the study carried out, ranging between 9-70%. These outcomes could underlie a number of reasons, like genotypic sampling, epistatic effects of the QTLs depending on the genetic background, differences in phenotyping and in environmental growth conditions and/or QTL modeling. However, the repeated mapping of a major QTL on chromosome 2 in different mapping populations and across studies points to the location of an important locus effected by natural variation for modulating trichome density.

In contrast to trichome patterning and flowering time traits, there was no major QTL detected for leaf size and morphology traits (Figure 3.4 B) (Table 3.3). For leaf length there was no QTL detected at all, although parental accessions differ significantly in leaf length (Table 3.1); this could be explained by leaf length underlying many small effect size QTL below the detection limit and/or high influence of environmental variation on this trait. However, H^2 estimates of leaf length are in the range of leaf width and edge trichomes of which QTL could be detected. Interestingly, the most QTL were detected for leaf shape index which also shows a high H^2 estimate (0.78). In the case that few QTL are interpreted as detection being hampered by environmental variation, the difference to leaf area genetic architecture with only two detected QTL and a low H^2 estimate (0.21) might point to a tight regulation of leaf shape regardless of leaf size. Further, leaf shape QTL do not overlap with leaf area or width QTL, pointing towards regulation by

different loci. Two studies have addressed the QTL architecture of *A. thaliana* leaf size and morphology. In an effort to complement the knowledge of leaf size and morphology gained in analyzing artificially induced mutants, leaf and petiole size were mapped in a RIL population derived of L*er*-0 and Col-4 (Perez-Perez *et al.* 2002). A further study investigated the relation between leaf and floral morphology in a L*er*-2×Cvi RIL popuation (Juenger *et al.* 2005). In comparison we find possibly the same QTL regions for leaf area and width on the bottom of chromosome 2 with both studies and of leaf width on the bottom of chromosome 5 with the study of Juenger et al (2005).

There is a long debate about the underlying nature of genetic architecture of complex traits, i.e. whether there is preponderance of a few large effect QTL or whether there are mainly many small effect QTL for any given trait. Initially, QTL mapping studies pointed to the former, while with the increase in studies with large mapping populations as well as a large number of markers and in the course of fine mapping studies it became evident that initial studies lacked power and therefore overestimated effect sizes due to undetected QTLs (reviewed in (Mackay et al, 2009)). Also, statistical considerations show that very large sample sizes are needed to detect small-effect size QTL (equation [21.3], page 367 and equation [15.37], page 471 in (Falconer & Mackay, 2005) and (Lynch & Walsh, 1998), respectively) and that QTL detection is dependent on standardized phenotypic differences between marker classes, that is the average difference δ scaled by the standard deviation σ_W of the trait in the marker classes (Mackay et al, 2009). Accordingly, in this study, the largest effect size QTL were detected for flowering time traits where the analysis was based on a smaller sample size (n=140). The second large-effect QTL was detected for trichome number based on a larger sample size (n=266); this was promoted by selecting for parental accessions with maximized phenotypic difference and the accurate description of the trait by using selected leaf positions for phenotyping in order to optimize for δ/σ_W.

Due to the presence of three genotypes per locus in an F2 mapping population, gene action of QTL can be modeled (Table 3.3). Of 19 QTLs detected for trichome patterning and leaf size and morphology traits, eight exhibit partial dominance and eight overdominance. Less frequent gene actions detected are near complete dominance (one locus) and near additivity (two loci). We could not detect epistatic (locus by locus) interactions in our mapping population for any of the traits. For trichome density, Symonds et al. (2005) detected an epistatic interaction between

RTN/TDL2, the location of the major QTL in this study, and a population specific QTL detected on chromosome 4 (*TDL6*) in a L*er*-2xCvi mapping population. Pfalz et al (2009) detected an epistatic interaction with a QTL on chromosome 3, which might colocalise with a trichome number QTL detected in this study and with *TDL3* (Symonds et al, 2005), and a QTL on the lower arm of chromosome 4, which might correspond to *TDL6*. However, *TDL6* does not seem to be polymorphic between Can-0 and Gr-1 or shows an effect size beyond the detection limit, further in the study of Symonds et al (2005) *TDL3* and *TDL6* were not detected in the same mapping population. The genomic location of *TDL6* might colocalize with *TRANSPARENTA TESTA8* (*TT8*), which has been shown to affect trichome density at leaf edges (Maes et al, 2008) and with *ACCELERATED CELL DEATH6* (*ACD6*) which has been associated with trichome density in a GWA (Atwell et al, 2010).

All traits displayed transgressive segregation, i.e. some F2 individuals show a more extreme phenotype than the parental accessions (Figure 3.3). For some traits (total trichome number, heteroblasty, leaf area, leaf width and leaf index) this can be explained either by the effects of overdominant loci and/or the occurrence of loci within the accessions with opposing effects. Furthermore, genetic evidence for transgressive segregation could stay undetected due to several minor QTLs beyond the detection limit. Unsurprisingly, we detected for each of the accessions only loci that decrease and increase trichome density or total trichome number for Gr-1 and Can-0, respectively, since the two parental accessions were selected based on their contrary and extreme phenotypes (Hauser *et al.* 2001) for trichome density. However, as shown by the previous QTL mapping study of trichome density in several populations (Symonds *et al.* 2005) several loci not detected in these two accessions can contribute to natural variation in trichome density pointing to the existence of accessions with even more extreme trichome phenotypes (under the assumption of additive gene action) and of the possibility to create extreme phenotypes by population hybrids. However, as analyzed by Mauricio (1998), even though high trichome density may serve protective functions, in the absence of these pressures high trichome density individuals exhibited fitness costs in this study. This may also explain the distribution of phenotypes sampled which shows a bias towards lower trichome density accessions (Hauser et al, 2001; Symonds et al, 2005).

4.2 Deductions following the identification of the QTN for trichome density
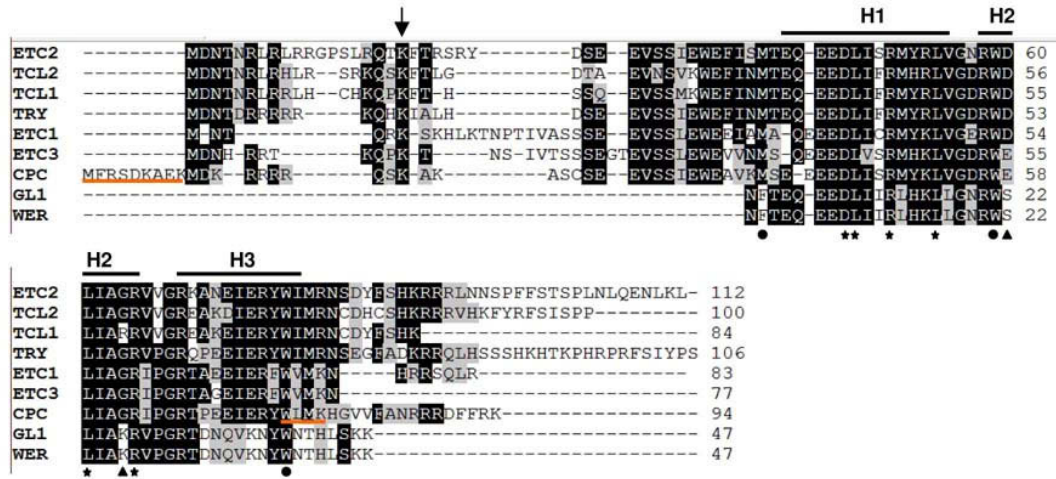
Figure 4.1 The K19E substitution in ETC2 modulating trichome density between Gr-1 and Can-0. The arrow indicates the site of lysine to glutamate exchange (K19E) associated with the high trichome density phenotype. H1, 2, 3 correspond to the aa forming α-helices 1, 2, 3 of the R3 MYB domain and filled circles indicate the regularly spaced tryptophan (phenylalanine/methionine) residues contributing to a hydrophobic core (Frampton et al, 1991). Asterisks indicate the bHLH interaction motif [DE]Lx2[RK]x3Lx6Lx3R (Zimmermann et al, 2004). Triangles indicate aa residues necessary for binding of WER to the *GL2* promoter (Tominaga et al, 2007). Orange bars mark aa residues required for CPC cell-cell movement (Kurata et al, 2005). Numbers to the right are equivalent to the number of aa residues of respective proteins.

To date, there is a lot information about natural variation for different traits in *A. thaliana*, however, identification of the very QTN is rare (examples are listed in (Alonso-Blanco et al, 2009)). Identification of natural variation for traits poses the possibility to learn more about molecular processes governing traits of interest, since natural variation is often quantitative in nature and underlying alleles are possibly functional alleles which might give insight into how traits are modulated. In this study, an attempt to identify a QTN for trichome density modulation in natural *A. thaliana* populations was carried out successfully. QTL mapping using two selected *A. thaliana* accessions showing opposite extreme phenotypes detected a major QTL for trichome number and density on chromosome 2 which was further fine mapped by selective genotyping to a 240 kbp QTL candidate interval. The fine mapped QTL candidate interval harboured a strong candidate locus with three members of the single-repeat R3 MYB gene family of trichome repressors *in tandem*. Association

analyses then excluded two of these genes, *TCL1* and *TCL2*, and after increasing the number of accessions for association mapping data indicated two SNPs at the *ETC2* locus as major candidate QTNs. Finally, functional tests showed that the nonsynonymous SNP leading to a lysine to glutamate substitution (K19E) in the trichome repressor protein ETC2 in low trichome density accessions is causative for trichome density modulation in natural *A. thaliana* accessions and thus constitutes a QTN.

The QTN is located in the N-terminal domain preceding the R3 MYB domain and therefore does not affect any of the previously annotated functional sites of single-repeat R3 MYB proteins (Figure 4.1). However alignment of the single-repeat R3 MYB proteins showed that the substitution is targeting a conserved lysine residue of the single-repeat R3 MYB protein family. As discussed in Hilscher et al., (2009), lysine residues are the target of ubiquitination and therefore it might be speculated that the K19E substitution renders the low trichome density allele insensitive to ubiquitination. One characterised role of ubiquitination is being a mark for proteolysis, so that under this scenario the low trichome density allele might be more stable and therefore represent a stronger trichome repressor protein. However, depending on the mode of ubiquitination, for example mono- and polyubiquitination or the pattern of linkage of polyubiquitin strands, post-translational modification by ubiquitination can also function in non-proteolytic pathways (Ye & Rape, 2009). Single-repeat R3 MYB family proteins constitute small proteins (for example, ETC2 = 18.1 kDa) and already mono-ubiquitination (for example, UBQ5 = 8.5 kDa) considerably changes their size. Thus alternatively, ubiquitination might lead to steric hindrance of ETC2 function. Further, it has been shown that CPC-tandemGFP fusions were only able to move between cells until they reached a size of ~119 kDa (Kurata et al, 2005), therefore, poly-ubiquitination of ETC2 might effect cell-cell movement. Accordingly, in all three mechanistic scenarios – proteolysis, steric hindrance, impairing cell-cell movement - the low trichome density allele lacking the ubiquitination site then would constitute a stronger trichome repressor.

Identification of QTN also sheds light on a discussion in evolutionary development whether morphological evolution is more likely driven by changes in *cis*-regulatory or structural sequences (chapter 1.1.2). Here, we find a major QTN affecting trichome patterning that targets the coding sequence of a transcriptional repressor. In *A. thaliana* there are only few descriptions of molecular causes of morphological natural variation, looking also at developmental (mostly flowering time) traits there

are examples of functional polymorphisms in *cis*-regulatory and structural sequences (Alonso-Blanco et al, 2009). Partly advancing the discussion might be the analysis of expression QTL (eQTL) mapping experiments since it will generate larger data on gene expression differences and show whether they are brought about by a preponderance of *cis*-regulatory or structural changes. As discussed in Hilscher et al., (2009), further characteristics of targets of natural variation may be taken into account to make general predictions regarding the patterns natural variation is shaping morphological evolution, as it is noted that *ETC2* shows low pleiotropy in contrast to the other members of the single-repeat R3 MYB family which function in both, trichome and root hair patterning. Modulation of ETC2 function therefore avoids disturbance of root hair patterning and might explain its targeting as a QTL for trichome patterning.

Comparison of *ETC2* alleles to other members of the single-repeat R3 MYB family members suggests that the low trichome density allele is the derived allele, since in the Col genomic background all other single-repeat R3 MYB family members possess a conserved QxK signature (Figure 4.1) and sequencing of *TCL1* and *TCL2* in other genomic backgrounds did not detect variant alleles at that position (data not shown). As discussed in Hilscher et al., (2009), the low trichome density allele at *ETC2* is not a minor allele since it is harboured by at least 20% of the collected accessions and the underlying QTL at chromosome two was detected in several QTL studies using different parental accessions. Further, the high sequence divergence to high trichome density alleles (d = 0.047) and the established sequence variation within low trichome density alleles (theta = 0.00333) suggest that the low trichome density allele is not of recent origin and not subject to a recent positive selection event (Hilscher et al., 2009). In a field study it has been shown that trichome density serves as a resistane trait against natural herbivores, however, in the absence of natural herbivores high trichome density is associated with fitness costs (Mauricio, 1998).

4.3   Novel insights into trichome density modulation

Trichome initiation is regulated in a complex fashion during *A. thaliana* development. Trichome formation varies on different organs as well as on the same organs initiated during different phases of the plants life cycle (for example rosette and cauline leaves, inflorescence internodes; (Gan et al, 2006; Martinez-Zapater et al,
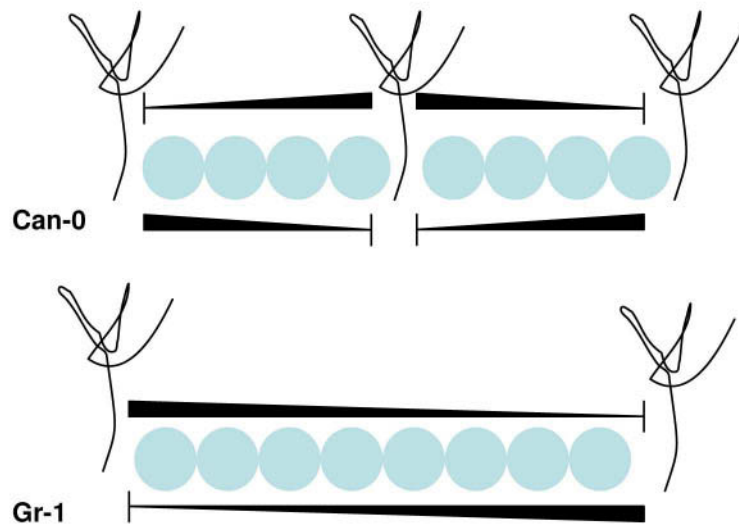
Figure 4.2. Novel insights into trichome density modulation. The cartoon vsiualizes that a speculated difference in strength of ETC2 repressor function, based on a lost ubiquitination site in ETC2^{Gr}, is in accordance to cellular analysis which showed a difference in mesophyll cell number in between trichomes in Can-0 and Gr-1. Blue circles and crosses represent palisade mesophyll cells and trichomes, respectively. Horizontal bars represent the strength of ETC2 function.

1995; Telfer et al, 1997)), trichome iniiation is responsive to biotic and abiotic factors (Nagata et al, 1999a; Traw & Bergelson, 2003) and finally, there is natural variation in trichome density on the same organs (analyzed mostly on the adaxial surface of rosette leaves) in *A. thaliana* populations (Hauser et al, 2001; Larkin et al, 1996). For the latter, a lot of information exists on how trichome initiation and patterning is achieved (Ishida et al, 2008), however, detailed information on genes and mechanisms governing the modulation of trichome density in different accessions is lacking. QTL analyses gave information on QTL regions and candidate genes annotated within, but are far from identifying the actual loci modulating trichome density (Larkin et al, 1996; Mauricio, 2005; Pfalz et al, 2007; Symonds et al, 2005). Further, an association analysis of naturally occurring alleles of *GL1* did not show a quantitative effect on trichome density modulation (Hauser et al, 2001). Here, the identification of a K19E substitution in the trichome repressor ETC2 and analysis of trichome density on the cellular level provides first insights into the modulation of trichome density by natural variation.

There are several non-exclusive mechanisms how trichome density might be regulated, (i) by correlation of trichome number to leaf cell number, (ii) by spacing of trichomes due to subsequent cell division and/or expansion of intervening epidermal cells, (iii) by a window of competence for trichome initiation (Larkin et al, 1996) and (iv) by the rate of trichome initiation, i.e. modulation of the activity of trichome cell fate regulators. Cellular analysis of Gr-1 and Can-0 on fully developed rosette leaves was able to eliminate the first two simple models as sole explanation for the modulation of trichome density and supports the latter two models. A further distinction between the two latter models based on cellular analysis will require measurement of trichome spacing at an earlier timepoint when trichome initiation is ongoing. However, cellular analysis clearly showed that the major difference between Can-0 and Gr-1 is the number of cells present in between trichomes (Figure 4.2). Thus, together with the finding that the molecular basis of the major QTL for trichome density between Can-0 and Gr-1 is caused by *ETC2*, in this study findings are presented corroborating a mechanism where the modulation of trichome density is caused by differences in a gene directly involved in trichome initiation. ETC2 is a member of the single-repeat R3 MYB family of trichome repressor proteins which are modelled to counteract the WD/bHLH/R2R3MYB trichome activator complex, and thus trichome initiation, by lateral inhibition (Figure 1.1) (Ishida et al, 2008). As discussed in Hilscher et al., (2009), there are several mechanisms by which the function of ETC2, and of single-repeat R3 MYB proteins in general, could be modulated to lead to different trichome densities, (i) strength of binding to GL3/EGL3, (ii) cell-cell movement ability and (iii) protein stability. As described above (chapter 4.2), the QTN leading to a K19E substitution in ETC2 possibly renders ETC2^{Gr-1} insensitive to ubiquitination, and thus it might be speculated that ETC2^{Gr-1} exerts its repressor function more stable which leads to a lower trichome initiation in Gr-1 than Can-0. This is the first indication that protein stability and/or ubiquitination might play a role in the regulation of trichome patterning. This proposed mechanism is also in agreement with the findings of the cellular analysis which has shown that there are more cells present in between trichomes in Gr-1 than in Can-0 Figure 4.2.

There is also evidence that the major QTL on chromosome two acts on the basis of a window of competence (Larkin et al, 1996). Monitoring trichome initiation as a function of leaf age suggested the rate of induction between Col and Ler being the same with an earlier cessation of trichome induction in the Ler accession. However,

this was done on the first leaf primordia where in the case of Can-0 and Gr-1 trichome density is different albeit to a lower level. Further, the fine mapping of the QTL in the F2 mapping population showed that there is the possibility of a second QTN inside the major QTL candidate interval which could act via a distinct mechanism to modulate trichome density. A strong candidate gene is *SAD2/URM9*, of which mutant alleles show a reduced trichome number phenotype but do not show a root hair phenotype (Gao et al, 2008). *SAD2* codes for an importin ß like protein and is functions in MYB4 nuclear trafficking (Zhao et al, 2007a). Importantly, *SAD2* was discovered to mediate JA induced trichome formation probably via affecting the nuclear distribution of GL3 (Yoshida et al, 2009). To date the specific role of *SAD2* in this process is unknown, however, it is thought that SAD2 protein mediates the nuclear trafficking of a further protein involved in trichome initiation other than GL1 and TTG1 which have been shown to be unaffected in nuclear trafficking by *SAD2* (Yoshida et al, 2009).

4.4   Assigning functions to *A. thaliana* trichomes

There are few studies addressing functional significance of the non-secreting trichomes of *A. thaliana*. The present natural variation in trichome density and number on rosette leaves of *A. thaliana* accessions (Hauser et al, 2001; Larkin et al, 1996; Symonds et al, 2005) and detected natural genetic variation for trichome density (Hauser et al, 2001; Mauricio, 2005; Pfalz et al, 2007; Symonds et al, 2005) indicate that they may be of adaptive value in response to biotic and abiotic stressors. Accordingly, studies in *A. thaliana* and *Arabidopsis lyrata* started to establish trichome density as a means against insect herbivory (Clauss et al, 2006; Handley et al, 2005; Kivimaki et al, 2007; Loe et al, 2007; Mauricio, 1998; Mauricio & Rausher, 1997), however, to date there is little information on the role of trichome density in abiotic stress defense in *A. thaliana*. In regard to the role of non-secreting trichomes in abiotic stress defense, UV-B tolerance is one of the most investigated stressors in other species (Karabourniotis & Bornman, 1999; Karabourniotis et al, 1995; Karabourniotis et al, 1992; Liakopoulos et al, 2006; Liakoura et al, 1997; Skaltsa et al, 1994). In the light of these studies, here, *A. thaliana* accessions exhibiting different trichome densities were tested for a difference in UV-B tolerance. Further, UV-B treated plants were analyzed for their anthocyanin content. Anthocyanins have been discussed as acting as a UV-B screen and genes acting late in flavonoid biosynthesis are regulated by the WD/bHLH/MYB transcription

factor module as are trichome initiation genes (see chapter 1.6). Therefore, it was of interest to test a possible co-regulation of these traits in regard to their function in UV-B protection.

There are two non exclusive strategies how trichome density might be regulated to provide UV-B protection, trichome density may be regulated irrespective of UV-B exposure and given for accessions originating from different habitats, further it may be regulated in response to UV-B exposure. In the former case, accessions with different trichome densities under conditions without UV-B should be associated with different UV-B tolerance, in the latter, trichome density should increase upon UV-B exposure.

A general issue became evident during the course of this pilot study. The UV-B conditions used here, chronic exposure with moderate and high fluence rates (according to (Brown & Jenkins, 2008)), led to severe growth retardation and tissue damage of plants in comparison to control conditions. Here, quantification of growth retardation detected natural variation for UV-B tolerance among *A. thaliana* accessions, however, these severe effects also pose a difficulty in determining a possible regulated response in trichome density upon UV-B exposure due to the plasticity of leaf size which indirectly influences trichome density. Related to that, one has to consider the recent findings that UV-B elicits distinct signalling pathways depending on its fluence rate. *UV RESISTANCE LOCUS8* (*UVR8*) is already activated at low UV-B fluence rates and activates the transcription factors *ELONGATED HYPOCOTYL5* (*HY5*) and *HY5 HOMOLOG* (*HYH*) and downstream genes thought to confer UV-B protection. High fluence rates causing severe growth retardation and tissue damage further activate *UVR8* independent genes that are thought to overlap with general stress responses and are therefore not specific to UV-B signalling (Brown & Jenkins, 2008). Brown and Jenkins (2008) speculate that the *UVR8* dependent pathway might be a means for UV-B acclimation, whereas the *UVR8* independent pathway might be protective of (sudden) strong UV-B exposures.

Keeping above in mind, *A. thaliana* accessions showed natural variation for UV-B tolerance (Figure 3.15 A, B), however, there was no association detected with trichome density - assigned under conditions lacking UV-B. *A. thaliana* grows in habitats with very different UV-B regimes and strengths which might be reflected in the natural variation in UV-B tolerance in the tested accessions. To date, there is virtually nothing known about natural variation for UV-B tolerance in *A. thaliana* and

the loci which are modulated. Here, no association of trichome density and UV-B tolerance was detected, however, increasing the number of accessions – in this study there were only five accessions used - and/or testing different UV-B regimes might lead to firmer conclusions. Further, it was tested whether there might be a regulated response of trichome density upon UV-B exposure, analogously to what has been shown for artifical wounding of leaves (Traw & Bergelson, 2003; Yoshida et al, 2009). Indeed, the two accessions tested, a low and a high trichome density accession, formed a higher trichome density (Figure 3.15 C). At the same time, as mentioned above, the individuals exposed to UV-B formed smaller leaves and less trichomes, so that the increase of trichome density is not distinguishable from a secondary effect of altering leaf size. A possibility to clarify the findings is to carry out cellular analysis determining the trichome number versus leaf cell number index. Also, further experiments might make use of a lower fluence rate UV-B regime or an earlier timepoint of measurement where there is less effect on leaf growth parameters and less leaf tissue damage.

As mentioned, in *A. thaliana* a WD/bHLH/MYB transcription initiation complex is central not only to regulation of trichome initiation but also to regulation of biosynthetic genes active late in the flavonoid pathway (Figure 1.6; (Ramsay & Glover, 2005; Zhang et al, 2003)), therefore, it became interesting to analyze anthocyanin content of *A. thaliana* accessions with different trichome densities (and) in reaction to UV-B treatment. The focus among flavonoids was set to anthocyanins, because they have been most prominently described in the course of studying the WD/bHLH/MYB module and they have been implicated as a UV-B screen.

The high variation in measurements and the small number of independent samples in the course of setting up anthocyanin content measurement posed a problem in interpreting the obtained results, the latter precluding significance testing of most of the data (Figure 3.16). Anthocyanin content among accessions tested were not significantly different under control conditions, however, a high variability of individual measurements might mask a possible difference. Upon long-term chronic UV-B treatment there seemed to be no increase in anthocyanin content in comparison to control conditions. On the contrary, most of the accessions treated for three days with UV-B seem to possess increased anthocyanin content in comparison to control conditions, among these are high and low trichome density accessions. Although preliminary, these data again raise the question of differential responses of *A. thaliana* to different UV-B regimes, in that anthocyanin biosynthesis

in response to UV-B might be upregulated only transiently or under moderate UV-B exposure.

Photometric analysis of plant extracts at OD_{530} serves as an initial analysis for anthocyanin content, since, as mentioned above, other flavonoids also absorb at this wavelength albeit at a lower extent. Therefore, high absorption could also be due to a high concentration of less absorbing flavonoid compounds. To get a first glimpse at a better resolution of the flavonoid composition, the samples of untreated plants at day 18 and the samples of the early response experiment were analyzed by Franz Hadacek (Department of Chemical Ecology and Ecosystem Research, University of Vienna) using HPLC analysis (Summit® HPLC System (Dionex); briefly, samples were separated on a 150 mm × 2 mm Synergi Max-RP C12 column with a 4 μm pore size (Phenomenex) using a 5-100% methanol gradient over 100 minutes and a stable 0.5% phosphoric acid concentration in H_20; detection was done with a UV Diode-Array). He found, based on a principal component analysis (PCA) using the whole profile between 5-60 minutes, that there might be a separation between the late and the early response samples (Figure 7.2). A further structuring within the early response experiment into control and UV-B treated samples is not as obvious; although it seems that the control plants are more clustered than the UV-B treated plants. Upon closer inspection he reports that only in the late response experiment, where only samples without UV-B treatment were analysed, anthocyanin can be detected albeit to a low extent. Further, it seems that the possible structuring between control and UV-B treated plants of the early response experiment might be partly due to the presence of kaempferol glycosides. These findings are in contrast to the photometric analysis, in that anthocyanins were detected in all samples. This discrepancy might be inherent to the method used, i.e. photometric detection cannot distinguish between anthocyanins and other flavonoids, or might be due to destabilization of anthocyanins. Photometric detection was carried out soon after the extracts were prepared whereas HPLC analysis after prolonged storage, however, a time series of photometric measurements of the extracts showed no decay in the photometric absorption units over time. The finding that kaempferol glycosides, belonging to the flavonoid subgroup of flavonols, might be accumulating in response to UV-B in the early response experiment is in accordance to their reported role as a UV-B screen (Taiz & Zeiger, 2006). The pathway leading to flavonols is identical to the anthocyanin pathway until the enzymatic step carried out by flavonoid 3´- hydroxylase (*F3´H*; Figure 1.6). F3´H is

the first flavonoid pathway enzyme whose expression is goverened by the WD/bHLH/MYB complex and categorized as a late flavonoid pathway gene, and therefore shares the same transcription regulation module with the trichome initiation pathway. Interestingly, At5g08640, encoding flavonol synthase 1 (*FLS1*; Figure 1.6) is amongst the 5% most highly expressed genes of trichomes (Jakoby et al, 2008b).

Irrespectively of the inconclusive results in respect to the role of trichomes (and anthocyanin content) in UV-B protection gained in this pilot study, there are arguments that substantiate further efforts to probe that particular function of trichomes. Central to that notion is the connection of trichomes and the flavonoid pathway; the expression of flavonoid pathway genes in trichomes, UV-B absorbing capacities of trichomes in other species and the use of the same transcription regulation module in trichome initiation and the flavonoid pathway. A critical point to elucidate a UV-B protective role of trichomes might be to mirror biological UV-B conditions in the lab and/or detection of the growth stage at where trichomes might primarily exert protective roles.

5   REFERENCES

Abiola O, Angel JM, Avner P, Bachmanov AA, Belknap JK, *et al.*, (2003) The nature and identification of quantitative trait loci: a community's view. *Nat Rev Genet* **4**(11)**:** 911-916

AGI (2000) Analysis of the genome sequence of the flowering plant *Arabidopsis thaliana*. *Nature* **408**(6814)**:** 796-815

Alonso-Blanco C, Aarts MG, Bentsink L, Keurentjes JJ, Reymond M, Vreugdenhil D, Koornneef M (2009) What has natural variation taught us about plant development, physiology, and adaptation? *Plant Cell* **21**(7)**:** 1877-1896

Alonso-Blanco C, Koornneef M (2000) Naturally occurring variation in *Arabidopsis*: an underexploited resource for plant genetics. *Trends Plant Sci* **5**(1)**:** 22-29

Alonso JM, Stepanova AN, Leisse TJ, Kim CJ, Chen H, Shinn P, *et al.,* (2003) Genome-wide insertional mutagenesis of *Arabidopsis thaliana*. *Science* **301**(5633)**:** 653-657

Appleby N, Edwards D, Batley J (2009) New technologies for ultra-high throughput genotyping in plants. *Methods Mol Biol* **513:** 19-39

Arpat AB, Waugh M, Sullivan JP, Gonzales M, Frisch D, Main D, Wood T, Leslie A, Wing RA, Wilkins TA (2004) Functional genomics of cell elongation in developing cotton fibers. *Plant Mol Biol* **54**(6)**:** 911-929

Asamizu E, Nakamura Y, Sato S, Tabata S (2000) A large scale analysis of cDNA in *Arabidopsis thaliana*: generation of 12,028 non-redundant expressed sequence tags from normalized and size-selected cDNA libraries. *DNA Res* **7**(3)**:** 175-180

Atwell S, Huang YS, Vilhjalmsson BJ, Willems G, Horton M, *et al.,* (2010) Genome-wide association study of 107 phenotypes in *Arabidopsis thaliana* inbred lines.

Nature

Balding DJ (2006) A tutorial on statistical methods for population association studies. *Nat Rev Genet* **7**(10)**:** 781-791

Baranowskij N, Frohberg C, Prat S, Willmitzer L (1994) A novel DNA binding protein with homology to Myb oncoproteins containing only one repeat can function as a transcriptional activator. *EMBO J* **13**(22)**:** 5383-5392

Beemster GT, De Veylder L, Vercruysse S, West G, Rombaut D, Van Hummelen P, Galichet A, Gruissem W, Inze D, Vuylsteke M (2005) Genome-wide analysis of gene expression profiles associated with cell cycle transitions in growing organs of *Arabidopsis*. *Plant Physiol* **138**(2)**:** 734-743

Berger F, Haseloff J, Schiefelbein J, Dolan L (1998) Positional information in root epidermis is defined during embryogenesis and acts in domains with strict boundaries. *Curr Biol* **8**(8)**:** 421-430

Bernhardt C, Lee MM, Gonzalez A, Zhang F, Lloyd A, Schiefelbein J (2003) The bHLH genes GLABRA3 (GL3) and ENHANCER OF GLABRA3 (EGL3) specify epidermal cell fate in the *Arabidopsis* root. *Development* **130**(26)**:** 6431-6439

Bernhardt C, Zhao M, Gonzalez A, Lloyd A, Schiefelbein J (2005) The bHLH genes GL3 and EGL3 participate in an intercellular regulatory circuit that controls cell patterning in the *Arabidopsis* root epidermis. *Development* **132**(2)**:** 291-298

Borevitz JO, Hazen SP, Michael TP, Morris GP, Baxter IR, Hu TT, Chen H, Werner JD, Nordborg M, Salt DE, Kay SA, Chory J, Weigel D, Jones JD, Ecker JR (2007) Genome-wide patterns of single-feature polymorphism in *Arabidopsis thaliana*. *Proc Natl Acad Sci U S A* **104**(29)**:** 12057-12062

Boudaoud A (2010) An introduction to the mechanics of morphogenesis for plant biologists. *Trends Plant Sci* **15**(6)**:**353-60

Bouyer D, Geier F, Kragler F, Schnittger A, Pesch M, Wester K, Balkunde R, Timmer J, Fleck C, Hulskamp M (2008) Two-dimensional patterning by a trapping/depletion mechanism: the role of TTG1 and GL3 in *Arabidopsis* trichome formation. *PLoS Biol* **6**(6)**:** e141

Broun P (2005) Transcriptional control of flavonoid biosynthesis: a complex network of conserved regulators involved in multiple aspects of differentiation in *Arabidopsis. Curr Opin Plant Biol* **8**(3)**:** 272-279

Brown BA, Jenkins GI (2008) UV-B signaling pathways with different fluence-rate response profiles are distinguished in mature *Arabidopsis* leaf tissue by requirement for UVR8, HY5, and HYH. *Plant Physiol* **146**(2)**:** 576-588

Browse J, Howe GA (2008) New weapons and a rapid response against insect attack. *Plant Physiol* **146**(3)**:** 832-838

Caro E, Castellano MM, Gutierrez C (2007) A chromatin link that couples cell division to root epidermis patterning in *Arabidopsis. Nature* **447**(7141)**:** 213-U216

Carroll SB (2008) Evo-devo and an expanding evolutionary synthesis: a genetic theory of morphological evolution. *Cell* **134**(1)**:** 25-36

Caspi R, Foerster H, Fulcher CA, Hopkinson R, Ingraham J, Kaipa P, Krummenacker M, Paley S, Pick J, Rhee SY, Tissier C, Zhang P, Karp PD (2006) MetaCyc: a multiorganism database of metabolic pathways and enzymes. *Nucleic Acids Res* **34**(Database issue)**:** D511-516

Chevalier D, Batoux M, Fulton L, Pfister K, Yadav RK, Schellenberg M, Schneitz K (2005) *STRUBBELIG* defines a receptor kinase-mediated signaling pathway regulating organ development in *Arabidopsis. Proc Natl Acad Sci U S A* **102**(25)**:** 9074-9079

Chien JC, Sussex IM (1996) Differential regulation of trichome formation on the adaxial and abaxial leaf surfaces by gibberellins and photoperiod in *Arabidopsis thaliana* (L.) Heynh. *Plant Physiol* **111**(4)**:** 1321-1328

Churchill GA, Doerge RW (1994) Empirical threshold values for quantitative trait mapping. *Genetics* **138**(3)**:** 963-971

Churchman ML, Brown ML, Kato N, Kirik V, Hulskamp M, Inze D, De Veylder L, Walker JD, Zheng Z, Oppenheimer DG, Gwin T, Churchman J, Larkin JC (2006) *SIAMESE*, a plant-specific cell cycle regulator, controls endoreplication onset in Arabidopsis thaliana. *Plant Cell* **18**(11)**:** 3145-3157

Clark RM, Schweikert G, Toomajian C, Ossowski S, Zeller G, Shinn P, Warthmann N, Hu TT, Fu G, Hinds DA, Chen H, Frazer KA, Huson DH, Scholkopf B, Nordborg M, Ratsch G, Ecker JR, Weigel D (2007) Common sequence polymorphisms shaping genetic diversity in *Arabidopsis thaliana. Science* **317**(5836)**:** 338-342

Clauss MJ, Dietel S, Schubert G, Mitchell-Olds T (2006) Glucosinolate and trichome defenses in a natural *Arabidopsis lyrata* population. *Journal of Chemical Ecology* **32**(11)**:** 2351-2373

Close D, Beadle C (2003) The ecophysiology of foliar anthocyanin. *The Botanical Review* **69**(2)**:** 149-161

Clough SJ, Bent AF (1998) Floral dip: a simplified method for *Agrobacterium-*mediated transformation of Arabidopsis thaliana. *Plant J* **16**(6)**:** 735-743

Cominelli E, Gusmaroli G, Allegra D, Galbiati M, Wade HK, Jenkins GI, Tonelli C (2008) Expression analysis of anthocyanin regulatory genes in response to different light qualities in *Arabidopsis thaliana. Journal of Plant Physiology* **165**(8)**:** 886-894

Costa S, Shaw P (2006) Chromatin organization and cell fate switch respond to positional information in *Arabidopsis. Nature* **439**(7075)**:** 493-496

Damiani RD, Jr., Wessler SR (1993) An upstream open reading frame represses expression of Lc, a member of the R/B family of maize transcriptional activators. *Proc Natl Acad Sci U S A* **90**(17)**:** 8244-8248

Davis SJ (2009) Integrating hormones into the floral-transition pathway of *Arabidopsis thaliana. Plant Cell Environ* **32**(9)**:** 1201-1210

De Neve M, De Buck S, Jacobs A, Van Montagu M, Depicker A (1997) T-DNA integration patterns in co-transformed plant cells suggest that T-DNA repeats originate from co-integration of separate T-DNAs. *Plant J* **11**(1)**:** 15-29

DePamphilis ML, Blow JJ, Ghosh S, Saha T, Noguchi K, Vassilev A (2006) Regulating the licensing of DNA replication origins in metazoa. *Curr Opin Cell Biol* **18**(3)**:** 231-239

Digiuni S, Schellmann S, Geier F, Greese B, Pesch M, Wester K, Dartan B, Mach V, Srinivas BP, Timmer J, Fleck C, Hulskamp M (2008) A competitive complex formation mechanism underlies trichome patterning on *Arabidopsis* leaves. *Mol Syst Biol* **4:** 217

Dolan L, Janmaat K, Willemsen V, Linstead P, Poethig S, Roberts K, Scheres B (1993) Cellular organisation of the *Arabidopsis thaliana* root. *Development* **119**(1)**:** 71-84

Donnelly PM, Bonetta D, Tsukaya H, Dengler RE, Dengler NG (1999) Cell cycling and cell enlargement in developing leaves of *Arabidopsis. DevBiol* **215**(2)**:** 407-419

Dubos C, Le Gourrierec J, Baudry A, Huep G, Lanet E, Debeaujon I, Routaboul JM, Alboresi A, Weisshaar B, Lepiniec L (2008) *MYBL2* is a new regulator of flavonoid biosynthesis in *Arabidopsis thaliana. Plant J* **55**(6)**:** 940-953

Duke SO, Canel C, Rimando AM, Tellez MR, Duke MV, Paul RN (2000) Current and potential exploitation of plant glandular trichome productivity. In *Advances in Botanical Research Incorporating Advances in Plant Pathology, Vol 31 2000* Vol. 31, pp 121-151.

Ebert B, Melle C, Lieckfeldt E, Zöller D, von Eggeling F, Fisahn J (2008) Protein profiling of single epidermal cell types from *Arabidopsis thaliana* using surface-enhanced laser desorption and ionization technology. *J Plant Physiol* **165**(12)**:** 1227-1237.

Esch JJ, Chen M, Sanders M, Hillestad M, Ndkium S, Idelkope B, Neizer J, Marks MD (2003) A contradictory *GLABRA3* allele helps define gene interactions controlling trichome development in Arabidopsis. *Development* **130**(24)**:** 5885-5894

Esch JJ, Chen MA, Hillestad M, Marks MD (2004) Comparison of *TRY* and the closely related At1g01380 gene in controlling *Arabidopsis* trichome patterning. *Plant J* **40**(6)**:** 860-869

Esch JJ, Oppenheimer DG, Marks MD (1994) Characterization of a weak allele of the *GL1* gene of *Arabidopsis thaliana*. *Plant Mol Biol* **24**(1)**:** 203-207

Falconer DS, Mackay TFC (2005) *Introduction to quantitative genetics*, Harlow [u.a.]: Pearson, Prentics Hall.

Fleming AJ (2005) The control of leaf development. *New Phytol* **166**(1)**:** 9-20

Frampton J, Gibson TJ, Ness SA, Doderlein G, Graf T (1991) Proposed structure for the DNA-binding domain of the Myb oncoprotein based on model building and mutational analysis. *Protein Eng* **4**(8)**:** 891-901

Galway ME, Masucci JD, Lloyd AM, Walbot V, Davis RW, Schiefelbein JW (1994) The *TTG* gene is required to specify epidermal cell fate and cell patterning in the *Arabidopsis* root. *Dev Biol* **166**(2)**:** 740-754

Gan Y, Kumimoto R, Liu C, Ratcliffe O, Yu H, Broun P (2006) *GLABROUS INFLORESCENCE STEMS* modulates the regulation by gibberellins of epidermal differentiation and shoot maturation in *Arabidopsis. Plant Cell* **18**(6)**:** 1383-1395

Gan Y, Liu C, Yu H, Broun P (2007a) Integration of cytokinin and gibberellin signalling by *Arabidopsis* transcription factors *GIS, ZFP8* and *GIS2* in the regulation of epidermal cell fate. *Development* **134**(11)**:** 2073-2081

Gan Y, Yu H, Peng J, Broun P (2007b) Genetic and molecular regulation by DELLA proteins of trichome development in Arabidopsis. *Plant Physiol* **145**(3)**:** 1031-1042

Gao Y, Gong X, Cao W, Zhao J, Fu L, Wang X, Schumaker KS, Guo Y (2008) *SAD2* in *Arabidopsis* functions in trichome initiation through mediating *GL3* function and regulating *GL1, TTG1* and *GL2* expression. *J Integr Plant Biol* **50**(7)**:** 906-917

Gaut BS, Long AD (2003) The lowdown on linkage disequilibrium. *Plant Cell* **15**(7)**:** 1502-1506

Gierer A, Meinhardt H (1972) A theory of biological pattern formation. *Kybernetik* **12**(1)**:** 30-39

Glazier AM, Nadeau JH, Aitman TJ (2002) Finding genes that underlie complex traits. *Science* **298**(5602)**:** 2345-2349

Gonzalez A, Zhao M, Leavitt JM, Lloyd AM (2008) Regulation of the anthocyanin biosynthetic pathway by the TTG1/bHLH/Myb transcriptional complex in *Arabidopsis* seedlings. *Plant J* **53**(5)**:** 814-827

Gould KS (2004) Nature's Swiss Army Knife: The Diverse Protective Roles of Anthocyanins in Leaves. *J Biomed Biotechnol* **2004**(5)**:** 314-320

Granier C, Tardieu F (2009) Multi-scale phenotyping of leaf expansion in response to environmental changes: the whole is more than the sum of parts. *Plant Cell Environ* **32**(9)**:** 1175-1184

Guan XY, Li QJ, Shan CM, Wang S, Mao YB, Wang LJ, Chen XY (2008) The HD-Zip IV gene GaHOX1 from cotton is a functional homologue of the *Arabidopsis GLABRA2*. *Physiol Plant* **134**(1)**:** 174-182

Guimil S, Dunand C (2007) Cell growth and differentiation in *Arabidopsis* epidermal cells. *J Exp Bot* **58**(14)**:** 3829-3840

Gutierrez-Alcala G, Gotor C, Meyer AJ, Fricker M, Vega JM, Romero LC (2000) Glutathione biosynthesis in *Arabidopsis* trichome cells. *Proceedings of the National Academy of Sciences of the United States of America* **97**(20)**:** 11108-11113

Hajdukiewicz P, Svab Z, Maliga P (1994) The small, versatile pPZP family of *Agrobacterium* binary vectors for plant transformation. *Plant Mol Biol* **25**(6)**:** 989-994

Handley R, Ekbom B, Agren J (2005) Variation in trichome density and resistance against a specialist insect herbivore in natural populations of *Arabidopsis thaliana*. *Ecological Entomology* **30**(3)**:** 284-292

Harborne JB, Williams CA (2000) Advances in flavonoid research since 1992. *Phytochemistry* **55**(6)**:** 481-504

Hauser MT, Adhami F, Dorner M, Fuchs E, Glossl J (1998) Generation of co-dominant PCR-based markers by duplex analysis on high resolution gels. *Plant J* **16**(1)**:** 117-125

Hauser MT, Harr B, Schlötterer C (2001) Trichome distribution in *Arabidopsis thaliana* and its close relative *Arabidopsis lyrata*: molecular analysis of the candidate gene GLABROUS1. *MolBiolEvol* **18**(9)**:** 1754-1763

Hauser MT, Morikami A, Benfey PN (1995) Conditional root expansion mutants of *Arabidopsis*. *Development* **121**(4)**:** 1237-1252

Hill WG, Mackay TF (2004) D. S. Falconer and Introduction to quantitative genetics. *Genetics* **167**(4)**:** 1529-1536

Hilscher J, Schlötterer C, Hauser MT (2009) A Single Amino Acid Replacement in *ETC2* Shapes Trichome Patterning in Natural *Arabidopsis* Populations. *Current Biology* **19**(20)**:** 1747-1751

Hirsch S, Oldroyd GE (2009) GRAS-domain transcription factors that regulate plant development. *Plant Signal Behav* **4**(8)**:** 698-700

Hoekstra HE, Coyne JA (2007) The locus of evolution: evo devo and the genetics of adaptation. *Evolution* **61**(5)**:** 995-1016

Horiguchi G, Ferjani A, Fujikura U, Tsukaya H (2006) Coordination of cell proliferation and cell expansion in the control of leaf size in *Arabidopsis thaliana*. *J Plant Res* **119**(1)**:** 37-42

Hülskamp M, Misra S, Jurgens G (1994) Genetic dissection of trichome cell development in *Arabidopsis*. *Cell* **76**(3)**:** 555-566

Humphries JA, Walker AR, Timmis JN, Orford SJ (2005) Two WD-repeat genes from cotton are functional homologues of the *Arabidopsis thaliana TRANSPARENT TESTA GLABRA1* (*TTG1*) gene. *Plant Mol Biol* **57**(1)**:** 67-81

Hung CY, Lin Y, Zhang M, Pollock S, Marks MD, Schiefelbein J (1998) A common position-dependent mechanism controls cell-type patterning and *GLABRA2* regulation in the root and hypocotyl epidermis of *Arabidopsis*. *Plant Physiol* **117**(1)**:** 73-84

Ishida T, Hattori S, Sano R, Inoue K, Shirano Y, Hayashi H, Shibata D, Sato S, Kato T, Tabata S, Okada K, Wada T (2007) Arabidopsis *TRANSPARENT TESTA GLABRA2* is directly regulated by R2R3 MYB transcription factors and is involved in regulation of *GLABRA2* transcription in epidermal differentiation. *Plant Cell* **19**(8)**:** 2531-2543

Ishida T, Kurata T, Okada K, Wada T (2008) A genetic regulatory network in the development of trichomes and root hairs. *Annu Rev Plant Biol* **59:** 365-386

Jakoby MJ, Falkenhan D, Mader MT, Brininstool G, Wischnitzki E, Platz N, Hudson A, Hulskamp M, Larkin J, Schnittger A (2008a) Transcriptional profiling of mature *Arabidopsis* trichomes reveals that *NOECK* encodes the MIXTA-like transcriptional regulator MYB106. *Plant Physiol* **148**(3)**:** 1583-1602

Jin H, Martin C (1999) Multifunctionality and diversity within the plant MYB-gene family. *Plant Mol Biol* **41**(5)**:** 577-585

Johnson CS, Kolevski B, Smyth DR (2002) *TRANSPARENT TESTA GLABRA2*, a trichome and seed coat development gene of *Arabidopsis*, encodes a WRKY transcription factor. *Plant Cell* **14**(6)**:** 1359-1375

Kang HM, Zaitlen NA, Wade CM, Kirby A, Heckerman D, Daly MJ, Eskin E (2008) Efficient control of population structure in model organism association mapping. *Genetics* **178**(3)**:** 1709-1723

Kang YH, Kirik V, Hulskamp M, Nam KH, Hagely K, Lee MM, Schiefelbein J (2009) The *MYB23* gene provides a positive feedback loop for cell fate specification in the Arabidopsis root epidermis. *Plant Cell* **21**(4)**:** 1080-1094

Karabourniotis G, Bornman JF (1999) Penetration of UV-A, UV-B and blue light through the leaf trichome layers of two xeromorphic plants, olive and oak, measured by optical fibre microprobes. *Physiologia Plantarum* **105**(4)**:** 655-661

Karabourniotis G, Kotsabassidis D, Manetas Y (1995) Trichome density and its protective potential against UV-B radiation-damage during leaf development *Canadian Journal of Botany-Revue Canadienne De Botanique* **73**(3): 376-383

Karabourniotis G, Papadopoulos K, Papamarkou M, Manetas Y (1992) UV-B radiation absorbing capacity of leaf hairs *Physiologia Plantarum* **86**(3): 414-418

Kim S, Plagnol V, Hu TT, Toomajian C, Clark RM, Ossowski S, Ecker JR, Weigel D, Nordborg M (2007) Recombination and linkage disequilibrium in *Arabidopsis thaliana. Nat Genet* **39**(9): 1151-1155

Kirik V, Baumlein H (1996) A novel leaf-specific myb-related protein with a single binding repeat. *Gene* **183**(1-2): 109-113

Kirik V, Lee MM, Wester K, Herrmann U, Zheng Z, Oppenheimer D, Schiefelbein J, Hülskamp M (2005) Functional diversification of *MYB23* and *GL1* genes in trichome morphogenesis and initiation. *Development* **132**(7): 1477-1485

Kirik V, Simon M, Hülskamp M, Schiefelbein J (2004a) The *ENHANCER OF TRY AND CPC1* gene acts redundantly with *TRIPTYCHON* and *CAPRICE* in trichome and root hair cell patterning in Arabidopsis. *DevBiol* **268**(2): 506-513

Kirik V, Simon M, Wester K, Schiefelbein J, Hülskamp M (2004b) *ENHANCER of TRY and CPC 2* (*ETC2*) reveals redundancy in the region-specific control of trichome development of Arabidopsis. *Plant MolBiol* **55**(3): 389-398

Kivimaki M, Karkkainen K, Gaudeul M, Loe G, Agren J (2007) Gene, phenotype and function: *GLABROUS1* and resistance to herbivory in natural populations of *Arabidopsis lyrata. Molecular Ecology* **16**(2): 453-462

Kliebenstein DJ (2004) Secondary metabolites and plant/environment interactions: a

view through *Arabidopsis thaliana* tinged glasses. *Plant, Cell & Environment* **27**(6)**:** 675-684

Koncz C, Schell J (1986) The promoter of TL-DNA gene 5 controls the tissue-specific expression of chimaeric genes carried by a novel type of *Agrobacterium* binary vector. *Molecular and General Genetics* **204**(3)**:** 383-396

Koornneef M (1981) The complex syndrome of *TTG* mutants. *Arabidopsis Information Service* **18:** 45-51

Koornneef M, Alonso-Blanco C, Vreugdenhil D (2004) Naturally occurring genetic variation in *Arabidopsis thaliana*. *Annu Rev Plant Biol* **55:** 141-172

Koornneef M, Dellaert LW, van der Veen JH (1982) EMS- and radiation-induced mutation frequencies at individual loci in *Arabidopsis thaliana* (L.) Heynh. *MutatRes* **93**(1)**:** 109-123

Kosambi DD (1944) The estimation of map distances from recombination values. *Annals of Eugenetics* **12:** 172-175

Koshino-Kimura Y, Wada T, Tachibana T, Tsugeki R, Ishiguro S, Okada K (2005) Regulation of *CAPRICE* transcription by MYB proteins for root epidermis differentiation in *Arabidopsis*. *Plant Cell Physiol* **46**(6)**:** 817-826

Koumproglou R, Wilkes TM, Townson P, Wang XY, Beynon J, Pooni HS, Newbury HJ, Kearsey MJ (2002) STAIRS: a new genetic resource for functional genomic studies of *Arabidopsis*. *Plant J* **31**(3)**:** 355-364

Kover PX, Valdar W, Trakalo J, Scarcelli N, Ehrenreich IM, Purugganan MD, Durrant C, Mott R (2009) A Multiparent Advanced Generation Inter-Cross to fine-map quantitative traits in *Arabidopsis thaliana*. *PLoS Genet* **5**(7)**:** e1000551

Kranz HD, Denekamp M, Greco R, Jin H, Leyva A, Meissner RC, Petroni K, Urzainqui A, Bevan M, Martin C, Smeekens S, Tonelli C, Paz-Ares J, Weisshaar B (1998) Towards functional characterisation of the members of the R2R3-MYB gene family from *Arabidopsis thaliana*. *Plant J* **16**(2)**:** 263-276

Kryvych S, Nikiforova V, Herzog M, Perazza D, Fisahn J (2008) Gene expression profiling of the different stages of *Arabidopsis thaliana* trichome development on the single cell level. *Plant Physiol Biochem* **46**(2)**:** 160-173

Kubasek WL, Shirley BW, McKillop A, Goodman HM, Briggs W, Ausubel FM (1992) Regulation of Flavonoid Biosynthetic Genes in Germinating *Arabidopsis* Seedlings. *Plant Cell* **4**(10)**:** 1229-1236

Kurata T, Ishida T, Kawabata-Awai C, Noguchi M, Hattori S, Sano R, Nagasaka R, Tominaga R, Koshino-Kimura Y, Kato T, Sato S, Tabata S, Okada K, Wada T (2005) Cell-to-cell movement of the CAPRICE protein in *Arabidopsis* root epidermal cell differentiation. *Development* **132**(24)**:** 5387-5398

Kwak SH, Schiefelbein J (2007) The role of the *SCRAMBLED* receptor-like kinase in patterning the *Arabidopsis* root epidermis. *Dev Biol* **302**(1)**:** 118-131

Kwak SH, Schiefelbein J (2008) A feedback mechanism controlling SCRAMBLED receptor accumulation and cell-type pattern in *Arabidopsis*. *Curr Biol* **18**(24)**:** 1949-1954

Kwak SH, Shen R, Schiefelbein J (2005) Positional signaling mediated by a receptor-like kinase in *Arabidopsis*. *Science* **307**(5712)**:** 1111-1113

Larkin JC, Oppenheimer DG, Lloyd AM, Paparozzi ET, Marks MD (1994) Roles of the *GLABROUS1* and *TRANSPARENT TESTA GLABRA* Genes in *Arabidopsis* Trichome Development. *Plant Cell* **6**(8)**:** 1065-1076

Larkin JC, Oppenheimer DG, Pollock S, Marks MD (1993) *Arabidopsis*

GLABROUS1 Gene Requires Downstream Sequences for Function. *Plant Cell* **5**(12)**:** 1739-1748

Larkin JC, Young N, Prigge M, Marks MD (1996) The control of trichome spacing and number in *Arabidopsis. Development* **122**(3)**:** 997-1005

Larkin MA, Blackshields G, Brown NP, Chenna R, McGettigan PA, McWilliam H, Valentin F, Wallace IM, Wilm A, Lopez R, Thompson JD, Gibson TJ, Higgins DG (2007) Clustal W and Clustal X version 2.0. *Bioinformatics* **23**(21)**:** 2947-2948

Lee MM, Schiefelbein J (1999) WEREWOLF, a MYB-related protein in *Arabidopsis*, is a position-dependent regulator of epidermal cell patterning. *Cell* **99**(5)**:** 473-483

Lee MM, Schiefelbein J (2001) Developmentally distinct MYB genes encode functionally equivalent proteins in *Arabidopsis. Development* **128**(9)**:** 1539-1546

Lee MM, Schiefelbein J (2002) Cell pattern in the *Arabidopsis* root epidermis determined by lateral inhibition with feedback. *Plant Cell* **14**(3)**:** 611-618

Li J, Ou-Lee TM, Raba R, Amundson RG, Last RL (1993) *Arabidopsis* Flavonoid Mutants Are Hypersensitive to UV-B Irradiation. Plant Cell **5**(2)**:**171-179

Li X-Q, Stahl R, Brown GG (1995) Rapid micropreps and minipreps of Ti plasmids and binary vectors from *Agrobacterium* tumefaciens. *Transgenic Research* **4**(5)**:** 349-351

Liakopoulos G, Stavrianakou S, Karabourniotis G (2006) Trichome layers versus dehaired lamina of Olea europaea leaves: differences in flavonoid distribution, UV-absorbing capacity, and wax yield. *Environmental and Experimental Botany* **55**(3)**:** 294-304

Liakoura V, Stefanou M, Manetas Y, Cholevas C, Karabourniotis G (1997) Trichome

density and its UV-B protective potential are affected by shading and leaf position on the canopy. *Environmental and Experimental Botany* **38**(3)**:** 223-229

Lieckfeldt E, Simon-Rosin U, Kose F, Zöller D, Schliep M, Fisahn J (2008) Gene expression profiling of single epidermal, basal and trichome cells of *Arabidopsis thaliana*. *J Plant Physiol* **165**(14)**:** 1530-1544

Linhart YB, Grant MC (1996) Evolutionary significance of local genetic differentiation in plants. *Annual Review of Ecology and Systematics* **27**(1)**:** 237-277

Lloyd AM, Schena M, Walbot V, Davis RW (1994) Epidermal cell fate determination in *Arabidopsis*: patterns defined by a steroid-inducible regulator. *Science* **266**(5184)**:** 436-439

Loe G, Torang P, Gaudeul M, Agren J (2007) Trichome production and spatiotemporal variation in herbivory in the perennial herb *Arabidopsis lyrata*. *Oikos* **116**(1)**:** 134-142

Long AD, Mullaney SL, Mackay TF, Langley CH (1996) Genetic interactions between naturally occurring alleles at quantitative trait loci and mutant alleles at candidate loci affecting bristle number in *Drosophila melanogaster*. *Genetics* **144**(4)**:** 1497-1510

Luikart G, England PR, Tallmon D, Jordan S, Taberlet P (2003) The power and promise of population genomics: from genotyping to genome typing. *Nat Rev Genet* **4**(12)**:** 981-994

Lynch M, Walsh B (1998) *Genetics and analysis of quantitative traits*: Sinauer Associates.

Mackay TF, Stone EA, Ayroles JF (2009) The genetics of quantitative traits: challenges and prospects. *Nat Rev Genet* **10**(8)**:** 565-577

Maes L, Inze D, Goossens A (2008) Functional specialization of the *TRANSPARENT TESTA GLABRA1* network allows differential hormonal control of laminal and marginal trichome initiation in *Arabidopsis* rosette leaves. *Plant Physiol* **148**(3)**:** 1453-1464

Mardis ER (2008) The impact of next-generation sequencing technology on genetics. *Trends Genet* **24**(3)**:** 133-141

Martinez-Zapater JM, Jarillo JA, Cruz-Alvarez M, Roladn M, Salinas J (1995) *Arabidopsis* late-flowering *fve* mutants are affected in both vegetative and reproductive development. *Plant Journal* **7**(4)**:** 543-551

Masucci JD, Rerie WG, Foreman DR, Zhang M, Galway ME, Marks MD, Schiefelbein JW (1996) The homeobox gene *GLABRA2* is required for position-dependent cell differentiation in the root epidermis of *Arabidopsis thaliana*. *Development* **122**(4)**:** 1253-1260

Matsui K, Umemura Y, Ohme-Takagi M (2008) AtMYBL2, a protein with a single MYB domain, acts as a negative regulator of anthocyanin biosynthesis in *Arabidopsis*. *Plant J* **55**(6)**:** 954-967

Mauricio R (1998) Costs of resistance to natural enemies in field populations of the annual plant *Arabidopsis thaliana*. *American Naturalist* **151**(1)**:** 20-28

Mauricio R (2005) Ontogenetics of QTL: the genetic architecture of trichome density over time in *Arabidopsis thaliana*. *Genetica* **123**(1-2)**:** 75-85

Mauricio R, Rausher MD (1997) Experimental manipulation of putative selective agents provides evidence for the role of natural enemies in the evolution of plant defense. *Evolution* **51:** 1435-1444

147

Meinhardt H, Gierer A (2000) Pattern formation by local self-activation and lateral inhibition. *Bioessays* **22**(8)**:** 753-760

Melaragno JE, Mehrotra B, Coleman AW (1993) Relationship between Endopolyploidy and Cell Size in Epidermal Tissue of *Arabidopsis*. *Plant Cell* **5**(11)**:** 1661-1668

Meyer K, Benning G, Grill E (1996) Cloning of plant genes based on genetic map location. In *Genome mapping in plants*, Paterson AH (ed), 12, pp 137-149. Austin: Landes Academic Press

Meyer K, Leube MP, Grill E (1994) A protein phosphatase 2C involved in ABA signal transduction in *Arabidopsis thaliana*. *Science* **264**(5164)**:** 1452-1455

Mitchell-Olds T, Schmitt J (2006) Genetic mechanisms and evolutionary significance of natural variation in *Arabidopsis*. *Nature* **441**(7096)**:** 947-952

Morohashi K, Grotewold E (2009) A systems approach reveals regulatory circuitry for *Arabidopsis* trichome initiation by the GL3 and GL1 selectors. *PLoS Genet* **5**(2)**:** e1000396

Morohashi K, Zhao M, Yang M, Read B, Lloyd A, Lamb R, Grotewold E (2007) Participation of the Arabidopsis bHLH factor GL3 in trichome initiation regulatory events. *Plant Physiol* **145**(3)**:** 736-746

Nagata T, Todoriki S, Hayashi T, Shibata Y, Mori M, Kanegae H, Kikuchi S (1999a) Gamma-radiation induces leaf trichome formation in *Arabidopsis*. *Plant Physiol* **120**(1)**:** 113-120

Nordborg M, Hu TT, Ishino Y, Jhaveri J, Toomajian C, Zheng H, Bakker E, Calabrese P, Gladstone J, Goyal R, Jakobsson M, Kim S, Morozov Y, Padhukasahasram B, Plagnol V, Rosenberg NA, Shah C, Wall JD, Wang J, Zhao K, Kalbfleisch T, Schulz V, Kreitman M, Bergelson J (2005) The pattern of

polymorphism in *Arabidopsis thaliana*. *PLoS Biol* **3**(7)**:** e196

Ogata K, Hojo H, Aimoto S, Nakai T, Nakamura H, Sarai A, Ishii S, Nishimura Y (1992) Solution structure of a DNA-binding unit of Myb: a helix-turn-helix-related motif with conserved tryptophans forming a hydrophobic core. *Proc Natl Acad Sci U S A* **89**(14)**:** 6428-6432

Oppenheimer DG, Herman PL, Sivakumaran S, Esch J, Marks MD (1991) A myb gene required for leaf trichome differentiation in *Arabidopsis* is expressed in stipules. *Cell* **67**(3)**:** 483-493

Page RD (1996) TreeView: an application to display phylogenetic trees on personal computers. *Comput Appl Biosci* **12**(4)**:** 357-358

Payne CT, Zhang F, Lloyd AM (2000) GL3 encodes a bHLH protein that regulates trichome development in *Arabidopsis* through interaction with GL1 and TTG1. *Genetics* **156**(3)**:** 1349-1362

Perez-Perez JM, Esteve-Bruna D, Micol JL (2010) QTL analysis of leaf architecture. *J Plant Res* **123**(1)**:** 15-23

Perez-Perez JM, Serrano-Cartagena J, Micol JL (2002) Genetic analysis of natural variations in the architecture of *Arabidopsis thaliana* vegetative leaves. *Genetics* **162**(2)**:** 893-915

Pesch M, Hülskamp M (2004) Creating a two-dimensional pattern de novo during *Arabidopsis* trichome and root hair initiation. *CurrOpinGenetDev* **14**(4)**:** 422-427

Pesch M, Hülskamp M (2009) One, two, three...models for trichome patterning in *Arabidopsis*? *Curr Opin Plant Biol*

Pfalz M, Vogel H, Mitchell-Olds T, Kroymann J (2007) Mapping of QTL for

resistance against the crucifer specialist herbivore Pieris brassicae in a new *Arabidopsis* inbred line population, Da(1)-12 x Ei-2. *PLoS One* **2**(6)**:** e578

Platt A, Horton M, Huang YS, Li Y, Anastasio AE, Mulyati NW, Agren J, Bossdorf O, Byers D, Donohue K, Dunning M, Holub EB, Hudson A, Le Corre V, Loudet O, Roux F, Warthmann N, Weigel D, Rivero L, Scholl R, Nordborg M, Bergelson J, Borevitz JO (2010) The scale of population structure in *Arabidopsis thaliana*. *PLoS Genet* **6**(2)**:** e1000843

Poethig RS (1990) Phase Change and the Regulation of Shoot Morphogenesis in Plants. *Science* **250**(4983)**:** 923-930

Pyke KA, Marrison JL, Leech AM (1991) Temporal and Spatial Development of the Cells of the Expanding First Leaf of *Arabidopsis thaliana* (L.) Heynh. *J Exp Bot* **42**(11)**:** 1407-1416

Ramsay NA, Glover BJ (2005) MYB-bHLH-WD40 protein complex and the evolution of cellular diversity. *Trends Plant Sci* **10**(2)**:** 63-70

Rea PA, Li Z-S, Lu Y-P, Drozdowicz YM, Martinoia E (1998) From vacuolar GS-X pumps to multispecific ABC transporters. *Annual Review of Plant Physiology and Plant Molecular Biology* **49**(1)**:** 727-760

Reiter RS, Williams JG, Feldmann KA, Rafalski JA, Tingey SV, Scolnik PA (1992) Global and local genome mapping in *Arabidopsis thaliana* by using recombinant inbred lines and random amplified polymorphic DNAs. *Proc Natl Acad Sci U S A* **89**(4)**:** 1477-1481

Rerie WG, Feldmann KA, Marks MD (1994) The *GLABRA2* gene encodes a homeo domain protein required for normal trichome development in *Arabidopsis*. *Genes Dev* **8**(12)**:** 1388-1399

Riano-Pachon DM, Dreyer I, Mueller-Roeber B (2005) Orphan transcripts in

Arabidopsis thaliana: identification of several hundred previously unrecognized genes. *Plant J* **43**(2)**:** 205-212

Rosinski JA, Atchley WR (1998) Molecular evolution of the Myb family of transcription factors: evidence for polyphyletic origin. *J Mol Evol* **46**(1)**:** 74-83

Rosso MG, Li Y, Strizhov N, Reiss B, Dekker K, Weisshaar B (2003) An *Arabidopsis thaliana* T-DNA mutagenized population (GABI-Kat) for flanking sequence tag-based reverse genetics. *Plant Mol Biol* **53**(1-2)**:** 247-259

Ryu KH, Kang YH, Park YH, Hwang I, Schiefelbein J, Lee MM (2005) The WEREWOLF MYB protein directly regulates *CAPRICE* transcription during cell fate specification in the *Arabidopsis* root epidermis. *Development* **132**(21)**:** 4765-4775

Sambrook J, Russell DW (2001) *Molecular cloning: a laboratory manual*, Cold Spring Harbor, NY: Cold Spring Harbor Laboratory Press.

Savage NS, Walker T, Wieckowski Y, Schiefelbein J, Dolan L, Monk NA (2008) A mutual support mechanism through intercellular movement of CAPRICE and GLABRA3 can pattern the *Arabidopsis* root epidermis. *PLoS Biol* **6**(9)**:** e235

Schellmann S, Hülskamp M, Uhrig J (2007) Epidermal pattern formation in the root and shoot of *Arabidopsis. Biochem Soc Trans* **35**(Pt 1)**:** 146-148

Schellmann S, Schnittger A, Kirik V, Wada T, Okada K, Beermann A, Thumfahrt J, Jurgens G, Hülskamp M (2002) *TRIPTYCHON* and *CAPRICE* mediate lateral inhibition during trichome and root hair patterning in *Arabidopsis. EMBO J* **21**(19)**:** 5036-5046

Schiefelbein J, Kwak SH, Wieckowski Y, Barron C, Bruex A (2009) The gene regulatory network for root epidermal cell-type pattern formation in *Arabidopsis. J Exp Bot* **60**(5)**:** 1515-1521

Schiefelbein JW, Benfey PN (1991) The development of plant roots: new approaches to underground problems. *Plant Cell* **3**(11)**:** 1147-1154

Schlötterer C, Zangerl B, Epplen JT, Lubjuhn T (1999) The use of imperfect microsatellites for DNA fingerprinting and population genetics. In *DNA Profiling and DNA Fingerprinting*, pp 153-165. Basel: Birkhäuser

Schmid KJ, Ramos-Onsins S, Ringys-Beckstein H, Weisshaar B, Mitchell-Olds T (2005) A multilocus sequence survey in *Arabidopsis thaliana* reveals a genome-wide departure from a neutral model of DNA sequence polymorphism. *Genetics* **169**(3)**:** 1601-1615

Schmid KJ, Torjek O, Meyer R, Schmuths H, Hoffmann MH, Altmann T (2006) Evidence for a large-scale population structure of *Arabidopsis thaliana* from genome-wide single nucleotide polymorphism markers. *Theor Appl Genet* **112**(6)**:** 1104-1114

Schnittger A, Folkers U, Schwab B, Jurgens G, Hulskamp M (1999) Generation of a spacing pattern: the role of *TRIPTYCHON* in trichome patterning in *Arabidopsis*. *Plant Cell* **11**(6)**:** 1105-1116

Serna L (2008) *CAPRICE* positively regulates stomatal formation in the *Arabidopsis* hypocotyl. *Plant Signal Behav* **3**(12)**:** 1077-1082

Serna L, Martin C (2006) Trichomes: different regulatory networks lead to convergent structures. *Trends Plant Sci* **11**(6)**:** 274-280

Shimizu KK, Purugganan MD (2005) Evolutionary and ecological genomics of *Arabidopsis*. *Plant Physiol* **138**(2)**:** 578-584

Shindo C, Bernasconi G, Hardtke CS (2007) Natural genetic variation in

Arabidopsis: tools, traits and prospects for evolutionary ecology. *Ann Bot* **99**(6)**:** 1043-1054

Siegal-Gaskins D, Grotewold E, Smith GD (2009) The capacity for multistability in small gene regulatory networks. *BMC Syst Biol* **3:** 96

Simon M, Lee MM, Lin Y, Gish L, Schiefelbein J (2007) Distinct and overlapping roles of single-repeat MYB genes in root epidermal patterning. *Dev Biol* **311**(2)**:** 566-578

Skaltsa H, Verykokidou E, Harvala C, Karabourniotis G, Manetas Y (1994) UV-B protective potential and flavonoid content of leaf hairs of *Quercus ilex*. *Phytochemistry* **37**(4)**:** 987-990

Smith JL, De Moraes CM, Mescher MC (2009) Jasmonate- and salicylate-mediated plant defense responses to insect herbivores, pathogens and parasitic plants. *Pest Manag Sci* **65**(5)**:** 497-503

Stern DL, Orgogozo V (2008) The loci of evolution: how predictable is genetic evolution? *Evolution* **62**(9)**:** 2155-2177

Steyn WJ, Wand SJE, Holcroft DM, Jacobs G (2002) Anthocyanins in vegetative tissues: a proposed unified function in photoprotection. *New Phytologist* **155**(3)**:** 349-361

Stirnimann CU, Petsalaki E, Russell RB, Muller CW (2010) WD40 proteins propel cellular networks. *Trends Biochem Sci*

Storz JF (2005) Using genome scans of DNA polymorphism to infer adaptive population divergence. *Mol Ecol* **14**(3)**:** 671-688

Stracke R, Werber M, Weisshaar B (2001) The R2R3-MYB gene family in

Arabidopsis thaliana. Curr Opin Plant Biol **4**(5)**:** 447-456

Symonds VV, Godoy AV, Alconada T, Botto JF, Juenger TE, Casal JJ, Lloyd AM (2005) Mapping quantitative trait loci in multiple populations of *Arabidopsis thaliana* identifies natural allelic variation for trichome density. *Genetics* **169**(3)**:** 1649-1658

Szakonyi D, Moschopoulos A, Byrne ME (2010) Perspectives on leaf dorsoventral polarity. *J Plant Res* **123**(3)**:** 281-290

Szymanski DB, Jilk RA, Pollock SM, Marks MD (1998) Control of GL2 expression in Arabidopsis leaves and trichomes. *Development* **125**(7)**:** 1161-1171

Szymanski DB, Marks MD (1998) *GLABROUS1* overexpression and *TRIPTYCHON* alter the cell cycle and trichome cell fate in *Arabidopsis. Plant Cell* **10**(12)**:** 2047-2062

Taiz L, Zeiger E (2006) *Plant Physiology* Sunderland, MA: Sinauer Associates, Inc.

Tanaka Y, Sasaki N, Ohmiya A (2008) Biosynthesis of plant pigments: anthocyanins, betalains and carotenoids. *Plant Journal* **54**(4)**:** 733-749

Telfer A, Bollman KM, Poethig RS (1997) Phase change and the regulation of trichome distribution in *Arabidopsis thaliana. Development* **124**(3)**:** 645-654

Tisne S, Reymond M, Vile D, Fabre J, Dauzat M, Koornneef M, Granier C (2008) Combined genetic and modeling approaches reveal that epidermal cell area and number in leaves are controlled by leaf and plant developmental processes in *Arabidopsis. Plant Physiol* **148**(2)**:** 1117-1127

Tominaga-Wada R, Iwata M, Sugiyama J, Kotake T, Ishida T, Yokoyama R, Nishitani K, Okada K, Wada T (2009) The *GLABRA2* homeodomain protein directly regulates *CESA5* and *XTH17* gene expression in *Arabidopsis* roots. *Plant J* **60**(3)**:**

564-574

Tominaga R, Iwata M, Okada K, Wada T (2007) Functional analysis of the epidermal-specific MYB genes *CAPRICE* and *WEREWOLF* in *Arabidopsis*. *Plant Cell* **19**(7)**:** 2264-2277

Tominaga R, Iwata M, Sano R, Inoue K, Okada K, Wada T (2008) *Arabidopsis CAPRICE-LIKE MYB 3* (*CPL3*) controls endoreduplication and flowering development in addition to trichome and root hair formation. *Development* **135**(7)**:** 1335-1345

Traw MB, Bergelson J (2003) Interactive effects of jasmonic acid, salicylic acid, and gibberellin on induction of trichomes in *Arabidopsis*. *Plant Physiol* **133**(3)**:** 1367-1375

Tsukaya H (2005) Leaf shape: genetic controls and environmental factors. *IntJDevBiol* **49**(5-6)**:** 547-555

Tsukaya H, Shoda K, Kim GT, Uchimiya H (2000) Heteroblasty in *Arabidopsis thaliana* (L.) Heynh. *Planta* **210**(4)**:** 536-542

van Nocker S (2003) CAF-1 and MSI1-related proteins: linking nucleosome assembly with epigenetics. *Trends Plant Sci* **8**(10)**:** 471-473

Verslues PE, Guo Y, Dong CH, Ma W, Zhu JK (2006) Mutation of SAD2, an importin beta-domain protein in *Arabidopsis*, alters abscisic acid sensitivity. *Plant J* **47**(5)**:** 776-787

Wada T, Kurata T, Tominaga R, Koshino-Kimura Y, Tachibana T, Goto K, Marks MD, Shimura Y, Okada K (2002) Role of a positive regulator of root hair development, *CAPRICE*, in *Arabidopsis* root epidermal cell differentiation. *Development* **129**(23)**:** 5409-5419

Wada T, Tachibana T, Shimura Y, Okada K (1997) Epidermal cell differentiation in *Arabidopsis* determined by a Myb homolog, CPC. *Science* **277**(5329)**:** 1113-1116

Wagner GJ, Wang E, Shepherd RW (2004) New approaches for studying and exploiting an old protuberance, the plant trichome. *Annals of Botany* **93**(1)**:** 3-11

Walker AR, Davison PA, Bolognesi-Winfield AC, James CM, Srinivasan N, Blundell TL, Esch JJ, Marks MD, Gray JC (1999) The *TRANSPARENT TESTA GLABRA1* locus, which regulates trichome differentiation and anthocyanin biosynthesis in *Arabidopsis*, encodes a WD40 repeat protein. *Plant Cell* **11**(7)**:** 1337-1350

Walker JD, Oppenheimer DG, Concienne J, Larkin JC (2000) *SIAMESE*, a gene controlling the endoreduplication cell cycle in *Arabidopsis thaliana* trichomes. *Development* **127**(18)**:** 3931-3940

Wang S, Basten CJ, Zeng ZB. (2005) Windows QTL Cartographer 2.5.

Wang S, Chen JG (2008) Arabidopsis Transient Expression Analysis Reveals that Activation of *GLABRA2* May Require Concurrent Bindings of GLABRA1 and GLABRA3 to the Promoter of *GLABRA2*. *Plant Cell Physiol*

Wang S, Hubbard L, Chang Y, Guo J, Schiefelbein J, Chen JG (2008) Comprehensive analysis of single-repeat R3 MYB proteins in epidermal cell patterning and their transcriptional regulation in *Arabidopsis*. *BMC Plant Biol* **8:** 81

Wang S, Kwak SH, Zeng Q, Ellis BE, Chen XY, Schiefelbein J, Chen JG (2007) *TRICHOMELESS1* regulates trichome patterning by suppressing *GLABRA1* in *Arabidopsis. Development* **134**(21)**:** 3873-3882

Wang ZY, Kenigsbuch D, Sun L, Harel E, Ong MS, Tobin EM (1997) A Myb-related transcription factor is involved in the phytochrome regulation of an *Arabidopsis* Lhcb

gene. *Plant Cell* **9**(4)**:** 491-507

Weigel D, Nordborg M (2005) Natural variation in *Arabidopsis.* How do we find the causal genes? *Plant Physiol* **138**(2)**:** 567-568

Werker E. (2000) Trichome diversity and development. *Advances in Botanical Research*, Vol. 31, pp. 1-35.

Wester K, Digiuni S, Geier F, Timmer J, Fleck C, Hülskamp M (2009) Functional diversity of R3 single-repeat genes in trichome development. *Development*

Weston K (1998) Myb proteins in life, death and differentiation. *Curr Opin Genet Dev* **8**(1)**:** 76-81

Wienkoop S, Zoeller D, Ebert B, Simon-Rosin U, Fisahn J, Glinski M, Weckwerth W (2004) Cell-specific protein profiling in *Arabidopsis thaliana* trichomes: identification of trichome-located proteins involved in sulfur metabolism and detoxification. *Phytochemistry* **65**(11)**:** 1641-1649

Willmann MR, Poethig RS (2005) Time to grow up: the temporal role of smallRNAs in plants. *Curr Opin Plant Biol* **8**(5)**:** 548-552

Wright SI, Gaut BS (2005) Molecular population genetics and the search for adaptive evolution in plants. *Mol Biol Evol* **22**(3)**:** 506-519

Xu CR, Liu C, Wang YL, Li LC, Chen WQ, Xu ZH, Bai SN (2005) Histone acetylation affects expression of cellular patterning genes in the *Arabidopsis* root epidermis. *Proc Natl Acad Sci U S A* **102**(40)**:** 14469-14474

Yanhui C, Xiaoyuan Y, Kun H, Meihua L, Jigang L, Zhaofeng G, Zhiqiang L, Yunfei Z, Xiaoxiao W, Xiaoming Q, Yunping S, Li Z, Xiaohui D, Jingchu L, Xing-Wang D, Zhangliang C, Hongya G, Li-Jia Q (2006) The MYB transcription factor superfamily

of *Arabidopsis*: expression analysis and phylogenetic comparison with the rice MYB family. *Plant Mol Biol* **60**(1)**:** 107-124

Ye Y, Rape M (2009) Building ubiquitin chains: E2 enzymes at work. *Nat Rev Mol Cell Biol* **10**(11)**:** 755-764

Yoshida Y, Sano R, Wada T, Takabayashi J, Okada K (2009) Jasmonic acid control of *GLABRA3* links inducible defense and trichome patterning in *Arabidopsis*. *Development* **136**(6)**:** 1039-1048

Yu J, Pressoir G, Briggs WH, Vroh Bi I, Yamasaki M, Doebley JF, McMullen MD, Gaut BS, Nielsen DM, Holland JB, Kresovich S, Buckler ES (2006) A unified mixed-model method for association mapping that accounts for multiple levels of relatedness. *Nat Genet* **38**(2)**:** 203-208

Yu N, Cai WJ, Wang S, Shan CM, Wang LJ, Chen XY (2010) Temporal Control of Trichome Distribution by MicroRNA156-Targeted *SPL* Genes in *Arabidopsis thaliana*. *Plant Cell* **22**(7)**:** 2322-35

Zeng ZB (1993) Theoretical basis for separation of multiple linked gene effects in mapping quantitative trait loci. *ProcNatlAcadSciUSA* **90**(23)**:** 10972-10976

Zeng ZB (1994) Precision mapping of quantitative trait loci. *Genetics* **136**(4)**:** 1457-1468

Zhang F, Gonzalez A, Zhao M, Payne CT, Lloyd A (2003) A network of redundant bHLH proteins functions in all *TTG1*-dependent pathways of *Arabidopsis*. *Development* **130**(20)**:** 4859-4869

Zhao J, Zhang W, Zhao Y, Gong X, Guo L, Zhu G, Wang X, Gong Z, Schumaker KS, Guo Y (2007a) SAD2, an importin -like protein, is required for UV-B response in *Arabidopsis* by mediating MYB4 nuclear trafficking. *Plant Cell* **19**(11)**:** 3805-3818

Zhao K, Aranzana MJ, Kim S, Lister C, Shindo C, Tang C, Toomajian C, Zheng H, Dean C, Marjoram P, Nordborg M (2007b) An *Arabidopsis* example of association mapping in structured samples. *PLoS Genet* **3**(1)**:** e4

Zhao M, Morohashi K, Hatlestad G, Grotewold E, Lloyd A (2008) The TTG1-bHLH-MYB complex controls trichome cell fate and patterning through direct targeting of regulatory loci. *Development* **135**(11)**:** 1991-1999

Zimmermann IM, Heim MA, Weisshaar B, Uhrig JF (2004) Comprehensive identification of *Arabidopsis thaliana* MYB transcription factors interacting with R/B-like BHLH proteins. *Plant J* **40**(1)**:** 22-34

Zou F (2009) QTL mapping in intercross and backcross populations. *Methods Mol Biol* **573:** 157-173

6 ABBREVIATIONS

µg: microgram

µl: micorlitre

aa: amino acid

AGI*: Arabidopsis* Genome Initiative

APS: ammonium persulfate

bp: base pair

Can-0: Canary Island-0

cDNA: complementary DNA

CDS: coding sequence

Col: Columbia

DDT: dithiothreitol

dH_20: deionized water

dATP: desoxiadenosine triphosphate

DIG: digoxigenin

DNA: desoxiribonucleic acid

dNTP: desoxinucleotide triposphate

DMSO: dimethyl sulfoxide

EDTA: ethylendiamintetra acetic acid

g: gram

g: gravitational force

GFP: green fluorescent protein

GUS: β-glucuronidase

gof: gain of function

Gr-1: Graz-1

HCl: hydrochloric acid

LALI: local activation, lateral inhibition

LIF: local activation with feedback

L*er*: Landberg *erecta*

lof: loss of function

M: molar

Ml: millilitre

mM: millimolar

mm^2: square millimetre

$MgCl_2$: magnesium chloride

mRNA: messenger RNA

N: normal

N_2: nitrogen

NaOH: sodium hydroxide

NASC: Nottingham *Arabidopsis* Stock Centre

ng: nanogram

nm: nanometre

OD: optical density

pmol: picomol

QTL: quantitative trait locus

QTN: quantitative trait nucleotide

RNA: ribonucleic acid

rpm: revolutions per minute

s: second

SNP: single nucleotide polymorpshism

TAIR: The *Arabidopsis* Information Resource

Taq: Thermophilus aquaticus

TEMED: tetramethylethylenediamine

Tris: tris-(hydroxylmethyl)aminomethan

U: unit

UTR: untranslated region

V: volt

v/v: volume/volume

w/v: weight/volume

YFP: yellow fluorescent protein

7 APPENDIX

7.1 Arabidopsis thaliana accessions

Table 7.1 *A. thaliana* accessions

Ecotype	Origin	Country	Stock nr.	Phenotyped by [1]	Obtained from [2]	Trichome number [3]	Trichome density	Nr. of individuals phenotyped	expected phenotype according to HS
Aa-0	Aua/Rhon	Germany	N934	MTH	NASC	nd	1.25		
An-1	Antwerpen	Belgium	N944	MTH	NASC	nd	0.68		
Ba-1	Blackmount	England	N952	MTH	NASC	nd	0.41		
Bla-1	Blanes	Spain	N970	MTH	NASC	nd	1.52		
Bur-0	Burren	Ireland	N1028	MTH	NASC	nd	1.64		
Can-0	Canary Island	Spain	N1064	MTH	NASC	nd	3.84		
Col	Columbia	USA		MTH	P.B.	nd	1.17		
Cond		Tadjikistan	N961	MTH	NASC	nd	1.73		
Di-0	Dijon	France	N1106	MTH	NASC	nd	0.58		
Es-0	Espoo	Finland	N1144	MTH	NASC	nd	1.42		

Gr-1	Graz	Austria	N1198	MTH	NASC	nd	0.30		
Hi-0	Hilversum	Netherlands	N1226	MTH	NASC	nd	0.95		
Ita-0	Ibel Tazekka	Morocco	N1244	MTH	NASC	nd	1.7		
Kas-1	Kashmir	India	N903	MTH	NASC	nd	1.53		
Ler	Landsberg	Poland		MTH	P.B.	nd	0.42		
Ms-0	Moscow	Russia	N1276	MTH	NASC	nd	1.57		
Mt-0	Martuba	Libya	N1380	MTH	NASC	nd	0.93		
Nd-0	Niederzenz	Germany		MTH	G.J.	nd	1.1		
No-0	Noordwijk	Germany	N1394	MTH	NASC	nd	0.67		
Ov-0	Ovstese	Norway	N1436	MTH	NASC	nd	0.57		
RLD-1	Rschew	Russia	N913	MTH	NASC	nd	0.88		
Sha	Shakdara	Tadjikistan	N929	MTH	NASC	nd	1.27		
Te-0	Tenela	Finland	N1550	MTH	NASC	nd	1.47		
Tsu-0	Tsu	Japan	N1564	MTH	NASC	nd	0.74		
Ws-0	Wassilewskaja	Ukraine		MTH	K.F.	nd	1.47		
Yo-0	Yosemite Ntl	USA	N1622	MTH	NASC	nd	1.15		
9481		Kasachstan	N22458	JH	NASC	511	1.43	1	
Ag-0	Argentat	France	N936	JH	NASC	ng	ng		
Bay	Bayreuth	Germany		JH	NASC	170	1.30	1	
Blh-1	Bulhary	Czech R.	N1030	JH	NASC	90	0.30	1	
Bor-0	Bou	Algerien	N993	JH	NASC	ng	ng		
BuckhornPass	California	USA	N8067	JH	NASC	108	0.42	1	
Ct-1	Catania	Italy	N1094	JH	NASC	218	0.96	1	
Est-1		Estland	N6701	JH	NASC	267	1.13	1	
Ga-0	Gabelstein	Germany	N6714	JH	NASC	98	0.54	1	
Ge-0	Genf	Switzerland	N1186	JH	NASC	138	0.94	1	

Gy-0	La Miniere	France	N6732	JH	NASC	267	2.07	1	
Kin-0	Kindalville	USA	N6755	JH	NASC	226	0.78	1	
Lind-0	Lindisfarne	UK	N22556	JH	NASC	ng	ng		
Lz-0	Lezoux	France	N6788	JH	NASC	222	0.55	1	
Mh-0	Mühlen	Poland	N6792	JH	NASC	339	0.93	1	
N7		Russia	N22458	JH	NASC	254	0.86	1	
Nok-0	Nordwijk	Netherlands	N6807	JH	NASC	80	0.45	1	
Pa-3	Palermo	Italy	N6827	JH	NASC	258	1.06	1	
Pi-0	Pitztal	Austria	N1454	JH	NASC	221	0.79	1	
Sf-2	San Feliu	Spain	N6857	JH	NASC	221	1.04	1	
St-0	Stockholm	Sweden	N1534	JH	NASC	191	1.15	1	
Sue-0	Sierra Nevada	Spain	N1543	JH	NASC	ng	ng		
Tscha-1	Tschagguns	Austria	CS22518	JH	NASC	362	0.94	1	
Uk-3	Umkirch	Germany	N6880	JH	NASC	249	1.33	6	
Van-0	Vancouver	Canada	N6884	JH	NASC	265	0.63	1	
Wt-5	Wietze	Germany	N6896	JH	NASC	131	0.56	1	
83-3				JH	K.S.	48	0.74	7	
84-1				JH	K.S.	100	2.01	7	
Brest-1				JH	K.S.	138	0.65	7	
Grivo-1				JH	K.S.	113	1.28	7	
Kara7-2				JH	K.S.	155	1.02	7	
Tein-1				JH	K.S.	162	1.49	5	
20-13	Population 8	Norway		JH	H.S.	290	2.46	7	
I-33	Population 6	Norway		JH	H.S.	71	0.86	6	
T-12-I	Population 7	Norway		JH	H.S.	164	0.86	6	
T-20-I	Population 7	Norway		JH	H.S.	154	0.83	6	

T-29-I	Population 7	Norway		JH	H.S.	181	0.92	7	
Ag-0/4	Argentat	France	N936	JH	H.Sch.	279	0.83	4	
Alc-0/1	Madrid	Spain	N1656	JH	H.Sch.	733	2.04	3	
Bas-2/3	Bastan	Russia		JH	H.Sch.	651	2.21	2	
Bur-0/1	Burren	Ireland		JH	H.Sch.	63	0.38	4	
Ct-1/4	Catania	Italy		JH	H.Sch.	125	0.65	2	
Dül/4	Dülmen	Germany		JH	H.Sch.	229	1.09	1	
Edi-0/2	Edinburgh	Scotland	N1122	JH	H.Sch.	647	2.07	5	
Kn-0/1	Kaunas	Lithuana	N1286		H.Sch.	ng	ng		low
Lim 3	Limeport	PA, USA		JH	H.Sch.	389	1.83	5	low
Lip-0/1	Lipowiec	Poland	N1336	JH	H.Sch.	272	0.87	4	
Ll-2/2	Llagostera	Spain	N1342	JH	H.Sch.	208	1.73	10	low
Mal-1/1	Mallorca	Spain			H.Sch.	ng	ng		
Mas/2	Masljacha	Russia		JH	H.Sch.	554	1.65	3	
Pa-1/1	Palermo	Italy		JH	H.Sch.	112	0.81	2	low
Per -1/5	Perm	Russia	N1444	JH	H.Sch.	390	1.76	1	
Pog-0/2	Point Gray	Canada		JH	H.Sch.	306	2.12	1	high
Rub-1/2	Rubezhnoe	Ukraine	N927	JH	H.Sch.	486	3.08	5	high
Ryb 2	Rybreka	Russia	N22479/N1	JH	H.Sch.	279	1.6	5	high
Sie/1	Siena	Italy		JH	H.Sch.	glabrous	glabrous		glabrous
Stoc 5	Stockholm	Sweden	N3114/M7943S	JH	H.Sch.	178	0.88	5	high
Tsar/1	Zarevichi	Russia	N22489	JH	H.Sch.	677	2.06	2	
Wa-1/3	Warschau	Poland	N1586	JH	H.Sch.	140	0.71	5	low

See table legend next page.

7.2 Primer sequences

Table 7.2 Primers used in marker analysis

Basic markers used for QTL mapping			Chr.	Gr/Can/Col length (bp)*
nga63	F	5´- ACCCAAGTGATCGCCACC - 3´	1	90/120/111
	R	5´- AACCAAGGCACAGAAGCG - 3´		
AtHZFP	F	5´- GACAGATAGAAGAGATAGGA - 3´	1	78/93/122
	R	5´- TCCAACATTTGCGTTTCCAC - 3´		
T27K12-	F	5´- GGAGGCTATACGAATCTTGACA - 3´	1	205/150/146
	R	5´- GGACAACGTCTCAAACGGTT - 3´		
T2K10	F	5´- TATGGCATCTTACCGTGTCG - 3´	1	high/low/182
	R	5´- CCAGGGTTTGGTGGTGAATA - 3´		
CIW2	F	5´- CCCAAAAGTTAATTATACTGT- 3´	1	105/90/105
	R	5´- CCGGGTTAATAATAAATGT- 3´		
F19G14	F	5´- CAATTCAAGTGTCTTATAAAGG- 3´	2	high/low/153
	R	5´- ACCATTTTATATTCTGGTTCT- 3´		
nga2g22	F	5´- GGGAGTTTTTCCTAATTGATCC- 3´	2	high/low/123
	R	5´- GCAACGCTTCTATCGGTTTC- 3´		
ngaT3B	F	5´- CCTTATTCTTTCCATGGAAATAAG - 3´	2	194/160/181
	R	5´- ATGACCATTTCTGTTCTGCA - 3´		
nga361	F	5´- AAAGAGATGAGAATTTGGAC - 3´	2	110/104/114
	R	5´- ACATATCAATATATTAAAGTAGC - 3´		
nga3470	F	5´- TGTTTTGTTTGTGTATTATTCTGAGG- 3´	2	high/low/89
	R	5´- TGTGATATTGATGCCTTGATGC- 3´		
nga3692	F	5´- GAATCCTTGCCAACATTTTGGA- 3´	2	high/low/120
	R	5´- CACAGAGATACTGTATGAGGGA- 3´		
ngaT2P	F	5´- CGTCTCGCATTCTTACCAAC- 3´	2	122/118/129
	R	5´- CCTAATGAAGCATCTGCTGCA- 3´		
nga162	F	5´- CATGCAATTTGCATCTGAGG - 3´	3	86/80/107
	R	5´- CTCTGTCACTCTTTTCCTCTGG - 3´		
3g2837	F	5´- TACGATAGATAGGGGAACAG - 3´	3	low/high/119
	R	5´- AAAACTCCATATGTTATTGGAC - 3´		
F1P2-	F	5´- GTCTGAAGATGTGGAGAGAG - 3´	3	130/100/130

	R	5´- GCTACTAATTCACTCTTCAGCT - 3´		
nga6	F	5´- TGGATTTCTTCCTCTCTTCAC - 3´	3	143/150/143
	R	5´- ATGGAGAAGCTTACACTGATC - 3´		
JV30/31	F	5´- CATTAAAATCACCGCCAAAAATTAG - 3´	4	108/112/194
	R	5´- GAACATTCAATCTAATACTATGAG - 3´		
nga8	F	5´- GAGGGCAAATCTTTATTTCGG - 3´	4	160/130/154
	R	5´- TGGCTTTCGTTTATAAACATCC - 3´		
CIW7	F	5´- AATTTGGAGATTAGCTGGAAT - 3´	4	130/100/130
	R	5´- CCATGTTGATGATAAGCACAA - 3´		
nga1139	F	5´- TAGCCGGATGAGTTGGTACC - 3´	4	150/120/114
	R	5´- TTTTTCCTTGTGTTGCATTCC - 3´		
nga151	F	5´- CAGTCTAAAAGCGAGAGTATGATG - 3´	5	125/170/150
	R	5´- GTTTTGGGAAGTTTTGCTGG - 3´		
nga139	F	5´- AGAGCTACCAGATCCGATGG - 3´	5	160/200/174
	R	5´- GGTTTCGTTTCACTATCCAGG - 3´		
AthSO1	F	5´- CTCCACCAATCATGCAAATG - 3´	5	130/160/148
	R	5´- TGATGTTGATGGAGATGGTCA - 3´		
nga129	F	5´- CACACTGAAGATGGTCTTGAG - 3´	5	90/120/102
	R	5´- TCAGGAGGAACTAAAGTGAGG - 3´		
Markers used for fine mapping				
ngaT3B	F	5´- CCTTATTCTTTCCATGGAAATAAG- 3´	2	194/160/181
	R	5´- ATGACCATTTCTGTTCTGCA- 3´		
nga3000	F	5´- ACAATCATCCACGCAACACA - 3´	2	155/160/153
	R	5´- TCAAACGGCTTATCGTGACA - 3´		
nga3023	F	5´- GATAGCATCACTGAGGATCTT - 3´	2	146/160/163
	R	5´- TTTCTCACCGGGCATGTT - 3´		
HDUP3	F	5´- TCCAAGTTTCTTCGTTATGTGAA - 3´	2	**SNP/486
	R	5´- CGAATGATGATTTGGTTGGA - 3´		
2g30420	F	5´- TATGTTGACTCCTGAATTTTG - 3´	2	***105/116/116
	R	5´- CTTCCTGCTATTAAATCCCAC - 3´		
nga3073	F	5´- AGGGATCTTCTTCGCTTAATG - 3´	2	156/162/282
	R	5´- CTCCGTCTTCATCATCAAGCA - 3´		
nga3098	F	5´- CATTGTTCACGAAAGAATCAATC - 3´	2	153/110/153
	R	5´- TTGAAACGTCGTCCCGATA - 3´		
nga361	F	5´- AAAGAGATGAGAATTTGGAC - 3´	2	110/104/114
	R	5´- ACATATCAATATATTAAAGTAGC - 3´		
nga3108	F	5´- CCCTACTGATCAGCGTTGGTAC - 3´	2	high/low/137
	R	5´- CTTGCGGACTAAAGAGTTGGA - 3´		
nga3119	F	5´- GAAGGGTCCAGGTCTAAGG - 3´	2	129/141/126
	R	5´- CAAAATGGAATCTGATTAATGC - 3´		
nga3142	F	5´- TCTTACTAAGGATTGCTCTTG -3´	2	112/107/111
	R	5´- GAACTAAAATAAAAATTTATCACTAG -3´		
nga3130	F	5´- CACCCGCTTACTTGCTCGA -3´	2	140/170/110
	R	5´- AGCCCAGAAATTCGCCGGA -3´		
nga3134	F	5´- AGAACATAATGTGAGGAAGGT -3´	2	****/107
	R	5´- TCTCTGCTTCCACTGTTCTAC -3´		
nga3139	F	5´- CATGTATCAGAACTTCTTCTAC -3´	2	120/114/110

	R	5´- CTCTGCACACATGTTACGATC -3´		
nga3142	F	5´- CTTGCTTCACAACACTCTGCT -3´	2	180/140/140
	R	5´- TCTCTTCGAAACCGGCCTAG -3´		
nga3145	F	5´- GTCTCTTTGAACCCTGTTTCA -3´	2	120/160/137
	R	5´- ATCTTTCTTGTTCCACAAGTTC -3´		
nga3168	F	5´- CTTCGTCATCGGACGACATC - 3´	2	120/114/110
	R	5´- CTCTATCATTTCCTTTGCCAGCTC - 3´		
nga3198	F	5´- GCTCATTGGTGCCTTGTTAG -3´	2	180/140/140
	R	5´- CTCTTAGATTTGTGATTCTCACT -3´		
nga3256	F	5´- CATTCAATTTCAAGTTCCAAAAC -3´	2	120/160/137
	R	5´- CTAACCAACTCATGGACACAA -3´		
nga3296	F	5´- TCGATCGGTTGATGGAATTAC -3´	2	140/150/128
	R	5´- TGGTAAATACCGACAAAAGC -3´		
nga3341	F	5´- TTGCTTTGATGAGCTCGATTT - 3´	2	high/low/166
	R	5´- GGATCAATGACCTTATTATTTGA - 3´		
Size standard preparation for denaturing PAA				
M13-40	F	5'- GTTTTCCCAGTCACGAC-3'		

*: marker lengths in Gr-1 and Can-0 genomic background were estimated from 5% non-denaturing PAA gels, except where indicated otherwise, and marker lengths in Col genomic background were derived from the AGI consensus sequence. high/low: relative marker states as seen on denaturing PAA gels using radioactively labelled PCR product, where approximate bp lengths could not be determined due to double loading of gels and/or non-functioning of the size standard

**: marker state at HDUP3038 was derived of a SNP state by sequencing

***: marker state at 2g30420 was derived from sequencing

****: marker state at nga31450 shows complex but distinguishable fragment patterning

Table 7.3 Primers used for cloning, sequencing, genotypic analysis and cosmid library screening

Primer name		Sequence
Cloning of *ETC2*, *TCL1* and *TCL2* genomic complementation constructs		
ETC2	F5_EcoRI	5´ - GAATTCTACAAGTTGTGCCACT - 3´
	R4_EcoR	5´ - GAATTCTGAGAATGGTTAATCATC - 3´
2g30432	F4_XbaI	5´ - TCCTGAGAATTGTTCTAGAAG - 3´
	R4_XbaI	5´ - AGTCTAGAACCCTTGCATACCACG - 3´
oRNA264	F1_XbaI	5´ - AGTCTAGACATCAATACACATGTTACAAG - 3´
	R1_XbaI	5´ - AGTCTAGAAGTCATGGACTAGAACGACT - 3´
Site directed mutagenesis of *ETC2*		
Gr-53F_Phusion		5´ - TCTCCAAACTCTACATTTTCAGTTTCTCT - 3´
Gr-53R_Phusion		5´ - ATGCAAGATATAGAAAAGATGTGAGGGA - 3´
Gr+55F_Phusion		5´ - GTTTTAGGCAAACCAAGTTCACTCG - 3´
+55R_Phusion		5´ - TGGGACCGCGACGAAGAC - 3´
Can-53F_Phusion		5´ - CATTCTCCAAACTCTAAATTTTCAGTTTC - 3´

Can-53R Phusion		5´ - CAAGATATAGAAAAGATGTGAGGGGA - 3´
Can+55F Phusion		5´ - GTCTTAGGCAAACTGAGTTCACTCGATC - 3´
Sequencing of *ETC2*		
2g30420	F1	5´- CATTCTGATTTCACGCTGAG - 3´
	R1	5´- CTATTACCGACAAGTCTGTAC - 3´
	F2	5´- GCATCGAATGGGAGTTTATCAG - 3´
	R2	5´- GAAGACATTCAAGATTTGTTCTAC - 3´
	F3	5´- GAGAAGTGTATTTGCATGTGATG - 3´
	R3	5´- CTTCCTGCTATTAAATCCCAC - 3´
	F4	5´- TATGTTGACTCCTGAATTTTG - 3´
	F5	5´- CTAAGTTCACTCGATCCCGAT - 3´
	R6	5´- CAGTCACTAAAATGGCGTGCT - 3´
	F6	5´- GTGCCCAATACTCTCAGGAC - 3´
Sequencing of *TCL1*		
2g30432	F1	5´- AATGTGTCTTATAATCATAGAG - 3´
	R1	5´- TCAGTAAGTTATGGTGTACC - 3´
	F2	5´- TTGAACAGTCTTAGAAAATATGGA - 3´
	R2	5´- TCGGATGTCGTGAGAGTCAG - 3´
	F3	5´- GAGTTTGGAGAATGCAAGCGA - 3´
	R3	5´- TCCGATTTGAGCGGATATAC - 3´
	R5	5´- GAATTAAGTCGCAACTGATTCAT - 3´
Sequencing of *TCL2*		
oRNA264	R1	5´- GTTGAACCCGAATTGTGGATA - 3´
	F2	5´- ATTGGGCAAGTTTTCGCTTAA - 3´
	R2	5´- ACAGTTATCTCGAGCATTATC - 3´
	F3	5´- GTATCTTAGCTATCTTTAGATTC - 3´
	R3	5´- CATGTGGGTGGAATTAACCT - 3´
	F4	5´- GGTTAAGAAAGAGTTCTGACGA - 3´
2goRNA264	R	5´- TTGATGAGAAGAATAAATATCG -3´
Genotyping of interaction study individuals		
LB CPC I		5´- CACATCATCTCATTGATGCTTGGT - 3´
2g46410	F	5´- GTATAAACTCGTTGGCGACAG - 3´
	R	5´- AGTAATTCAAGGACAGGTAC - 3´
nga5g53150	F	5´- GTGGTTTTTGGATTTGGTTTATAG - 3´
	R	5´- GGTTTTTCACTTTTTAACGCTATAAC - 3´
nga3034	F	5´- TGTGGAATTGTGTTATTTTGTG - 3´
	R	5´- AATGGGTTCCATTACCATACT - 3´
2g30420	F4	5´- TATGTTGACTCCTGAATTTTG - 3´
	R3	5´- CTTCCTGCTATTAAATCCCAC - 3´
nga3098	F	5´- CATTGTTCACGAAAGAATCAATC - 3´
	R	5´- TTGAAACGTCGTCCCGATA - 3´
Genotyping of Col *etc2* lines		
LBa1		5´- TGGTTCACGTAGTGGGCCA - 3´
Cosmid library screening		
nga3023	F	5´- GATAGCATCACTGAGGATCTT - 3´
	R	5´- TTTCTCACCGGGCATGTT - 3´
At2g30280	F	5´- AAGCCATATTTTGCTTGTGG - 3´

	R	5´- TTCTCATTATGATCAGACTC - 3´
HDUP3032	F	5´- CTGATTCTGATGCTTTGATTG - 3´
	R	5´- GATAGGTTGCAAGCTCATAC - 3´
At2g30340	F	5´- TGTGGAATTGTGTTATTTTGTG - 3´
	R	5´- AATGGGTTCCATTACCATACT - 3´
At2g30350	F	5´- TGCTAATCTGTCTTCTTCATCA - 3´
	R	5´- GAGATGTTTAGTGATTGATTGC - 3´
HDUP3037	F	5´- CGGCAACAAGTTGTACATGC - 3´
	R	5´- TGTTATTGGGCTTTTGGTTT - 3´
HDUP3038	F	5´- TCCAAGTTTCTTCGTTATGTGAA - 3´
	R	5´- CGAATGATGATTTGGTTGGA - 3´
At2g30420	F2	5´- GCATCGAATGGGAGTTTATCAG - 3´
	R2	5´- GAAGACATTCAAGATTTGTTCTAC - 3´
At2g30432	F1	5´- AATGTGTCTTATAATCATAGAG - 3´
	R2	5´- TCGGATGTCGTGAGAGTCAG - 3´
At2g30432	F3	5´- GAGTTTGGAGAATGCAAGCGA - 3´
	R3	5´- TCCGATTTGAGCGGATATAC - 3´
At2g30440	F	5´- TGAAACCAAATGGGTGGTCT - 3´
	R	5´- GGTTTGAGAAATCAAATCGAG - 3´
At2g30470	F	5´- TTTCGTTCACTTGCATGCTC - 3´
	R	5´- CGCCATTTACATGTTGCCTA - 3´
At2g30490	F	5´- ACCTTTTGCCGTTGGTCCTC - 3´
	R	5´- CGGCGACATTGATGTTCTCG - 3´
At2g30520	F	5´- CAACGGTGGAGACTTCAACA - 3´
	R	5´- ACAGAATTTGCGGGCATAAG - 3´
At2g30575	F	5´- TGCTGAATTGCTGATGAAGC - 3´
	R	5´- ATAAACTGCATCCAGATTGC - 3´
At2g30590	F	5´- GCACACGTGAATTAGTTTCGAC - 3´
	R	5´- ACAAATTTAATTGTTCTCTGAC - 3´
At2g30600	F	5´- AAAGTGGGTGTTGAAACCTAC - 3´
	R	5´- GATCATACGTTTTGAGAAGAC - 3´
At2g30640	F	5´- CTTCCATGAACCACAGCAAC - 3´
	R	5´- GAATCTGTAAGAGATATTAGTG - 3´
At2g30670	F	5´- ATACACTTCTCATTCTTATGTC - 3´
	R	5´- GGATTCATTATCATTATGTTGG - 3´
At2g30700	F	5´- GCTGCTTGGTTTATCGCTTC - 3´
	R	5´- CTTGGACACTGAAATCTTTG - 3´
nga3073new	F	5´- AGGGATCTTCTTCGCTTAATG - 3´
	R	5´- CTCCGTCTTCATCATCAAGCA - 3´
At2g30780	F	5´- GGTTTGATGCACCGGTCTAC - 3´
	R	5´- AATTTGCATACCCACGAAGC - 3´
nga3082	F	5´- GCGAGTGTAAAAACGTACGA - 3´
	R	5´- GGTCTGAGTCTCTGTGAGTC - 3´
At2g30880	F	5´- TTGATCGCGTTGAAAGAGTG - 3´
	R	5´- AGATTCCAATCAACTATCTCC - 3´
At2g30920	F	5´- TCGAGAATTCGTCATTCCAC - 3´
	R	5´- TAACCCTCAAACGCTCAACC - 3´

At2g30942	F	5´- GATTACCCGGTCACATGAGG - 3´
	R	5´- GAAAATGGCAAGAGCTCTGG - 3´
nga3098	F	5´- CATTGTTCACGAAAGAATCAATC - 3´
	R	5´- TTGAAACGTCGTCCCGATA - 3´
At2g31020	F	5´- CGCCGCAATTTCCTACAAC - 3´
	R	5´- ACTCCTTCCTCAACCAATCG - 3´
nga361	F	5´- AAAGAGATGAGAATTTGGAC - 3´
	R	5´- ACATATCAATATATTAAAGTAGC - 3´
Sequencing of Cosmid insert borders		
pBIC20	F	5´- GAGCAAGTCCTTTCTGAGC - 3´
	R	5´- CATCTGTGGGTTAGCATTCT - 3´

Table 7.4 Primers used in expression analysis

			Fragment length (bp)	
Gene	Primer	Sequence	genomic	cDNA
UBIQUITIN5	CUB_Q	5'- AACCCTTGAGGTTGAATCATCC -3'	426	426
	NQ	5'- GTCCTTCTTTCTGGTAAACGT -3'		
TUBULIN9	TUB9-F	5'- GTACCTTGAAGCTTGCTAATCCTA -	470	360
	TUB9-R	5'- GTTCTGGACGTTCATCATCTGTTC -		
ETC2	ETC2 F2	5´- GCATCGAATGGGAGTTTATCAG -3'	840	301
	ETC2 R2	5´- GAAGACATTCAAGATTTGTTCTAC -		
TCL1	30432-RT_F	5´- GATAACACAAACCGTCTTCG -3'	1292	255
	30432RT_R	5´- TCATTTGTGGGAGAAATAGTC -3'		
TCL2	oRNA264_F2	5´- GTCACCTTCGCAGTCGTAAG -3'	1023	363
	2goRNA_264_R	5´- TTGATGAGAAGAATAAATATCG -3'		

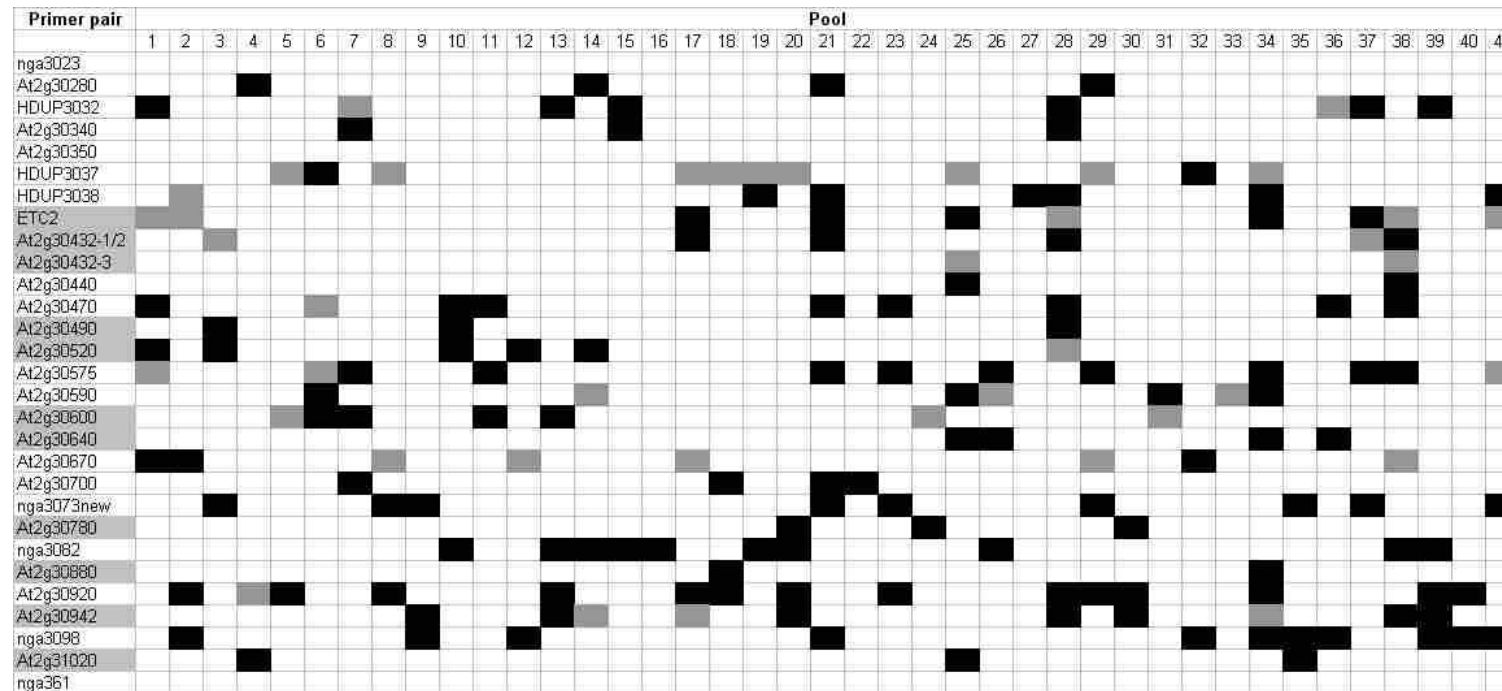## 7.3 Screening of *Arabidopsis thaliana* L*er* genomic library

Figure 7.1. PCR screen results of the A. thaliana L*er* cosmid library for subpools containing genomic regions of the major QTL candidate interval on chromosome 2. Black and grey squares indicate strong and week PCR product, respectively. Primer pairs annotated grey indicate successful isolation of clones containing the respective regions via further library screen steps. Primer sequences are listed in Table 7.3.

Table 7.5 Genomic sequences at pBiC20 vector borders of successfully isolated clones

Marker	Primer (pBIC20)	Sequence at vector border	AGI position (bp)	Insert length (bp)
At2g30280	F	5´- **AAGCTT**GAATCATTGGTACAGGAAGTTCATGGAG - 3´	12914341	12644
	R	5´- **AAGCTT**CTTCACGTTGAGACGTGTGAAAAA - 3´	12926985	
HDUP3032	F	5´- TTGTTGTTGCTATGCNTTGGTATCCATTTTC - 3´	12942075	16146
	R	5´- GAAACAAATCAAATAAGATGGAACAAGGGTNAGATGAG - 3´	12925929	
nga3037	F	5´- **GCTT**TATGCCGTGAAACATTCTCCGAACAATGTATGA - 3´	12956153	14026
	R	5´- **AAGCTT**GATCTTACTAGGCAACCCCAG - 3´	12942127	
HDUP3038	F	5´- CAATTGTTACTTGNTTAGATCACGCAAGAGAGTAAGAGGTATA - 3´	12948829	15358
	R	5´- **GCTT**TCTCTACCGAATCAATCACTTTGACC - 3´	12964187	
At2g30420	F	5´- **AAGCTT**AAGTTGTTGAGTAGAACAAAACTTCGATCGAT - 3´	12971557	15866
	R	5´- **AAGCTT**TTCGACATTGTTTCATCGCTTAAGCTAGCGTATCTTGAGA	12955691	
At2g30432	F	5´- **AAGCTT**CTATCCAAGATCATTTTTACCTTG - 3´	12976682	12490
	R	5´- TGCAAGCAAGCCGATTAAGAAACCGCAGAAAAGCCATCTTTCTG -	12964192	
At2g30490_1	F	5´- **AAGCTT**CAGCACTTTGAGAAAGAGACTTATTCTC - 3´	13006137	16119
	R	5´- **AAGCTT**TAGCTAAGACATGAACTATATTAAAAGTACCTGTATCACC -	12990018	
At2g30490_2	F	5´- GTCCACATAAATTGTAAGATTCTAATCCG - 3´	13019237	18958
	R	5´- **AAGCTT**CGACAGTATCTGAATCGCGTCC - 3´	13000279	
At2g30520	F	5´- TCACATTCACCGAATTTGCCTACACTAGTCTACCAA - 3´	13009397	16012
	R	5´- **AAGCTT**TATCAAGTTCTGCAGTTGTTTATTTG - 3´	13025409	
At2g30600	F	5´- GAAGCTTCCTCATCGACCACAGATTTTCCATCTACCTGAAT - 3´	13044763	19358
	R	5´- **GCTT**CCCTAACATTCAACAACAATTAAATAAACGAAATTGCATAAA -	13025405	
	F	5´- **AAGCTT**CTGCCATGACAACTAATATAACTTGATGCAGT - 3´	13034750	

173

	R	5´- **AAGCTT**TGCTTCTTTCATTG---CTTGCCAAGNTAGCCAT - 3´	13060452	
At2g30780	F	5´- **AAGCTT**ACCCGTTGTTAGATGGGTCAGTCAAACTTGTA - 3´	13111657	18900
	R	5´- **AAGCTT**GATTTGACGGATGAGGATAAACTTGCTTTAG - 3´	13130557	
At2g30880	F	5´- **AAGCTT**CTAATAAAAGCCGAAGCACATCGTCAACAA - 3´	13166718	19004
	R	5´-	13147714	
At2g30942	F	5´- **AAGCTT**TGCCTTCAAGCGTTTGTATTTTCGGATGC - 3´	13166711	17003
	R	5´- TCATCAGGCTCCAGCATAACTAATGTGAAGCTGAACGTG - 3´	13183714	
At2g31020	F	5´- **AAGCTT**GATCAAGAAGATATGAATACTCCAAATCTTCAAAGC - 3´	13210540	14126
	R	5´- ACCGAGAACTATTACTCTTTGCATCCTCCACAAGATATTTATC - 3´	13196414	

Sequences in bold correspond to (partial) *Hind*III restriction site used for construction of the L*er* genomic library

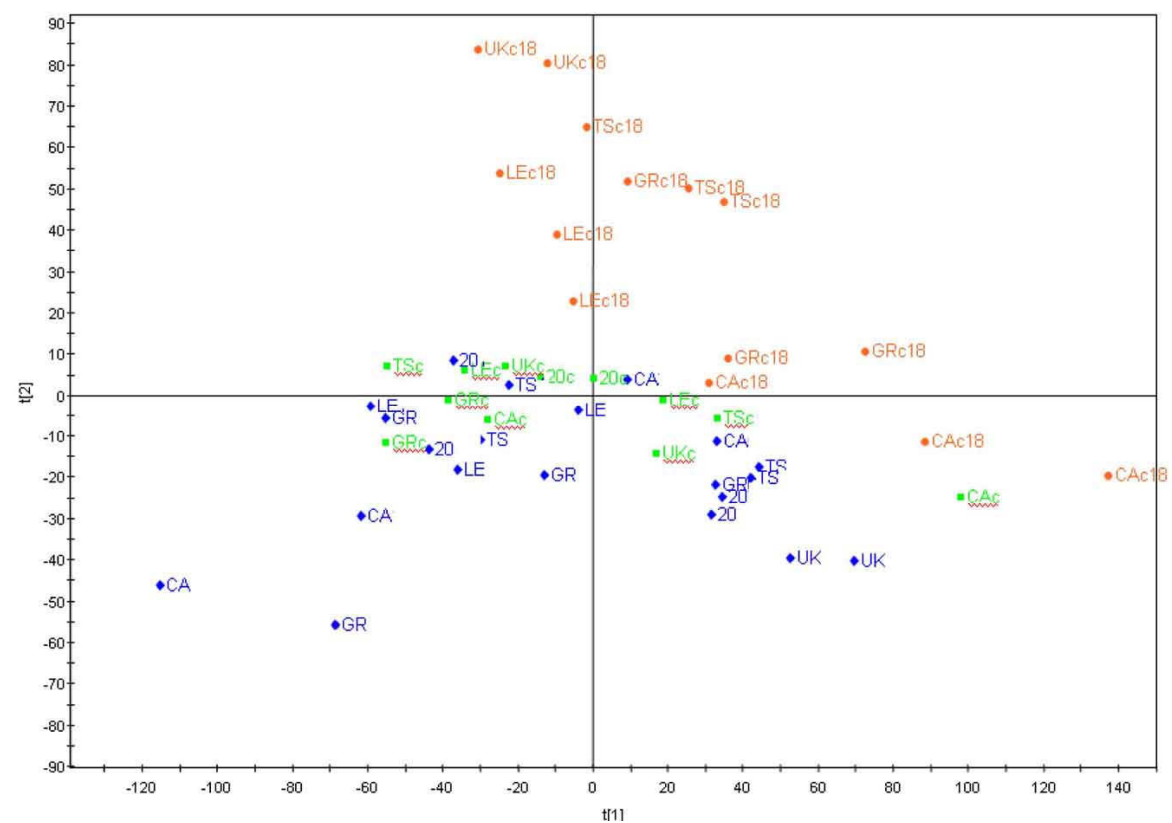## 7.4   HPLC analysis of UV-B treated *A. thaliana* accessions

Figure legend see next page.

Figure 7.2. Principal component analysis summarizing data of HPLC analysis of *A. thaliana* accessions analyzed for flavonoids of UV-B treated and control plants as described in chapter 3.5 and discussed in chapter 4.4. HPLC analysis was carried out in collaboration with Franz Hadacek (Department of Chemical Ecology and Ecosystem Research, University of Vienna).

Red: control plants of late response experiment. Green: control plants of early response experiment. Blue: UV-B treated plants of early response experiment under moderate UV-B regime. CA: Can-0, GR: Gr-1, LE: L*er*, UK: Uk-3, 20: 20-13, TS: Tscha-1.

8 Curriculum vitae

Name: Julia Hilscher

Geburtsdatum: 24. 3. 1978

Staatsbürgerschaft: Österreich

Universitätsausbildung:

10/1996 – 12/2002: Studium der Biologie, Studienzweig Genetik, Universität Wien

Titel der Diplomarbeit: „Characterization of Arabidopsis SR Protein Splicing Factors: Localization, Intercellular Trafficking, and Impact of Phosphorylation on Protein-Protein Interactions", Institut für medizinische Biochemie, Universität Wien

Seit 06/2004: Dissertation in der Forschungsgruppe von Dr. Marie-Theres Hauser

Titel: Genetic and molecular Analysis of Trichome Patterning in natural Accessions of *Arabidopsis thaliana*", Department für angewandte Genetik und Zellbiologie, Universität für Bodenkultur Wien

Publikationen:

Hilscher J, Schlötterer C, Hauser MT. 2009. A single amini acid replacement in ETC2 shapes trichome patterning in natural *Arabidopsis* populations. Current Biology 19:1747-1751.

Lorkovic ZJ, Hilscher J, Barta A. 2008. Co-localisation studies of *Arabidopsis* SR splicing factors reveal different types of speckles in plant cell nuclei. Experimental Cell Research 314: 3175-3186.

Lorkovic ZJ, Hilscher J, Barta A. 2004. Use of fluorescent protein tags to study nuclear organization of the spliceosomal machinery in transiently transformed living plant cells. Molecular Biology of the Cell 15: 3233-3243.

Lopato S, Forstner C, Kalyna M, Hilscher J, Langhammer U, Indrapichate K, Lorkovic ZJ, Barta A. 2002. Network of interactions of a novel plant-specific Arg/Ser-rich protein, atRSZ33, with atSC35-like splicing factors. Journal of Biological Chemistry 277: 39989-39998.